Investigating the role of microRNA-31 as a modulator of chemosensitivity in malignant pleural mesothelioma

by Hannah Louise Moody, BSc

A thesis for the degree of Doctor of Philosophy

The University of Hull and the University of York

Hull York Medical School

September 2016

Abstract

Malignant pleural mesothelioma (MPM) is associated with an extremely poor prognosis and the majority of patients are initially or rapidly become unresponsive to platinum-based chemotherapy. MicroRNA-31 (miR-31) is encoded on a genomic fragile site, 9p21.3, which is reportedly lost in approximately half of MPM tumours, and its prognostic value is currently ambiguous. Based on previous findings in a variety of other cancers, it was hypothesised that miR-31 loss confers chemoresistance and that miR-31 reconstitution may enhance sensitivity to chemotherapeutics in MPM. Surprisingly, reintroduction of miR-31 into epithelioid miR-31-null NCI-H2452 cells significantly enhanced clonogenic resistance to cisplatin and carboplatin. Conversely, suppression of endogenous miR-31 in P31 epithelioid cells significantly increased chemosensitivity. Interestingly, while miR-31 overexpression increased resistance to platinum-containing therapeutics, paradoxically, a higher relative intracellular concentration of platinum was observed versus controls. While the expression of the drug influx transporter CTR1 was increased upon miR-31 re-expression, a significantly decreased intranuclear concentration of platinum was observed, with associated reduction in DNA damage, potentially explaining the increase in cisplatin accumulation but decreased chemosensitivity. The converse relationship was demonstrated in P31 cells upon endogenous miR-31 suppression, further suggesting a mechanism underpinning resistance that involves altered nuclear transport. Linked with a downregulation of OCT1, a bipotential transcriptional regulator with multiple miR-31 target binding sites, we subsequently identified an indirect miR-31-mediated upregulation of ABCB9, a transporter associated with drug accumulation in lysosomes, and increased uptake of platinum to lysosomes. However, when overexpressed directly, ABCB9 promoted cellular chemosensitivity, suggesting the miR-31 promotes

1

chemoresistance largely via an ABCB9-independent mechanism. Overall, these data suggest that miR-31 loss from MPM tumours does not promote chemoresistance in MPM, and may be prognostically beneficial in the context of therapeutic sensitivity. As such, endogenous miR-31 suppression may actually enhance sensitivity to platinum-based treatment in patients with MPM.

Dedication

This thesis is dedicated to two persons, firstly, my son, Oliver. Without Oliver, I would not have had the inspiration or commitment to complete this research. Secondly, I dedicate this to my Mum, a woman whom I could not admire more, her resilience, strength and guidance has made me into the person I am today, thank you Mum.

"*Promise me you'll always remember: You're braver than you believe, and stronger than you seem, and smarter than you think*"

- A. A. Milne

Author's declaration

I confirm that this work is original and that if any passage(s) or diagrams(s) have been copied from academic papers, books, the internet or any other sources these are clearly identified by the use of quotation marks and the references(s) fully cited. I certify that, other than where indicated, this is my own work and does not breach the regulations of HYMS, the University of Hull or the University of York regarding plagiarism or academic conduct in examinations. I have read the HYMS Code of Practice on Academic Misconduct, and state that this piece of work is my own and does not contain any unacknowledged work from any other sources. I confirm that any patient information obtained to produce this piece of work has been appropriately anonymised.

Publications

• H.L. Moody, M.J. Lind, S.G. Maher (2016) 'MicroRNA-31 regulates chemosensitivity in malignant pleural mesothelioma' [under review with *Molecular Therapy – Nucleic Acids*].

• H. Moody, M. Lind, S. Maher (2016) 'MicroRNA-31 regulates chemosensitivity in malignant pleural mesothelioma via altered intracellular drug localisation', *European Journal of Cancer*, Vol. 61, S140 [published abstract].

• Hannah Moody, Michael Lind, Stephen Maher (2015) 'BACR 14: MicroRNA-31 mediates chemoresistance in malignant pleural mesothelioma via reduced cisplatin intranuclear accumulation', http://abstracts.ncri.org.uk [online abstract].

• H.L. Moody, M.J. Lind, S.G. Maher (2015) 'MicroRNA-31 expression mediates chemoresistance in malignant pleural mesothelioma', *Lung Cancer*, Vol. 87, S1–S2 [published abstract].

• Maher, S., Bibby, B., Moody, H. and Reid, G. (2015) 'MicroRNA and Cancer', in Epigenetic Cancer Therapy, Elsevier [book chapter].

Presentations

• International Mesothelioma Interest Group Conference, Birmingham, 2016 (oral).

• Hull York Medical School Postgraduate Research Conference, York, 2016 (oral).

• 12th International Medical Postgraduate Conference, Charles University, Czech Republic, 2015 (oral).

• National Cancer Research Institute Conference, Liverpool, 2015 (poster).

• British Thoracic Oncology Group Conference, Dublin, 2015 (poster).

• HYMS Postgraduate Research Conference, York, 2014 (poster).

Awards received

• Hull York Medical School Postgraduate Researcher of the Year, 2016.

• Young Investigator Award, iMig 2016.

• EACR Biennial Congress Student Travel Award, 2016.

• 12th International Medical Postgraduate Conference, Charles University, Czech Republic, 1st prize awarded from 33 PhD students from 10 European countries.

• BACR/CRUK Student Award, 2015.

• Teesside Science Award 2013, for outstanding academic achievement in Biological Sciences.

Chapter 1:

General introduction

Partially published in Maher, S., Bibby, B., Moody, H. and Reid, G. (2015) 'MicroRNA

and Cancer', in Epigenetic Cancer Therapy, Elsevier, 4: 67:90.

1.1 Malignant mesothelioma

1.1.1 *Overview*

Malignant mesothelioma is a relatively rare tumour that originates in the cells that compose the mesothelial surface of the body cavities. There are four reported anatomical areas in which mesothelioma can establish, these are namely the pleura, pericardium, peritoneum and *tunica vaginalis* [1]. The pleural form of malignant mesothelioma (MPM) is the most widespread in presentation, detailed in Fig 1.1, with the other areas of the body contributing to approximately 22.1% of the total noted cases of malignant mesothelioma [2-4]. Primary pericardial mesothelioma relates to 0.7% of mesothelioma cases, with no clarity on a causative agent, although Mensi *et al.* [3] supported that the pathogenesis of the disease is promoted by exposure to asbestos. Peritoneal presentation accounts for 10-20% of cases, with most patients suffering with progressive ascites, however, as Markaki *et al.* [2] reported, there are complications with accurate diagnosis due to misinterpretations as serous papillary carcinoma and ovarian carcinoma. The *tunica vaginalis* represents the most exceptional area for mesothelioma to develop with, in 2011, only 223 cases known [4]. Initial symptoms include scrotal enlargement with a paratesticular mass, which is then identified as malignant mesothelioma intraoperatively [4].

1.1.2 *Clinical presentation and diagnosis*

The diagnosis of MPM represents a challenge as there is an extensive delay between the onset of symptoms and accurate diagnosis [5]. The symptoms of the disease are multifaceted and can progress with time; many patients have non-specific ailments when presenting to a clinic. Symptoms comprise lethargy, chest pain, sweating, coughing, breathlessness and constipation [6, 7], all of which have a range of different diseases to which they can be attributed. An additional issue is the latency period of the
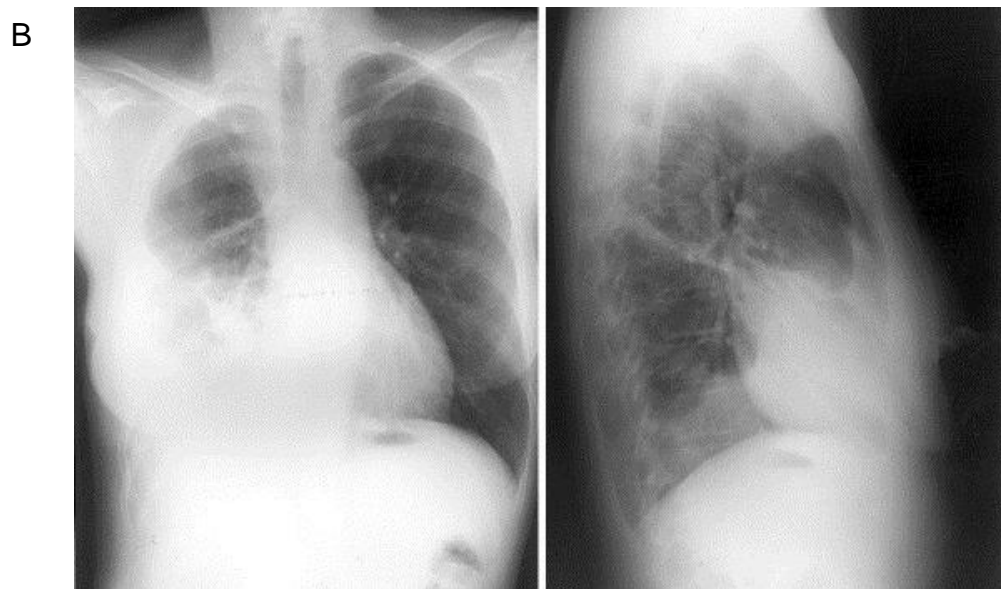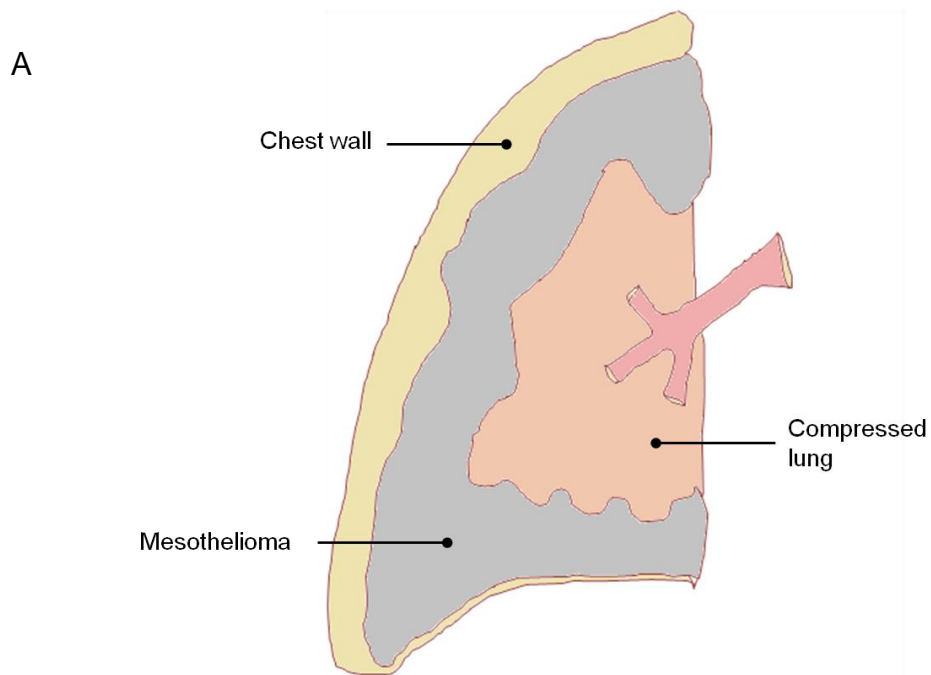
Figure 1.1 Malignant pleural mesothelioma. (A) Diagram demonstrating the anatomical presentation of malignant pleural mesothelioma. Lung is encased by mesothelioma tumour developing in the pleural cavity. Adapted from Thompson and Mason [8]. (B) Chest radiographs of a 55-year-old woman with MPM. Postero-anterior (PA) (left) and lateral (right) radiographs demonstrate circumferential thickening, which is encasing and compressing the right lung. Adapted from Bonomo *et al.* [9].

disease; the time lapse from the carcinogenic agent exposure to the onset of disease can be many years. The median latency period in review of 1690 cases, as described by Linton *et al.* [10], is 32 years, with 20-40 years being the most common latency period. The production of a chest radiograph is often a first line of enquiry when a patient presents with dyspnoea, an antero-posterior (AP) or postero-anterior (PA) chest typically reveals a unilateral pleural effusion or thickening also visible on a lateral view in MPM [1]. A chest CT may then follow, although accurate diagnosis is not possible; a "rind-like" tumour on the pleural cavity is suggestive of the disease [1]. Haberkorn [5] reported that the primary investigative procedure for relatively accurate diagnosis (>90 %) is thoracoscopy, although there may be complications affecting the patient, such as tumour seeding. Evidence of less invasive accurate diagnosis is growing, with procedures such as 18F-fluorodeoxyglucose-positron emission tomography (FDG-PET) gaining attention due to MPM cells taking up more of the FDG marker and thus determining such vital aspects as prognosis and staging [5]. In respect of the medico-legal aspects, a biopsy specimen of the tissue must accurately diagnose MPM via histology [1].

1.1.3 *Staging*

The staging of MPM is complex, but the need to stratify patients quickly into different treatment regimes according to survival data is prominent. It is well recognised that patients who have advanced disease who would not benefit from surgery, for example, should be considered for other treatments or palliative care, the primary aim being to minimise stress to the patient [11]. Table 1.1 details a summary of treatment at differing stages. CT and PET imaging are used for diagnosis and staging purposes, as well as video-assisted thoracoscopic surgery (VATS). Additionally, sonography with a transthoracic ultrasound can be of benefit in the diagnosis and staging of the disease,

wherein the pleural effusion, so often noted in MPM cases, can be used as an acoustic window to view intrapleural and intrapulmonalary processes, although this technique is not widely adopted [12]. The international association for the study of lung cancer, along with the international mesothelioma interest group (iMig) have developed TNM classification for MPM, as detailed in Table 1.1 and Table 1.2. Unfortunately, it is common for patients to present at stage IIIA/B or stage IV of disease (Table 1.2), with poorer prognosis associated with advanced staging.

1.1.4 *Histological subtypes*

Mesothelioma can be categorised into four cellular subtypes, these are epithelioid, biphasic, sarcomatoid and desmoplastic, as in Fig. 1.2 [13]. Proportionally, the subtypes constitute approximately 60%, 20%, 20% and 1-2% of cases respectively [13]. The more common epithelioid subtype is associated with increased survival, and the more aggressive sarcomatoid and desmoplastic subtypes are associated with the poorest survival [14, 15]. Primarily, epithelioid tumours have a papilla-tubular structure of flat cells present, sarcomatoid has a high ratio of spindle type cells and mimics sarcoma, biphasic have features of both epithelioid and sarcomatoid cells. Desmoplastic mesothelioma is rare, however, histologically tumours feature granulated areas and/or fibrous pleuritis [13].

1.2 Epidemiology

From an epidemiological aspect, MPM is comparatively rare [16] in comparison to other cancer types, however, as the disease is so destructive, there is particular interest in geographical areas with high mortality quotients. Bianchi and Bianchi [17] reported that from a global perspective, incidence rates are highest in Australia, Belgium and

Great Britain, with incidence rates at around 30 per million. Australia has its own register dedicated to mesothelioma, and from reported cases it is clear that only 16 cases were described in 1980, whereas 490 were recorded in 2000 [17], an astounding 30-fold increase, which may be partially due to increased diagnosis due to better service provision. MPM, according to Pinto *et al.*, [18] cannot be considered an uncommon disease due to the sharp and constant increase in incidence since the 1980s. The peak of prevalence is approximated to be from 2010-2020, thus connoting many current studies relating to the disease.

1.2.1 *Prevalence in the United Kingdom*

The Health and Safety Executive [19] established statistical evidence from 1981-2005 relating to mesothelioma mortality amongst the British population. According to figures, West Dunbartonshire, Barrow-In-Furness, Plymouth and North Tyneside have the greatest number of male deaths, with cities such as Kingston-upon-Hull rating in the middle. In the Yorkshire city of Leeds a study was conducted from 2002 to 2005 to determine the incidence of MPM in the population. The research concluded that 77% of the 146 cases were male patients with a median survival of 8.9 months from diagnosis [20]. Although not as prevalent, MPM in female patients has also been noted, especially in areas of manufacturing including Barking and Dagenham, and Sunderland [21].

More recently, the Health and Safety Executive published mortality rates in Great Britain from 1968 to 2014 [22]. In 2014, there were 2,515 mesothelioma deaths, a similar number was reported for the preceding 2 years, and this roughly equates to 7 people per day dying of mesothelioma. In projection, statistical modelling forecasts this rate will remain steady, until 2020, thereafter annual rates are predicted to decline. The

Table 1.1 Staging of MPM (adapted from IASLC 8th TNM classification for MPM).

T – Primary tumour	
T1	Tumour only found in the ipsilateral parietal or visceral pleura
T2	Tumour involves the ipsilateral pleura with invasion to diaphragmatic muscle and/or pulmonary parenchyma
T3	Tumour involves the ipsilateral pleura with invasion to endothoracic fascia and/or mediastinal fat and/or chest wall with or without rib destruction and/or pericardium
T4	Tumour involves the ipsilateral pleura with invasion to chest wall (unresectable) and/or peritoneum and/or contralateral pleura and/or mediastinal organs and/or vertebra and/or pericardium
N- Regional lymph nodes	
NX	Regional lymph node cannot be assessed
N0	No regional lymph node metastases
N1	Metastases to ipsilateral intrathoracic lymph nodes
N2	Metastases to contralateral intrathoracic lymph nodes, metastases to ipsilateral or contralateral supraclavicular lymph nodes
M- Distant metastasis	
M0	No distant metastasis
M1	Distant metastasis present

T- tumour stage; N- lymph node status; M- metastasis status

Table 1.2 Stage grouping of MPM and treatments utilised (adapted from IASLC 8th TNM classification for MPM).

Stage	T	N	M	Treatment utilised
IA	T1	N0	M0	Surgery, Chemotherapy, Radiotherapy
IB	T2, T3	N0	M0	Surgery, Chemotherapy, Radiotherapy
II	T1, T2	N1	M0	Surgery, Chemotherapy, Radiotherapy
IIIA	T3	N1	M0	Some surgery, Chemotherapy, Radiotherapy
IIIB	T1, T2, T3	N2	M0	Some surgery, Chemotherapy, Radiotherapy
	T4	N0, N1, N2	M0	
IV	Any T	Any N	M1	Chemotherapy, Radiotherapy
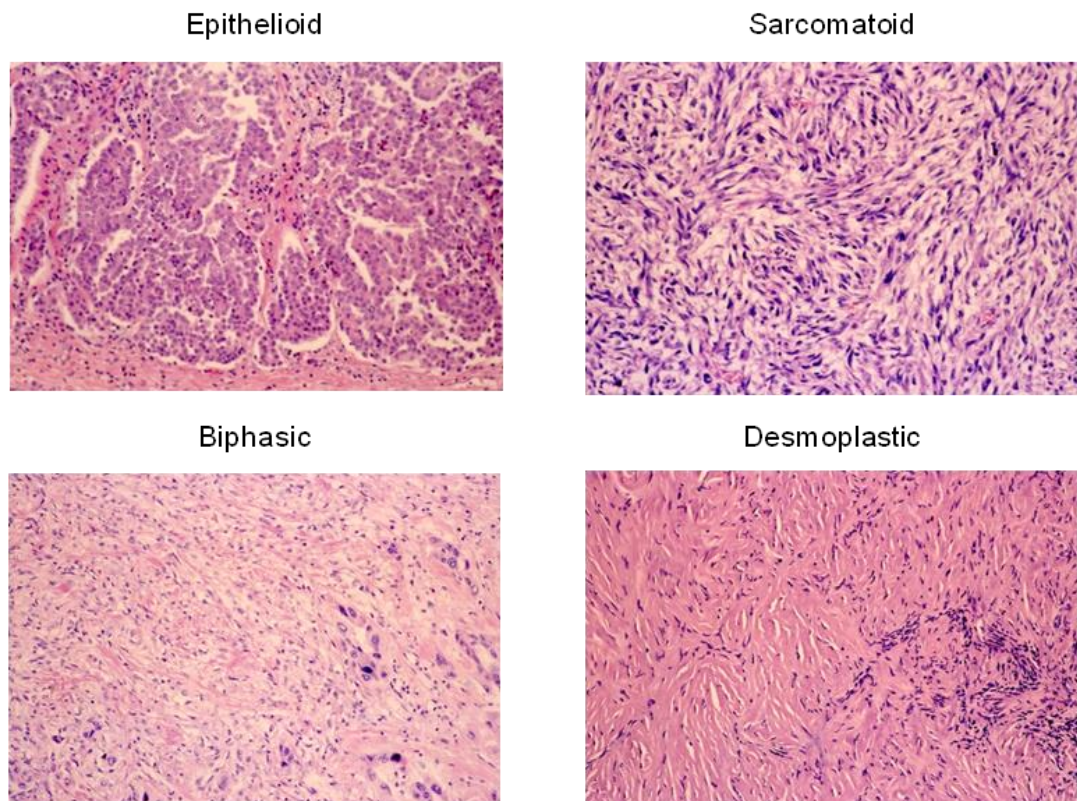
Figure 1.2 Histological subtypes of malignant pleural mesothelioma. Epithelioid represents the most common subtype of MPM, desmoplastic representing the rarest subtype. Epithelioid cells have a tubular more uniformed morphology. Sarcomatoid cells, which represent the most aggressive form of MPM, are spindle-like. Biphasic cells are a mixture of both epithelioid and sarcomatoid subtypes within one tumour. Desmoplastic cells have fibrous formations and often feature granulation. Microphotographs taken with H & E staining. Figure adapted from Inai [13].

most recent epidemiological data suggests mesothelioma rates are falling in Scotland, the East Midlands, London, and the South East [22].

1.2.2 *Prevalence in specialised industry*

Interestingly, epidemiology indicates a higher mortality in areas that have a relationship to the shipping industry. In Sweden, rates of disease were much higher in the counties of Gothenburg and Malmö, both of which are known for their large shipyard sites [17]; this appears to be reflected in similar British areas. In 2003, Hilliard *et al.* [23] produced a study relating to the Devonport Naval Base in Plymouth. The site employed circa 19,000 people during World War II, with no protection for workers from inhalation of asbestos. During the 1960s asbestos usage had diminished in the dockyard, and employees were provided with some respiratory equipment to protect their airway. The leading occupation by which asbestos-related deaths occurred was as a shipwright. The shipwrights were continuously exposed to asbestos at high levels, with a correlation of heavy exposure associated with a shorter latency period, and also a high risk of peritoneal forms of mesothelioma [23].

1.3 Causative agents

1.3.1 *Asbestos*

The primary agent for MPM pathogenesis is asbestos [24]. As Linton *et al*. [10] reported, asbestos is a polyfilamentous fibrous substance composed of crystalline hydrated silicates. Amphibole minerals are a natural product found in dilated rock that actually composes around 5% volume of the earth's crust [25]. There are primarily six different forms of asbestos fibres, five of which are amphiboles, and one of which is a serpentine. The double chain amphiboles consist of actinolite, amosite, anthophyllite,

crocidolite and tremolite, all of which are traditionally incorporated into tiles or cement. The serpentine, chrysotile, is structured in crystallised rolled-up sheets; it is incredibly pliable and can be woven into fabrics and flexible products [10].

Ross *et al.* [25] described the desirable commercial properties of asbestos being high absorbency, high tensile strength, low thermal and electrical conductivity, and resistance to acids and bases. A wide variety of industrial and household products were manufactured when asbestos was at its highest usage, including wallboards, firemen's clothing, talcum powder, steam equipment, mechanical brake linings, theatre scenery and hair dryers, thus affecting a broad population and various occupational roles [26]. Asbestos was banned or severely restricted in many developed nations almost two decades ago, due to the realisation of implicated health issues associated with the fibres. Although the prohibition and tight regulation of demolitions exists, due to the latency period of asbestos-related diseases, it is only within the past decade that the burden of disease has been particularly felt; this is set to increase within this decade [24].

Domestic exposure to asbestos fibres is an indirect route by which contact occurs. From a traditional perspective, many women are affected by the disease without working in a contaminated environment; the dose they received has been due to washing clothes by hand [10]. There has furthermore been prevalence in asbestos workers' children becoming diseased with MPM [27]. The fibres of amphibole that constitute asbestos contain varying amounts of mono-, di- and tri-valent metals like iron. It is proposed that amphiboles are more pathogenic in comparison to that of the short-fibred serpentine structure since they contain metal, and are considered insoluble in the lung [24]. Nymark *et al.* [24] describes that asbestos alone is non-toxic to humans, although the way by which iron is bound to the fibre can promote free radical generation. Fibres can also radically interact with DNA, which induces DNA damage and may result in

mutational and deleterious events [28]. Additionally, the modification of mitochondrial function, interruption of cell cycle progression and activation of cell signalling pathways have been noted [24].

1.3.2 *Erionite*

In addition to asbestos there is another mineral that has been linked to the onset of MPM. Erionite is a fibrous zeolite that is found in volcanic tuffs, particularly in the Cappadocian region of Central Anatolia, Turkey [29, 30]. Erionite, as Bertino *et al.* [31] described, is a mutagen and can be deemed more carcinogenic than asbestos fibres due to its ability to accrue iron on its exterior. The mineral fibres are believed to be higher in potency, as comparisons between villagers environmentally exposed to tremolite, and that of erionite-exposed villagers showed that residents from Tuzköy retained significant amounts of the mineral [29].

There is evidence of genetic susceptibility to erionite promoted carcinogenesis in the villages of Tuzköy and Karain in Turkey, wherein 50% of deaths are attributed to MPM [32]. Six families in the region are thought to have a common ancestor with genetic susceptibility to MPM through erionite exposure, as families in other villages with housing made from the same erionite containing rock have a greatly decreased incidence by contrast. It has been noted that the families affected marry in an endogamous manner, and so the indication is that there is an autosomal dominant pattern of inheritance [33].

1.3.3 *Simian Virus 40*

Polyomaviruses are a family of double-stranded DNA viruses. Two isolated polyomaviruses, JC and BK, have previously been identified as being of human origin. There is a third known polyomavirus that affects humans, however, the isolate derives

from simians [34]. The DNA-based tumour virus, Simian Virus 40 (SV40), is an endogenous virus in Rhesus monkeys that consists of a 5,234 base pair circular genome [32]. There was a singular event that is alleged to be the route by which humans were infected with the virus; this is thought to be the inadvertent contamination of oral poliovirus vaccines administered to the population of many countries from 1954 to 1963, and possibly until the 1970s in some areas [35]. The monkey kidney cells used to grow the vaccine were contaminated with live SV40, which was then administered to more than 30 million people in the USA alone [32, 34].

The pathogenicity of SV40 lies with two antigens, the large T antigen (Tag) that is approximately 90 kDa and small t antigen (tag) that is approximately 17 kDa in size [35]. The large Tag binds and inactivates both p53 and Rb, which in turn induces insulin-like growth factor 1. In addition to tumour suppressors being targeted, PP2A is inactivated by tag, which results in the upregulation of the AP1 transcription factor, and the ensuing activation of the Wnt pathway, signifying alterations to cell migration and fate determination [34-36]. Chromosomal anomalies additionally occur in the host cell, which consequently affects oncogenesis-related genes and promotes genetic instability [36].

The tumour promoting effect of SV40 varies when in contact with different cell types. Monkey and *Homo sapien* fibroblast cells are tolerant of infection; however, human mesothelial cells are vulnerable in relation to the carcinogenicity of SV40 [32]. SV40 was specifically linked to mesothelioma in 1991, when 100% of hamsters injected intrapleurally with the virus developed MPM within 6 months [35]. The mesothelial cells that line the pleura and other body cavities are amongst the most undifferentiated cells in the adult human body, they possess the ability to arise in different morphologies, such as epithelial-like or fibroblast-like cells [37]. Mesothelial cells are

predisposed to expressing large amounts of the tumour suppressor gene p53, generally five times greater than in fibroblasts [35]. As Rizzo *et al.* [35] reported, and as previously discussed, Tag binds p53, which inactivates it, and at the same time the physical interaction between the two components discontinues the replicase activity of SV40, this could be viewed as a benefit, however, as viral replication is at a slow rate, there is evasion of the host immune response and the infection persists [32]. Interestingly, the virus and mesothelial cells appear to exist in a parasitic relationship, where the virus may effectively live inside the cellular environment, as exposure to a few isolated SV40 can cause an infection and therefore release of viral particles from contaminated cells; thus infecting neighbouring mesothelial cells. Where the expression of the oncoproteins perseveres, and in the absence of normal cell lysis, the rate of transformation in the mesothelial cells is around 1 in 103 in comparison with 1 in 109 in other cell types [32]. By the evasion and inactivation of various modulators, cellular proliferation becomes autonomous and fundamental checkpoints are avoided, enabling the passage from the G1 to the S phase of the cell cycle [38].

It is apparent that SV40 single-handedly does not normally cause carcinogenic events in humans; it is rather viewed as a contributing factor, or initiator. Millions of people immunized with the contaminated polio vaccine would now have cancer if SV40 were to be the sole pathogenic agent for the onset of MPM [32]; however, there have been alternative suggestions, in that SV40 may play a synergistic part alongside asbestos exposure to contribute to the pathogenesis of MPM, where SV40 is the initiator and asbestos-related inflammation is the promoter. Carbone and Rdzanek [32] discussed the observation that mutant SV40 transfected cells that are consequently exposed to asbestos appear to become malignantly transformed, which correlates to a co-carcinogenic effect.

1.3.4 *BAP1*

Due to the observations that mesothelioma developed in family groups, as established with erionite exposure, Testa *et al.*[39] investigated the potential for genetic pre-dispositions to the disease. Interestingly, the research established germline mutations in *BAP1*, a gene encoding BRCA1-associated protein. As well as the correlation with sporadic mesothelioma, the results identified that *BAP1* mutation carriers could also develop uveal melanoma. Promisingly, recent studies have indicated *BAP1* immunostain representing 100% specificity in distinguishing between benign and malignant mesothelial proliferations [40], encouraging *BAP1* as a reliable marker for mesothelioma pre-disposition.

1.4 Treatment

There are three main modalities by which MPM can be treated; these are surgery, radiotherapy and chemotherapy.

1.4.1 *Surgery*

The foremost surgical treatments involve extrapleural pneumonectomy (EPP), or pleural decortications [41]. Pleurectomy/decortication (P/D) is a lung sparing procedure where the visceral and parietal pleurae are dissected [42]. Where patients are deemed to have operable mesothelioma, EPP may be considered, however, this is a demanding procedure. The parietal and visceral pleura, ipsilateral diaphragm, ipsilateral pericardium and underlying lung are resected in EPP, followed by the reconstruction of the pericardium and diaphragm. Where patients are able to tolerate the procedure, there can be relief of chest wall pain and shortness of breath [42]. The EPP approach can be deemed highly aggressive; however, patients in the early stages of the disease appear to

31

respond better to this treatment [43]. P/D can improve survival in patients who present with early stage disease; while EPP can be more appropriate for more advanced tumours. However, the MARS trial in 2011 [44] reported no benefit to patients with the use of EPP, and actually warned against EPP due to the harm that the procedure causes to patients. A further developed randomised trial, MARS2 [45, 46], which compares chemotherapy only with chemotherapy and lung-sparing surgery is currently recruiting patients and the analysis is expected early 2018. This trial will be vital in stratifying patients to give them the best quality of life possible.

As well as surgical resection, there are surgical procedures to alleviate the symptoms of mesothelioma, including the insertion of chest drains to alleviate pleural effusion [47]. Interestingly, post drainage pleurodesis can be applied by means of talc poudrage, however, where the lung is entrapped, a tunnelled intrapleural catheter can provide relief from dyspnea [48].

Overall, surgery is most beneficial to patients who present with early stage disease, and according to Flores [49], median survival for P/D is 46 months at stage I, 18 months at stage II, 13 months at stage III and 9 months at stage IV. In comparison, the more radical EPP surgery has median survival of 22 months at stage I, 19 months at stage II, 10 months at stage III and 4 months at stage IV. There can be complications resulting from either surgery, with diagphragmatic rupture, empyema, air leaks, mediastinal shift, bleeding, pulmonary embolus and cardiac failure all being noted [50].

1.4.2 *Radiotherapy*

MPM represents a challenge to radiotherapy, as the tumour surrounds and encases the lungs making accurate radiation exposure difficult. Radiotherapy is most often used for palliative care in MPM to alleviate chest wall pain, and at sites of chest drains [51, 52]. The phase II SYSTEMS (The SYmptom Study of radioThErapy in MeSothelioma)

multi-centre study in 2015 [53] reported that radiotherapy was effective for the treatment of pain in MPM, a symptom that greatly affects patient quality of life [54]. Radiotherapy is widely and often utilised within the clinical setting to ensure patient quality of life is optimal [55]. Currently, SYSTEMS-2 is recruiting patients for investigation of higher dose radiotherapy to treat pain; patient recruitment will end in 2018 [56].

Radiation can aid the prevention of the subcutaneous nodules that mesothelioma forms along the tracts of biopsies, incisions and chest tubes [48]. New and adaptive technologies are currently being developed in attempt to irradiate areas surrounding the thorax without penetrating vital tissues [51]. The IMPRINT study focussed on hemi-thoracic intensity-modulated pleural radiation therapy in combination with chemotherapy and, in some cases, pleurectomy/decortication, and found it may contribute a lung-sparing approach to treatment [57].

1.4.3 *Chemotherapy*

1.4.3.1 *Chemotherapy interactions*

Chemotherapy drugs act on rapidly proliferating cells, by either damaging DNA, or interrupting vital biochemical processes [58]. Generally, chemotherapeutic molecules aim to initiate or promote cell death pathways mainly through the induction of apoptosis [59]. Although the outcome of chemotherapy treatment is cell death, the means by which this occurs can be variable, and is often poorly understood, although damage to DNA, RNA[60] and important regulatory proteins [61] is thought to be a common initial event whereby a cellular stress response is initiated [62]. The activation of intrinsic apoptosis through targeting of the Bcl-2 family and p53, as well as extrinsic targeting of tumour necrosis factor, and FLICE-inhibitory protein have all been observed with varying success in many cancer cell lines [63-66]. Additionally, it is

possible to trigger cell death through targeted activation of necrosis, disabling the mitotic checkpoint, and activation of senescence [67].

The activation of apoptosis by chemotherapies has been linked with the extrinsic pathway, where a death signal from the cell surface leads to the triggering of intracellular signalling pathways ultimately leading to the death of the cell [68]. Death receptors including TNF-related apoptosis-inducing ligand-receptor 1 and 2 (TRAIL-R1/2), TNF receptor 1 (TNFR1) and CD95 (APO-1/Fas), and their ligands TRAIL, TNFα and CD95L (FasL) are implicated in resistance to chemotherapy. Interestingly, the overexpression of death receptor ligands has been thought to aid the explanation as to how tumour cells can suppress anti-tumour T cells through the stimulated CD95/CD95L interaction [62].

Although the extrinsic pathway is implicated, it is widely accepted that many chemotherapy drugs activate the intrinsic cytochrome c/Apaf-1/caspase-9-dependent pathway via the mitochondrion. Protein kinases that are activated by stress signals have been shown to inactivate Bcl-2 family members, which contributes to many drug-resistant phenotypes [69]. Defects in either pathway can promote chemotherapy resistance, and the targeting of these pathways may restore some sensitivity[62].

1.4.3.2 *Cisplatin*

Cisplatin or *cis*-diamminedichloroplatinum(II) ($Cl_2H_4N_2Pt$), Fig. 1.3, is a chemotherapeutic drug frequently used in the treatment of many cancers including MPM. On association of cisplatin with the plasma membrane, the uptake of the drug is mediated by the copper transporter CTR1 [70]. Whilst within the cell, Atox1 chaperones the cisplatin through the intracellular environment [71], and the platinum compound is then effluxed via the transporters ATP7A, ATP7B and multidrug resistant proteins (MRPs) [72, 73]. Cisplatin is activated upon contact with the cytoplasmic

environment, wherein chloride atoms are displaced by water; this hydrolysed product binds to the N7 reactive centre on purines leading to observable 1,2-intrastrand cross-links [72]. The formation of platinum-DNA adducts results in DNA double- and single-strand breaks that consequently instigate cell death [74, 75].

1.4.3.3 *Carboplatin*

Carboplatin, or *cis*-diammine(cyclobutane-1,1-dicarboxylato)platinum(II), Fig.1.3, is a platinum-based chemotherapy which is used to treat a variety of cancers. Generally, it is thought that carboplatin enters the intracellular environment via passive diffusion [76]. Carboplatin is utilised in many gynaecological tumours and is myelosuppressive [77].

The mechanism of action of carboplatin is similar to that of cisplatin; treatment with carboplatin induces DNA adducts, however, a 20-40 fold increase in concentration is needed to emulate that of cisplatin treatment, and the formation of adducts is at a 10-fold slower rate [78]. Originally, carboplatin was developed to improve the efficacy of cisplatin, and was found to be much less nephro- and neuro-toxic, therefore better tolerated by patients who may not otherwise endure cisplatin treatment [76].

1.4.3.4 *Pemetrexed*

Pemetrexed disodium or N-[4-[2-(2-amino-3,4-dihydro-4-oxo-7H-pyrrolo[2,3-d] pyrimidin-5-yl)ethyl] benzoyl L-glutamic acid ($C_{20}H_{19}N_5Na_2O_6$), Fig. 1.3, is an antifolate commonly used in treatment of MPM and non-small cell lung cancer [79, 80]. Pemetrexed has a high affinity for many membrane bound folate transporters including reduced folate carriers, folate receptors $-\alpha$ and $-\beta$, the proton-coupled folate transporter as well as members of the SLC organic acid family of carriers [79]. Additionally, export out of the cell relies upon the ABC family of proteins to transport antifolate monoglutamates [79]. Pemetrexed inhibits the action of three critical folate metabolism

enzymes, namely thymidylate synthase, glycinamide ribonucleotide formyl transferase (GARFT) and dihydrofolate reductase (DHFR) [81]. The folate metabolism pathway is essential for the synthesis of both purines and pyrimidines, signifying replication halt due to the block in DNA production by the inhibition of thymidylate synthase [80].

1.4.3.5 *Chemoresistance mechanisms*

Although the standard treatment for MPM is to utilise cisplatin and pemetrexed in combination, the average prognosis for patients who are treated with these chemotherapeutics is still relatively poor, with average survival of ~12.1 months, compared to just ~9.3 months when treated with cisplatin alone [82]. The poor prognosis can be at least partially attributed to the inherent resistance that MPM appears to have toward chemotherapy. Patients can therefore be defined by either having refractory or resistant disease. Patients with innate resistance to chemotherapy, also termed refractory disease, are inherently resistant to the treatment and equate to ~50% of MPM cases [83-85], patients who initially respond but then relapse are termed to have acquired resistance [86].

As reviewed in Shi and Gao [87], there are five main mechanisms by which the development of chemoresistance may occur. Firstly, modifications in drug transport can signify cross-resistance to many chemotherapeutics via the overexpression of ATP-binding transporters, which can lead to greater efflux of drugs and therefore decreased drug accumulation. O'Reilly [88] described resistance to PARP inhibitors through overexpression of MDR pumps in triple negative breast cancer, conversely, in Singh *et al.* [89] the decrease of MDR efflux proteins resulted in greater sensitivity to paclitaxel in prostate cancer. Alternatively, the decreased expression of drug influx transporters can be responsible for reduced accretion within cells, as demonstrated in Peng *et al.* [90], where down regulation of transporters responsible for influx enhanced
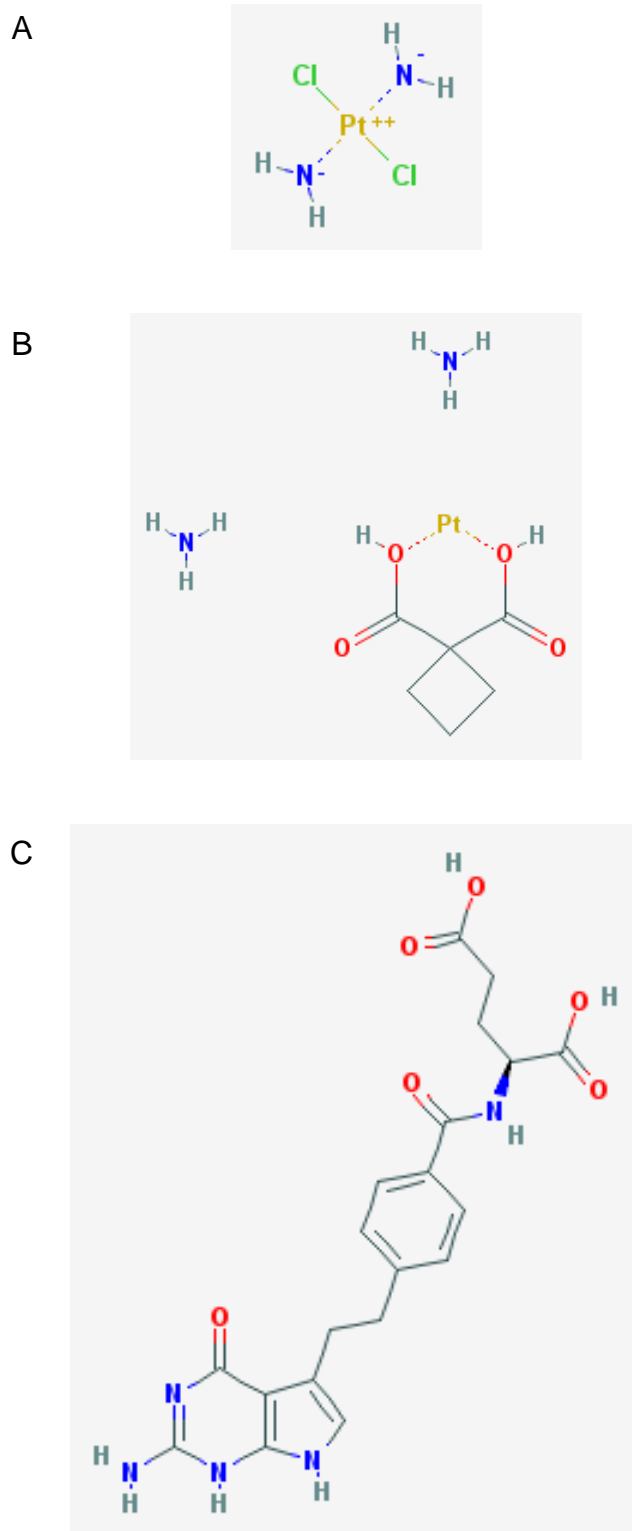
Figure 1.3 Chemical structures of chemotherapies frequently used in MPM. (A) Cisplatin (300.01 g/mol), is a platinum based compound with a square planar geometry with two chlorine ligands. (B) Carboplatin (371.249 g/mol) has a bidentate dicarboxylate ligand in place of the two chloride ligands and (C) Pemetrexed disodium (471.37 g/mol) is a synthetic pyrimidine-based antifolate. Figure adapted from PubChem, the open chemistry database [91].

resistance in leukaemia cells. Alterations in proteins involved in the detoxification of drugs can also modulate resistance to chemotherapy, including overexpression of glutathione and glutathione S transferases, this was noted in cervical cancer cells that were resistant to doxorubicin, partially due to an upregulation of glutathione-related genes [92]. Changes in drug targets, such as topoisomerase gene mutations can also ascribe to resistance to some chemotherapeutics, as in non-small cell lung cancer, where point mutation in top1 led to enhanced chemoresistance [93]. The increase in DNA repair activity, including nucleotide excision repair (NER) is also thought to be means of resistance, especially to that of platinum containing agents. Rocha *et al.* [94] demonstrated the influence of NER in fibroblasts and skin biopsies from patients wherein increased NER-associated proteins increased resistance to mitoxantrone. Similarly, an amplified ability to tolerate drug damage has also been viewed in cisplatin chemoresistance, wherein the upregulation of pro-apoptotoic factors is imbalanced with the downregulation of some survival factors [95-98].

Chemotherapeutics are the standard and most common modalities by which to treat MPM [99, 100]. Platinum-based chemotherapy as well as antifolate-based chemotherapy is often employed in combination, due to well established improvements in treatment efficiency, with response rates significantly higher in dual treated MPM patients [82, 101]. However, the ability of cells to acquire and maintain resistance to chemotherapy in MPM remains both a clinical and scientific challenge. Therefore the investigation into the affected molecular pathways and how these pathways are modulated is of high importance to the improvement of prognosis and survival times in patients whom unfortunately, with this disease, have limited options.

1.4.4 *Targeted therapies*

Similarly to non-small cell lung cancer (NSCLC), the presence of epidermal growth factor overexpression in MPM suggested that the use of EGFR inhibitors such as gefitinib and erlontinib may provide a reduction in tumour burden within MPM. In contrast to NSCLC cohorts, unfortunately, there was no benefit to MPM patients [102, 103].

Immunotherapy with both anti-CTLA-4 (a protein receptor expressed on T cells) and anti–PD-1 (a cell surface receptor expressed on T cells), resulted in profound effects on solid tumours, with rapid tumour shrinkage, even after the antibody had been discontinued, implying the immune system within these patients had been altered [104]. Immune checkpoint blockade has shown promise as a targeted treatment in many different cancer types, including malignant melanoma, where anti-CTLA-4 treatment produced an impressive increase in survival. It has also been reported that in combination with anti-PD-1 there was a rapid and extensive regression of melanoma tumours [78, 104]. Immunotherapy is a promising an emerging treatment field in MPM, and recently a PDL-1 blocking drug, pembrolizumab, attained a 76% disease control rate [105]. The modification of the body's immune system to recognise cancer cells is currently of prominent interest within MPM research, but also in the landscape of cancer treatment as a whole.

1.5 Tumour biology

The pioneering principle to explicate the understanding of neoplastic disease, named the hallmarks of cancer, was developed by Hanahan and Weinberg in 2000 [106]. More

recently, in 2011 [107], the original 6 hallmarks noted in 2000 have been developed to incorporate 10 different aspects that contribute to cancer, as in Fig. 1.4.

1.5.1 *Proliferative signalling*

Actively proliferating cells are required for growth, function, embryogenesis and tumourigenesis [108]. In tumourigenesis, the absence of regulation for proliferative signals signifies that cancer cells are effectively in control of their own division. The production of growth factors by the cancer cells themselves can stimulate proliferation, as well as the cancer cells signalling normal neighbour cells in the supporting stroma, which may excrete growth factors that the cancer cell can utilise [107]. Among the contributing factors associated with proliferation, mutations in the PI3K/Akt/mTOR pathway can mean differences in the response to growth factors, which may result in changes to downstream effectors such as Akt and mTOR, both of which play vital roles in regulation of proliferation, the cell cycle and metabolism [108]. Investigation of the PI3K/Akt/mTOR pathway has been shown to be active in many MPM tumours; however Phase II trials of an mTOR inhibitor have concluded limited clinical activity [109].

1.5.2 *Tumour-led inflammation*

Immune cells are regularly found within the tumour microenvironment. Crucially, many reports detail that the presence of innate immune cells in the area of the tumour promotes inflammation and can release chemicals that influence many of the hallmarks of cancer [107]. Particularly in MPM, tumour associated inflammation is chronic, with many immune cells being associated with asbestos induced damage to mesothelial cells [110]. Within the lung, inhaled asbestos fibres cause an infiltration of macrophages into the pleura, this causes frustrated phagocytosis, wherein the macrophages attempt to phagocytose the fibres; these efforts fail and lead to reactive oxygen species (ROS)

generation and production of pro-inflammatory cytokines. Although the disease may be initiated by the immune system, there have been studies correlating the anti-tumour effects of CD8+, with higher CD8+ T cells linked with prolonged survival and reduced lymph node metastasis [110].

The inflammatory response outside of the direct tumour microenvironment can promote carcinogenesis in many ways. Inflammation associated tumour growth, EMT transition, angiogensis and metastasis have all been established in a variety of cancers [111]. In the context on MPM, it is well established that the immune system heavily contributes to the biogenesis and growth of MPM through ROS and cytokine production, as well as damage induced by the immune response in mesothelial cells [112].

1.5.3 *Evading immune destruction*

Avoidance of immune cell mediated destruction is fundamental to cancer development. The ability of cancer cells to 'hide' their maladies appears to be reliant upon several factors including the secretion of immune suppressive factors such as TGF-β, or recruitment of immunosuppressive inflammatory cells including T_{regs} and MDSCs, which can suppress the actions of cytotoxic lymphocytes [107]. Additionally, tumours elude observation by the down regulation of antigen processing machinery, which alters the MHC I pathway, consequentially leading to enhancement of cancer development due to the failure of cytotoxic T lymphocytes to identify target antigens on tumour cells [113]. In MPM, once asbestos has been phagocytosed by macrophages, there is a local and systemic affect on immunity, the influence of an altered immune response may facilitate the expression of antigens that aid the evasion of immune detection [114].
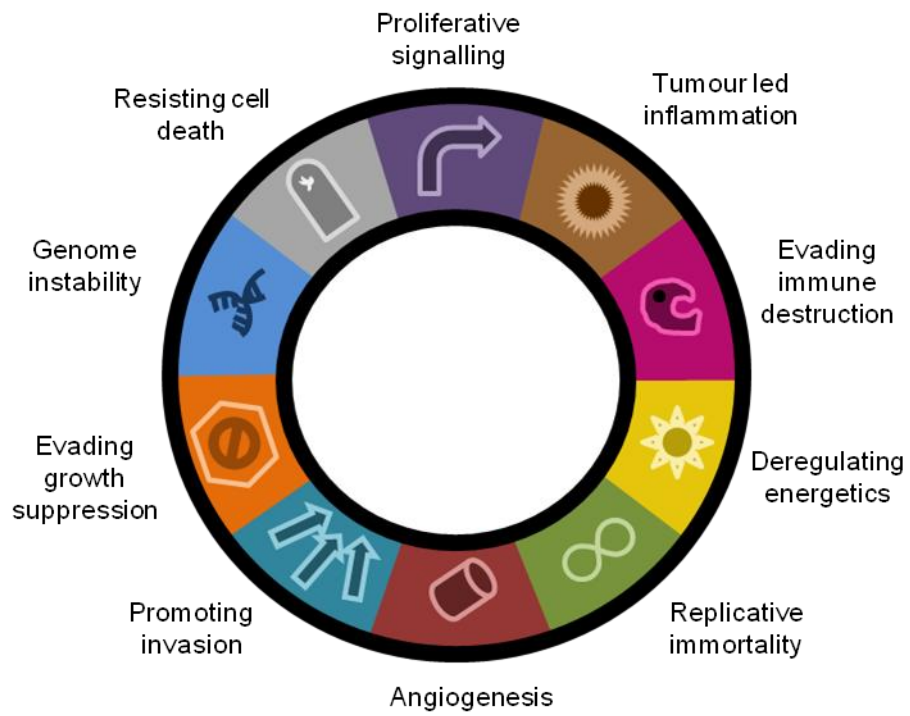
Figure 1.4 Hallmarks of cancer. Conceptual diagram illustrating the 10 revised hallmarks of cancer (from top, clockwise), maintaining proliferative signaling, encouraging tumour led inflammation, evading immune destruction, deregulating cellular energetic, allowing replicative immortality, promoting angiogenesis, promoting invasion and metastasis, evading growth suppression, genome instability, and resisting cell death. Figure adapted from Hanahan and Weinberg [107].

1.5.4 *Deregulating cellular energetics*

Alongside the differences in cellular proliferation in cancer cells, understandably, there needs to be a shift in cellular energetics to respond to the higher metabolic and proliferative state of the cancer cell. In a normal cell, aerobic respiration occurs through glucose processing to pyruvate via glycolysis, and eventually to carbon dioxide in the mitochondrial environment [107, 115]. In anaerobic conditions, glycolysis is primarily utilised, with little mitochondrial involvement. Glycolysis is a primitive method of energy metabolism, and is an inefficient pathway that yields 2 mol of ATP per mole of glucose, whereas 38 mol of ATP is generated in complete aerobic oxidation, also known as oxidative phosphorylation [115]. Interestingly, as Warburg discovered, in cancer, despite a relatively good oxygen supply to cells, the process of energy metabolism is largely performed through glycolysis. This seemingly is an unusual method for cells to produce ATP; however it has been hypothesised that the functional justification for this may relate to increased glycolysis allowing the diversion of intermediates into various cellular pathways, some of whom generate nucleosides and amino acids, which assists the biosynthesis of organelles and large molecules which are needed to create new daughter cells [107, 116]. In MPM, as in most cancer cells, an increase in anaerobic glycolysis is observed. Interestingly, in animal models, the use of a glycolysis inhibitor, 3-Bromopyruvate, led to significant benefits to survival when treated in combination with cisplatin [117].

1.5.5 *Replicative immortality*

The ability of cancer cells to evade the constraints of the normal limited number of cell cycles has long been investigated. Normally the barriers of proliferation are either senescence, where a cell is viable but unable to replicate, or crisis, which normally leads to cell death. Cancer cells have an innate change in telomerase expression, a polymerase

that functions to add telomere repeats, is highly expressed in immortalised cells [107, 118]. Normally, telomeres become progressively shorter as cells divide, however, the high expression of telomerase means the telomeric DNA is extended, effectively defying the typical shortening. Ensuing resistance to the barriers of proliferation ensures that cancer cells can persist in division. Telomerase antagonists have been trialled, including that of imetelstat, however the phase II trial conducted showed disappointing progression free survival in patients with NSCLC [119]. Despite the early disappointments of imetelstat, there are ongoing studies relating to other telomerase effecting drugs including targeted therapies, phytochemicals, gene therapies, small molecule inhibitors and other oligonucleotide inhibitors [118]. Au *et al.* [120] demonstrated that in MPM, telomere length maintenance was observed in 100% of MPM, concluding that MPM may benefit from second generation anti-telomerase therapy.

1.5.6 *Angiogenesis*

Nutrients and oxygen are commodities essential for both normal and cancerous cells. These are delivered via the vascular system within the body. The generation of new vasculature, normally only transient in an adult human, is turned 'on' in cancer cells [107]. The angiogenic switch is maintained by a variety of different progressive and suppressive factors including VEGF and TSP-1, these proteins are often dysregulated within cancer leading to problems with vasculature and potentially an increase in new vessels forming in the tumour and its microenvironment [107, 121]. VEGF gene expression can be modulated by several factors including posttranscriptional regulation [122], hypoxia [123] and oncogene signalling [124]. Interestingly, Chen *et al.* [125] reported the targeting of hypoxia-associated HIF-1α with its target VEGF led to a reduction in invasive and metastatic potential of liver tumours. Recently, in MPM, there

has been a trial investigating the targeting of proteins involved in tumour vasculature, however, as a single agent these have proven inefficient, as there were no partial or complete responses observed [126].

1.5.7 *Invasion and metastasis*

Invasion and metastasis are governed by alterations to cellular shape, attachment and role within an extracellular matrix [107]. Epithelial cells progress to a mesenchymal state in a process known as epithelial-mesenchymal transition (EMT), where cell to cell adhesion and apicobasal polarity is lost. EMT is regulated by a complex network of pathways involving the transcriptional regulators Snail, Slug, Twist and Zeb1 and Zeb2 [127]. Additionally, it has been established that the margins of some tumours can be seen to have a greater number of transitioned cells, suggesting a role for stimuli resulting from the tumour microenvironment. Furthermore, the loss or downregulation of adherins such as E-cadherin, which effectively hold cells together in a sheet like formation, are well established as regulators of invasion and are recognised as suppressors of this process. However, N-cadherin normally functions in migratory cells, often associated with embryogenesis, with the upregulation of this cadherin noted in many invasive cancers [107]. Clinically, often tumour sections are stained for the presence of epithelial markers such as E-cadherin and CK5, as well as mesenchymal markers such as vimentin, N-cadherin and C-cadherin to establish how invasive the tumour potentially is [128]. MPM tumours have demonstrated EMT activation, and it has recently been proposed that MPM histologies can be well characterised through specific gene expression patterns involving EMT markers [129].

Remarkably, it is noted that once cancer cells have initially progressed through EMT to invade surrounding tissue, they can reverse the process so that colonies of tumour cells can form in a new site. This plasticity can be observed with modulation of Frizzled-7,

which can suppress the mesenchymal state or enhance migratory ability of cancer cells depending upon on the context [130].

1.5.8 *Evading growth suppression*

Within the normal cellular environment growth is restrained by tumour suppressors such as RB and TP53. Malfunctioning RB expression can connote that cancer cells are effectively missing a "gatekeeper" of cell cycle progression [107]. TP53 is a complex suppressor which can trigger apoptosis or can halt cell cycle progression in the event of damage or other cellular issues. TP53 suppressor gene mutations are one of the most frequently observed abnormalities in cancer, with ~40% of patients being affected. Ivanova *et al.* [131] established that a novel tumour suppressor TUSC2 was downregulated in ~84% MPM tumours, and particularly interestingly, TUSC2-deficient mice were found to display an immuno-inflammatory driven phenotype that had a predisposition to cancer development. Wheler *et al.* [132] made a correlation between VEGF inhibition and TP53, in that patients with TP53 mutation respond better to anti-angiogenesis agents, again relaying the complexity of feedback loops within the hallmarks.

1.5.9 *Genome instability*

Mutant genomes that provide selective advantages to the cell enable the growth and expansion of the cancer. Multistep tumour progression is broadly characterised as a subset of clonal expansions, where each expansion event is driven by a further mutation. Mutations and corresponding dysregulation of so called caretakers of the genome, including TP53, effect the detection of DNA damage and DNA repair, and are well characterised in many cancers including MPM [107, 133]. In addition to TP53, the well known tumour suppressor BRCA2 has recently been verified as regulator of genome stability, the protein functions to repair DSB and has the ability to limit replication

stress, demonstrating its dysregulation being of great importance in regulation of damage [134].

Conversely there is another theory, developed in colorectal cancer, which takes a different perspective to the classical clonal expansion theory. Here, rather than a mutant by mutant basis expansion, the theory is that the early alterations accrue in a mixing of subclones, suggesting that some tumours may essentially be "born to be bad". The theory is known as the 'big bang model' of tumour growth, and is supported by analysis of colorectal tumours, wherein subclonal populations that comprise the intratumoral heterogeneity have been isolated to present early alteration rather than late clonal expansions [135].

1.5.10 *Resisting cell death*

Apoptosis, or programmed cell death, can be divided into two processes, the extrinsic and intrinsic pathways. Briefly, the extrinsic pathway obtains and processes extracellular death-inducing signals, and the intrinsic processes the intracellular signals. Within the context of cancer, the cell is able to avoid apoptosis despite multiple mutagenic events and dysregulation of key cellular pathways. Apoptosis regulatory proteins, such as Bcl-2, are well characterised as inhibitors of apoptosis and correspondingly suppress proapoptic proteins Bax and Bak [107, 136]. The dysregulation of Bcl-2 and the kinase mTOR are noted in many cancers, including MPM [137], however their regulation is noted to be controlled by a variety of posttranscriptional regulators or microRNA [138]. A recent study [139] has portrayed the importance between the interactions of the apoptosis associated regulators TP53, KRAS, BCL2, PLK1 and the microRNA-143. Additionally, microRNA-206 was noted to be downregulated in glioblastoma, whilst Bcl-2 was upregulated, as is often the case in tumours. Overexpression of microRNA-206 led to a reduction in Bcl-2 and reduced

proliferation; it was shown that microRNA-206 directly targeted Bcl-2, which led to suppression in the progression of glioblastoma *in vivo* [138].

1.6 MicroRNAs

1.6.1 *MiRNA biogenesis and functionality*

MicroRNAs (miRNA/s) are a species of the non-protein-coding RNA family, represented by short, single-stranded RNA approximately 18-22 nucleotides in length [140]. MiRNAs are regulators of gene expression at a post-transcriptional level [140]. In combination with an RNA-induced silencing complex (RISC), miRNA specifically target complementary messenger RNA (mRNA) transcripts, typically via imperfect complementary base pairing, and repress their translation, as in Fig. 1.5 [140, 141]. Although miRNAs are generally regarded as regulators of gene expression at the post-transcriptional level, newer miRNA functions are being identified. The role of miRNAs as bystanders and effectors within the epigenetic landscape of the cell is becoming apparent [142]. The complex relationship between miRNAs and epigenetics is uncovering a new understanding of cancer cell biology.

In 1993, Lee and colleagues identified the first miRNA in the worm *Caenorhabditis elegans* [143]. The lin-4 gene encodes two small non-protein-coding RNA transcripts approximately 22 and 61 nucleotides in length, and is essential for post-embryonic development in *C.elegans* [143]. The sequences of the RNA transcripts have complementarity to the 3' UTR (3' untranslated region) of the lin-14 mRNA, and bind to the mRNA via antisense RNA:RNA interactions, repressing mRNA translation, which results in downregulation of LIN-14 protein levels [143-145]. Several years later a second miRNA was identified in *C.elegans*. The let-7 gene encodes a 21 nucleotide

RNA transcript with complementarity to the 3' UTR of five heterochronic genes involved in normal development; lin-14, lin-28, lin-41, lin-42 and daf-127, [146]. Expression of lin-4 and let-7 are essential to post-embryonic development and developmental timing in *C.elegans*. In 2001, numerous small non-protein-coding RNAs were identified and were collectively termed miRNA [147, 148], and included 21 novel human miRNA; miR-1 to miR-339. Intensified research efforts identified additional miRNA in mammals, fish, worms, flies and plants [140]. To date ~1880 human miRNA precursor sequences have been identified, but the functional roles of many miRNA are still unknown.

The genes encoding miRNA are located throughout the genome as individual genes, polycistrons or within introns of pre-mRNA [140]. MiRNA genes located within the introns of pre-mRNA are ideally located for translational repression of their mRNA host [140]. Polycistronic miRNA genes encode a cluster of miRNA precursors, which are transcribed as a single transcript then processed into individual mature miRNA that may have related or non-related functions as in Fig. 1 [140]. MiRNA genes are transcribed in the nucleus by RNA polymerase II or III, most often RNA polymerase II, producing a single stranded RNA transcript 1-7 kb in length [149, 150] (Fig. 1.4).

This primary miRNA (pri-miRNA) transcript folds into an imperfect hairpin structure as a result of Watson-Crick base pairing and is processed in the nucleus by Drosha and DGCR [151, 152]. The 5'- and 3'-ends of the hairpin structure are asymmetrically cleaved producing a precursor-miRNA (pre-miRNA), which is exported to the cytoplasm via exportin-5 in the nuclear membrane [153]. In the cytoplasm, Dicer and TRBP cleave the loop structure off the hairpin, forming the miRNA duplex, termed miR-5p/-3p (formerly known as miRNA-miRNA*) [154, 155]. The relative thermodynamic stability of the strands determines which arm of the duplex will be
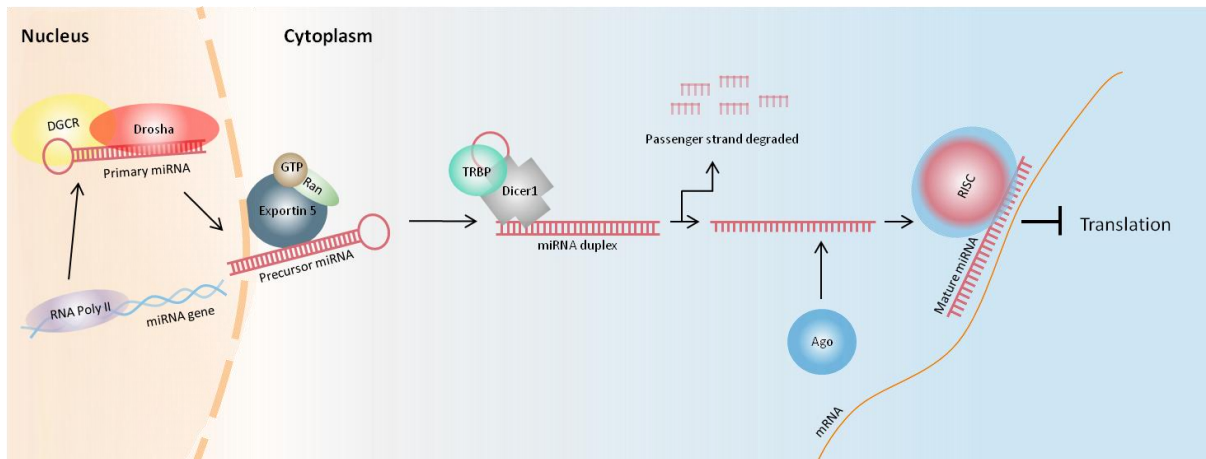
Figure 1.5 Biogenesis of miRNA. MiRNA genes are transcribed in the nucleus by RNA polymerase II to produce a long, single stranded RNA. The primary-miRNA (pri-miRNA) folds into a hairpin structure and is processed by Drosha and DGCR, the 5' and 3' ends of the hairpin structure are asymmetrically cleaved to produce the precursor-miRNA (pre-miRNA). The pre-miRNA is exported from the nucleus to the cytoplasm via exportin-5 and Ran-GTP on the nuclear membrane and is further processed in the cytoplasm by Dicer and TRBP. The loop of the hairpin structure is cleaved to produce the miRNA duplex. Within the miRNA duplex one arm is the passenger strand and the other is the mature miRNA. The passenger strand is degraded whilst the mature strand complexes with Argonaute proteins. The Ago proteins constitute the major functional element of the RNA induced silencing complex (RISC). The exposed bases of the mature miRNA bind to complementary mRNA via imperfect complementary base pairing. Subsequently, translation of the mRNA is repressed thereby downregulating gene expression at the protein level. Figure adapted from Gray *et al.*[156], originally devised and drawn by H Moody.

incorporated into the RISC as the mature miRNA, whilst the passenger strand (miRNA*) is subsequently degraded [154, 157]. Argonaute (Ago) proteins constitute the major functional element of the RISC. In mammals there are four Ago proteins, all of which are capable of repressing mRNA translation as part of the RISC, but only Ago2 is able to directly cleave the mRNA target [158]. The piwi-argonaute-zwille (PAZ) domain of the Ago protein binds the 2-nucleotide overhang at the 3' end of the mature miRNA strand [157]. The duplex then unwinds and the 5' end of the mature miRNA strand is bound by the Ago MID (middle) domain (Fig. 1.4) [140]. Exposed bases of the mature miRNA within the RISC bind to target mRNA sequences via complementary base pairing [154]. The mRNA may be regulated by an RNAi mechanism involving direct cleavage and degradation by the RISC, or the translation of the mRNA can be repressed, as is most frequently the case in mammals [140].

Within the target mRNA, the 'seed site' is a sequence of approximately seven nucleotides, and is essential for miRNA binding. These sequences are often highly conserved between species [159-161]. The mRNA seed site is frequently, but not exclusively, located in the 3'-UTR. The 'seed region' at the 5'-end of the miRNA binds the seed site in the mRNA [159, 162]. The 5'-UTR and coding sequence of the mRNA can also contain 'seed sites'; the miRNA RISC complex can potentially bind to any region of the mRNA [162, 163]. The general consensus is that the 3'-UTR is the most accessible region of the mRNA, as the RISC has less competition binding to the mRNA furthest away from the ribosome and translational machinery [140, 164, 165]. Furthermore, regulated target mRNA generally have longer 3'-UTR compared to ubiquitously expressed genes which tend to have shorter 3'-UTRs that are depleted of miRNA binding sites [166]. A mature miRNA within the RISC guides the complex towards complementary mRNA targets, stringent seed sites have perfect Watson-Crick base pairing between the mRNA and miRNA [164]. However, the RISC can also

tolerate G:U wobble and mismatch binding between the miRNA seed region and mRNA seed site [164]. In mammals, miRNA:mRNA binding is generally the result of imperfect complementary base pairing, while in contrast, near-perfect complementary base pairing is most common in plants [140]. The imperfect nature of miRNA target binding enables a single miRNA to target multiple mRNA targets, hence there is a degree of redundancy between miRNA, conversely a single mRNA can be targeted by multiple miRNA [167]. This variation and flexibility in miRNA:mRNA binding can make it difficult to predict mRNA targets using bioinformatic tools [164].

Once incorporated into the RISC, the mature miRNA downregulates target gene expression at the post-transcriptional level. There are a range of mechanisms by which this may occur and these are broadly divided into two categories: translational repression and mRNA degradation [168]. In metazoans mRNA targets are typically translationally repressed by their regulating miRNA; the imperfect base pairing between the miRNA and mRNA is generally associated with translational repression, as opposed to mRNA cleavage [140]. Experimental evidence in mammals has demonstrated that the levels of target mRNA can remain unchanged upon miRNA targeting, but a decrease in protein expression is observed (Fig. 1.4) [140, 143]. However, studies also demonstrate that miRNA binding to targets can frequently result in degradation, with the miRNA promoting translational quiescence, followed by degradation of the target as a secondary consequence. The exact mechanism of translational repression is unclear; the RISC complex may repress translation at the initiation or post-initiation stage, or both [168]. Alternatively, mRNA targets can be guided by the RISC into processing (P)-bodies, sequestering them from ribosomes and the translational machinery [157, 168]. Endonucleases can subsequently enter P-bodies and degrade the sequestered mRNA, or these mRNA can later be released back into the cytoplasm for translation if protein levels decrease below the requirements of the cell, thus demonstrating miRNA-

mediated repression is reversible [169, 170]. Near-perfect base pairing between the miRNA:mRNA is associated with direct cleavage of the mRNA by the RISC [140]. MiRNA are also destabilised by the gradual shortening of the poly A tail, resulting in mRNA degradation by progressive decay catalysed by the exosome or degradation by endonucleases [171].

Generally, miRNA are recognised as functioning to downregulate gene expression via translational repression. However, there is evidence of further functional roles of miRNA, including links between miRNA and epigenetics [142]. The expression of miRNA genes is regulated by their epigenetic status and miRNA are known to have specific epigenetic functions [142]. Although miRNA are processed and function in the cytoplasm there is evidence that mature miRNA are associated with Ago proteins found in the nucleus [172]. The miRNA in the nucleus are reported to have epigenetic functions, such as modulating mRNA splicing and targeting gene promoters to activate or repress transcription [172, 173].

MiRNAs account for approximately 1% of the genome and are estimated to regulate ~30% of genes [140]. The imperfect nature of miRNA target binding enables a single miRNA to target multiple mRNA targets, therefore miRNA essentially regulate all cellular pathways. As different cell types have specialised functions and express a specific set of genes related to the function of the cell, this is reflected in tissue-specific miRNA expression profiles [174]. Disrupting the highly complex miRNA regulatory network within the cell can induce abnormal cell behaviour and disease initiation or progression [175], and as such, dysregulated miRNA expression is a common feature in human diseases [176, 177], especially cancer [178].

1.6.2 *MiRNAs in cancer biology*

MiRNAs are involved in all pathways and cellular processes within the cell, hence it is not surprising that miRNA dysregulation is viewed as a fundamental feature of cancer and is considered instrumental in the acquisition of the hallmarks of cancer; such as invasion, angiogenesis and evasion of apoptosis. Tumours most often have a reduced level of mature miRNA, due to the loss of genetic material, alterations to the machinery associated with biogenesis, and epigenetic silencing [179]. It is proposed that cancer-associated miRNAs either have an oncogenic or tumour suppressive activity [180], as detailed in Table 1.3. Again, this relates to tissue type and location of the cancer. The link between miRNA and cancer was first established over a decade ago, when

Calin *et al.* [181] reported the deletion or down-regulation of miR-15a and miR-16-1 encoded at the 13q14 loci in a majority of B-cell chronic lymphocytic leukaemia cases. The same group later reported that the alterations in expression of miRNA in various cancers could be critical to the understanding of cancer pathophysiology [182]. Interestingly, Calin *et al.* [182] revealed that many miRNA are encoded at fragile sites and within common breakpoint regions in the genome, thus increasing their susceptibility to mutation and deletion.

As miRNA play a significant role in the regulation of many aspects of cellular machinery, it has been suggested that the deregulation of these small non-coding molecules could profoundly and substantially affect the cell and its progression through the cell cycle. It is considered that during carcinogenesis, miRNA become either upregulated or downregulated; however, this can vary depending on the tissue of origin. The frequently altered miRNA, miR-31, is disrupted in opposing directions in a wide

Table 1.3 MicroRNA expression in MPM. MicroRNAs that have known functions with MPM (adapted from Reid [183]).

MicroRNA	Expression change in MPM vs. normal	Function in disease	Disease outcome	Reference
Let-7a	Up	Inhibits RAS	Attenuates tumour growth	Khodayari *et al.* [184]
miR-1	Down	Inhibits growth	ND	Xu *et al.* [185]
miR-15	Down	Inhibits growth	Inhibition of tumour growth with miRNA restoration	Reid *et al.* [186]
miR-16	Down	Downregulates cell cycle and anti-apoptotic genes	Sensitisation to pemetrexed and gemcitabine	Reid *et al.* [186]
miR-29c-5p	Down	Inhibits growth and migration	Stratifies patients by time to progression post surgery	Pass *et al.* [187]
miR-31	Down/Up	Inhibits growth and migration/unclear, associated with sarcomatoid subtype	Downregulation leads to pro-tumourigenesis. Upregulation in aggressive subtype.	Ivanov *et al.* [188] Matsumoto *et al.* [189]
miR-34b/c	Down	Inhibits growth	Restoration of miRNA leads to increased radiosensitivity	Maki *et al.* [190]
miR-126	Down	Induces autophagy	Failure of tumour to progress with miRNA restoration	Tomasetti *et al.* [191]
miR-145	Down	Inhibits migration, accelerated senescence	Restoration increased pemetrexed sensitivity	Cioce *et al.* [192]
miR-205	Down	Affects migration	Mesenchymal phenotype, more aggressive tumour	Fassina *et al.* [193]

ND: Not Detailed

range of tumour types [194], for example, in mesothelioma it has been established that miR-31 is significantly downregulated, which effects the expression of PPP6C, a pro-survival phosphatase [188]. Conversely, the same miRNA within the colorectal cancer microenvironment is highly upregulated across all stages of the disease [195].

A cluster of miRNA associated with tumour formation was discovered by He *et al.* [196]. The multiple component miRNA polycistron miR-17~92 was found to be amplified in B-cell lymphomas in both cell line studies and samples of tumour tissue [196]. Further investigation by Suarez *et al.* [197] concluded that the cluster carries out pleiotropic functions and modifies postnatal angiogenesis in response to vascular factors, such as vascular endothelial growth factor (VEGF). The cluster has also been shown to promote carcinogenesis by altering cell cycle phase distribution, as in Sylvestre *et al.* [198]. MiR-17~92 is activated by members of the E2F family, which stimulate a number of S phase genes, including thymidine kinase. E2F1, E2F2, and E2F3 are all modulated by the miR-17~92 cluster, via their 3'-UTR binding sites. Additionally, overexpression of a member of the cluster, miR-20a, decreased apoptosis in a prostate cancer cell line whilst the inhibition of miR-20a produced an increase in cell death. The miR-20a anti-apoptotic properties may elucidate some of the oncogenic capabilities of the miR-17-92 cluster. The study suggested that the auto-regulation between E2F1-3 and miR-20a may contribute to the regulation of apoptotic events and proliferation [198].

Recently, Gao *et al.* [199] investigated miR-184 for regulatory functions within hepatocellular carcinoma (HCC). It had previously been established that miR-122 had a significant role within HCC [200]; however, miR-184 was novel in the research into both the development and onset of HCC. Using the inositol polyphosphate phosphatase-like 1 (INPPL1) insulin regulator as a recognized target, miR-184 was found to be

central in HCC cell proliferative activity, and that silencing of miR-184 leads to the overexpression of INPPL1. The miRNA was also allied to the inhibition of caspase-3 and -7, suggesting a role in the evasion of apoptosis [199].

In pancreatic cancer, miR-106a is highly expressed in tumour tissue and in four cell lines, one of which, SW-1990, is a highly invasive line [201]. Interestingly, results have indicated that the highest expression of miR-106a was present in the most invasive line. In cells transfected with a miR-106a mimic, tumour cell growth was stimulated, whereas a miR-106a inhibitor decreased cell viability [201]. Mace *et al.* [202] investigated miRNA in relation to pancreatic tumour cells under hypoxia; findings suggested that miR-21 was induced via hypoxia inducible factor (HIF)-1α upregulation, and that miR-21 overexpression promoted the evasion of apoptosis in a hypoxic environment.

Let-7a, a tumour suppressor miRNA, is lost in malignant melanoma, where it has been demonstrated to regulate integrin β3 expression [203]. The integrin β3 subunit αvβ3 family of adhesion receptors is involved in the transition from dysplastic nevi to tumourigenic melanomas, and overexpression has been linked to increased cellular motility [204]. MiR-143 and miR-145, located at the 5q33 fragile site represent tumour suppressive miRNA [205]. The miR-143-145 cluster is downregulated in many cancers, suggesting a 'protective' role for the miRNA. MiR-143 and miR-145 are recurrently co-ordinately downregulated in endometrial cancer, with a connection made between downregulation of miR-143/-145 and overexpression of DNA methyltransferase (DNMT) 3B [206]. The DNMT group contribute to the coordination of mRNA expression in normal tissues and overexpression in many tumours [207]. Additionally, miR-29 has been identified to target DNMT2A and DNMT3B, which have been found to be upregulated in lung carcinoma [208]. The miR-29 family has been identified as

being upregulated in induced and replicative senescence, and functions to inhibit DNA synthesis and repress the B-Myb oncogene in combination with Rb; this may be beneficial as the tumorigenic cell may become senescent as a result [209, 210].

The well-established hallmarks of cancer are integrally linked with miRNA expression, and indeed hundreds of miRNAs have been found to be novel regulators of these distinctive carcinogenic hallmarks. MiR-519 has demonstrated the ability to inhibit proliferation in cervical, colon, and ovarian cell lines, through one of its targets, HuR, an RNA binding protein [211]. Furthermore, the RhoA pathway can be modulated through miR-146a in prostate cancer [212]. This results in the downregulation of the serine/threonine protein kinase ROCK1, leading to dysregulation of the actin cytoskeleton [212], and alterations in cellular motility. The expression of miR-34a correlates with p53 expression, and so can be termed a regulator of apoptosis [213]. The cluster of miR-290 can directly regulate the DNMT expression in Dicer1-null cells, which indirectly affects telomere integrity and length, thus implying significance in the regulation of replicative potential [214]. An example relating to angiogenesis regulation is that of miR-378, which binds to 3'-UTR region of VEGF, which promotes neovascularisation [215]. Other miRNAs, such as miR-10b and miR-23a, are implicated in the regulation of invasion and genomic stability, respectively [216].

Biomarkers can be defined as diagnostic, prognostic and predictive, with some being candidate for therapeutic targeting. Diagnostic biomarkers aid the identification of a disease, prognostic biomarkers helped estimate the likely course of the disease, and predictive biomarkers suggest a possible treatment based on whether the disease is likely to respond [217]. MiRNAs are novel therapeutic targets and promising cancer biomarkers with potential applications in diagnostics, prognostic, tumour staging, patient response to treatment, determination of developmental lineages and clinical

subtypes, all of which are important to stratify patients into the best treatment or management of disease for the optimal quality of life [218], as in Table 1.4.

Interestingly, miRNA treatment in the form of a nucleic acid-modified DNA phosphorothioate antisense oligonucleotide has already entered human clinical trials in treatment of disease, specifically viral infection. MiR-122, an abundant liver-expressed miRNA, essential for the replication of the hepatitis C virus (HCV), is sequestered by the oligonucleotide and is bound in a duplex that inhibits its function [219]. Results thus far have shown promise, with long-standing dose-dependent decreases in viral titre levels without evidence of acquired resistance [219].

In summary thus far, miRNA function as regulators of gene expression in all cellular pathways, and aberrant miRNA expression is associated with cancer initiation, promotion and progression. MiRNAs are globally downregulated in cancer and tissue-specific expression profiles have been determined for several cancer types. However, the functional roles of many miRNAs are yet to be determined. MiRNAs are involved in all cancer-associated pathways and the acquisition of the hallmarks of cancer, and thus

represent promising cancer biomarkers and in translational therapeutics, which will be discussed later. More specifically, miRNA may play a fundamental role in the epigenetic changes observed within carcinogenesis, and understanding the dysregulation of these small, non-coding molecules could be imperative in our understanding of cancer biology [220].

Table 1.4 MiRNA associated with MPM. MiRNA that have been identified as potential biomarkers, adapted from Sheff *et al.* [221]

Diagnostic	Prognostic	Therapeutic
miR-30c	miR-17-5p	let-7
miR-126	miR-29c*	miR-7
miR-141	miR-30c	miR-17-92 cluster
miR-192	miR-299-3p	miR-21
miR-193a-3p	miR-301	miR-30c
miR-200a/b/c	miR-379	miR-31
miR-429	miR-455-3p	miR-34a

1.6.3 *Inhibition of miRNAs in treatment*

The overexpression of miRNAs that target tumour suppressor genes in cancer led to the development of the term oncomiR [222]. In order to efficiently target the overrepresented miRNA, many therapeutic strategies have been developed which are sequence based inhibitors of the overexpressed miRNA. The specific inhibitors can potentiate the cleavage or sequestering of the target miRNA into P-bodies. Broadly, miRNA inhibitors can be classified into antagomiR or decoys known as miRNA sponges [223].

Direct miRNA inhibitors are essentially antisense oligonucleotides that are complimentary to the mature miRNA target. Often the oligonucelotide based inhibitors are administered without delivery vehicle *in vivo*, although conjugation may be used to improve the uptake of the inhibitor in tumours [224]. MiR-21 is commonly upregulated in a range of cancer types and it has been linked to inhibition of a range of tumour suppressor genes [225] and importantly suppression of drug resistance [226]. Several studies have identified that the administration of miR-21 inhibitors of differing types using various courses of administration in xenograft models can provide success. Zhou *et al.* [227] utilised direct intratumoral injection of antimiR-21 and was able to inhibit growth of glioblastoma [227], multiple myeloma [228] and tongue squamous cell carcinoma [229], which sequentially effected the expression of miR-21 targets. Furthermore, miR-21 antimiR has been administered via intraperitoneal injection in mice with subcutaneous breast or colon cancer xenografts, leading to inhibition of tumour growth [230].

Currently, one of the leading antimiR is antimiR-122, which targets and suppresses miR-122 in the liver. MiR-122 is the most abundantly expressed miRNA within the liver environment, and is essential for hepatitis C virus replication [219]. Utilising

different administration methodologies [231, 232], it was astonishingly found that HCV infection could be decreased by up to 300 fold with the administration of antimiR-122 [231], demonstrating the power behind modulation of a single miRNA.

1.6.4 *Replacement of miRNAs in treatment*

In addition to miRNAs that target tumour suppressors, miRNAs themselves can be tumour suppressors, thus meaning the downregulation of these miRNA can lead to cancer progression. Primarily, the synthetic reintroduction or overexpression of tumour suppressing miRNA has been facilitated by miRNA plasmid or lentiviral based expression vectors, although miRNA mimics are also utilised [223]. Similar approaches to that of inhibition can be utilised in order to administer overexpression of suppressor miRNAs, however there have been developments in therapeutic delivery that involve the use of nanoparticles and lipid based systems to facilitate the delivery of tumour suppressive miRNA, such as the miR-34 family [233] or miR-15/16 [223, 234].

Interestingly, Reid *et al.* [235] developed TargomiRs, a nanocell based delivery system to transport a miR-15/107 sequence that targets the tumour due to the nanocell being coated in anti-EGFR antibody in non small cell lung cancer and MPM patients. The research entered Phase I trial in MPM in 2014, named MesomiR-1, and has thus far isolated five out of six patients benefitting through disease control, with acceptable tolerance for the drug.

1.6.5 *MiRNAs in MPM*

Many studies have indicated, as in other cancers, that miRNA play pivotal roles in the onset and progression of MPM cancer, making them possible targets for therapy, or indeed markers of prognosis [183]. Aberrant miRNA expression in MPM is the subject

of over 400 studies and reviews. Balatti *et al.* [236] observed dysregulation of many miRNA, including miR-214 which has been associated with targeting PTEN, leading to increased Akt activity and promoted cell survival. Williams *et al.* [237] observed that the transient transfection miR-193a-3p using a mimic-based system induced apoptosis and inhibited MPM growth *in vitro*. When this was followed up *in vivo* with the use of minicells, the mimic inhibited MPM xenograft growth. Tomasetti *et al.* [191] reported that miR-126 expression in mesothelioma induces autophagic flux, and that mice injected with miR-126 expressing cells failed to progress in tumour growth possibly suggesting that the relative increase in autophagy could have a protective role in mesothelioma.

Furthermore, Ivanov *et al.* [188] reported a general downregulation of the miRNA miR-31 in MPM; it was observed that the re-introduction of miR-31 inhibited factors involved in cell cycle progression and DNA repair. However, in contrast to Ivanov *et al.* [188], a more recent study by Matsumoto *et al.* [189] correlated miR-31 downregulation with increased long term survival in patients, with the proposition that miR-31 acts as a tumour suppressor within MPM. Interestingly, the research indicated a significant negative relationship between miR-31 expression and survival time in an aggressive sarcomatoid subtype MPM patient cohort. The existing correlation between miR-31 dysregulation in differing MPM subtypes remains unclear, however increased expression in the sarcomtoid subtype within patient derived samples may elucidate that miR-31 expression could be utilised as potentially a predictive or prognostic biomarker, with potential to further investigate the miRNA in terms of therapeutic targeting.

Quinn *et al.* [238] comprehensively reviewed the role of miRNAs within MPM, with particular reference to the dysregulation of miR-31, due to it being encoded in the frequently lost 9p21.3 chromosomal region.

1.7 Project rationale

Regrettably, patients who present with MPM in the clinic are either inherently resistant, or become resistant to the first line of treatment, chemotherapeutics. Currently, there is a need to understand the functionality of this resistance, not only to identify why cells are chemoresistant, but also to develop clinically viable routes by which sensitivity can be enhanced. Additionally, the ability of patients to be stratified into relatively poor or good responders to chemotherapy pre-treatment would be of great benefit to reduce the treatment burden on patients who may benefit more from alternative therapies.

MiRNAs are pivotal regulators of many cancer pathways due to their ability to target hundreds of different mRNA species. Their pleiotropic nature connotes that many miRNAs are closely associated with resistance to treatment modalities. Particularly in MPM, the miRNA miR-31 is encoded on a commonly deleted fragile site, 9p21.3. The dysregulation of miR-31 is currently of ambiguous conclusion in MPM, there are studies correlating positive and negative influences. MiR-31 has been associated with re-sensitisation to radiation therapy in OAC; therefore, the understanding and exploration of miR-31 in the context of MPM chemosensitivity may reveal a possible therapeutic target or potentiate a biomarker for response to chemotherapy treatment.

1.7.1 *Project hypothesis*

MiR-31 is established as a modifier of therapeutic response. Thus, it is hypothesised that manipulation of miR-31 *in vitro* confers a modulatory effect on chemosensitivity in MPM.

The objectives for the study were to investigate miR-31 in the context of response to therapy within an *in vitro* model, by assessing whether the miRNA had potential to be

utilised as a predictive biomarker, and also, potentially, a target for therapeutics to enhance cellular sensitivity to existing chemotherapy in refractory MPM.

The overall aims of the investigation are therefore 1) to modulate miR-31 expression in MPM cells in order to assess the affects, if any, on MPM sensitivity to therapy, 2) to explore the mechanism behind this alteration in chemosensitivity in order to elucidate potential pathways modified by miR-31 dysregulation in MPM.

Chapter 2:

Material and methods

2.1 Reagents and materials

Chemicals and consumables were purchased from Fisher Scientific UK, unless otherwise specified. To measure weight, an OHAUS Explorer analytical balance (OHAUS, Switzerland) was used within a 4 decimal place accuracy range, and an OHAUS Scout Pro balance was used to measure weights up to 2 decimal places. Fluidic volumes over 25 mL were measured using graduated cylinders, while volumes over 1 mL up to 25 mL were measured using serological pipettes and an electronic pipette controller (Pipetboy Integra, Switzerland). Volumes less than or equal to 1 mL were measured using calibrated adjustable volume pipettes (Pipetman Gilson, USA).

2.1.1 *Cytotoxic drug preparation*

Cisplatin [*cis*-Dichlorodiamineplatinum(II)] was purchased from Acros Organics (Thermo Fisher Scientific, Geel, Belgium) and solubilised in sterile 1X phosphate buffered saline (PBS) (Lonza, Basel, Switzerland) at a stock concentration of 5 mM. Carboplatin [cis-diammine(1,1-cyclobutanedicarboxylato)platinum(II)] was purchased from Selleckchem (Stratech, Newmarket, UK) and solubilised in sterile PBS (Lonza) at a stock concentration of 10 mM. The chemotherapeutic 5-Flurouracil (5-FU) was solubilised in sterile dimethyl sulfoxide (DMSO) and prepared at a stock concentration of 5 mM. Aliquots were stored at -20°C and thawed at 37°C immediately prior to use to ensure all drugs were in solution.

2.1.2 *Radiation treatment*

Irradiation was performed with a RS-2000 Pro biological research X-ray irradiator (Rad Source Technologies, Georgia, USA) at a dose rate of 1.87 Gy/min. Detailed dosimetry and warm up cycles were performed regularly to ensure the irradiated dose

was accurate. The irradiator was validated and calibrated to National Physical Laboratory standards.

2.2 Cell lines

The MPM cell lines NCI-H2452, P31, MSTO-211H and NCI-H2052 were kind gifts from Dr Steven Gray (Department of Oncology and Clinical Medicine, Institute of Molecular Medicine, Trinity Sciences Health Centre, St James's Hospital, Dublin, Ireland). All cell lines were confirmed as mycoplasma negative, as described in section 2.2.5.

2.2.1 *Tissue culture*

Cell lines were maintained in RPMI-1640 medium (Lonza) supplemented with 10% heat inactivated foetal bovine serum (HyClone, UT, USA), 1% Penicillin/Streptomycin (Lonza) and 1% Glutamax (Gibco, Paisley, UK). All cell lines were cultured in supplemented RPMI-1640, henceforth termed complete medium. Cell culture reagents were stored at 4°C and warmed to 37°C in a water bath with armor beads (Lab Armor, USA) for at least 1 h prior to use. Cells were maintained in 95% humidified incubators at 37°C, 5% CO_2 (Nuaire IR Direct Heat CO_2 Incubator, Red Laboratory Technology, USA). Aseptic technique was adopted for all procedures involving cells. Tissue culture work was carried out in Faster BH-EN 2004 laminar air flow units (Faster S.r.l, Italy). Before entering the laminar flow hood, the area was thoroughly cleaned with 1% Virusolve (Amity International Healthcare, UK), followed by 70% Ethanol (EtOH). All reagents and equipment were sterilised prior to entering the laminar air flow unit with 70% EtOH. Spent reagents and materials were decontaminated in Presept sterilising solution for at least 20 min out of the laminar flow area, prior to flushing down the sink with copious amounts of water.

2.2.2 *Subculturing*

All cell cultures were maintained in an exponential growth phase in T75 cm^2 tissue culture flasks (Greiner Bio-One, UK), and subcultured at 70-85% confluency. Spent media was discarded to waste (containing decontaminating Presept (Asya Medica, Philippines)) and cells were briefly washed with 5-10 mL sterile 1X PBS. Cells were detached from the plastic surface of the flask using 1 mL trypsin-EDTA (Lonza). Cells were incubated with trypsin-EDTA for 5 min at 37°C to promote detachment. Cells were checked for complete detachment with the aid of light microscopy (Olympus, MA, USA). Trypsin-EDTA was inactivated with 4 mL complete medium. Cell suspension was split into fresh T75 cm^2 flasks at a varying ratio of 1:2-1:12, depending upon experimental needs. Further complete medium was added to each flask to ensure a total volume of 20 mL. Cells were passaged approximately 2-3 times weekly, with passage numbers recorded.

2.2.3 *Frozen cell stocks*

All cell lines were regularly frozen and stored in liquid nitrogen. Regular freezing ensured passage numbers were kept low. In order to freeze down cells, confluent (80%) T75 cm^2 flasks were 1X PBS washed, incubated with Trypsin-EDTA and inactivated with complete medium, as described in section 2.2.2. Cells were then collected in 50 mL sterile tubes and centrifuged for 5 min at $300 \times g$ to pellet cells. Spent media was discarded to waste. Cells were then resuspended in 1.5 mL freezing media (90% FBS, 10% DMSO), drop wise. Cryovials (Sarstedt, Germany) were labelled and 500 μL of the cell freeze mix suspension added to each 2 mL cryovial. Cell suspensions were stored at -80°C for a period of at least 48 h in a Mr Frosty freezing container, which ensures gentle lowering of cellular temperature at a rate of 1 °C/min. After equilibrating at -80°C, cryovials were moved into liquid nitrogen

dewar for long term storage. A liquid nitrogen stock spreadsheet containing cell line name, date and passage number was used to log each vial within the dewar.

Cells were reconstituted by removal from liquid nitrogen, and quick thawing to 37°C. Defrosted suspension was added to a labelled T25 cm^2 tissue culture flask, and warm complete media added to a total of 10 mL. Cells were then immediately incubated at 37ºC, 5% CO_2. After 24 h post defrosting, cells were subjected to a PBS wash and complete media was refreshed on cells to remove any residual DMSO.

2.2.4 Cell counting

Cells were subjected to a PBS wash, Trypsin-EDTA and concurrent inactivation. In order to pellet cells, cells were centrifuged for 5 min at $300 \times g$. Spent media was disposed into waste. Cells were then resuspended in 1 mL warm complete media and thoroughly mixed with pipetting. Cells were either enumerated at a 1:2 dilution or a 1:10 dilution. For example, 20 µL of cell suspension (well mixed) was added to a 1.5 mL Eppendorf tube containing 180 µL of Trypan blue (Gibco). The Trypan blue cell solution was mixed thoroughly and 9 µL loaded onto a haemocytometer (Superior Marienfeld, Germany) covered with a glass cover slip. The haemocytomter was checked for sufficient loading, if any air bubbles had resulted, the process was repeated after washing the haemocytometer. To assess the viable cell count, the haemocytometer was put under the inverted microscope (Olympus CKX41, 10X objective). Cells that remained viable appeared white due to exclusion of the dye from the cell membrane interface, whereas cells that had the membrane disrupted, therefore non-viable, were stained dark blue and not counted. Cells lying in the four large corners of the haemocytometer were enumerated. Cells lying on the right or bottom edge of the squares were not counted to avoid repeat counting of the same cell. To ensure reliable and rapid counting, a tally counter was used. Once the total

number of cells in the large corners had been counted, the total number of cells was divided by 4, and then multiplied by the dilution factor (2 or 10), then multiplied by 10^4 to achieve a total number of cells/mL.

2.2.5 *Mycoplasma testing*

Cells were subjected to routine mycoplasma testing approximately every 3 months. Mycoplasma testing was carried out with the MycoAlert Mycoplasma Detection Kit from Lonza. Briefly, 1 mL of spent medium was taken from an actively culturing flask and centrifuged for 5 min at $300 \times g$. An aliquot (100 µL) of the supernatant was pipetted in triplicate into a white-walled 96-well plate. A 100 µL volume of MycoAlert Reagent was added to each well containing supernatant and incubated at room temperature for 5 min. Luminescence was then measured with 1000 ms integration time (Fluoroscan Ascent FL, ThermoScientific, UK). Following the initial reading, 100 µL of MycoAlert Substrate was added to each reagent containing wells; this was then incubated at room temperature for 10 min. Luminescence was then again measured with 1000 ms integration time. In order to determine mycoplasma status, the second reading was divided by the first reading to give a ratio. Where the ratio was less than 0.9, the sample was considered negative; where the value was more than 1.2 cells would have been identified as mycoplasma positive.

2.3 Manipulation of gene expression

2.3.1 *MiRNA plasmids*

Overexpression and suppression of specific miRNA was achieved by transfection with miRNA plasmids from Origene (MD, USA) and System BioSciences (CA,

USA) respectively (appendix 1). Plasmids were CMV promoter driven, and included a bacterial resistance gene (ampicillin or kanamycin) and a GFP reporter sequence. The miR-31 overexpression plasmid (MI0000089) encoded a miRNA precursor, which was then processed to the mature miRNA by the normal cellular machinery. The vector control plasmid (PCMVMIR) was exactly the same as the miR-31 overexpression, aside from the coding miR-31 sequence, which in the control was a scrambled sequence. The miR-31 suppression (zip-down) plasmid (MZIP31-PA-1), produced an antisense oligonucleotide to the miR-31 sequence, which physically binds miR-31 and irreversibly inhibits its activity. The vector control plasmid (MZIP000-PA-1) was exactly the same as the miR-31 suppressive, aside from the coding miR-31 suppressing sequence, which in the control was a scrambled sequence. The overexpression plasmid and its vector control equivalent had a mammalian selection marker, conferring geneticin (G418) resistance. The suppression (zip) plasmid and its equivalent vector control had a mammalian selection marker encoding puromycin resistance.

The NCI-H2452 miR-31-null cell line and the P31 endogenous miR-31-expressing cell lines were transfected with miR-31-overexpressing or miR-31-suppressing plasmids, respectively. Cells were transfected and seeded into 100 mm^2 tissue culture dishes at a density of 1×10^6 per dish and left to adhere overnight. Spent medium was removed, and dishes washed with PBS, following which Opti-MEM low nutrient medium (10 mL) was added to each dish. Transfections were performed using diluted Lipofectamine 2000 reagent (9 µL in 150 µL Opti-MEM). A total of 14 µg plasmid vector, and vector control equivalents, were used to transfect the miR-31 overexpression (for NCI-H2452 cell line) or suppression plasmid (for P31 cell line), diluted in 700 µL Opti-MEM. The transfected NCI-H2452 cell line were kept under 500 µg/ml G418 selection for 3 weeks. Zip-miR-31 plasmid and Zip vector control

were stably transfected into the P31 cell line and maintained under 3 µg/ml puromycin selection for 10 days. Concentrations of G418 and puromycin were determined by literature based analysis. Both plasmids encoded a GFP reporter, which was regularly checked for expression via fluorescence microscopy and Western blot analysis. Transfected cell lines were maintained as mixed populations.

2.3.2 *Bacterial transformation*

One Shot TOP10 (Thermo Fisher, ThermoScientific, UK) or XL-10 Gold (Agilent, CA, USA) chemically competent *E.coli* were used to facilitate the production of miRNA plasmid stocks. On ice, 2 µL of each plasmid was added to thawed *E.coli* species. The bacterial suspension was then heat shocked at 42 °C for 30 s, then put straight onto ice for 2 min. Using aseptic technique, the culture was added to 5 mL LB broth (Fast-media *E.coli* LB broth, InvivoGen, USA) in a 50 mL tube, incubated for 4-6 h at 30°C, 220 rpm. The culture was checked for turbidity, indicating bacterial growth. The entirety of the broth was then poured into 200 mL LB ampicillin or kanamycin selection medium, which was then incubated at 30°C, 220 rpm overnight. Following incubation, the *E.coli* were collected via centfriguation at $6000 \times g$ for 15 min. Pellets were either immediately extracted for purified plasmid, or frozen at -20°C for up to 4 months.

2.3.3 *Plasmid extraction*

Pellets of bacteria previously transformed, as in section 2.3.1, were defrosted on ice and extracted using the NuceloBond Xtra Midi Plus Kit (Macherey-Nagel, UK). Cell pellets were resuspended in 8 mL RNase A resuspension buffer, with the addition of 8 mL lysis buffer. The solution was gently mixed via inversion and incubated at room temperature for 5 min to ensure optimal bacterial lysis. During incubation,

column filters were equilibrated with 12 mL equilibration buffer. After incubation, 8 mL neutralisation buffer was added to the cell suspension and inverted to allow mixing. The suspension was then applied to the equilibrated column filter. The column filter strained the suspension of precipitate, whilst the plasmid DNA was isolated via binding to the silica based resin at the bottom of the column, which was positively charged, ensuring the negatively charged plasmid DNA was bound with high specificity. The cell suspension was allowed to fully flow through the filter, by suspending the filter over the column with a clamp and stand. The filter was then washed with 5 mL equilibration buffer, after which it was disposed to waste. To ensure purity of plasmid DNA, the column was washed with 8 mL wash buffer. Elution of the plasmid DNA was then achieved by the addition of 5 mL elution buffer, to precipitate the plasmid DNA from the solution, 1.5 mL isopropanol was added and vortexed (Stuart SA7 Vortex, UK) thoroughly. The plasmid solution was added to a fresh column and washed with 100% EtOH, and elution achieved with 250 μL 5 mM Tris-HCl pH 8.5. The DNA concentration of the final product was measured with a NanoDrop ND-100 (Thermo-Scientific). The measuring pedestal was gently cleaned with deionised water and blanked with the appropriate reference. The pedestal was loaded with 2 uL of plasmid product and a reading taken, and concentration measured in ng/mL. Purified plasmid DNA was then stored in aliquots to at -20 °C. Further details of the Nanodrop ND-100 are detailed in section 2.4.2.

2.3.4 *ABCB9 plasmids*

Overexpression of the protein ABCB9 was achieved by transfection with ABCB9 encoding plasmids from GeneCopoeia (MD, USA) (appendix 1). Plasmids were CMV promoter driven, and included a bacterial resistance gene (ampicillin). The ABCB9 overexpression plasmid (EX-T8156-M68) and its empty vector control

equivalent (EX-NEG-M68) encoded a puromycin resistance gene for stable mammalian selection. Plasmids were grown up to create plasmid stocks as in sections 2.3.2 and 2.3.3.

2.3.5 *Transfection of cell lines*

Stable transfections were performed using Lipofectamine 2000 liposomal-based reagent from Invitrogen (UK) according to the manufacturer's instructions. Lipofectamine 2000 relies upon lipofection to enter the cellular environment. The transfection reagent is a cationic formulation that forms complexes with negatively charged DNA, which therefore allows passage across the cell membrane [239]. Cells were seeded at appropriate densities for the vessels in which they were to be transfected in (2×10^5 - 4×10^5 for 6-well plates and 1×10^6 for 100 mm dishes) and left to adhere overnight. Subsequently, spent medium was removed and discarded from wells/plates. Cells were subjected to a PBS wash, Opti-MEM (Invitrogen, UK) reduced serum media was then added to the well/dish. Lipofectamine 2000 was diluted, with 9 µL of Lipofectamine being added to 150 µL Opti-MEM. The plasmid stock was initially diluted so that 14 µg plasmid was used to transfect the miRNA plasmids. The ABCB9 and EX-NEG (vector control) plasmids were diluted to 10 µg. The Lipofectamine and diluted plasmid stock solutions were then combined at a ratio of 1:1 and incubated at room temperature for 10-15 min. Following incubation, 250 µL of the combined plasmid/transfection reagent was added drop wise to each well of a 6-well plate. Where the utilisation of a 100 mm (60 cm^2) dish was necessary for transfection, reagents were scaled accordingly. Following 6 h of incubation with the plasmid/transfection reagent in the Opti-MEM filled wells, spent Opti-MEM was removed and fresh complete media added. Cells were assessed for GFP expression

by fluorescence microscopy, where appropriate, 24 h post transfection, as described in section 2.3.6.

2.3.6 *Fluorescence microscopy*

The Zeiss Axio Vert.A1 inverted microscope was used to visualise transfected cells on the bright field and FITC channels to check for the presence for GFP. The exposure time was kept constant between untransfected controls and transfected cells to ensure autofluorescence did not provide false positives. The Zeiss LSM710 AxioObserver Confocal microscope (Zeiss, Germany) was used for immunoflourescence studies. Zeiss ZEN 2012 software was utilised to analyse images.

2.4 Gene expression analysis

2.4.1 *RNA extraction*

Extraction of both miRNA and mRNA was achieved through the use of an RNeasy column based Mini kit (Qiagen, Netherlands) according to manufacturer's protocols. The RNeasy kit relies upon a silica-based membrane for RNA capture and purification. The kit achieves cell lysis via a guanidine-thiocynate-based buffer, with the addition of ethanol to allow the optimal binding conditions.

Surfaces and equipment were cleaned using 1% Virusolve prior to procedures involving RNA. Filtered, RNase and DNase free sterile pipette tips (TipOne, StarLab, UK) were used throughout all RNA/DNA based experiments. Cells (up to 1×10^7) were harvested in an exponential growth phase from T75 cm^2 flasks via scraping (using sterile cell scraper) into sterile cold 1X PBS. Cells were then pelleted at $300\times g$ for 5 min and immediately placed on ice. The supernatant of each sample

was carefully removed via pipetting and disposed to waste. To initialise the lysis procedure, 350 µL Buffer RLT was added to the sample and vigorously mixed via pipetting to ensure total disaggregation of the cell pellet. One volume (350 µL) 70% EtOH was then added to the cell solution and mixed thoroughly. The total sample was then added to an RNeasy spin column complete with collection tube. The sample was then centrifuged at $9000 \times g$ for 20 s, after which the flow-through was discarded to waste. The column was checked for full flow-through to ensure no obstructions. A volume of 700 µL Buffer RW1 was then added to the column, and centrifuged at $9000 \times g$ for 20 s, flow-through subsequently discarded. A volume of 500 µL of Buffer RPE was then added to the column and centrifuged at $9000 \times g$ for 20 s, flow-through discarded. The sample was repeat washed with 500 µL of Buffer RPE and centrifuged at $9000 \times g$ for 2 min. The RNeasy column was then inputted into a collecting 1.5 mL RNase- and DNase-free sterile Eppendorf tube. A volume of 30 µL RNase-free water was added directly onto the column membrane, the column was then centrifuged at $9000 \times g$ for 1 min to elute RNA; this was then repeated using the flow-through from the elution step to ensure maximal RNA recovery.

2.4.2 *RNA quantification*

Total RNA extracted was asssessed for concentration and quality using the NanoDrop Lite Spectrophotometer (Thermo Scientific, UK). The NanoDrop Lite relies upon optic technology, wherein a sample is loaded onto a receiving fibre, which is then contacted with a source fibre, and the liquid bridge created by the sample then allows a light emitting diode (LED) to create light, and a silicon photodiode to then analyse the light that has passed through the sample, giving indication of its content.

Prior to running samples, the loading pedestal was cleaned using deionised H_2O and lens cleaning tissue. Initially, the NanoDrop was blanked using the appropriate control (RNase-free H_2O for RNA). The loading pedestal (receiving fibre end) then had a sample volume of 2 µL placed upon it and absorbance measured at 260 nm. Concentration of RNA was measured and recorded in ng/µL format, and a 260/280 ratio recorded for indication of protein contamination, a ratio of ~2 was indicative of optimal quaility.

Post quantification, extracted RNA was immediately reverse transcribed to cDNA; any surplus RNA was stored at -80°C.

2.4.3 *cDNA synthesis for miRNA*

Reverse transcription for miRNA was completed using the miScript II RT kit (Qiagen) according to manufacturer's instructions. Reverse transcription used the miScript HiSpec buffer, which ensures mature miRNA are polyadenylated and reverse transcribed with oligo-dT primers, which have a 3' degenerate anchor and a universal tag sequence on the 5' end, allowing amplification of mature miRNA.

Previously extracted RNA was placed on ice, or thawed on ice, alongside thawing the reverse transcriptase mix. MiScript Nucleics Mix (10X), 5X miScript HiSpec buffer and RNase free water were thawed at room temperature. On a volume per reaction basis, master mix for cDNA synthesis was prepared. Briefly, 4 µL 5X miScript HiSpec buffer, 2 µL 10X miScript Nucleics Mix, and 2 µL miScript Reverse Transcriptase Mix were added together to form a master mix (hereafter termed miScript RT MM). A volume of 8 µL of the miScript RT MM was then added to 0.5 mL flat-topped tubes and variable amounts of RNA sample (2 µg of RNA reverse transcribed for each sample) and RNase-free H_2O were added, giving a total reaction volume of 20 µL (for each sample). Each time a set of samples was run

through the procedure, a blank was also performed to ensure no contamination of the RT reagents (all components were used for the blank aside from the RNA sample; RNase-free H_2O was used as a substitute). The total reaction was then placed into a thermal cycler (C1000 Thermal Cycler, BioRad, UK) that was programmed to incubate the samples for 60 min at 37°C and then 5 min at 95°C to inactivate the miScript RT MM. Reverse transcribed RNA, now termed cDNA, was either placed on ice ready for quantitative PCR (qPCR), or frozen at -20°C for later investigation.

2.4.4 *Quantitative PCR for miRNA*

To assess miRNA expression, SYBR Green-based quantitative PCR (qPCR) was employed. The miScript SYBR Green PCR kit and miScript primer assays (Qiagen) were used along with cDNA synthesised from the miScript II RT kit, as described in section 2.4.3. MiScript primer assays were purchased as they are known to amplify the desired gene of interest and have been meticulously quality controlled. The process of SYBR Green qPCR acts by the binding of the SYBR Green dye to double stranded DNA (dsDNA).The PCR reaction amplifies the sequence it is targeting, the SYBR Green binds to each new copy of the dsDNA product, thus proportionately elevating the fluorescent signal, which relates to the amount of amplified product.

Each sample anlaysed by miScript qPCR was plated in triplicate into 96-well qPCR plates to limit the influence of outliers in the dataset. A volume of 1 μL cDNA (equal to 100 ng) was added to each well of a 96-well PCR plate (Applied Bioscience, UK). Two qPCR reaction master mixes (qPCR MM) were prepared on a volume per reaction basis, with the only difference between the mixes being one having the primer assay of interest, and one having a PCR loading control primer assay (Table 2.1). The reaction volumes were 10 μL Quantitech SYBR Green, 2 μL Universal primer (reverse), 2 μL primer assay and 5 μL RNase free H_2O, making the total

volume in the well 20 μL. To control for anomalies within the qPCR reagents, an RNase-free H_2O sample that had been through the cDNA synthesis process was run as a non-treated control on every qPCR plate. The prepared qPCR plate was covered with an adhesive clear film (Applied Bioscience) and sealed by scoring with a pipette tip. The plate was then subjected to a short spin in a Miniplate Spinner MPS1000 (Labnet, USA) to pool the contents of each well. The qPCR machine (StepOne Plus Real Time PCR System, Applied Bioscience) was then programmed to run for 40 cycles after the initial activation at 95°C for 15 min. Each cycle was set to denature at 94°C for 15 s, anneal primers at 55°C for 30 s and extend primer at 70°C for 30 s. Data collection was collected during the primer extension step.

Data was collated using StepOne software v2.0 (Applied Bioscience), with adjustments made to the baseline threshold if the software had not automatically detected early exponential phase, to ensure C_t determination was as accurate as possible. Analysis of qPCR data was achieved using the Livak method [240].

2.4.5 *cDNA synthesis for mRNA*

For samples previously extracted from section 2.4.1, to assess mRNA levels, a QuantitTect RT kit was utilised (Qiagen). A total of 1 μg of previously extracted RNA was loaded into the cDNA synthesis reaction; this was made up to a total of 12 μL with RNase free H_2O. Initially, 2 μL (making a total reaction volume of 14 μL) of genomic DNA wipeout buffer was added to each individual sample to ensure potential contamination from genomic DNA was eliminated. A negative control with RNase-free H_2O only was also prepared for each set of reactions. After addition of the gDNA wipeout buffer, samples were placed into a thermal cycler for 2 min at 42°C, after which samples were immediately placed on ice prior to cDNA synthesis. A master mix (RT MM) was prepared on a volume by reaction basis, with 1 μL RT

MM Quantitect Reverse Transcriptase, 4 µL of Quantiscript RT buffer and 1 µL RT primer mix (total of 6 µL) added to each sample post gDNA wipeout, thus making a total volume per reaction of 20 µL. The samples were added to a thermal cycler and reverse transcription completed for 15 min at 42°C, followed by 3 min at 95°C to inactivate the reverse transcriptase. cDNA was either placed immediately on ice after reverse transcription prior to qPCR, or was frozen at -20°C for longer term storage.

2.4.6 *Quantitative PCR for mRNA*

To assess relative mRNA levels within samples, QuantiTect SYBR Green PCR was adopted (Qiagen). The QuantiTect SYBR Green PCR kit and QuantiTect primer assays were used along with cDNA synthesised from the Quantitect RT kit. QuantiTect primer assays were purchased as they are known to amplify the desired gene of interest and have been meticulously quality controlled.

Each sample analysed by QuantiTect qPCR was plated in triplicate to extrapolate any outliers in the dataset. Initially, cDNA from section 2.4.5 was diluted to 20 ng/µL, so that 20 ng cDNA would be loaded into the qPCR reaction. A volume of 1 µL cDNA (20 ng) was added to each well of a 96-well PCR plate (Applied Bioscience, UK). As for miRNA analysis, two separate qPCR reaction master mixes (qPCR MM) were prepared on a volume per reaction basis, with the only difference between the mixes being the one had the primer assay of interest, and one had a PCR loading control primer assay (Table 2.1). The reaction volumes were 10 µL Quantitech SYBR Green, 2 µL primer assay and 7 µL RNase-free H$_2$O, making the total volume in the well 20 µL. To control for anomalies within the qPCR reagents, an RNase free water sample was run as a non-treated control on every qPCR plate. The prepared qPCR plate was covered with an adhesive optically clear film (Applied Bioscience). Each plate was then subjected to a pulse spin in a Miniplate Spinner MPS1000 (Labnet,

Table 2.1 Primer assays utilised in qPCR

Target	miRNA or mRNA	Manufacturer	Catalogue number
miR-31	miRNA	Qiagen	MS00003290
RNU-6	miRNA (loading control)	Qiagen	MS00033740
CTR1	mRNA	Qiagen	QT00099267
ABCB9	mRNA	Qiagen	QT00089047
ATP7A	mRNA	Qiagen	QT00075852
ATP7B	mRNA	Qiagen	QT00075782
B2M	mRNA (loading control)	Qiagen	QT00088935

USA) to pool the contents of each well. The qPCR machine (StepOne Plus Real Time PCR System, Applied Bioscience) was then programmed to run for 40 cycles after the initial activation at 95°C for 15 min. The cycle was set to denature at 94°C for 15 s, anneal primers at 55°C for 30 s and extend primer for 72°C for 30 s. Data collection was collected during the extension step.

Data was collated on the StepOne software v2.0 (Applied Bioscience), with adjustments made to the baseline threshold if the software had not automatically detected early exponential phase, to ensure C_t determination was as accurate as possible. Analysis of qPCR data was achieved using the Livak method [240].

2.5 Protein expression analysis

2.5.1 *Protein lysate preparation*

Cells previously seeded into 100 mm dishes had spent medium discarded to waste and were washed with 2 mL sterile 1X pre-warmed PBS, this was then discarded and cells were scraped into approximately 2 mL of fresh sterile pre-warmed 1X PBS. The cell mix was then inserted into 15 mL tubes, where samples were subjected to centrifugation for 5 min at $300 \times g$ to pellet cells. From this point onward, all reagents and cells were kept on ice.

The supernatant was carefully pipetted from the tube, avoiding disturbance of the pellet. The cell pellet was then resuspended in complete cold RIPA lysis buffer (50 mM Tris-HCl pH8, 1% Triton-X, 0.5% sodium deoxycholate, 0.1% SDS, 150mM NaCl, with the addition of protease and phosphatase inhibitor tablets (Pierce, IL, USA)), hereafter termed complete RIPA. The volume of the complete RIPA was dependent upon the size of the pellet; a range of 25 µL to 40 µL per pellet was used

to ensure optimal concentration of protein. Cells were thoroughly resuspended in complete RIPA and transferred to fresh, sterile 1.5 mL Eppendorf tubes. Cells with complete RIPA were kept on ice for 30 min to ensure efficient lysis, and then centrifuged at $6000 \times g$, 4°C for 5 min. The supernatant was then determined.

2.5.2 *Extraction of nuclear proteins*

Cells were harvested and washed with ice cold NEB buffer A (10 mM HEPES pH 7.9, 1.5 mM $MgCl_2$, 10 mM KCl, 1 mM DTT, PIC, ultrapure H_2O) and pelleted at $20,000 \times g$ for 2 min. Cells were washed a further two times with NEB buffer A for 5 min. Cell lysis was achieved by resuspending cells in NEB buffer A plus 0.1% (v/v) NP40 with incubation on ice. Lysate was separated by centrifugation at $20,000 \times g$ for 15 min, followed by nuclear lysis with NEB buffer C (20 mM HEPES pH7.9, 1.5 mM $MgCl_2$, 420 mM NaCl, 1 mM DTT, PIC, ultrapure H_2O). Insoluble material was removed via centrifugation at $20,000 \times g$ for 15 min. Protein concentration in the supernatant was then quantified.

2.5.3 *Protein quantification*

Quantification of protein was completed using Pierce bicinchoninic acid assay (Thermo Scientific), or BCA assay. In short, the assay chelates copper with protein within an alkaline environment, this is also known as the biuret reaction. Chains of peptides form a coloured chelate complex with cupric Cu^{1+} ions, which is light blue in colouration. The colour is then further developed when the BCA reacts with the formed Cu^{1+}. A purple colouration occurs as two BCA molecules chelate with one ion, which can be measured at approximately 562 nm. A linear increase in absorbance is observed with increasing protein concentration.

Initially, a standard curve using 2 mg/mL bovine serum albumin (BSA) was created for each BCA assay run. The protein concentration of a sample was calculated using the standard curve. Serial dilutions of the concentrated BSA were completed so that a series of 8 known protein concentrations from 25 μg/mL to 2000 μg/mL (diluted in RIPA buffer, with RIPA only as a blank or 0 μg/mL) were produced. The prepared standards created were frozen at -20°C after use, and freeze thawed up to ~5 times. When standards became non-linear upon analysis, new standards were made to avoid problems in quantification. In a non-sterile 96-well clear bottomed plate, 10 μL standards were aliquotted in duplicate. In order for protein concentrations to be within the range of the assay, sample protein was diluted 1 in 10 within the well, so that 1 μL sample was added to 9 μL RIPA buffer. The BCA assay reagent was made in a 15 mL tube at a ratio of 50 parts of reagent A (BCA) to 1 part reagent B (4% Cu^{1+} sulphate). Once thoroughly mixed, 200 μL of the BCA assay reagent was then added to all protein containing wells, including standards. The 96-well plate was then covered in foil and placed in a 37 °C incubator for 30 min. Post incubation, absorbance was measured at 595 nm on an Absorbance Microplate Reader ELX800 (Biotech, USA). The blank absorbance was subtracted from all sample and standard absorbance and all duplicated wells were averaged. Using Microsoft Excel, a standard curve was plotted with BSA concentration on the x-axis, and absorbance at 595 nm on the y-axis. The concentration of protein within samples was therefore calculated using the equation of the standard line (y=mx+c) as overleaf (x: protein concentration, y: absorbance, c: y intercept, m: gradient).

$$x = \frac{\left(\frac{(y-c)}{m} \times 10\right)}{1000}$$

2.5.4 *Protein sample preparation*

Quantified samples were prepared (30-50 μg per sample) to be loaded onto a gel for SDS-PAGE protein separation. Samples were prepared with RIPA buffer and normalised to a total volume of 20 μL in 1.5 mL tubes. A volume of 5 μL loading buffer (3.3% SDS; 6 M Urea; 17 mM Tris-HCl pH 7.5; 0.01% bromophenol blue and 0.07 M β-mercarptoethanol) was added to each sample, and samples pulse centrifuged (Sprout mini-centrifuge, Heathrow Scientific, UK) to pool the contents of the 1.5 mL tubes. Samples were then heated to 95°C for 8 min (Techne Dri-Block DB-3D, Sigma Aldrich, UK), after which tine samples were cooled to room temperature and pulse centrifuged again prior to gel loading.

2.5.5 *SDS-PAGE*

Prepared proteins were loaded onto polyacrylamide gels and electrophoresed to separate proteins according to size within the gel matrix. Gels were hand-cast (6-12%) according to recipes detailed in appendix 2. Gel casting apparatus, mini-PROTEAN Tetra System (Bio-Rad, UK), was assembled with a glass spacer plate sandwiched with a short plate, clamped into a casting stand. The plates were checked for leaks by gently introducing 1 mL isopropanol in between the plates with a Pasteur pipette. Where leaks were present, the casting equipment was taken apart and reassembled. Isopropanol was poured out of the plates and plates were concurrently left to dry before gel solutions were added. The resolving gel was prepared in a 50 mL tube and gently pipetted in between the plates with a Pasteur pipette, stopping ~1-1.5 cm from the top of the short plate to allow for the stacking gel. Carefully, a layer of isopropanol was pipetted on top of the resolving gel to ensure an even gel, and to assist polymerisation. Surplus resolving gel was left in the 50 mL tube to act as a proxy for polymerisation. Once the surplus resolving gel had polymerised after

~20 min, the isopropanol was carefully poured off and the prepared stacking gel was pipetted on top. Once the top of the short plate had been reached with the stacking gel solution, a 10-well comb was pushed in between the plates ensuring no bubbles underneath the wells. The stacking gel was then left for ~10 min to polymerise; surplus stacking gel was left in the 50 mL tube to ensure the gel had polymerised within the plates. In general, gels were prepared at least 1 day in advance of electrophoresis, and soaked in 1X running buffer before storage in the fridge overnight which ensures a firmer gel.

Following gel casting, the mini-PROTEAN Tetra Cell (Bio-Rad) was assembled. Two to four gels per tank were run simultaneously. Once removed from the fridge, gels were clamped into a gasket and the gasket fitted into a tank, with short plates facing inward toward the central buffer reservoir. A small amount of 1X running buffer (diluted from 10X stock: 30.2 g Tris base, 144 g glycine, 100 mL 10% SDS, H_2O up to 1 L) was poured in between plates to ensure no leakage. Further 1X running buffer was then added to the space between plates, up to the top of the gasket. After removal of the well combs, using a 1 mL syringe and 25 gauge needle, wells were flushed with 1X running buffer to ensure residual polymerised stacking gel did not interrupt loading of the gel.

In general, gels were loaded with molecular weight markers for the first two wells (5 µL 1kB PageRuler Plus Prestained Protein Ladder (Thermo Scientific) and 2 µL Precision Plus Protein WesternC Standard (Bio-Rad)). A volume of 20 µL sample was added to each well using a gel loading tip. Gels were then electrophoresed (PowerPac Universal, Bio-Rad) for 1 h 30 min to 1h 50 min at 100 V to 120 V. Gels were stopped when the dye front became proximal to the bottom of the gel, however very large proteins required the dye front to be run off the gel, ensuring the proteins

had sufficiently migrated into the resolving gel. Glass plates were carefully separated post electrophoresis and the wells cut off from the gel, the gel was then transferred to a box tray containing 1X transfer buffer (diluted from 10X stock: 30.2 g Tris base, 144 g glycine, dH_2O up to 1 L) for ~5 min until equipment and reagents for transferring were prepared.

2.5.6 *Western blotting*

Proteins separated by SDS-PAGE were subsequently transferred onto PVDF (polyvinylidene fluoride) 0.2 µM membrane (Thermo Scientific). Briefly, proteins are probed on the PVDF membrane with specific primary antibodies directed against a protein of interest. After washing, the PVDF membrane is then probed with horseradish peroxidise (HRP) linked secondary antibodies, which bind to the primary antibodies and can be detected through the application of a chemiluminescent substrate.

Cassettes were assembled and all components were thoroughly soaked in 1X transfer buffer. Assembly of the cassette was performed with the clear side down. Firstly, a transfer sponge was placed on to the clear side of the cassette, followed by 2 filter papers (cut to the same dimensions as a short plate), PVDF membrane activated for 10 s in methanol, the polyacrylamide gel, 2 filter papers and finally another sponge. Between each layer of the cassette, a roller was used to ensure no air bubbles can disrupt the transfer process. The sandwich cassette was then carefully closed and fastened and inserted into the transfer gasket, with the black side of the cassette facing the black side of the gasket (negative electrode). The transfer gasket was then slotted into the tank and filled with 1X transfer buffer. The tank had a magnetic stir bar and cool pack added to control temperature and circulate buffer during transfer. The tank was then placed on a magnetic stirrer and run at 100 V for 1 h 30 min.

After transfer, the cassette was removed and carefully disassembled using forceps to minimise contact with the PVDF membrane. Filter papers and gel remains were discarded to waste. The orientation of the membrane was noted, and using a scalpel, the top right hand corner of the membrane cut. The PVDF was then transferred into a box tray to block the membrane (thus preventing non-specific binding of antibody), which contained 5 mL 5% w/v non-fat dried milk (Marvel, UK)/1X TBST (TBS diluted from 10X: 24 g Tris HCl (Melford, UK), 5.6 g Tris base, 88 g NaCl, up to 1 L with dH$_2$O, with the addition of 0.1% Tween 20) solution, hereafter termed milk solution. Membranes were incubated at room temperature on a gyrorocker (Stuart 3D gyratory rocker, Bibby Scientific, UK) set at 40 rpm for 1 h. After blocking, the milk solution was discarded and membranes were washed in 1X TBST for 10 min with 2 changes of wash during that period. Post brief washing, membranes were incubated in primary antibody overnight at 4 °C on a roller (Stuart Analogue tube roller, Bibby Scientific). Primary antibodies, Table 2.3, were prepared in 50 mL tubes, with either 5% milk solution, or 5% BSA solution (prepared with 1X TBST), depending upon recommendations of the manufacturer on antibody datasheets. Membranes were then washed in 1X TBST for 30 min, with at least 4 changes of wash during that period. Secondary antibodies, Table 2.3, were then prepared in 50 mL tubes in milk solution. A volume of 0.25 μL Streptactin HRP conjugate (Bio-Rad) was added to secondary antibody solutions to ensure the concurrent visualisation of the Protein WesternC Standards. Membranes were incubated in secondary antibody for 1-2 h at room temperature on a roller. Membranes were then washed in 1X TBST for 40 min with 5 changes of wash during the period to ensure milk residues did not defile the membrane.

Imaging of the membranes was completed either through a chemiluminescent imaging system (Molecular Imager ChemiDoc XRS with ImageLab 3.0 Software,

Bio-Rad) or autoradiography. Firstly, a chemiluminescent substrate was prepared by combining two Clarity Western ECL Substrate (Bio-Rad) reagents (1:1). Membranes were put onto a sheet of clean acetate and 2 mL ECL was poured onto each membrane, ensuring the entirety of the surface was covered. An additional sheet of acetate was then placed over the top of the membrane, and the surface rolled to ensure no air bubbles were trapped in between the sheets. Membranes were then inputted into the imaging system and imaged intermittently over a 5 min period.

Where autoradiography was utilised, sandwiched membranes (with ECL) were secured into a developing cassette (Hypercassette, Amersham Biosciences, USA). The process was henceforth carried out in a dark room. A sheet of X-ray film (Fuji Super Rx X-ray Film, Fujifilm, Germany) was placed securely over the sandwiched membranes and the cassette shut firmly. Exposure time varied from 2 s to 120 s depending upon relative protein abundance. The exposed film was removed from the cassette and immediately placed into a large tray containing developing solution (Universal, Champion Photochemistry, Malaysia), the solution was circulated over the film until bands were visible. The exposed film was then placed into a tray containing fixer solution (Universal) and agitated until the film turned from opaque to transparent. Films were then briefly washed in water and left to air dry.

To complete densitometry analysis, Western blots developed on film were imaged using white light on the imaging system or alternatively opened from previously saved files on the Image Lab software. Using the volume tool, boxes were drawn around bands of interest; this then displayed volume intensity. The volume intensity of a band was normalised to the volume density of the loading control, mainly

Table 2.2 Antibodies for Western blot

Target protein	Manufacturer	Catalogue no.	Species	Dilution used
TurboGFP	Origene	TA150041	Mouse	1:10,000 (in 5% w/v milk/TBST)
CTR1	Santa Cruz	sc-66847	Rabbit	1:1000 (in 5% w/v milk/TBST)
ATP7A	Santa Cruz	sc-376467	Mouse	1:1000 (in 5% w/v milk/TBST)
ATP7B	Santa Cruz	sc-373964	Mouse	1:1000 (in 5% w/v milk/TBST)
OCT1	Santa Cruz	sc-28334	Mouse	1:1000 (in 5% w/v milk/TBST)
ABCB9	Santa Cruz	sc-393431	Mouse	1:1000 (in 5% w/v milk/TBST)
LAMP1	Santa Cruz	sc-17768	Mouse	1:2000 (in 5% w/v milk/TBST)
Phospho-53bp1	R & D Systems	AF3405	Rabbit	1:1000 (in 5% w/v BSA/TBST)
Phospho-histone H2A.X (ɣH2AX)	Cell Signalling	2577	Rabbit	1:1000 (in 5% w/v BSA/TBST)
β-actin	Santa Cruz	sc-69879	Mouse	1:10,000 (in 5% w/v milk/TBST)
Anti-mouse (2°)	Dako	P0260	Rabbit	1:2000 (in 5% w/v milk/TBST)
Anti-rabbit (2°)	Santa Cruz	7074	Goat	1:2000 (in 5% w/v milk/TBST)

β-actin, by dividing the band of interest by the β-actin band. Where appropriate, volume densities of bands were then normalised to densities of a control sample.

2.5.7 *Immunofluorescence microscopy*

Cell lines were seeded on sterile glass cover slips (sterilised in 70% EtOH and air dried in laminar air flow unit) within a 6-well plate at a density of 4×10^{5} per well. Spent media was aspirated and cells were fixed by pipetting 4% formaldehyde solution (prepared with warm 1X PBS) to a depth of 2 mm on top of cover slips. Cells were fixed for 15 min at room temperature. The fixative was aspirated and wells rinsed three times with 1X PBS for 5 min. Henceforth, the process was completed in the dark (by covering the plate in foil). After initial washing, cells were blocked with blocking solution (1X PBS, 5% FBS, 0.3% Triton X-100) for 60 min at room temperature. Blocking solution was aspirated, and primary antibody, Table 3, was applied in antibody dilution buffer (1X PBS, 1% BSA, 0.3% Triton X-100) and incubated at 4ºC overnight. Following washing three times with 1X PBS for 5 min, cells were incubated with Alexa Fluor 555 (Thermo Fisher Scientific), Table 3, secondary antibody diluted in antibody dilution buffer for 2 h at room temperature. Secondary antibody was aspirated and cells were rinsed four times with 1X PBS for 5 min. Cover slips were then reverse mounted onto glass slides with ProLong® Gold Antifade Mountant with DAPI (Thermo Fisher Scientific), and sealed with clear nail varnish. Slides were left to cure overnight before imaging on Zeiss LSM710 AxioObserver Confocal microscope or Zeiss Axio.Vert A1 Fluorescence microscope. Images were captured with AxioCamIC with 0.5x Camera Adapter.

Table 2.3 Antibodies for immunofluorescence studies

Antibody	Manufacturer	Catalogue no.	Species	Dilution
ABCB9	Santa Cruz	sc-393431	Mouse	1:100
LAMP-1	Santa Cruz	sc-17768	Mouse	1:200
Anti-mouse Alexa-Fluor 555 (Red)	Thermo Scientific	A-21422	Goat	10 µg/mL

2.6 Cell based assays

2.6.1 *Clonogenic assay*

Clonal survival was determined by seeding cells at a density of between 5×10^2 and 1.5×10^3 per well with 1.5 mL complete medium into 6-well plates and allowing them to adhere and settle overnight in a 37ºC, 5% CO_2 humidified incubator. Spent media was carefully aspirated so as not to disturb the single cells adhered. Cells were then subjected to chemotherapy treatment using established doses for 24-48 h, following which treatment was carefully aspirated and 2 mL fresh complete medium applied to each well. For radiation treated clonogenics, plates were transported to the irradiator and were exposed to a range of doses from 2 Gy to 8 Gy, after which they were returned to incubation. Plates were incubated for 8-10 days post seeding. Colonies were fixed by firstly aspirating and discarding media, then a gentle wash with room temperature 1X PBS to each well. A crystal violet solution (0.1% w/v crystal violet, 70% v/v MeOH, 30% v/v dH_2O) was then used to stain colonies. The fixative was incubated on the wells for 30 min, after which it was carefully removed with a Pasteur pipette into a waste bottle containing sodium hydroxide to inactivate crystal violet. Plates were washed carefully with water, until colonies were distinct and crystal violet deposits no longer remained. Plates were then air dried at room temperature for at least 24 h. Colonies were counted using the GelCount instrument (Oxford Optronix, UK), using optimised CHARM (compact Hough and radial map) image processing algorithms for each cell line, as in appendix 3. Plating efficiency was calculated as the colony count divided by the number of cells seeded. Surviving fraction was therefore calculated as the colony count, divided by the plating efficiency of the control, multiplied by the number of cells seeded.

The clonogenic assay was optimised so that ~200 colonies were present on a fixed and stained 6-well plate; this varied across cell lines and took into consideration the visible overlap of colonies. Cell seeding densities were adjusted according to treatments, with a greater density of cells seeded where treatment would indicate lower countable colonies. The CHARM algorithm was optimised to distinguish and detect individual colonies; this was of benefit where two colonies arose in close proximity to one another. The CHARM algorithm was able to distinguish between colonies by using a range of functional features, including the optical density of a given colony.

2.6.2 *Longitudinal cumulative cell count-based proliferation assay*

A basic cumulative cell count assay was employed to detect subtle changes in proliferative capacity, wherein 3×10^5 cells were seeded into 100 mm tissue culture dishes and allowed to adhere overnight. Subsequently, spent media was discarded to waste and chemotherapy treatment was then applied for 24 h, after which time treatment was aspirated and 10 mL fresh complete medium added to each dish. Cells were re-seeded at 3×10^5 every 3 days, for a total of 9 days, and a cumulative cell count taken at each time of re-seeding.

2.6.3 *MTS assay*

Cellular viability in response to chemotherapeutic treatment was established via the CellTiter 96® AQueous One Solution Cell Proliferation Assay (Promega, UK), according to manufacturer's instructions. Briefly, Aqueous One Solution is a colourmetric-based assay that contains the tetrazolium compound MTS, which is reduced by metabolically active cells, producing a coloured formazan product which can then be measured at an absorbance of ~490 nm on a plate reader.

Cells were seeded at a density of 1×10^3 cells per well in 100 μL complete media within a 96-well clear bottomed plate, with each experimental condition plated in triplicate. Cells were incubated overnight, after which the spent media was removed from each well, and appropriate treatment medium added (including on each plate at least one media only well). A volume of 20 μL of MTS reagent was added to each well 72 h after chemotherapy treatment. Post addition of the MTS reagent, plates were measured at 495nm on a plate reader (Absorbance Microplate Reader ELX800, USA). The triplicate absorbance readings were averaged, and the media only reference subtracted from the readings. Data was then subjected to normalisation to vehicle control wells and corresponding variance from that value calculated.

2.6.4 *GSH/GSSG-Glo Assay*

The GSH/GSSG-Glo assay (Promega, UK) was performed according to manufacturer's instructions. GSH/GSSG-Glo measures oxidised and reduced glutathione content in cells. Glutathione is the most abundant antioxidant found in eukaryotes, and oxidised glutathione is an indicator of oxidative stress, thus measuring the ratio of GSH (reduced) to GSSG (oxidised) can be beneficial to gain insights into the health of cells [241]. The GSH/GSSG Glo assay relies upon GSH-dependent conversion of a GSH probe to luciferin by glutathione S-transferase.

Briefly, 5×10^2 cells per well were seeded into 96-well white bottomed plates, cells were left to adhere overnight, and then treated with appropriate treatment for 24 h. A standard curve of known GSH concentrations was pipetted in triplicate on each plate. Preparation of reagents for the assay occurred 30 min prior to the commencement of the procedure. Following treatment, spent media was discarded to waste, and 50 μL total glutathione or oxidised glutathione lysis was applied to each well, this was then shaken using a luminometer (Fluoroscan Ascent FL, Thermo Scientific) for 5 min. A

volume of 50 µL of luciferase generation reagent was then added to all wells, following a short shake of 30 s, after which the plate was incubated for 30 min. A volume of 100 µL of luciferase detection reagent was then applied to all wells and the plate shaken for a further 30 s. After 15 min of incubation at room temperature, luminescence was read with the Fluoroscan Ascent FL with an integration time of 1000 ms.

2.6.5 *ROS-Glo H_2O_2 Assay*

The ROS-Glo H_2O_2 assay (Promega, UK) was performed according to manufacturer's instructions. ROS-Glo measures H_2O_2 content in cells by providing a substrate to H_2O_2 that generates a luciferin precursor; this is then detected by the addition of a detection reagent with luciferase and d-Cysteine.

Briefly, 5×10^3 cells per well were seeded into 96-well white bottomed plates, cells were left to adhere overnight, and then treated with appropriate treatment for 24 h. A volume of 20 µL of H_2O_2 substrate was added to treatment for the final 6 h of incubation. A volume of 100 µL ROS-glo detection reagent was then added to all wells. The plate was incubated for 20 min at room temperature. Plates were then measured for luminescence signal using the Fluoroscan Ascent FL, with 1000 ms integration time.

2.7 Elemental analysis

2.7.1 *Subcellular fractionation*

Initially, cells were seeded, left to adhere overnight, and treated with high doses (50-500 µM) of chemotherapy or vehicle control for 24 h before scraping with 1X PBS to harvest into 15 mL tubes. From this point onward, the procedure was carried out

on ice or at 4°C. Cells were centrifuged at $200 \times g$ to pellet cells, and PBS discarded to waste. Cells were subjected to homogenisation with 10 strokes of a tight fitting pestle B in a glass Dounce homogeniser in the presence of 5 volumes of a sucrose-based solution (250 mM sucrose, 50 mM Tris-HCl, 5 mM $MgCl_2$ up to 100 mL with 1XPBS). Homogenised cells were then subjected to $600 \times g$ for 3 min to isolate nuclei; this fraction was collected from the separated solution. Further fractionation at $6000 \times g$ for 8 min separated mitochondria, lysosomes and peroxisomes, this fraction was collected separately. Supernatant from fractionation was collected for analysis.

2.7.2 *Lysosomal pull down*

To improve the yield of lysosomes from cell suspension, a novel immuno-pull down based methodology was developed, where an antibody directed against the lysosomal marker LAMP-1 and protein A/G magnetic beads were used to effectively pull lysosomes from homogenised cells. The lysosomal marker LAMP-1, makes ~50% of the total protein present on the lysosomal membrane [242], thus making this an ideal candidate to utilise to attempt pulling intact lysosomes from the pool of organelles present in the homogenised cell population.

Similarly to section 2.7.1, cells were treated and harvested, then resuspended in 100 µL ice cold PBS, and homogenised with 10 strokes of Dounce homogeniser. Briefly, the homogenised samples were combined with 5 µg LAMP-1 antibody; the sample/antibody solution was then incubated overnight at 4 °C on a tube rotator (Stuart, Bibby Scientific) set at 20 rpm. A volume of 25 µL Pierce Protein A/G magnetic beads (#88802, Thermo Scientific) was then aliquotted into a 1.5 mL tube. A volume of 175 µL wash buffer (1X TBST) was then added to the beads, and gently vortexed (Stuart SA7 Vortex) to mix. The magnetic beads were then collected to the

side of the tube by placing tubes in a magnetic stand (PureProteome Magnetic Stand, Merck Millipore, UK). The excess wash buffer was discarded, and 1 mL of fresh wash buffer added to the beads, this was then inverted several times. Beads were then collected with the magnetic stand; the supernatant was discarded to waste. The previously incubated antibody/sample solution was ten added to the pre-washed beads and incubated at room temperature on a tube rotator. Beads were then collected with a magnetic stand; the supernatant was saved for further analysis. A volume of 500 µL wash buffer was then gently added to the tubes and carefully mixed, beads were then collected via the magnetic stand, and this was repeated twice. A volume of 500 µL of PBS was then used to gently wash beads, with beads being collected using a magnetic stand, the supernatant was discarded to waste. For inductively coupled plasma mass spectroscopy and transmission electron microscopy (appendix 6), beads were weighed and frozen at -20°C at this point, otherwise, for Western blot analysis, beads were heated to 95°C for 10 min to dissociate the bead from the lysosomes (appendix 5).

2.7.3 *Inductively Coupled Plasma Mass Spectroscopy*

Inductively coupled plasma mass spectroscopy, or ICP-MS, measures the trace elements within a given sample. Here, we adopted ICP-MS to analyse platinum at the most abundant isotope 195. Platinum is the main component of cisplatin, not normally found within the cellular environment at more than absolute trace levels, making this element ideal to analyse via ICP-MS [243].

Cells were treated with 50 µM cisplatin for 24 h, after which cells were harvested and counted, fractionated, or pulled down to isolate organelle areas of interest. Cells (1×10^6) or fractions were incubated in HNO_3 for 72 h at room temperature. Following incubation, HCl was added to each sample to form *aqua regia* at a ratio of

1:3, ensuring total platinum was in solution (a bright orange colour was visualised). Samples were then diluted to 10 mL with dH_2O and analysed by Perkin Elmer DRCII (MA, USA) inductively coupled plasma mass spectrometry. An autosampler (Cetac ASX-510) was programmed to facilitate the ICP-MS run. Standard curves were generated using aqueous serial dilutions of known standards. Each measurement taken was representative of 3 technical replicates from an individual sample.

2.8 Bioinformatics

Gene promoter bioinformatics analysis was performed using the DECODE database http://www.sabiosciences.com/chipqpcrsearch.php?app=TFBS. Genes of interest were inserted, with analysis showing the potential binding sites of over 200 transcription factors 20 kb upstream and 10 kb downstream of the gene. Target prediction for miRNA binding to genes of interest was carried out through miRcode and Targetscan, available at the following:

http://mircode.org/?gene=pou2f1&mirfam=&class=&cons=&trregion= (accessed 290615)

http://www.targetscan.org/cgibin/targetscan/vert_61/view_gene.cgi?taxid=9606&rs=NM_001198783&members=&showcnc=0&shownc=0&showncf=#miR-31 (accessed 290615)

2.9 Statistical analysis

The standard error of the mean (±SEM) was used for all data analysis and relates to the standard deviation (SD) and sample size (n) (SEM $= \frac{SD}{\sqrt{n}}$). The SEM is a measurement of the standard deviation of all sample means over the means drawn from the population.

Statistical analysis was performed using GraphPad InStat v3 (GraphPad software), and graphical data completed on GraphPad Prism software 7.00 (GraphPad Software Inc, USA). All statistical tests generated a p value, which was considered significant if $p \leq 0.05$. Where data comparisons involved one (where hypothetical means were set to 1.0) or two sets of data, t-tests were performed, where there were more than two groups of interest to compare, ANOVA (analysis of variance) with Tukey's post-hoc test adopted.

Chapter 3:

The role of miR-31 in modulating MPM sensitivity to treatment

3.1 Introduction

Multimodality treatment for MPM is not commonly practised. The benefit to patients who have trimodality treatment, including chemotherapy, radical surgery and radiotherapy is limited [244]. The mainstay of treatment for MPM is administration of chemotherapeutics [100], although targeted therapies are in development and currently in clinical trials alone or in combination with chemotherapy [245]. There have been many targets identified for drug development, including EGFR [103], BAP1 [246] and PDL1 [247] however, a lack of sufficient randomised trials and poor target definition has meant chemotherapy, namely cisplatin and pemetrexed, as identified in the EMPHACIS trial [82], is the only recommended systemic standard of care for MPM [245, 248]. Patients, despite treatment, are still faced with an extremely poor prognosis [245], where the median PFS remains at just over 1 year, and the median overall survival post diagnosis being 4-18 months [249]. Unfortunately, due to the inherent resistance of the disease to chemotherapy, regression post treatment is generally short lived and patients relapse quickly.

MiRNAs are a group of small non-coding molecules that function to regulate gene expression at the posttranscriptional level. A single miRNA can regulate possibly hundreds of different genes, via imperfect complementarity to its target mRNA, consequentially inhibiting translation [250]. Additionally, a single gene can be regulated by multiple miRNA. It is approximated that ~50% of miRNAs are encoded in fragile sites within the genome [182], explicating the current interest in miRNA as potential contributory modulators of cancer biology. MiRNA play a significant role within the regulation of many aspects of cellular machinery, it has been extensively described that the dysregulation of these small non coding molecules could profoundly and substantially affect cell biology and functionality [251]. The

103

investigation of miRNA in the context of MPM is a prominent subject matter in current MPM research [238, 252]. A particular miRNA, namely miR-31, has a widely reported dysregulated expression profile in a extensive range of tumour types [194]. The role of miR-31 in cancer is complex; its dysregulated expression is associated with inhibition of colorectal cancer progression [253], inhibition of invasion in glioma [254] and protective roles against ionizing radiation [255]. The roles of miR-31 and its up- and down-regulation according to cancer type is comprehensively reviewed by Laurila and Kallioniemi [194].

Recently, Ivanov *et al.* [188] reported a general downregulation of miR-31 in MPM, following the deletion of the encoding chromosomal location 9p21.3 in 54% of a MPM patient cohort. It was observed that the re-introduction of miR-31 inhibited factors involved in cell cycle progression and DNA repair, in line with our previous groups' findings in oesophageal adenocarcinoma radioresistance [256]. However, in contrast, there has been correlation of miR-31 downregulation with increased long term survival in patients, with the proposition that miR-31 acts as a tumour suppressor in MPM [189]. Interestingly, the research indicates a significant negative relationship between miR-31 expression and survival time in an aggressive sarcomatoid MPM patient cohort [189]. The role of miR-31 in MPM remains unclear, with conflicting results indicating a pro-tumourigenic role for miR-31, as well as tumour suppressor functionality. Therefore, the investigation of miR-31 and the elucidation as to whether it modulates chemosensitivity in MPM is to be elucidated within this chapter.

3.2 Rationale, Aims and Objectives

Patients diagnosed with MPM face an extremely poor prognosis, mainly attributed to the lack of response to chemotherapeutics, the mainstay of MPM treatment [257]. MiRNAs have thus far shown promise as potential biomarkers, and can be targeted to modify response to treatment in MPM and other cancers [234, 258]. With previously established results indicating miR-31 re-expression leading to re-sensitisation to therapeutics [256], we hypothesized that miR-31 loss promotes resistance to chemotherapy in MPM, and that synthetic miR-31 replacement would enhance cellular sensitivity to chemotherapy.

The objectives of this chapter were to 1) determine whether the dysregulation of miR-31 contributes to MPM chemoresistance, in order to identify whether the miRNA may potentiate a therapeutic target or predictive biomarker 2) explore the effect of miR-31 modulation on biological endpoints relating to chemoresistance to begin to characterise any alterations observed, and to further elucidate and clarify the role of miR-31 within the landscape of MPM response to therapy.

3.3 Experimental design

3.3.1 *Assessing miRNA expression in MPM cell lines*

In order to analyse the status of miR-31 within a range of MPM cell lines to establish and verify which lines would be candidates for transfection of miR-31 overexpressing and suppressing plasmids, qPCR was utilised. A range of subtypes were assessed via qPCR including biphasic (MSTO-211H), sarcomatoid (NCI-H2052), and the most prevalent epithelioid subtype (NCI-H2452 and P31), a brief characterisation of which is noted in Table 3.1.

3.3.2 *Stable expression of miR-31 in NCI-H2452 and P31*

To establish the cell line models using NCI-H2452 as a reintroduction model and P31 as a suppression model, cell lines were lipofectamine transfected with miR-31-overexpressing or miR-31-suppressing plasmids, respectively. Successful transfection was confirmed by Western blot and fluorescent microscopy with GFP as a marker, although this did not directly confirm miR-31 was being expressed within the system, it supported the plasmid integration within the cellular environment and ensured support of the miR-31 expression measured in the transfected cells via qPCR.

3.3.3 *Analysis of the affect of miR-31 manipulation on cytotoxic drug response*

MPM cell response to chemotherapy with altered miR-31 expression was measured with clonogenic assay and a cumulative cell count. The clonogenic assay is the gold standard for assessing response to agents as it takes into account all forms of cell death, both early and late events [259].

Table 3.1 Cell line characteristics utilised with the *in vitro* cell model of refractory MPM. The NCI-H2452 and P31 comparatively have similar characteristics; however miR-31 is contrastingly expressed in both cell lines.

NCI-H2452	P31
Hsa malignant pleural mesothelioma cell line	Hsa malignant pleural mesothelioma cell line
Epithelioid subtype	Epithelioid subtype
Loss of 9p21.3 including p16	Loss of p16
✖ **NO endogenous miR-31**	✓**Endogenous miR-31**
Stably transfected to **REINTRODUCE miR-31**	Stably transfected to **SUPPRESS / ZIP DOWN miR-31**
NCI-H2452 miR-VC (vector control) NCI-H2452 miR-31 (miR-31 overexpression)	P31 Zip-miR-VC (vector control) P31 Zip-miR-31 (suppressing miR-31)

The cumulative cell count allows the observation of gross changes to basal proliferation over a similar period of time to that of the clonogenic assay, and importantly allowed the observation as to whether miR-31 alone was contributing to basal proliferation changes, or whether this was a specific response to drug treatment.

3.4 Results

3.4.1 *Confirmation of miR-31 status in MPM cell lines*

As miR-31 has previously been associated with resistance to therapy, the effect of either reintroducing or silencing miR-31 was assessed, in order to reveal any alterations to the chemosensitivity phenotype of MPM cells. The NCI-H2452 (parent) epithelioid subtype cell line demonstrated no endogenous expression of miR-31 (Fig. 3.1), confirming the results of other groups [188], and indicating deletion of this miRNA from this cell line. The P31 epithelioid subtype cell line was shown to have expression of miR-31 (Fig. 3.1). This provided an opportunity wherein within the same subtype we had the possibility of creating an antagonistic modified miR-31 expression system, whereby the NCI-H2452 cell line had miR-31 functionally restored, and the P31 cell line had miR-31 functionally silenced.

3.4.2 *Establishing a stable model*

The miR-31 deficient NCI-H2452 was stably transfected with either miR-VC (VC/vector control) or miR-31 overexpression plasmids, and P31 cells expressing endogenous miR-31 were stably transfected with silencing plasmids Zip-miR-VC or Zip-miR-31. In order to confirm the expression of miR-31, the relative expression level of miR-31 was measured via qPCR (Fig. 3.1); this was repeated over a 6 month period in order to confirm miR-31 was stably expressed. To confirm the expression of the miR-VC or Zip-miR-VC control within cells, analysis of the GFP reporter was undertaken via fluorescent microscopy (Fig. 3.2), and Western blot (Fig. 3.3). Utilising both methodologies ensured successful transfection of both the control plasmids and both the overexpression and suppression miR-31 vectors. Periodically, stable cell lines in culture were monitored for GFP expression using fluorescent microscopy, as in Fig. 3.2.
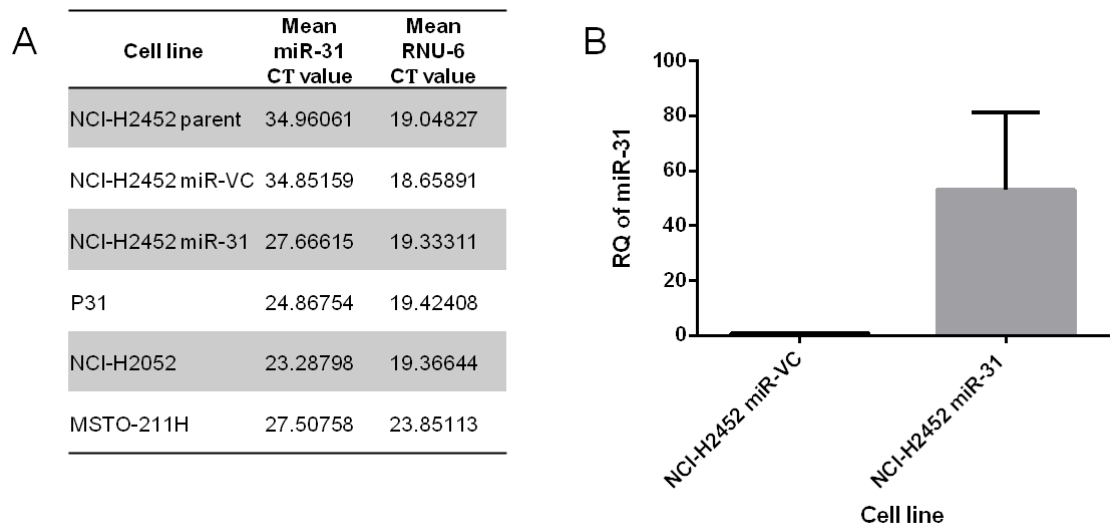
Figure 3.1 MiR-31 status in MPM cell lines. (A) C_t values of MPM cell lines comparing miR-31 expression. A comparable C_t value of ~39 between the NCI-H2452 parent and NCI-H2452 miR-VC is apparent, whereas the NCI-H2452 miR-31 transfected line has a C_t value of ~27, connoting successful transfection. The sarcomatoid cell line NCI-H2052 has the highest relative C_t value, indicating this cell line has the highest level of miR-31 expression. (B) qPCR evaluating the relative level of expression miR-31 between NCI-H2452 miR-VC control and NCI-H2452-miR-31 transfected cells (*n*=5). All qPCR runs were loaded with the maximum template of 100ng cDNA. As well as probing for miR-31, relative values were normalised to the endogenous control RNU6.
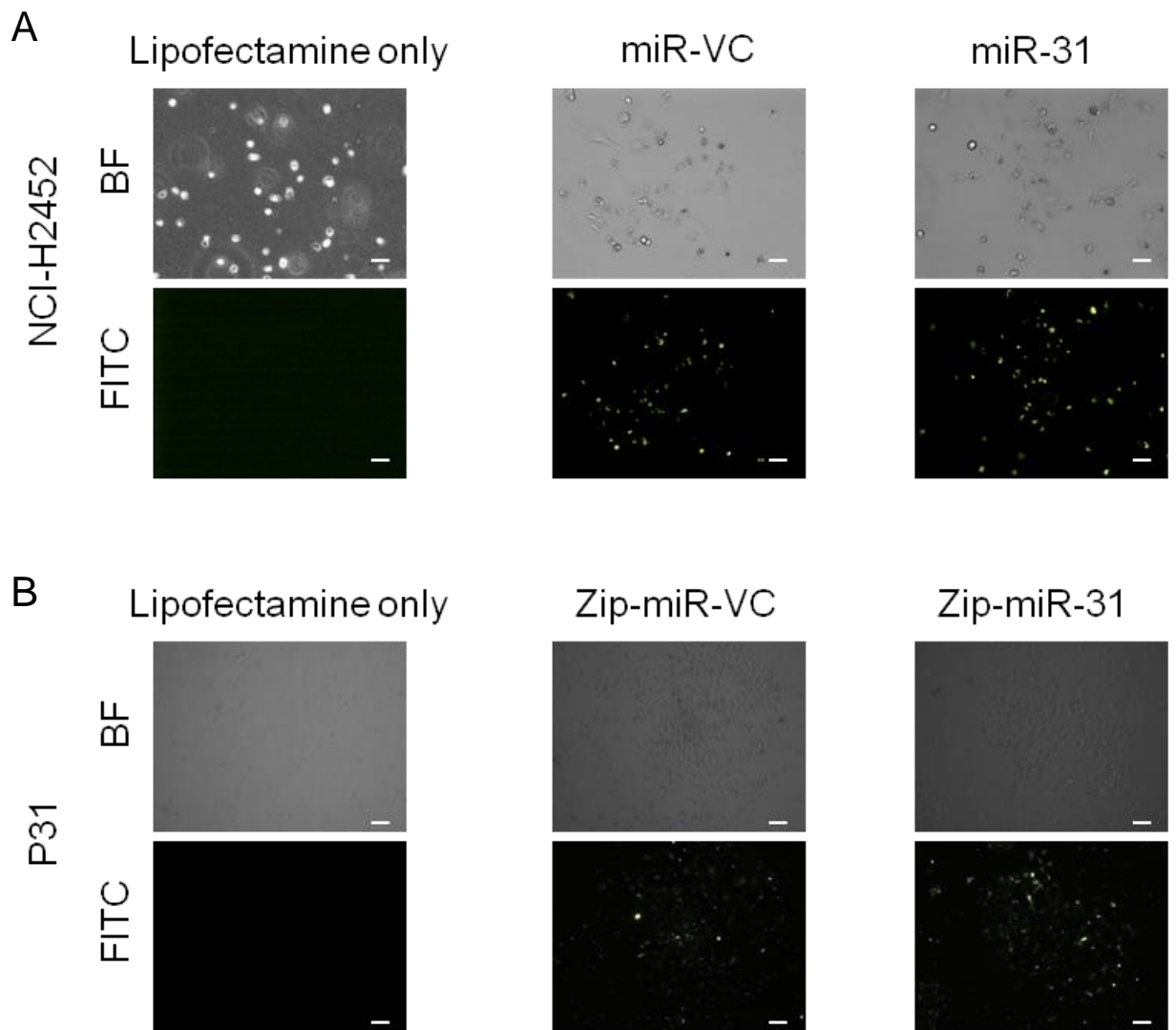
Figure 3.2 Confirmation of stable transfection. (A) The NCI-H2452 cell line was stably transfected with miR-31 overexpression vectors which had a GFP reporter sequence. (B) The P31 cell line was stably transfected with Zip-miR-31 silencing vectors which had GFP reporter sequence. The data demonstrates successful transfection and stable selection of the overexpressing NCI-H2452 miR-31 cell line model and the P31 Zip-miR-31 cell line model. Images shown from Fluorescein isothiocyanate (FITC) channel of Zeiss Axio Vert.A1 microscope, captured with AxioCamIC with 0.5x Camera Adapter. The objective used was LD A-Plan 10x/0.25 Ph1. Scale line equates to 100 μm.
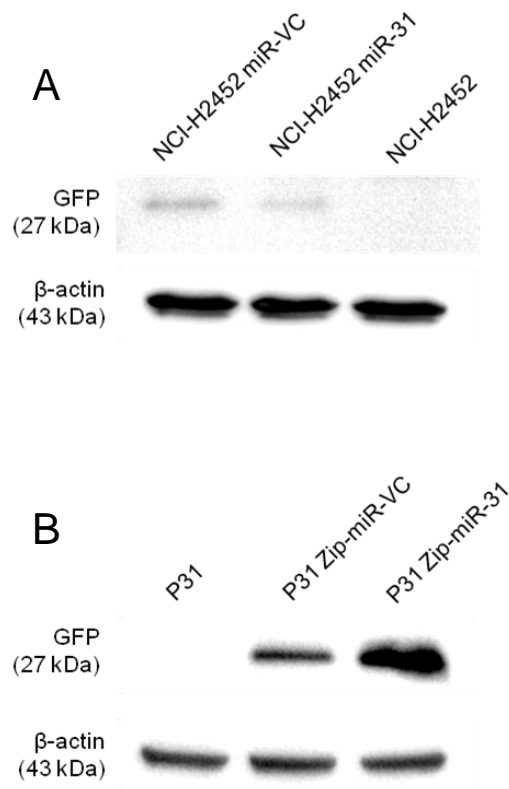
Figure 3.3 Confirmation of stable transfection. (A) Representative Western blot indicating GFP expression in transfected NCI-H2452 cell line; with β-actin as a loading control. (B) Representative Western blot indicating GFP expression in transfected P31 cell line; with β-actin as a loading control. The data demonstrates successful transfection of stably selected plasmids in both cell lines, and illustrates the Zip-down plasmids confer stronger GFP signal (B) than the overexpression plasmids (A). Blots detailed are representative of *n=2*.

3.4.3 *MiR-31 modulates sensitivity to platinum-based therapy in MPM*

In order to establish if miR-31 modulation altered clonality of cells treated with platinum-based chemotherapy, the clonogenic assay was applied using the appropriate IC_{50} doses (Fig. 3.4) of 1 μM and 2 μM cisplatin for the NCI-H2452 overexpression model and the P31 suppression model, respectively; as well as 10 μM and 40 μM carboplatin for the NCI-H2452 overexpression model and the P31 suppression model, respectively. It was established that there was a 9.6% ± 1.6% significant increase in resistance with miR-31 reintroduction in the NCI-H2452 cell line with cisplatin treatment (Fig. 3.5). Furthermore, there was an 8.4% ± 0.2% significant increase in sensitivity to cisplatin with the silencing of miR-31 in the P31 cell line (Fig. 3.6), and a 19.3% ± 0.2% increase with carboplatin treatment with miR-31 suppression (Fig. 3.7). However, the silencing of miR-31 in the P31 cell line led to no significant difference in surviving fraction when treated with carboplatin (Fig. 3.8). There may be a partial explanation to this, relying on the silencing of a particular miRNA potentially leading to a modification in the modulation of the cellular membrane integrity. Carboplatin relies upon passive diffusion to enter the cell [260]; hence potential alterations to the cell membrane may modulate the ability of the molecule to enter the cellular environment. Overall, these data demonstrate that miR-31 influences the response to platinum-based chemotherapeutics.

3.4.4 *MiR-31 re-expression does not affect response to radiation treatment in vitro*

In order to assess whether the miR-31 mediated alterations in resistance were specific to chemotherapy, radiosensitivity was analysed using the clonogenic assay with a range of treatment doses, from 2 to 6 Gy. No alterations in surviving fraction
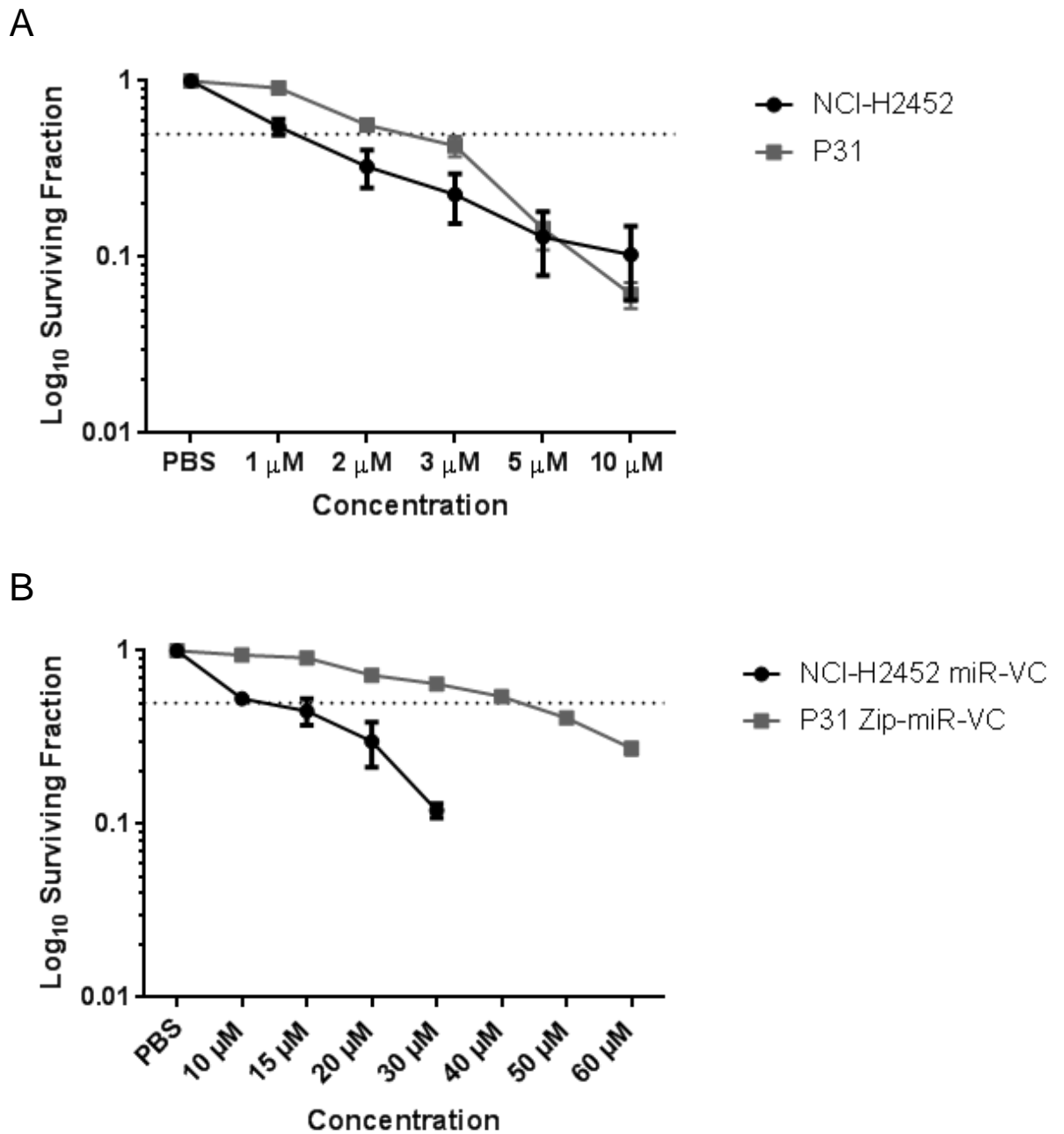
Figure 3.4 IC_{50} doses of chemotherapeutics in MPM cell lines. (A) Dose response for cisplatin treatment for 24 h in the miR-31-deficient NCI-H2452 cell line (*n*=5) and P31 miR-31-positive cell line (*n*=3). Dose of 1 μM cisplatin determined for NCI-H2452, and 2 μM determined for P31. (B) Dose response for 48 h treatment with carboplatin in control transfected cell lines (*n*=3). Dose of 10 μM carboplatin determined for NCI-H2452 miR-VC, and 40 μM determined for P31 Zip-miR-VC. Cisplatin treatment was utilised for 24 h and carboplatin for 48 h in line with current literature, and due to more moderate effect of carboplatin treatment. All clonogenic assays were vehicle controlled with the analysis of PBS treated controls taken into account in surviving fraction calculations. Although plotted, where error bars are not visible, data replicates are within 0.05 surviving fraction.
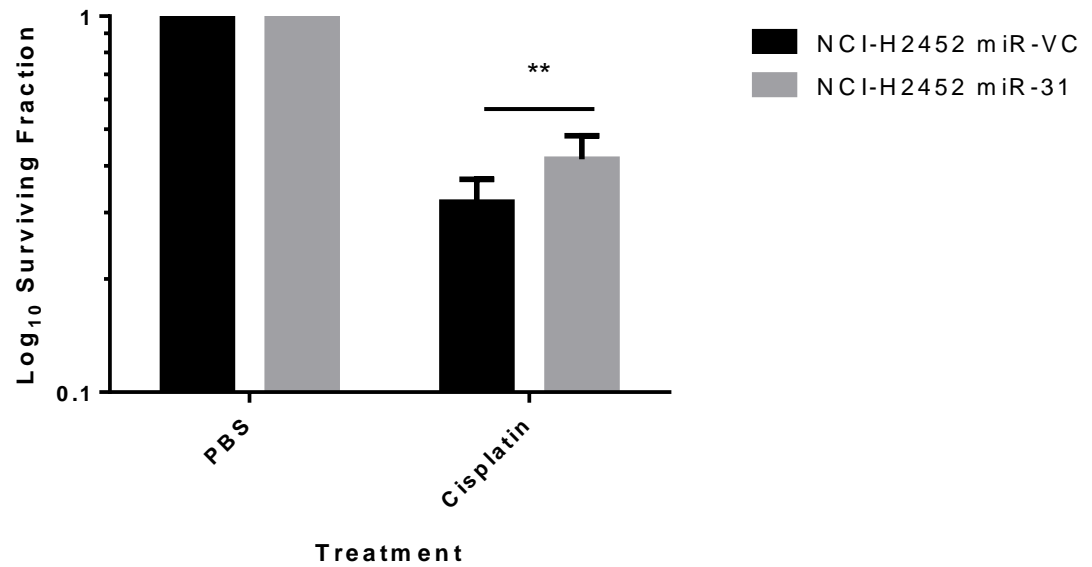
Figure 3.5 MiR-31 reintroduction in MPM cells increases cellular resistance in response to cisplatin treatment. Clonogenic analysis of miR-31 reintroduction illustrated a significant difference (**p=0.0028) between the surviving fractions of miR-VC transfected cells treated with 1 μM cisplatin for 24 h, compared to miR-31 transfected equivalent (*n*=7). Data demonstrate that miR-31 influences the response to cisplatin treatment by increasing the surviving fraction of NCI-H2452, connoting miR-31 reintroduction increasing resistance to cisplatin. All clonogenic assays were vehicle controlled; as such no error is associated for PBS treatment (set to 1), with the analysis of controls taken into account in surviving fraction calculations. Data presented as the mean ± SEM. Student's *t*-test applied between NCI-H2452 miR-VC and NCI-H2452 miR-31 cell lines.
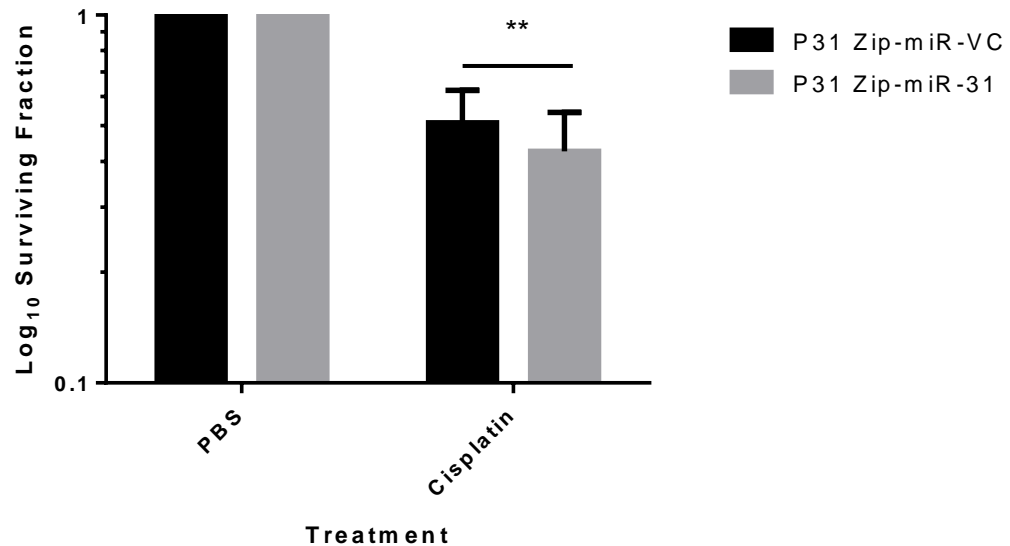
Figure 3.6 MiR-31 suppression in MPM cells increases cellular sensitivity in response to cisplatin treatment. There is a significant difference (**p=0.0084) between the surviving fractions of P31 Zip-miR-VC transfected cells treated with 2 μM cisplatin for 24 h, compared to Zip-miR-31 equivalent (n=3). Data demonstrates that conversely to that of miR-31 reintroduction, miR-31 suppression leads to a significant increase in sensitivity to cisplatin treatment. All clonogenic assays were vehicle controlled; as such no error is associated for PBS treatment (set to 1), with the analysis of controls taken into account in surviving fraction calculations. Data presented as the mean ± SEM. Student's t-test applied between P31 Zip-miR-VC and P31 Zip-miR-31 cell lines.
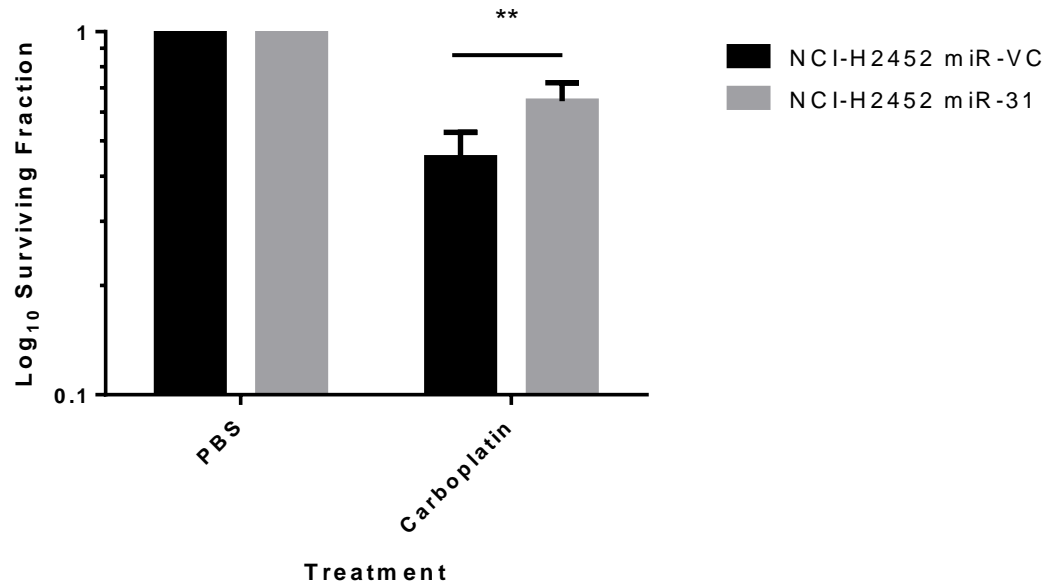
Figure 3.7 MiR-31 reintroduction in MPM cells increases cellular resistance in response to carboplatin treatment. MiR-31 reintroduction significantly increases the surviving fraction of NCI-H2452 cells treated with 10 μM carboplatin for 48 h (**p=0.0073) (*n*=3). Data demonstrates that as in cisplatin treatment, miR-31 reintroduction increases chemoresistance. All clonogenic assays were vehicle controlled; as such no error is associated for PBS treatment (set to 1), with the analysis of controls taken into account in surviving fraction calculations. Data presented as the mean ± SEM. Student's *t*-test applied between NCI-H2452 miR-VC and NCI-H2452 miR-31 cell lines.
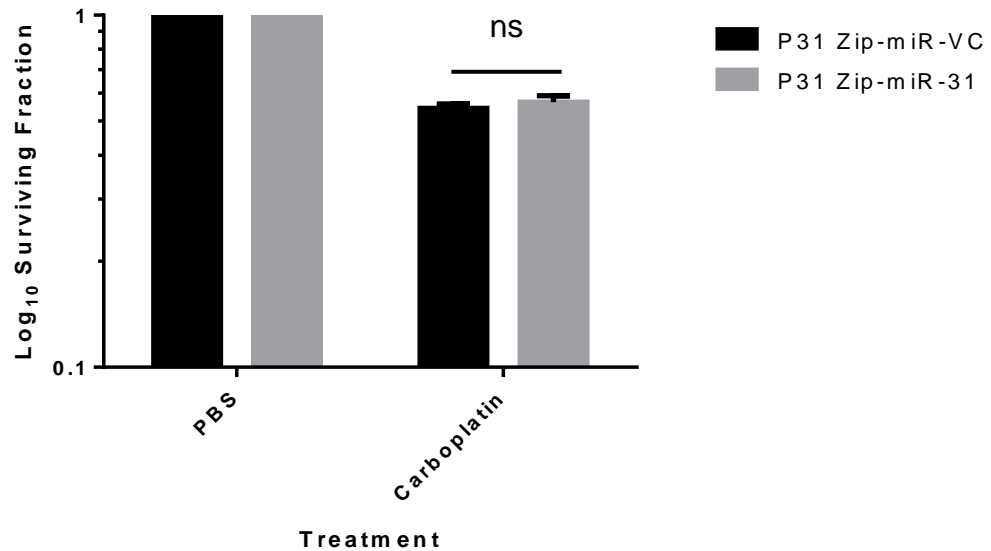
Figure 3.8 MiR-31 suppression in MPM cells does not alter sensitivity to carboplatin treatment. Suppression of miR-31 does not significantly alter the surviving fraction of MPM cells treated with 40 µM carboplatin for 48 h (p=0.0198) (n=3). Data demonstrates that suppression of miR-31 does not affect carboplatin chemoresistance. All clonogenic assays were vehicle controlled; as such no error is associated for PBS treatment (set to 1), with the analysis of controls taken into account in surviving fraction calculations. Data presented as the mean ± SEM. Student's *t*-test applied between P31 Zip-miR-VC and P31 Zip-miR-31 cell lines.

between vector control and miR-31 expressing cells were found at any dose (Fig. 3.9), although large errors in the dataset may cloud the clarity and resolution of the assay. Although chemo- and radio-therapy both target DNA, they have very different mechanisms of action. Our results indicate a chemotherapy specific enhancement of resistance, most likely attributed to a mechanism that is chemotherapy limited.

3.4.5 *Reintroduction of miR-31 confers a delay in the cellular response to cisplatin*

Following on from the increase in resistance to chemotherapy observed with miR-31 reintroduction into MPM cell lines, we analysed whether there were general phenotypic differences between the cell populations. In NCI-H2452 reconstituted with miR-31, cellular viability remained unchanged, despite the clonogenic assay revealing an increase in surviving fraction (Fig. 3.10). This may be partially attributed to the timescale on which the methods are measured. Subsequently, by employing a 9-day cumulative cell count assay which covers a similar period of time to the clonogenic assay, we observed a disparity in the ability of the miR-31 overexpressing NCI-H2452 cells to respond to cisplatin; only after 9 days post treatment with cisplatin was there a significant change in proliferation of NCI-H2452 miR-31, whereas the vector control equivalent was significantly affected by cisplatin 3 days post treatment, suggesting a delay in response to cytotoxics (Fig. 3.11). The lapse in response may be consistent with differing modes of cell death, with apoptosis completing in 2-3 h post induction, whereas non-apoptotic events such as mitotic catastrophe can take days to accrue [68], importantly the NCI-H2452 has a doubling time of 30 h compared to the 24 h for P31 cell line, meaning the P31 could be more susceptible to more rapid forms of cell death [261].
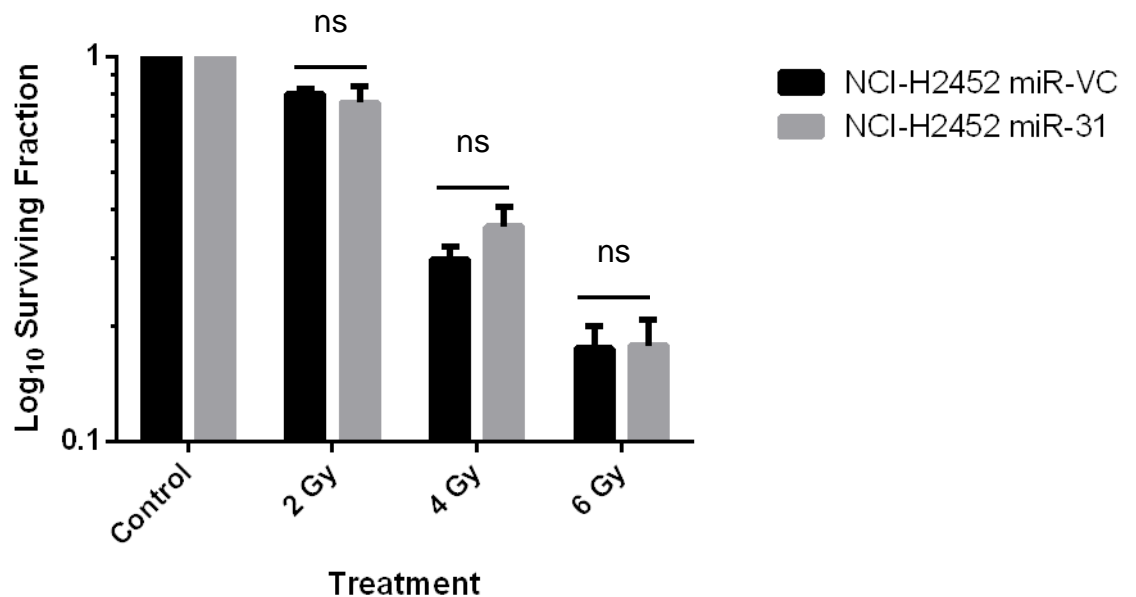
Figure 3.9 The reintroduction of miR-31 does not modulate radiosensitivity in NCI-H2452. To determine the dose response for NCI-H2452 miR-VC and NCI-H2452 miR-31 cells, cells were irradiated with 2 Gy, 4 Gy and 6 Gy at a rate of 1.87 Gy/min (*n*=3). Data demonstrates no difference in response to irradiation at any dose with miR-31 reintroduction, suggesting the resistance observed with cisplatin and carboplatin may be chemotherapy limited. Controls were mock irradiated, and used to normalise surviving fractions, as such no error is associated. Data presented as ± SEM. ns= non significant. Student's *t*-test were utilised between individual treatment groups.
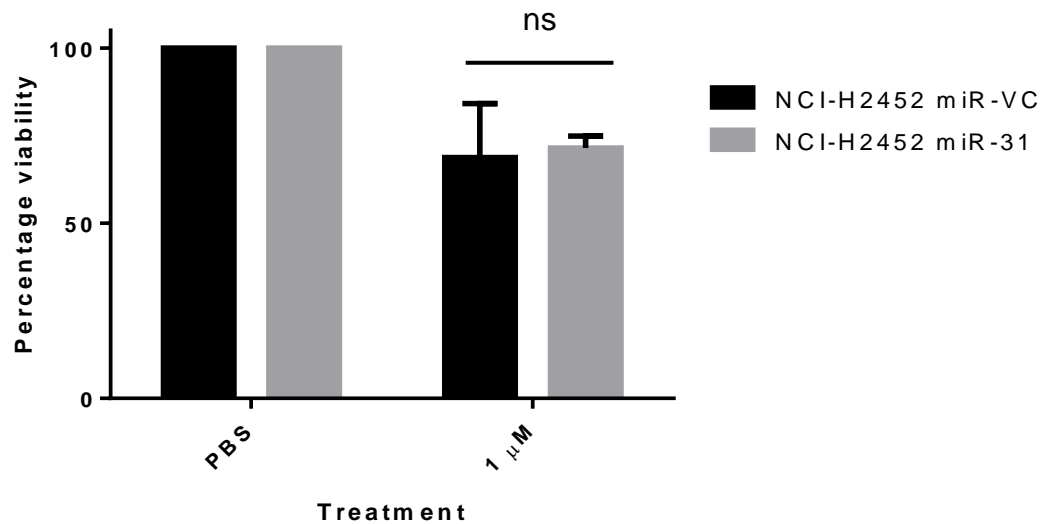
Figure 3.10 The reintroduction of miR-31 does not alter cellular viability. As measured by the MTS cellular viability assay, the percentage viability of cisplatin treated (1 μM) relative to the control PBS treated cells remains unaltered by miR-31 status (*n*=3). Data demonstrates that cellular viability, as measured by metabolism, remains unaltered despite of miR-31 status, this may relate however to the 4 day period in which the MTS assay in conducted, rather than the longitudinal 10 day assay of the clonogenic. Data was normalised firstly to medium only wells, then to vehicle control PBS treated wells. Data presented as ± SEM. ns= non significant. Student's *t*-test were utilised between individual treatment groups. PBS treatment utilised as relative control and is set to 100, as such no error is associated.
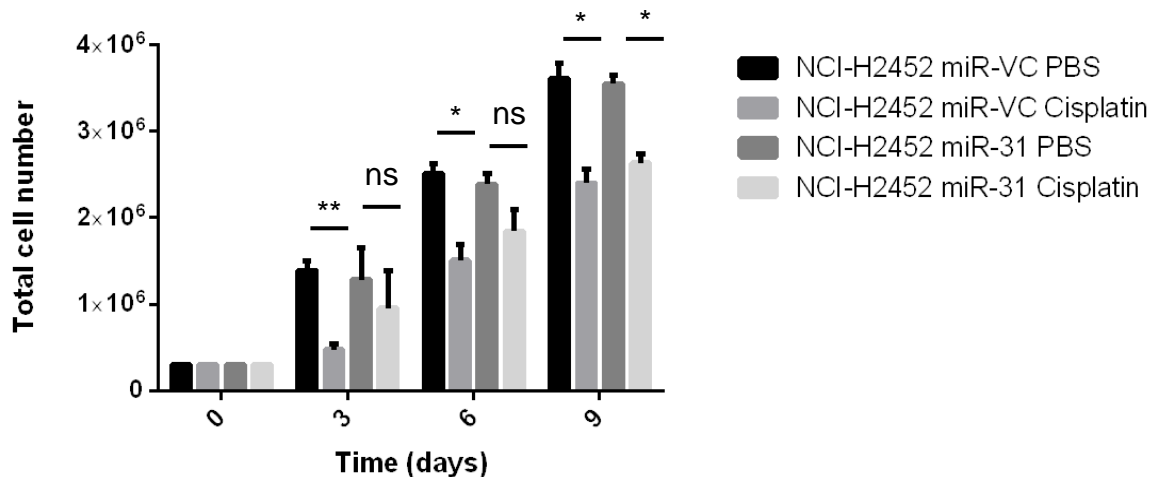
Figure 3.11 MiR-31 modulation in MPM cells alters cellular sensitivity in response to platinum-based chemotherapy treatment. Assaying cumulative proliferation with cisplatin treatment revealed a significant decrease in proliferation at all time points in miR-VC cells, whereas miR-31 cells appear less sensitive to the chemotherapeutic agent. The reintroduction of miR-31 in NCI-H2452 cells alters cellular proliferation in response to cisplatin treatment. NCI-H2452 miR-VC cells treated with 1 µM cisplatin have a significant difference in proliferation compared to NCI-H2452 miR-VC untreated cells at day 3 (**p=0.0027), day 6 (*p=0.0366) and day 9 (*p=0.0191) (n=3). There is no significant difference between NCI-H2452 miR-31 cells treated with 1 µM cisplatin until day 9 (*p=0.0306), when compared to the untreated equivalent (n=3). Data presented as the mean ± SEM. ANOVA with Tukey's post-hoc test adopted for statistical analysis. Day 0 results are all seeded with 3×10^5 cells; as such no error is associated.

The diameters of colonies were significantly increased in the presence of miR-31 with cisplatin treatment (Fig. 3.12), suggesting miR-31 may be influencing proliferation, however suppression of miR-31 did not affect colony diameter, this may be explicated by the large errors in the dataset. Although in contrast to the proliferation data of Fig.3.11, rather than a measure of proliferation, colony diameter may be an indication of how diffuse colonies are, as colonial cells could be spread over a greater area according potentially to how migratory or invasive the cells are; this observation could be supported by an invasion or migratory assay.
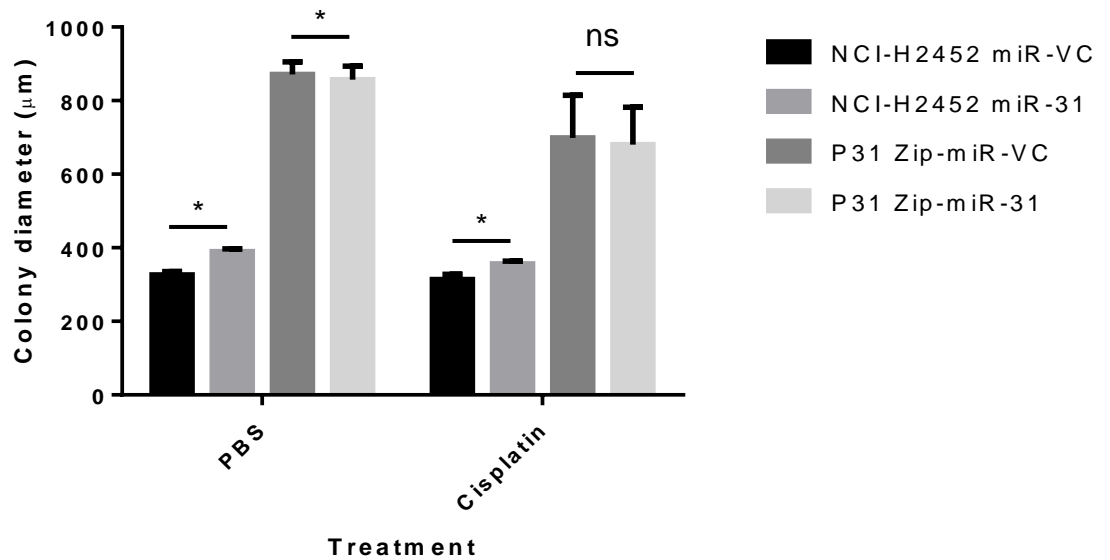
Figure 3.12 MiR-31 modulation in MPM cells affects colony size. Colony diameter is significantly increased in miR-31 expressing cells ($p = 0.0284$) with and without chemotherapy treatment (*$p = 0.0359$). Suppression of miR-31 significantly (*p=0.0489) reduces the diameter of colonies with vehicle control treatment; however this is unsignificant in the cisplatin treated miR-31 suppressed MPM cells (n=3). Data demonstrates that miR-31 is influencing colony diameter irrespective of treatment. Data presented as the mean ± SEM. Student's *t*-test were utilised between individual treatment groups.

3.5 Discussion

It is apparent that the role of miR-31 within differing tumour types remains unclear, and there is evidence supportive of oncogenic and tumour suppressive functions [195, 254, 256]. Within MPM, the fragile site at which miR-31 is encoded has been correlated with poor prognosis [188], however, it has also been reported that miR-31 expression is allied with aggressive subtypes, those with a poor prognosis, in patient cohorts [189]. Surprisingly, here, we have determined that miR-31 expression in MPM promotes resistance to platinum-based therapy *in vitro*. Consequently, loss of miR-31 in MPM tumours might actually confer a chemosensitive phenotype. Contrasting with our original hypothesis, the data support the alternative hypothesis that miR-31 loss in MPM may confer a positive prognostic influence.

With the data presented in this chapter, miR-31 expression promotes resistance to platinum-based chemotherapy in MPM cell lines. MiR-31 overexpression has been generally associated with tumour suppression [262], however, it is noted to amplify oncogenesis in many cancers, including lung cancer [263], a summary of miR-31 realtionship in MPM is in Table 3.2. Within cervical cancer, it has been reported that miR-31 is highly expressed, and is significantly correlated with higher stage of disease, deep stromal invasion, as well as lymph node metastasis. The downregulation of miR-31 was demonstrated to impair migration, invasion, cell proliferation, colony formation *in vitro* in cervical cell lines, and inhibited cervical xenograft tumour growth *in vivo*, suggesting higher expression of miR-31 increases the aggressiveness of cervical cancer [264].

Of the publications relating to miR-31 in MPM, the observations here agree with miR-31 overexpression promoting a more aggressive disease [189], due to the chemoresistant phenotype observed. Matsumoto *et al.* [189] used 25 FFPE patient

Table 3.2 Summary of miR-31 expression effects in MPM

miR-31 effect	Summary of investigation	Reference
Pro-tumorigenic, effects PPP6C expression	- Loss of miR-31 expressed in many MPM cell lines - miR-31 inhibits progression of MM cells to S-phase - Reintroduction of miR-31 suppressed genes involved in DNA repair, replication, and cell cycle	Ivanov *et al.*[188]
Upregulation of microRNA-31 associates with a poor prognosis	- miR-31 status assessed in 24 FFPE samples - Wide variation in miR-31 expression amongst subtypes - High miR-31 expression strongly correlated with sarcomatoid subtype	Matsumoto *et al.*[189]
Reintroduction of miR-31 increases chemoresistance	- Reintroduction of miR-31 increased resistance to cisplatin and carboplatin - Suppression of miR-31 led to increased sensitivity to cisplatin - Basal proliferation is unaltered by miR-31 status, however colony size may be increased	Moody *et al.* (under review)

derived MPM samples, of different clinical subtypes, to examine miRNA content. Their focus upon miR-31 was due to the coding chromosomal location neighbouring the often-deleted chromosomal region encoding p16 [189, 256]. The deletion of the chromosomal region 9p21.3, encoding the p16/CDKN2A/CDKN2B tumour suppressor genes and the methylthioadenosine phosphorylase mTAP, promotes disruption in the regulation of the cell cycle and apoptosis [265-267]. In their study there was no difference in overall survival between normal and miR-31 downregulated groups (30.1 months vs 27.3 months), this is in contrast to the correlation reported in Ivanov *et al.* [188] for MPM. However, there was a significant decrease in overall survival in high miR-31 expressing MPM tumours, with an average OS of 5.3 months.

In contrast with the observations made here, and Matsumoto *et al.* [189], Ivanov *et al.* [188] correlated miR-31 expression with the repression of pro-tumourigenic properties, such as a reduction in migratory, invasive and proliferative ability. Similarly to the methodology adopted for this research, an antagonistic model was implemented to overexpress, or reintroduce, miR-31 into a cell line devoid of miR-31 expression, and conversely to suppress the expression of miR-31 within an endogenously expressing cell line. To facilitate the manipulation of miR-31, mimics and inhibitors were used. Alongside differences in observational endpoints, it was concluded that miR-31 re-introduction led to a reduction in cells in S-phase, and inhibition of miR-31 led to an increase in the S-phase cell ratio alluding to miR-31 significantly affecting cell cycle progression. Here, our results oppose the conclusions drawn by Ivanov *et al.* [188]. The investigation here focussed upon the relationship between chemoresistance and miR-31 within MPM, Ivanov *et al.* [188] made no observations with any mode of treatment. Additionally, the use of mimics and inhibitors was transient rather than the stable system adopted here. Transient

expression systems are useful for observational studies, but without data showing the status of miR-31 for the duration of assays, the point at which miR-31 ex- or sup-pression is optimal is not clear, this issue is resolved with the use of constitutively ex- or sup-pressing miR-31 stable cell lines. Cell cycle distribution was not assessed as the analysis was not deemed necessary as the available evidence from other experiments precluded a need to do this. For example, the data on cumulative cell counts (Fig. 3.11), indicated no significant influence of miR-31 expression on basal proliferation rates of NCI-H2452 cells, indicating that cell cycle is not obviously affected by altered miR-31 expression.

Ivanov *et al.* [188] also investigated potential miR-31 targets using KEGG analysis. Kyoto Encyclopaedia of Genes and Genomes (KEGG) is a database that connects systemic functions with chemical and genomic analysis [268]. As is widely understood, databases that are predictive of miRNA targets are extremely useful as an initial starting point to investigate potential targets, however, validation is essential [269]. One of the predicted miR-31 targets was identified for further investigation, namely the protein phosphatase PPP6C. According to Ogoh *et al.* [270], PPP6C encodes PP6, which targets IκBε for degradation, subsequently triggering DNA repair. Ivanov *et al.* [188] reported an elevated expression of PPP6C in mesothelioma tissue compared to matched normal samples, however more recently in malignant melanoma, mutations in the gene encoding PPP6C have been linked to B-Raf or N-Ras driven tumourigenesis, meaning that PPP6C deficiency confers a predisposition to skin carcinogenesis [271].

The observation that miR-31 reintroduction increases chemoresistance in MPM cells, and suppression of miR-31 increases sensitivity to chemotherapy in MPM cells contradicted our initial hypothesis, which was based upon previous findings in other

cancers [256]. These preliminary investigations have uncovered an interesting conclusion that appears to be chemotherapy specific, rather than broadly therapy responsive. If miR-31 potentiated modulation of both radio- and chemo-therapy treatment, this would allude to miR-31 possibly modulating targets involved in the regulation of DNA damage response, or repair, as Wouters *et al.* [272] comprehensively reviewed. Rather than a generalised response to DNA damaging agents, the cytotoxic specificity has lead the investigation to focus upon the possibility that miR-31 may regulate the quantity of chemotherapy within MPM cells, as chemoresistance has been attributed to altered influx and efflux of drugs within the cellular environment in a wide variety of cancers [75, 273-275], and is noted as a major contributing factor to cancer chemoresistance [274].

There are interesting differences between cisplatin and carboplatin functionality within the cellular environment that may help to explicate the differences in response to cisplatin vs carboplatin. Cisplatin is a small compound, however, carboplatin is larger and has less toxicity per mol, with an improvement on side effects of treatment in patients [276]. Although some literature exists to support active transport of carboplatin, by proteins such as CTR1, or by ion channels, carboplatin is thought to be more reliant upon passive diffusion to enter the cellular environment [76, 260]; hence, potential alterations to the cell membrane may modulate the ability of the molecule to enter the cellular environment. Here, it may mean that miR-31 suppression leads to an alteration in transport across the membrane, perhaps suggesting that miR-31 suppression is driving alterations in membrane structure or composition, as in Llado *et al.* [277]. The next chapter explores the relationship between miR-31 and how it might modulate the response to platinum-based chemotherapeutics. A summary of chapter 3 in pictorial form is depected in Fig. 3.13.
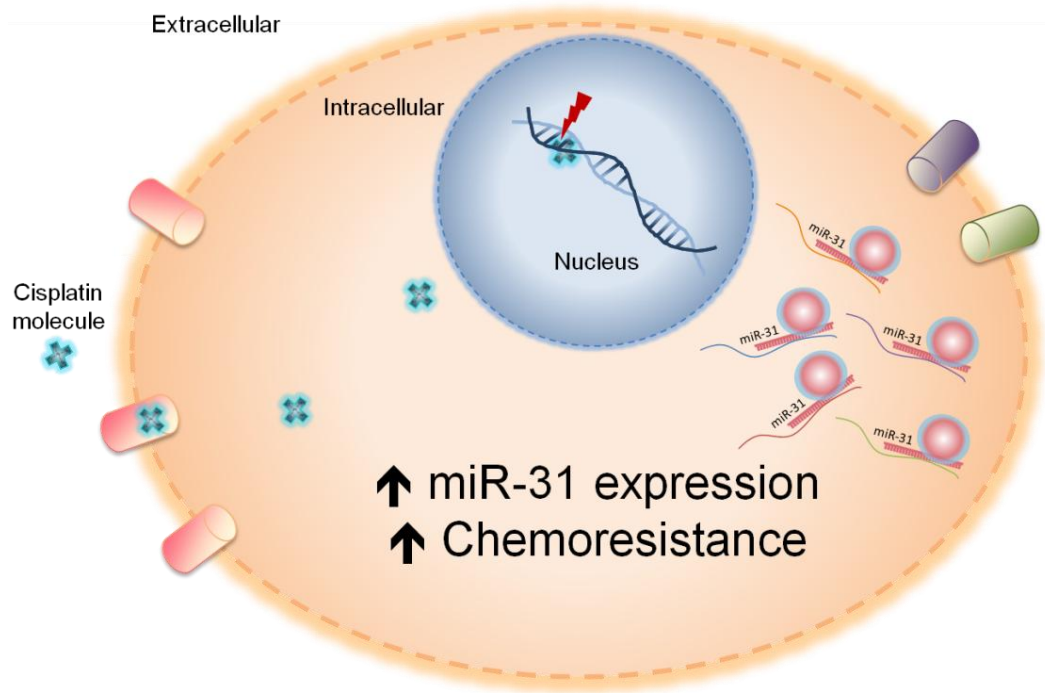
Figure 3.13. Summary of the effect of miR-31 reintroduction on MPM cell. The MPM cell (orange) has notable increased resistance to chemotherapy (blue cross structures) with miR-31 reintroduction. The pleiotropic nature of miR-31 may mean that the miRNA is targeting multiple pathways which ultimately lead to a less chemosensitive phenotype.

Chapter 4:

MiR-31 modulates the intracellular accumulation of chemotherapeutics in MPM

4.1 Introduction

The mechanisms underpinning drug resistance in cancer cells are substantial and complex [274]. MiRNAs have previously been linked to the modulation of many different pathways associated with multi-drug resistance [278-281]. MiR-31-mediated posttranscriptional regulation of genes that potentiate resistance has been investigated in other cancer types [282]. Within the context of this study, a correlation between miR-31 re-expression and increased therapeutic resistance has been observed; this was noted only in MPM cells subjected to chemotherapy, not radiation. Pathways that respond to both chemo- and radio-therapy, such as the nucleotide excision repair (NER) and base excision repair (BER) pathways, act to repair non-specific DNA damage that is induced by both chemotherapy and radiation treatment [283]. With no evidence of miR-31 modulated alterations to overall radioresistance (Figure 3.9), changes to cellular drug metabolism and drug transportation may well be contributing to the resistance observed [273, 284, 285].

The foundation of treatment for MPM is a platinum-based chemotherapy, most often cisplatin, administered in combination with the antifolate pemetrexed [79, 82]. Cisplatin resistance has broadly been attributed to altered DNA repair, altered accumulation and cytosolic inactivation, which as individual mechanisms can enhance resistance [286]. Cisplatin enters cells via active or passive transport [75]; the copper transporter CTR1 has previously been identified as the major facilitator of cisplatin influx into the intracellular environment, with reports of CTR1-deficient cells accumulating 2.3-fold less platinum in their DNA compared to CTR1-competent cells, interestingly CTR1-deficient cells were also more resistant to cisplatin [70, 287]. CTR1 expression levels have been correlated with chemoresistance in other cancers, where reduced expression, or reduced influx,

resulted in decreased cisplatin accumulation leading to resistance [288]. Post influx, cisplatin can be chelated with glutathione throughout the intracellular environment, which also has a role as a redox regulating protector in response to cisplatin treatment [289]. An additional chaperone of cisplatin has been identified in Atox1, which binds with cisplatin via its conserved metal-binding motif, and reportedly convoys the molecule through the cytoplasmic compartment [71, 290]. The relationship between Atox1 expression and resistance has not been documented, but has been highlighted as an area of potential investigation, due to the protein potentially contributing to the regulation of cisplatin accumulation [61, 291]. The proteins mainly responsible for efflux of copper, and thus cisplatin, are the ATPases ATP7A and ATP7B. ATP7A and ATP7B segregate intracellular cisplatin into the vesicular secretory pathway in preparation for efflux from the cell, and can also be located on the plasma membrane [292-294]. There have been studies associating ATP7A and ATP7B with oxaliplatin resistance, where it is described that the dysregulation of these proteins leads to greater efflux of chemotherapy, reducing the potential for reactions with chemotherapeutic targets, such as DNA [295-297]. Oxaliplatin is generally not utilised for MPM treatment, however, interestingly, it is thought to have a different mechanism of action to other platinating agents. Oxaliplatin has a DACH (diaminocyclohexane) carrier ligand, which similarly to cisplatin, can induce DNA cross links, however it can be argued that oxaliplatin has greater efficiency. Cisplatin-induced cell death depends on an intact MMR (mismatch repair) complex for its optimal cytotoxicity. In contrast, oxaliplatin adducts are poorly recognised by MMR protein complexes, thus meaning oxaliplatin can retain cytotoxicity in MMR-proficient and MMR-deficient cells [298].

The role of chemotherapy transport in MPM is poorly understood, despite cisplatin being one of the most commonly used treatments. This chapter therefore aims to

explore the potential mechanisms as to why miR-31 re-expression promotes chemoresistance.

4.2 Rationale, Aims and Objectives

MPM cells expressing miR-31 display increased resistance to platinum-based chemotherapeutic treatment. MiRNAs have been shown to alter many different resistance associated pathways, including modulation of drug transportation. We hypothesised, based upon current information, that miR-31 may modulate the transportation of chemotherapy within MPM cells. With this in mind, the ability of miR-31 to modulate drug trafficking within the cellular environment was assessed.

The objectives of this chapter were 1) to explore the effect of miR-31 expression on the levels of uptake of platinum-based chemotherapy in MPM cells 2) to identify potential molecular mechanisms underpinning any miR-31 mediated alterations in chemotherapy transport in MPM cells.

4.3 Experimental design

4.3.1 *Assessing the concentration of platinum within MPM cells*

In order to analyse the platinum content, thus indicating cisplatin content, ICP-MS was utilised. ICP-MS has been adopted for the analysis of chemotherapy within the cellular environment in a range of publications, including the investigation by Barr *et al.* [299] of NSCLC cisplatin resistant cell lines and their ability to alter intracellular cisplatin content.

4.3.2 *Analysis of transport related proteins*

To establish whether influx, efflux and sequestration related proteins were involved in the chemoresistant phenotype observed within the miR-31 modulated MPM cells Western blot and immunoflourescent microscopy was adopted, as is often used in support of protein expression analysis [300]. The Western blot analysis indicated the up- or down-regulation of respective proteins; however immunoflourescent microscopy additionally added information regarding the gross location of the proteins within the cellular environment, when confocal microscopy was applied and a nuclear stain utilised. To analyse whether there were transcriptional as well as translational alterations to the molecules of interest, qPCR was performed with commercially available primers.

4.3.3 *Isolation of the lysosomal compartment*

The investigation of the platinum content within lysosomes was approached using a novel technique involving the magnetic separation of lysosomes from other intracellular components via a LAMP-1 linked Protein A/G bead. Although fractionation has long been utilised to facilitate lysosome separation in research [301], the technique does not delineate between lysosomes and other membrane

bound organelles including mitochondria and peroxisomes [302], meaning the analysis of the fraction may potentiate misleading results. Therefore, the development of a novel immune-based capture of lysosomes was analysed in order to specifically pull out lysosomes in order to analyse platinum content.

4.4 Results

4.4.1 *MiR-31 alters intracellular distribution of cisplatin in MPM*

To begin to establish a potential mechanism underpinning miR-31-mediated chemoresistance, the overall concentration of platinum was assessed in the miR-31 manipulated NCI-H2452 and P31 cell lines (Fig. 4.1). Surprisingly, the intracellular level of platinum was increased in NCI-H2452 cells reconstituted with miR-31 (Fig. 4.1A). The connotation of this observation is that despite miR-31 enhancing resistance, the more resistant population of cells actually had a higher concentration of chemotherapy within them. With the observed accumulation in miR-31 expressing cells, cellular flux of chemotherapeutics was investigated. Recent studies have implicated the importance of influx and efflux of drugs in chemoresistance [273, 284]. There appeared to be a trend (p=0.0722) toward increased expression of CTR1 (Fig. 4.2), a copper transporter well established to facilitate influx of cisplatin into the cell [288, 303, 304]. No statistically significant differences in the expression of the efflux proteins ATP7A and ATP7B were ascertained (Fig. 4.3 and 4.4). The increase in influx could potentially explain, at least in part, the increased overall concentration of platinum in the miR-31 expressing cells; yet did not explain the resistant phenotype observed. To this end the cytoplasmic to nuclear levels of platinum following treatment were assessed.

4.4.2 *MiR-31 modulates nuclear accumulation of cisplatin*

To further attempt to determine how miR-31-expressing MPM cells remained resistant to cisplatin despite an increase in the level of intracellular cisplatin, subcellular fractionation was employed to separate the nuclear compartment and organelles of the cells and determine platinum burden in each fraction. The nuclear fraction was collected and analysed via ICP-MS in order to determine whether there
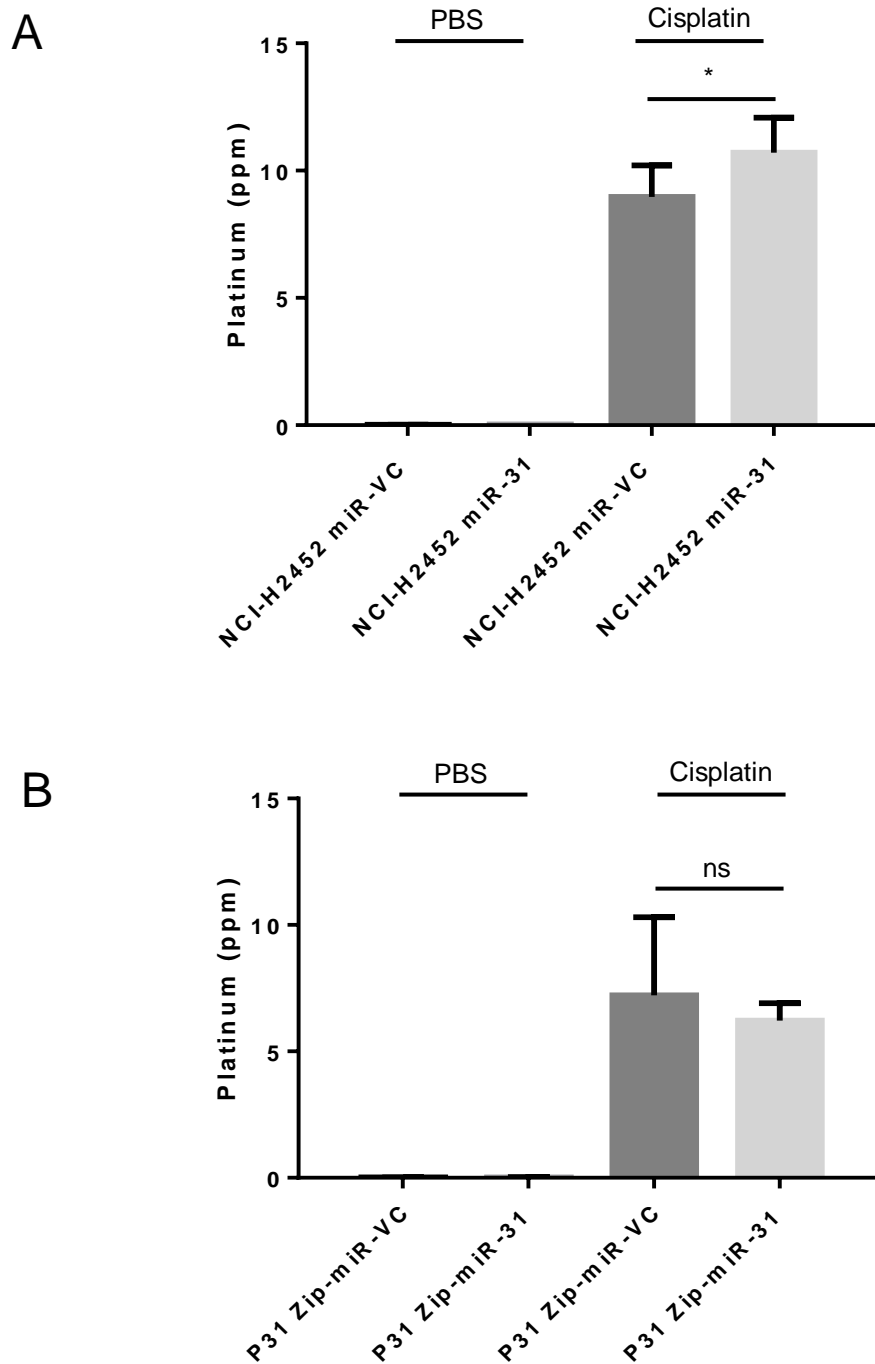
Figure 4.1. Intracellular cisplatin content is altered with miR-31 manipulation. ICP-MS analysis of whole cells with treated with 50 μM cisplatin for 24 h. (A) There is a significant (*p=0.0112) increase in levels of platinum in NCI-H2452 miR-31 cells compared to miR-VC equivalent (n=3). (B) There may be a decrease in platinum content in MPM cells with miR-31 suppressed (n=3). Data demonstrates that miR-31 reintroduction facilitates a greater burden of platinum within the intracellular environment; however the converse is not apparent with miR-31 suppression. Data presented as the mean ± SEM. ns= non significant. Statistical analysis performed using Student's t-test.
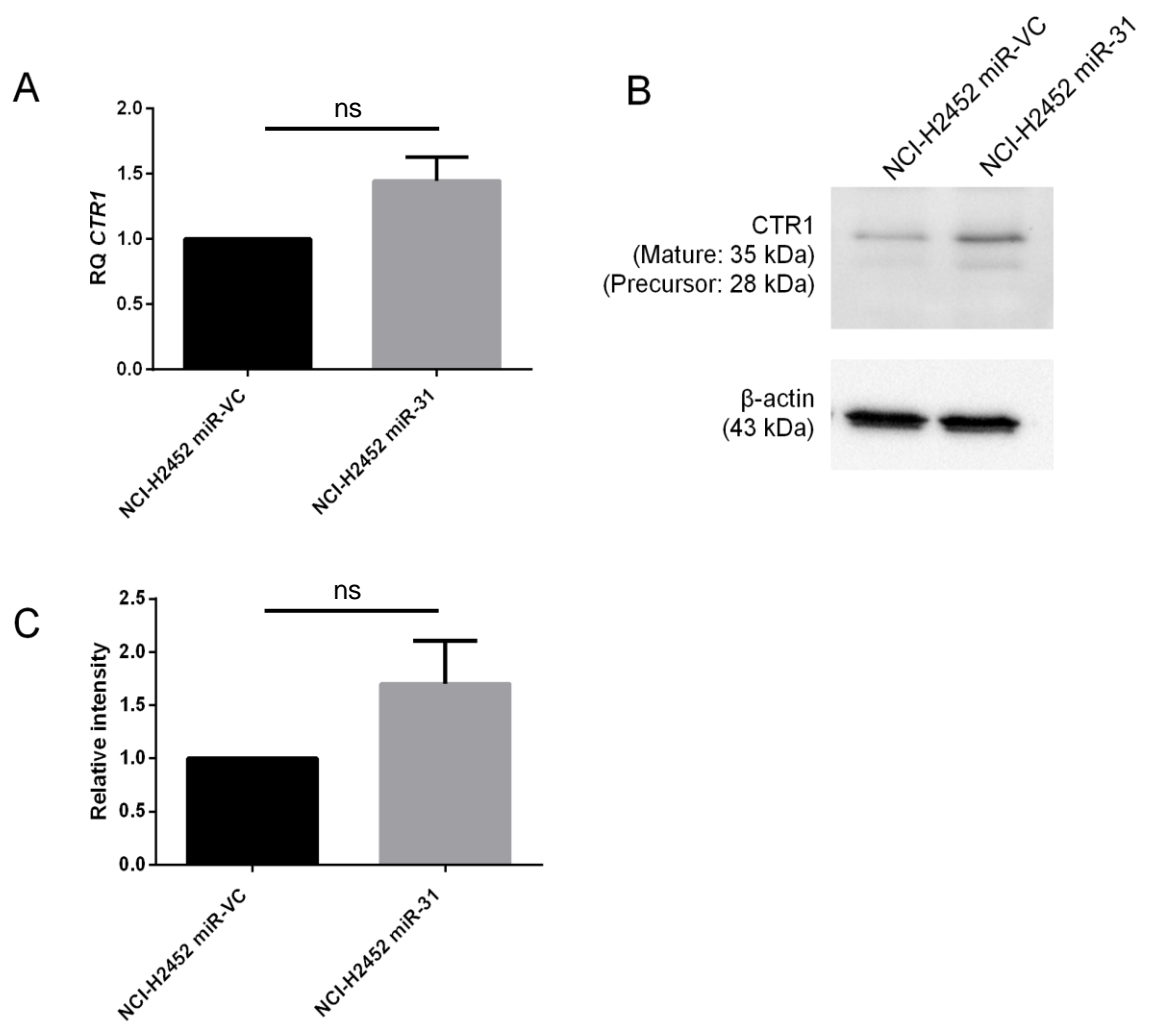
Figure 4.2 MiR-31 re-expression in MPM cells may alter the expression of drug influx transporter CTR1. (A) Expression levels of drug influx transporter *slc31a1* (copper transporter 1, CTR1) were analysed via quantitative PCR (qPCR). RQ relates to relative fold change (*n*=4). (B) Representative Western blot illustrating CTR1 expression to be moderately amplified by miR-31 reintroduction. (C) Densitometry analysis revealing upregulation of the CTR1 protein, although unsignificant (*n*=3). Data demonstrates an observable increase in the cisplatin transporter CTR1 at both transcript and translational levels, possibly contributing to the increase in intracellular platinum. Data presented as the mean ± SEM. ns= non significant. Statistical analysis performed using Student's *t*-test. NCI-H2452 miR-VC utilised as relative control and is set to 1, as such no error is associated.
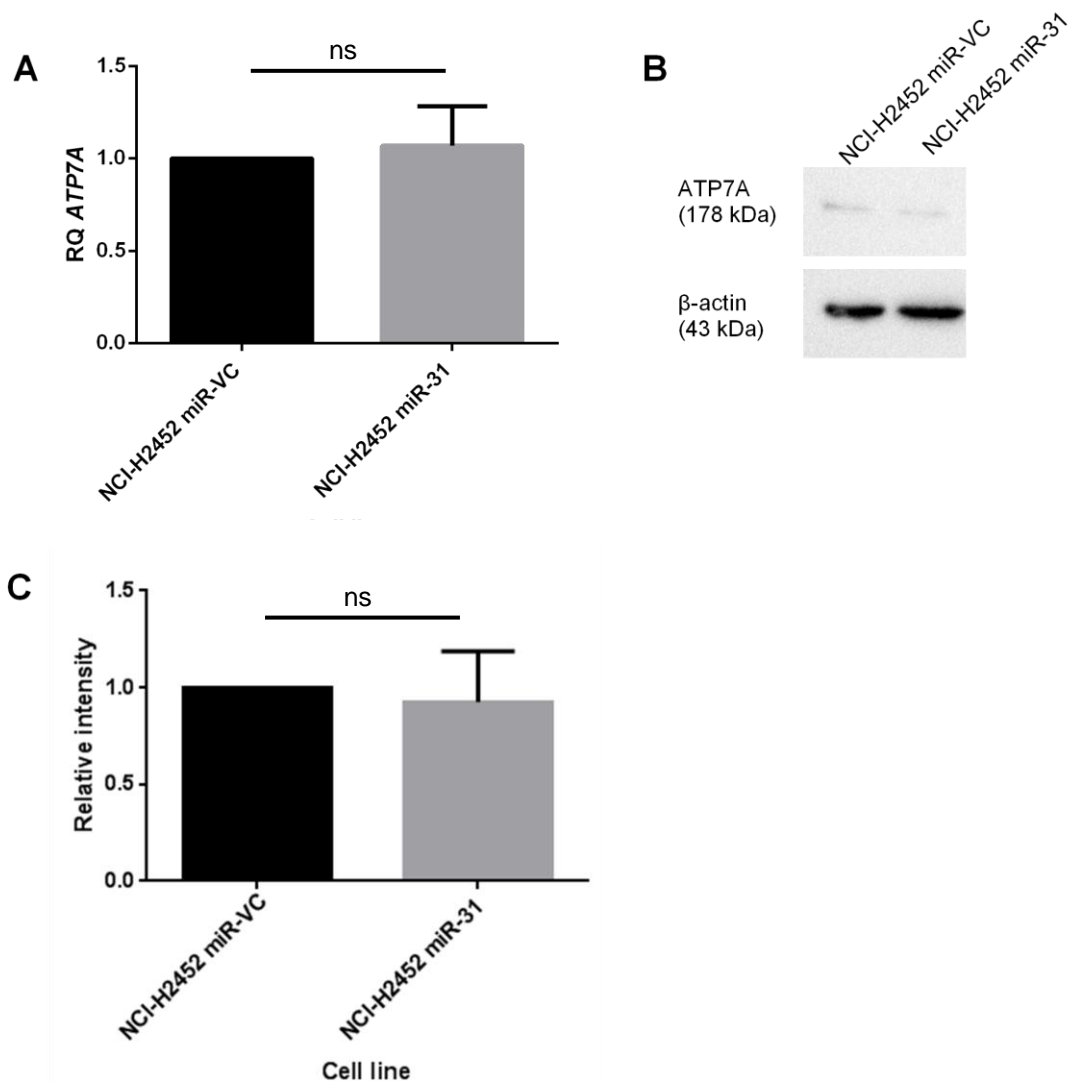
Figure 4.3 MiR-31 expression in NCI-H2452 cells does not significantly alter the expression of copper efflux transporter ATP7A. (A) There is no significant modulation in relative expression level of the transporter *ATP7A* in miR-31 expressing cells compared to miR-VC equivalent (*n*=5). (B) ATP7A protein levels appear to be unaltered by miR-31 reintroduction. (C) Densitometry of ATP7A protein levels show no change with miR-31 overexpression (*n*=3). Data demonstrates that whilst influx via copper transporter 1 (CTR1) may be of importance in the increase in intracellular platinum burden, the efflux of cisplatin is unaffected by miR-31 status. Data presented as the mean ± SEM. ns= non significant. Statistical analysis performed using Student's *t*-test. NCI-H2452 miR-VC utilised as relative control and is set to 1, as such no error is associated.
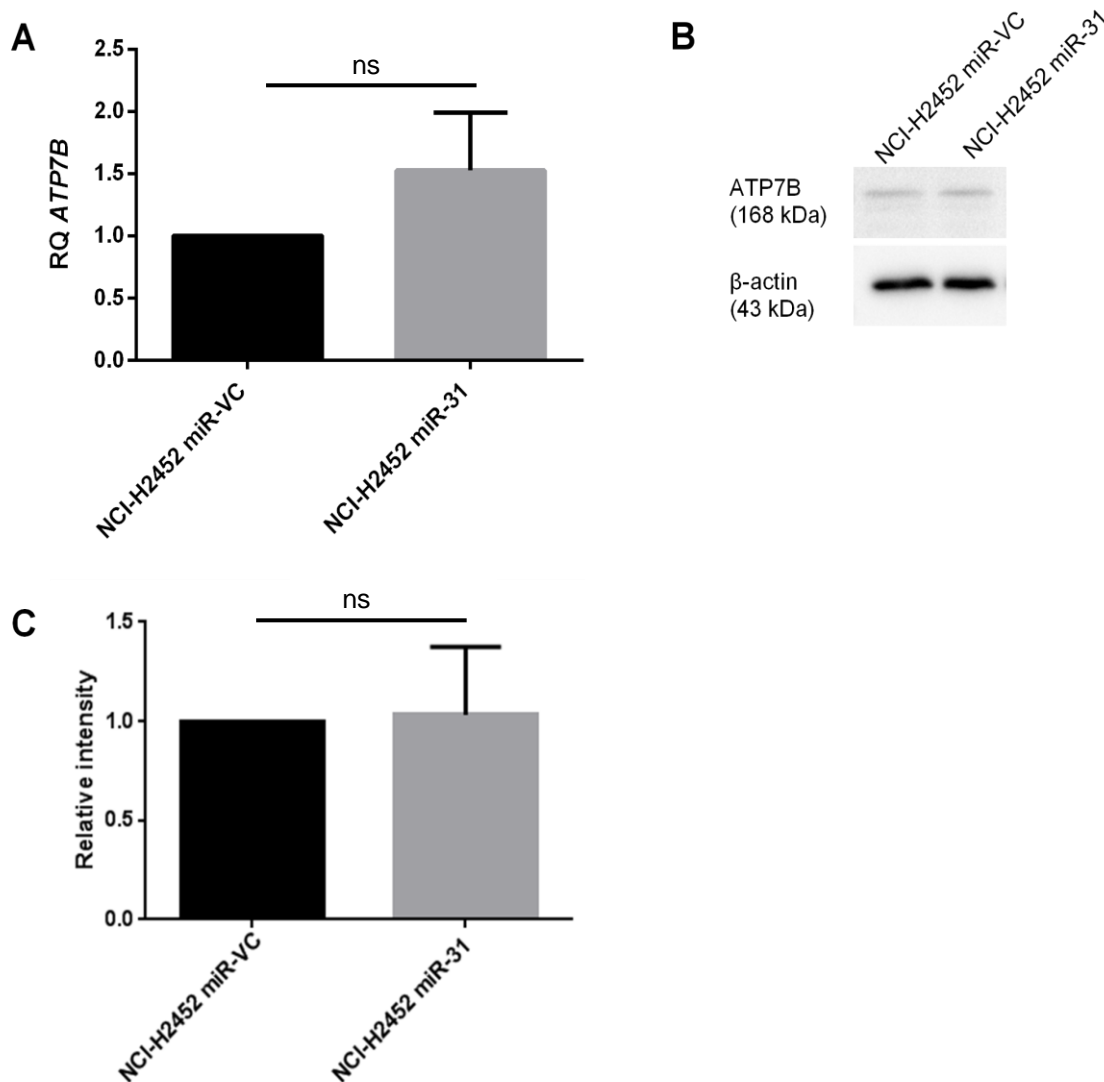
Figure 4.4 MiR-31 expression in NCI-H2452 cells does not significantly alter the expression of copper efflux transporter ATP7B. (A) There is no significant difference in the relative expression level of the transporter *ATP7B* in miR-31 compared to miR-VC equivalent (*n*=5). (B) ATP7B protein levels appear to be unaltered by miR-31 reintroduction. (C) Densitometry of ATP7B protein levels show no change with miR-31 overexpression (*n*=2). Data demonstrates that whilst influx via copper transporter 1 (CTR1) may be of importance in the increase in intracellular platinum burden, the efflux of cisplatin is unaffected by miR-31 status. Data presented as the mean ± SEM. ns= non significant. Statistical analysis performed using Student's *t*-test. NCI-H2452 miR-VC utilised as relative control and is set to 1, as such no error is associated.

was a differential in accumulation of platinum in the nuclear region, where it would be expected to promote cross-linking damage. ICP-MS analysis revealed that there was a decrease by approximately 50% in nuclear accumulation of platinum observed upon miR-31 re-expression in NCI-H2452 cells (Fig. 4.5) compared to vector control. Conversely, there may be an increased burden of platinum within miR-31 suppressed cells, as observed in Fig. 4.5; however, the error within the replicates clouds any significance in this comparison. These data indicate that the increased resistance to chemotherapy observed upon miR-31 expression is likely due to altered trafficking of drugs to the nucleus.

In order to support and confirm the reduction in nuclear accumulation with miR-31 re-expression, the influence of miR-31 on DNA damage induction was assessed, via levels of phospho-histone H2A.X (γH2A.X), which is phosphorylated on serine 139 in response to DNA damage [305]. NCI-H2452 miR-31 re-expressed cells displayed a reduction in γH2A.X levels compared to vector control, whereas P31 Zip-miR-31 cells demonstrated an increase in γH2A.X, both in response to cisplatin and carboplatin treatment (Fig. 4.6), suggesting a role for miR-31 in either antagonising DNA damage induction or promoting repair (Fig. 4.7). The alteration to γH2A.X was not platinum-based therapy limited, as a similar trend was apparent upon treatment with 5-FU (Fig. 4.8), which has a different mechanism of action in mediating damage, but still relies upon active transport into the intracellular environment. The utilisation of 5-FU rather than pemetrexed, due to pemetrexed toxicity issues (appendix 3), illustrated a decrease in γH2A.X with miR-31 re-introduction. Both 5-FU and pemetrexed treatment can affect thymidylate synthase, which leads to dTTP depletion and eventual DNA damage, this is why, with pemetrexed ineffectiveness, 5-FU was utilised as a substitute agent. However, it is important to note that as 5-FU

is a fluoropyrimidine and pemetrexed is an antifolate, they have other mechanisms of action. 5-FU can affect not only DNA, but also RNA by altering the expression of uridine-cytidine kinase which leads a cascade affect that can increase RNA damage. Pemetrexed, as well as other antifolates such as ralitrexed and methotrexate, which were not available during this study, all inhibit thymidylate synthase, however pemetrexed can also affect DHFR, GART and AICART, which not only can deplete dTTP pool, but also directly affect purine synthesis, also leading to DNA damage [306]. Interestingly, a differential expression of γH2A.X was also observed in response to DMSO treatment with miR-31 reintroduction. In order to determine whether the alterations to DNA damage were due to a gross alteration in DNA damage induction or repair pathways, levels of phospho-53BP1 were analysed post irradiation treatment (Fig. 4.9). No change was observed in radiation treated groups, strongly suggesting reliance upon altered transport and accumulation within the intracellular environment in miR-31 positive cells rather than alterations in DNA damage induction or repair.

As an alternative to analyse DNA damage, the Comet assay may have been utilised in support of the data obtained. The Comet assay relies upon electrophoresis such that cells with damaged DNA leave a 'tail' compared to those who have intact DNA, this can be quantified and modified to include analysis of cross-linking damage, particularly relevant with chemotherapy treated cells [307].

Previously, oxidant and antioxidant levels have been linked to resistance to treatment and detoxification of platinum-based therapies [307, 308]. In order to determine whether oxidant and antioxidant levels contributed to chemoresistance in this system, reactive oxygen species (ROS) generation and glutathione levels were assessed.
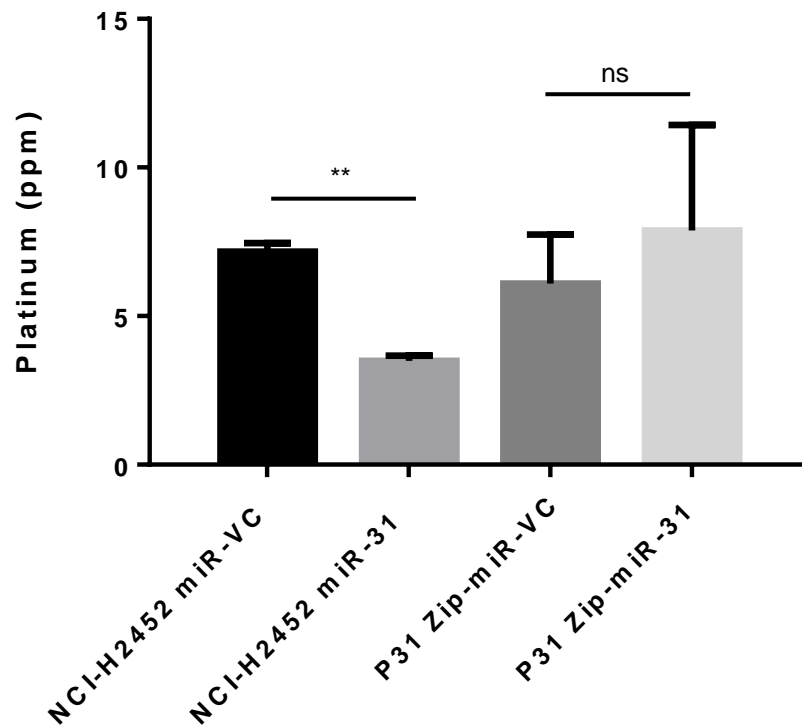
Figure 4.5 MiR-31 status affects platinum content of the nuclear region. ICP-MS analysis indicating a significant difference (**p=0.0028) in platinum concentration within the nuclear fraction of miR-31 expressing cells following 50 μM cisplatin treatment for 24 h. Platinum content within the nuclear region of miR-31 suppressed cells remains unsignificant (n=3). PBS controls were also analysed with a platinum (Pt) concentration of less than 0.1 ppm (not presented). Data demonstrates that there is approximate halving in the total amount of Pt within the nuclear region of miR-31 re-expressing MPM cells compared to vector control. Data presented as the mean ± SEM. ns= non significant. Statistical analysis performed using Student's t-test of miR-31 reintroduction or suppression cell line models.
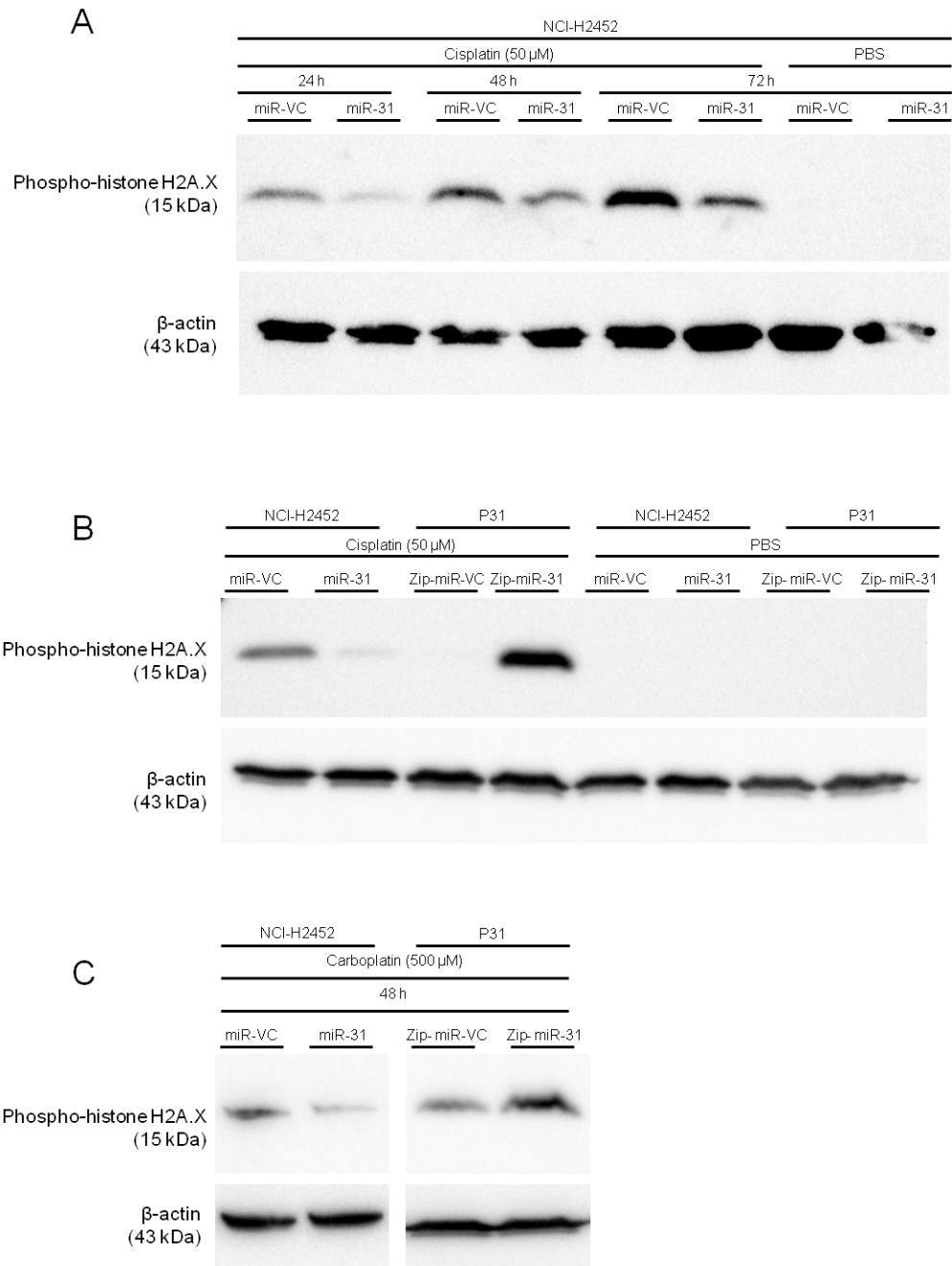
Figure 4.6 The expression of miR-31 correlates with DNA damage incurred when treated with platinum-based chemotherapeutics. (A) Representative Western blot time course for phospho-histone H2A.X as a marker of DNA damage with cisplatin treatment (50 µM). Across all time points it is evident that levels of phospho-histone H2A.X are decreased in miR-31 positive cells. (B) Representative Western blot for phospho-histone H2A.X with cisplatin treatment (50 µM). The confirmation of a reduction in DNA damage with miR-31 can be viewed in the second band (*left to right*), with an increase in DNA damage evident in the miR-31 suppressed P31 cell line. (C) Representative Western blot for phospho-histone H2A.X with carboplatin treatment (500 µM). A similar response as seen in with cisplatin is evident with carboplatin treatment. All vehicle control treated samples (PBS) were treated with the equivalent dose as utilised for drug treatment.
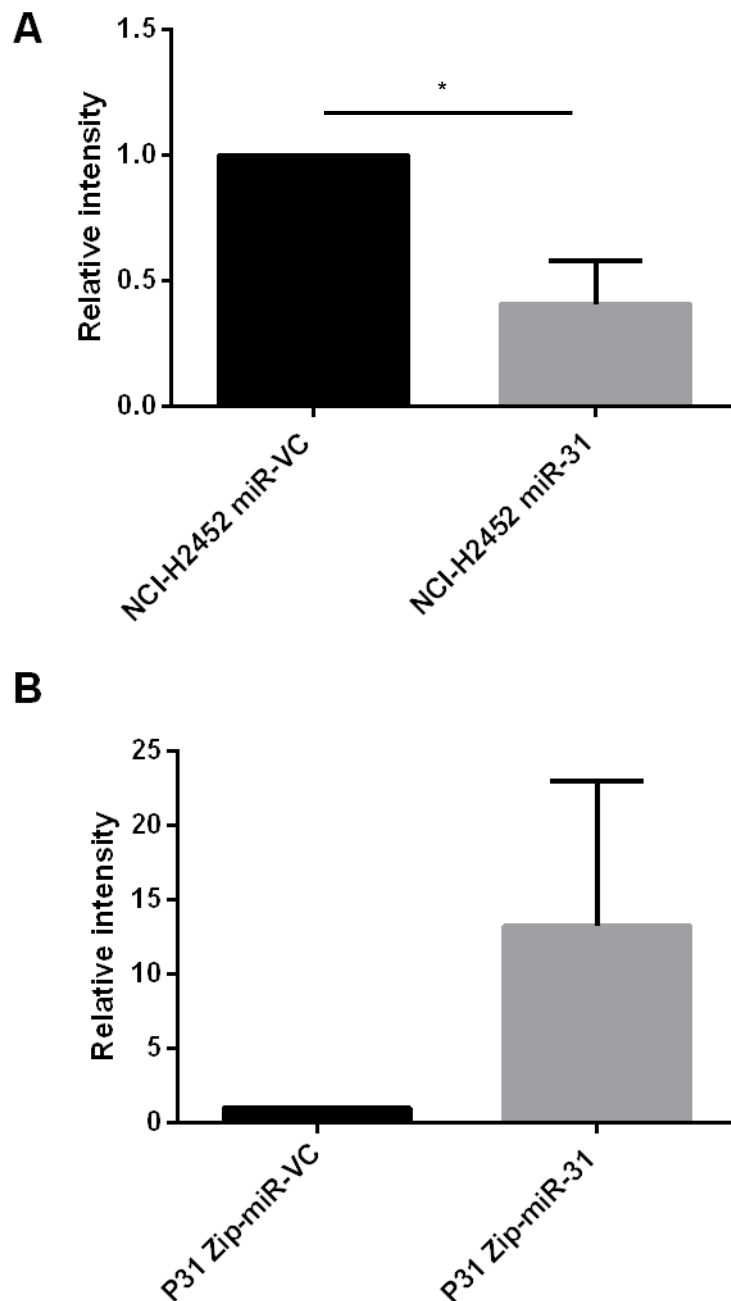
Figure 4.7 Densitometry analysis for phospho-histone H2A.X in cisplatin treated samples. (A) There is a downregulation in the DNA damage marker phospho-histone H2A.X with miR-31 reintroduction (p=0.0371) (n=3), and an upregulation (B) with miR-31 suppression (n=2). Data demonstrates that DNA damage induction is greatly decreased in miR-31 re-expressing cells; conversely this is increased upon suppression of miR-31. Data presented as the mean ± SEM. Statistical analysis performed using Student's t-test. NCI-H2452 miR-VC and P31 Zip-miR-VC utilised as relative control and are set to 1, as such no error is associated.
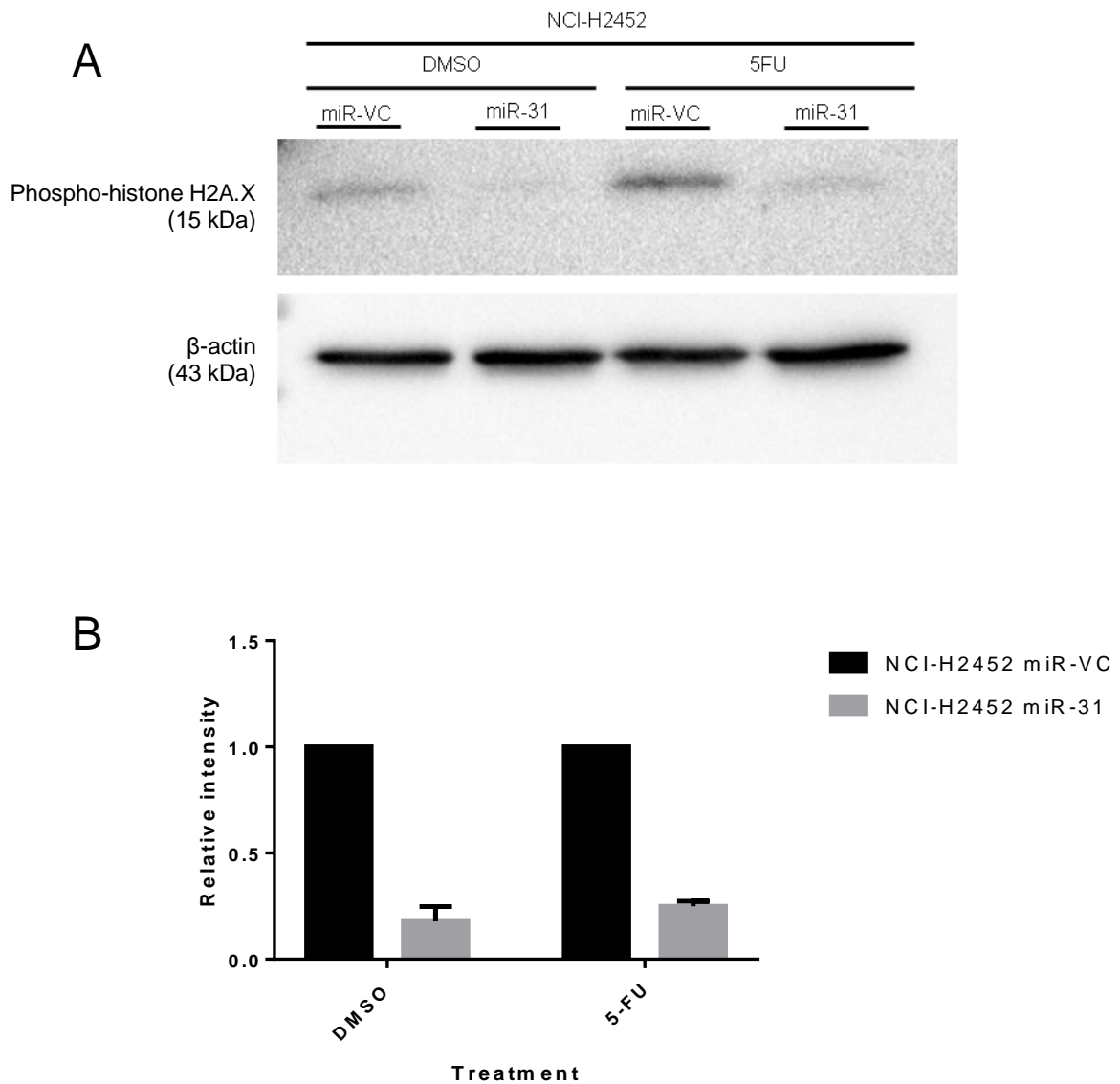
Figure 4.8 MiR-31 reintroduction decreases DNA damage induction with non-platinum based chemotherapeutics. (A) Treatment with 5-FU induced minor DNA damage when miR-31 was reintroduced in the NCI-H2452 cell line, in accordance with cisplatin and carboplatin treatment. DMSO treatment, here used as the vehicle control, also affected phospho-H2A.X levels with miR-31 reintroduction. (B) Densitometry analysis of phospho-H2A.X levels for DMSO and 5-FU treated NCI-H2452 transfected cell lines (*n*=2). Cells were treated with 500μM 5-FU for 24 h. Data demonstrates that miR-31 re-expression influences on DNA damage initiation are not platinum-based chemotherapy limited. Due to the statistical limitations of *n*=2, statistics were not applied, however alterations may pertain significance if *n*=3 achieved. NCI-H2452 miR-VC utilised as relative control and is set to 1, as such no error is associated.
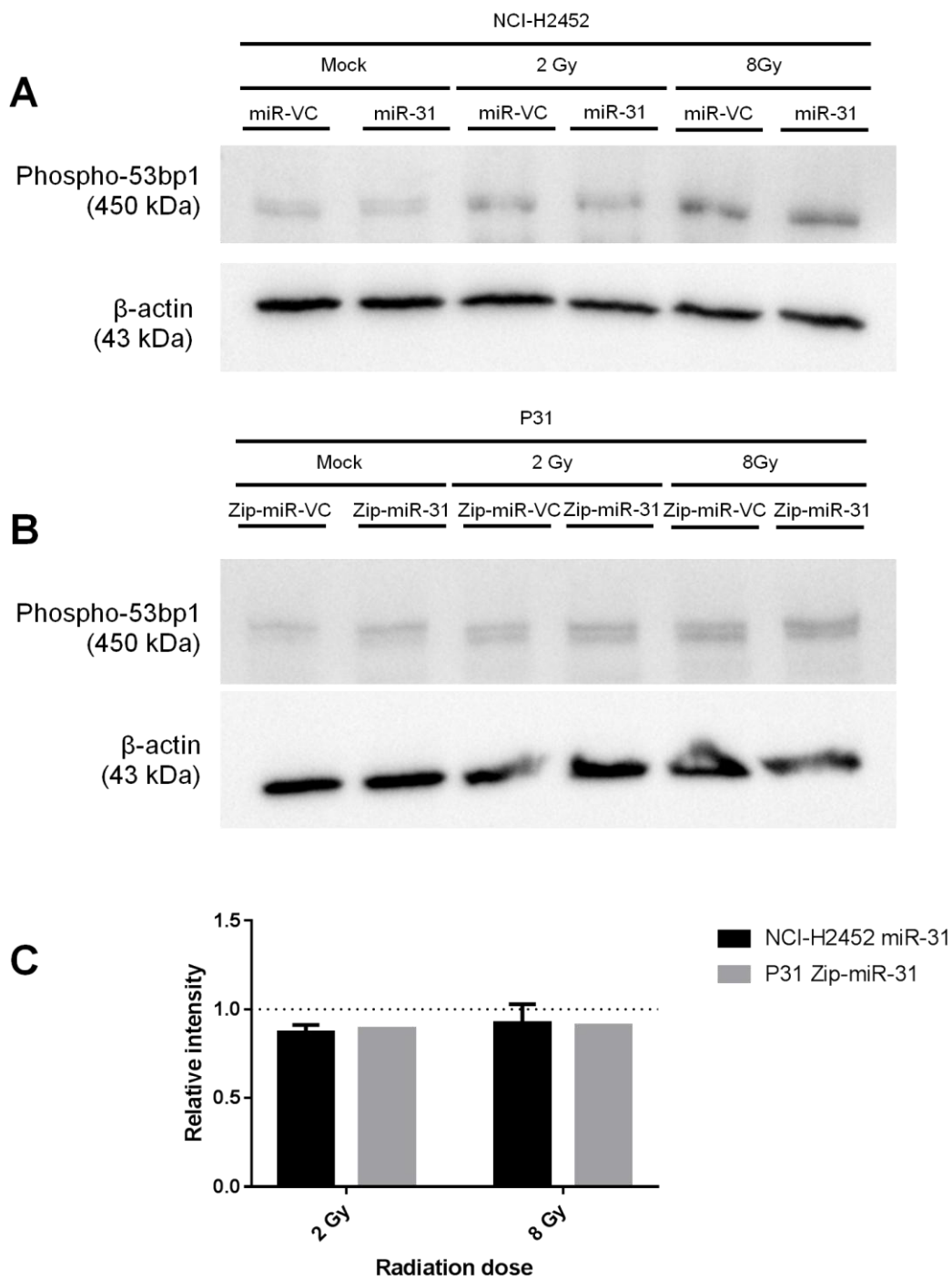
Figure 4.9 MiR-31 does not modulate DNA damage induced by radiation treatment in MPM cells. (A, B) Representative Western blots measuring phosphorylation of 53bp1 found no correlation between DNA damage induced by radiation treatment and miR-31 manipulation. (C) Densitometry analysis of phospho-53bp1 for miR-31 manipulated cell lines. Dotted line is vector control equivalents (set to 1). Cells were irradiated with 2 Gy and 8 Gy at a rate of 1.87 Gy/min. Data demonstrates that the manipulation of miR-31 does not affect DNA damage in the context of radiation treatment. Controls were mock irradiated.

There were no great changes between vector control and miR-31 expressing cells (Fig. 4.10), indicating that miR-31 enhanced chemoresistance is largely independent of ROS biology. The analysis of ROS was completed *n*=2, therefore statistics were not applied, however if a trend existed whereby cisplatin increased ROS this would not correlate with a model of enhanced resistance, as an increase in ROS would promote DNA damage, which is not observed here.

Although the overall burden of platinum was greater within miR-31 expressing cells, importantly, the increased chemotherapeutic levels were not localised to the nuclear compartment, leading to questioning as to where the chemotherapy was located within the miR-31 positive, more resistant, MPM cells. In order to explain the observed miR-31-mediated chemoresistant phenotype, despite a greater concentration of platinum within the cellular environment and reduced accumulation within the nuclear region, the literature was thoroughly reviewed. There are many routes by which accumulation within the extranuclear environment may be facilitated, including the efficiency of exosome packaging of cisplatin [308], changes in the structure of the nuclear region [309], rearrangements of cytoskeletal components [310] and lysosomal transport [311]. Interestingly, a link has been established between miR-31 expression, resistance to therapy, and a lysosomally bound drug transporter ABCB9 [312, 313].
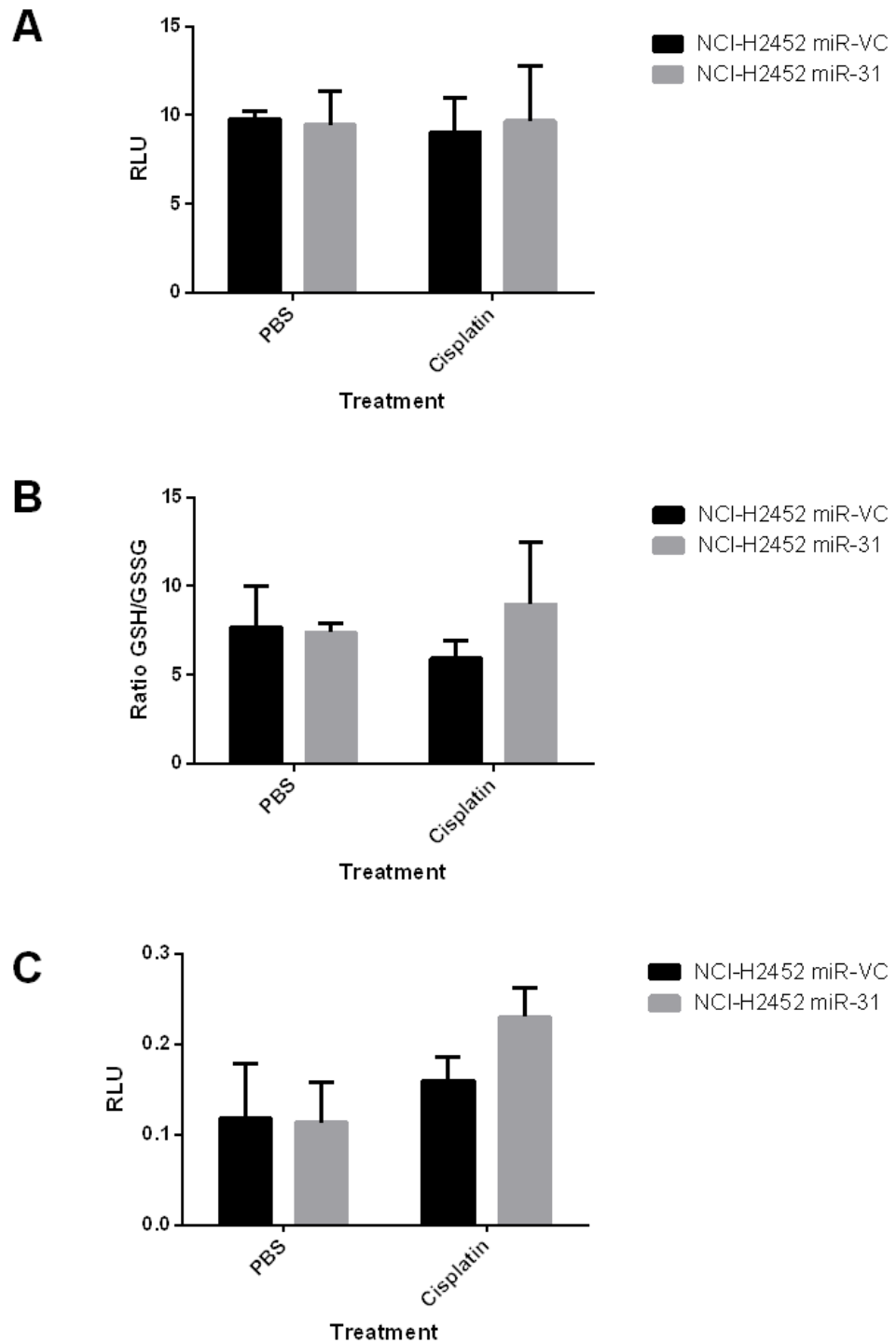
Figure 4.10 Antioxidant and oxidant levels are not significantly altered by re-expression of miR-31. (A) Total glutathione levels were unaltered upon re-expression of miR-31in the NCI-H2452 miR-31 re-expression model, as measured by GSH/GSSG-Glo assay (*n*=2). (B) Glutathione/Oxidised glutathione ratio was unaltered with miR-31 reintroduction, as measured by GSH/GSSG glo assay (*n*=2). (C) Reactive oxygen species levels were moderately increased by re-expression of miR-31 with cisplatin treatment, as measured by ROS glo assay (*n*=2). Data presented as ± SEM.

4.4.3 Lysosomally bound ABCB9 is upregulated with miR-31 re-expression in MPM cells, potentially via an OCT1-mediated mechanism in the extranuclear compartment

With an increase in overall concentration of cisplatin, increased drug influx, and reduced nuclear accumulation of drug, the potential capability of miR-31 expressing cells to sequester cisplatin into cytosolic organelles within the cell was investigated. One route by which cells can sequester cytotoxic drugs away from the nucleus is through packaging into intracellular vesicles such as lysosomes [314]. Following further subcellular fractionation, the lysosomal fraction, as analysed via ICP-MS, illustrated a 0.28 ppm ± 0.07 ppm increase in platinum concentration; this pattern was not conversely replicated within the miR-31 suppression model (Fig. 4.11). Unfortunately, the process of gradient centrifugation does not separate individual groups of organelles; therefore denoting that the fraction collected likely also have contained peroxisomes, endosomes and other vesicular structures. In order to attempt to better isolate lysosomes, a novel pull down method was adopted using magnetic Protein A/G beads (see section 2.7.2) (Fig. 4.11B). The result of the pull down methodology led to a great reduction in the amount of platinum measured (ppm to ppb), and the process was not confirmed to select for intact lysosomes post isolation, despite attempts including the use of transmission electron microscopy to visualise lysosomes (appendix 6).

With ICP-MS data from lysosomal platinum content unclear, a modulating effect of miR-31 on lysosomal biology was investigated to further determine if the lysosome may be involved in miR-31 mediated chemoresistance and the cytoplasmic sequestration of drugs. An association between miR-31 and the lysosomal bound transporter ABCB9 had been previously established in NSCLC [313], thus prompting the investigation as to whether miR-31 may modulate ABCB9
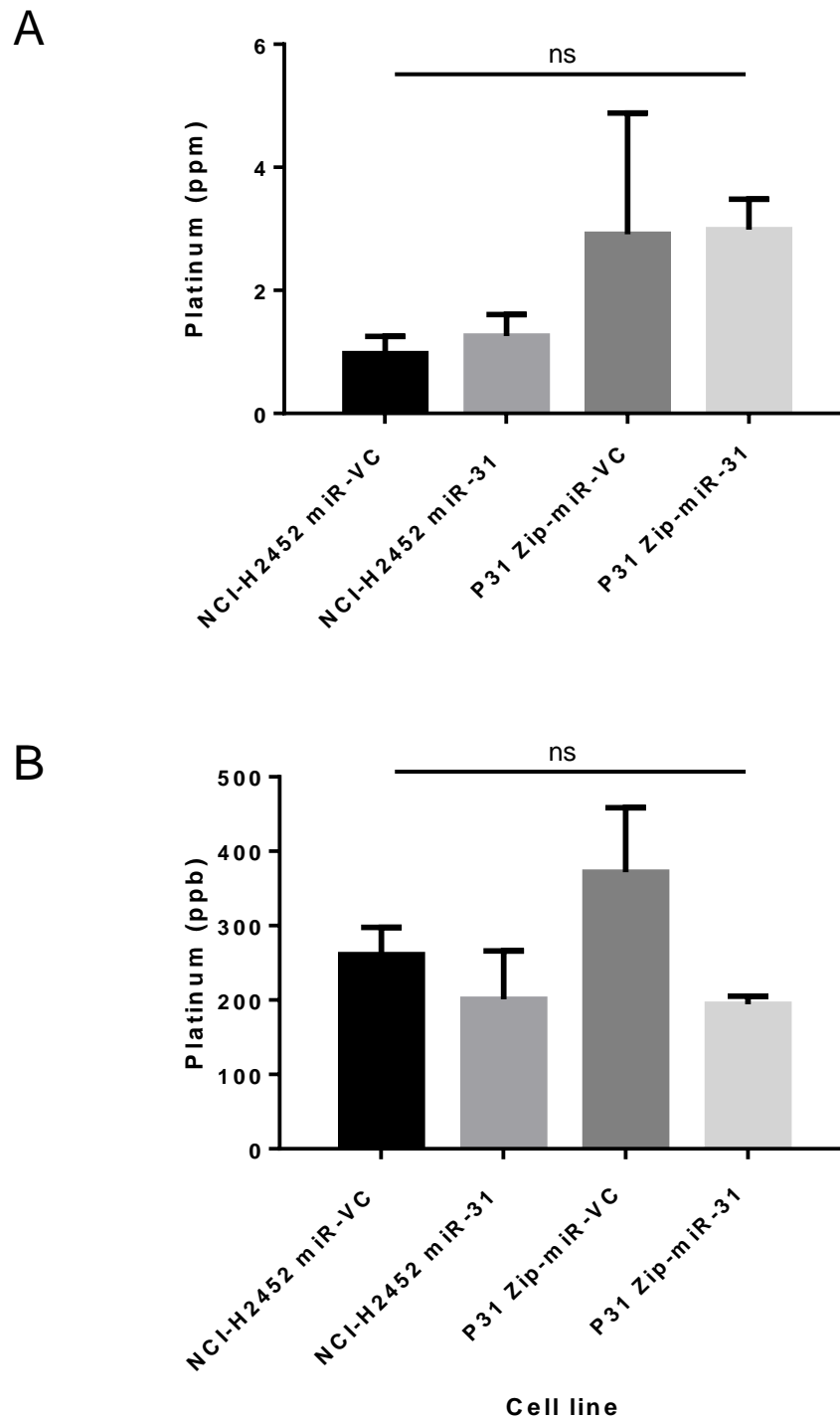
Figure 4.11 MiR-31 status may affect platinum content of the lysosomal region.
(A) ICP-MS of lysosomal fraction following 50 μM cisplatin treatment for 24 h
illustrated a trend toward an increased platinum concentration with miR-31
reintroductions, however this is not significant (*n*=3). (B) ICP-MS of lysosomal pull
down following 50 μM cisplatin treatment for 24 h illustrated a trend toward an
decreased platinum concentration with miR-31 suppression, however this is not
significant (*n*=3). Data presented as the mean ± SEM. ns= non significant. Statistical
analysis performed using Student's *t*-test of miR-31 reintroduction or suppression cell
line models.

expression, which consequently may regulate cisplatin transport across the lysosomal membrane. Here, it was identified that there was an upregulation of ABCB9 at both gene and protein level upon re-introduction of miR-31 (Fig. 4.12). This was supported by immunoflourescent studies examining intracellular ABCB9 localisation (Fig. 4.13). To establish whether the change in ABCB9 expression levels may be accounted for by an increase in the overall burden of lysosomes within the miR-31 expressing cells, the expression of the lysosomal marker LAMP-1 was analysed as a proxy for lysosomal burden. It was established that there were no significant changes in LAMP-1 expression as determined by immunofluorescence and Western blot, supporting a specific upregulation of the ABCB9 transporter rather than an increase in the density of lysosomes in the NCI-H2452 miR-31-expressing cell population (Fig. 4.13).

Presently, this data supports a role for miR-31 in regulating aspects of lysosomal biology. However, as the mechanism of action for miRNA typically involves the negative regulation of target genes at the posttranscriptional level, the observed upregulation of ABCB9 upon miR-31 reintroduction indicated the involvement of a potential intermediate negative regulator of ABCB9 expression. Here, bioinformatic tools were used to identify potential negative transcriptional regulators of ABCB9, which may be altered by miR-31 (Fig. 4.14, Table 4.1, which is adapted from http://mircode.org/?gene=pou2f1&mirfam=&class=&cons=&trregion=, http://www.targetscan.org/cgibin/targetscan/vert_61/view_gene.cgi?taxid=9606&rs= NM_001198783&members=&showcnc=0&shownc=0&showncf=#miR-31, accessed 290615). OCT1 has previously been recognised as a bipotential transcription factor [315], which we propose, within our system, is a negative regulator of *abcb9* transcription. In line with the present model, it was observed that there was a
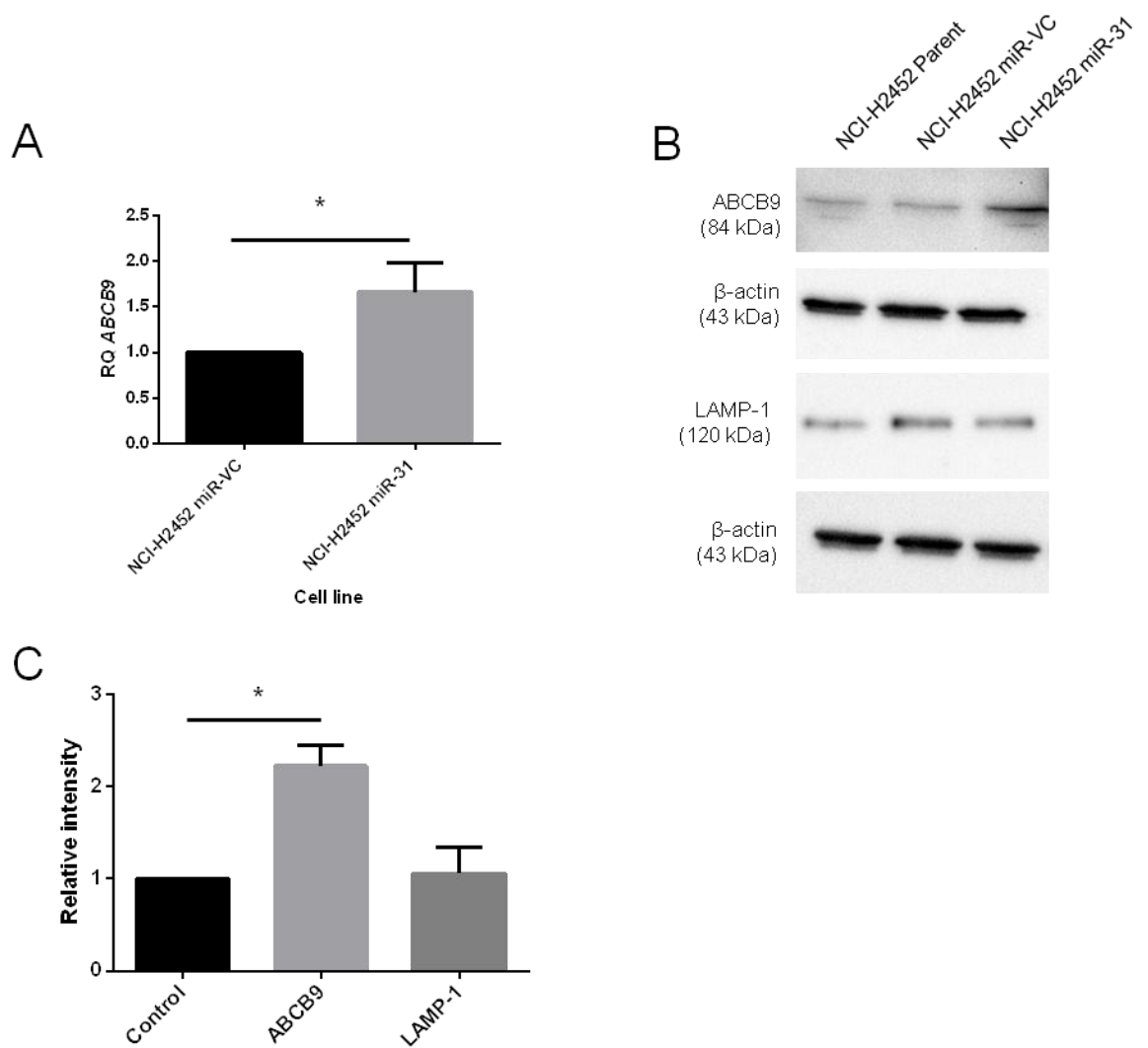
Figure 4.12 Reintroduction of miR-31 affects lysosomal drug transport. (A) Expression levels of drug influx transporter *abcb9* were analysed via qPCR. There is a significantly greater relative expression level (*p=0.0251) of ABCB9 in miR-31 transfected cells compared to miR-VC transfected equivalent (*n*=4). RQ relates to relative fold change. (B) Representative Western blot illustrating an increase in ABCB9 expression level with miR-31 re-expression, with no apparent change in lysosomal marker LAMP-1. (C) Densitometry analysis revealing significant (*p=0.0325) upregulation of ABCB9 (*n*=3). Data demonstrates that there is a significant increase in lysosomal transport through the upregulation of ABCB9, this is not due to an increase in lysosomal burden, as LAMP-1 is unaffected by miR-31 re-expression. Data presented as the mean ± SEM. Statistical analysis performed using Student's *t*-test. NCI-H2452 miR-VC and 'Control' utilised as relative control and are set to 1, as such no error is associated.
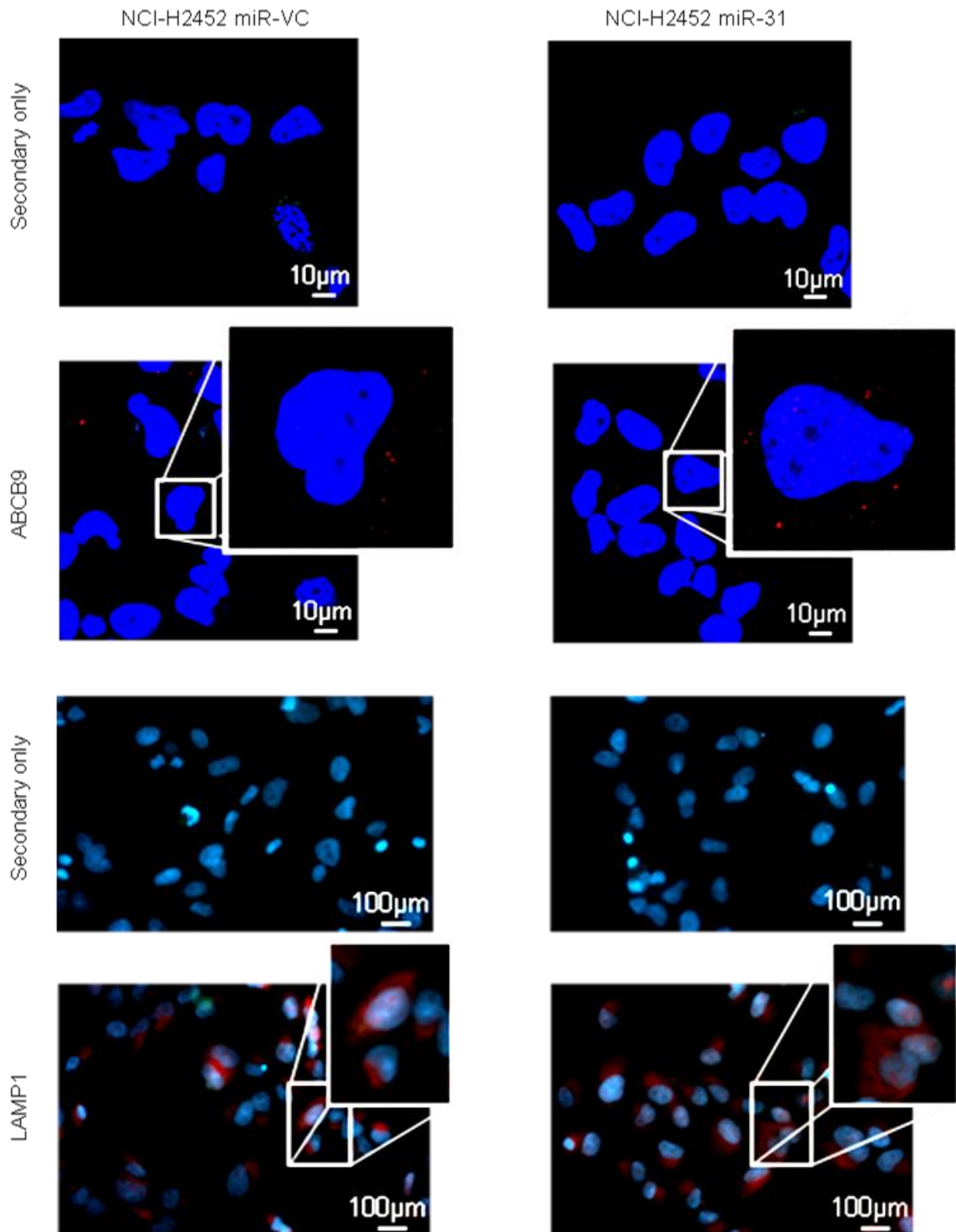
Figure 4.13 Reintroduction of miR-31 affects lysosomal drug transporter ABCB9.
Immunoflourescent images showing ABCB9 (red) or LAMP-1 (red) expression. Nuclei
stained with DAPI (blue). Images captured on LSM 710 with 63x/1.40 Oil DIC M27
objective for ABCB9 images, and 10x/0.25 Ph1 objective for LAMP-1 images. Data
demonstrates that ABCB9 is present in foci type pattern across the intracellular
environment. LAMP1 expression is the equivalent irrespective of miR-31 status.
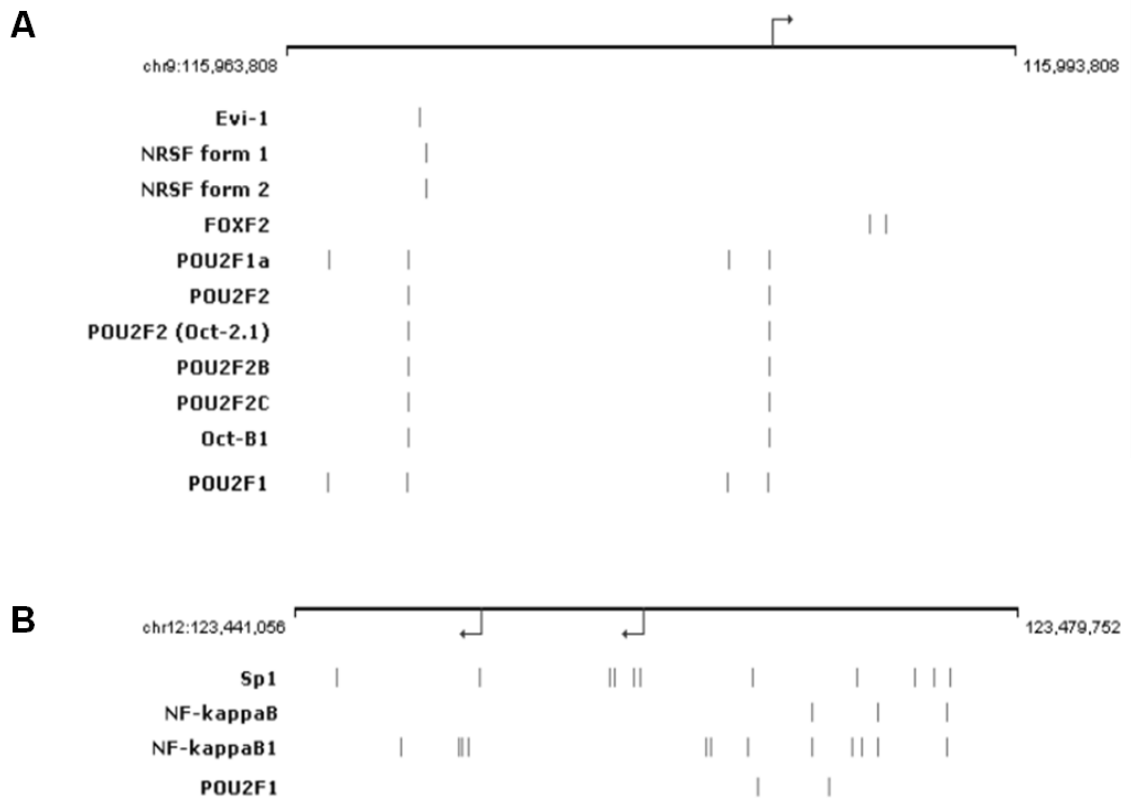
Figure 4.14 Potential transcriptional regulators of genes *slc31a1* (CTR1) and *abcb9* (ABCB9). (A) Transcription factors regulating gene *slc31a1*. The image displays transcription factor binding sites in this gene promoter as predicted by SABiosciences' Text Mining Application and the UCSC Genome Browser. The *pou2f1* gene relates to the bipotential transcription factor OCT1. (B) Transcription factors regulating gene *abcb9*. The image displays transcription factor binding sites in this gene promoter as predicted by SABiosciences' Text Mining Application and the UCSC Genome Browser. The *pou2f1* gene relates to the bipotential transcription factor OCT1. The arrows are indicative of transcription start sites within the gene promoters.

Adapted from http://www.sabiosciences.com/chipqpcrsearch.php.

Table. 4.1 Target prediction for OCT1. Utilising bioinformatic tools, pairing of miR-31 with the *pou2f1* (OCT1) gene was performed. Of the approximately 190 predicted miRNA that may potentially bind to OCT1, miR-31 appears to be one of the most conserved.

microRNA family	Predicted consequential pairing of target region (top) and miRNA (bottom)	Seed position	Transcript region	Conservation		
				Primates	Mammals	Other vertebrates
miR-31	5'...UUCUUAGUGAGAUCAUCUUGCCA... ||||||| 3' UCGAUACGGUCGUAGAACGGA	chr1:167389158	3pUTR	78%	61%	0%
miR-31	5'...UUUUUCUUAUAUCUGUCUUGCCA... ||||||| 3' UCGAUACGGUCGUAGAACGGA	chr1: 167391236	3pUTR	100%	65%	23%

concomitant reduction in OCT1 expression upon miR-31 reintroduction into NCI-H2452 cells (Fig. 4.15), which may connote miR-31 targeting OCT1, thus facilitating the increased transcription of downstream proteins, such as CTR1 and ABCB9, both of which have binding sites for OCT1. OCT1 binds to the CTR1 gene downstream of the transcription start site at potentially 4 different transcription factor binding sites, whereas OCT1 binds to the ABCB9 gene upstream of the transcription start site at potentially 2 different transcription factor binding sites. In the next section, the role of ABCB9 will be further assessed by functional manipulation of ABCB9 expression.
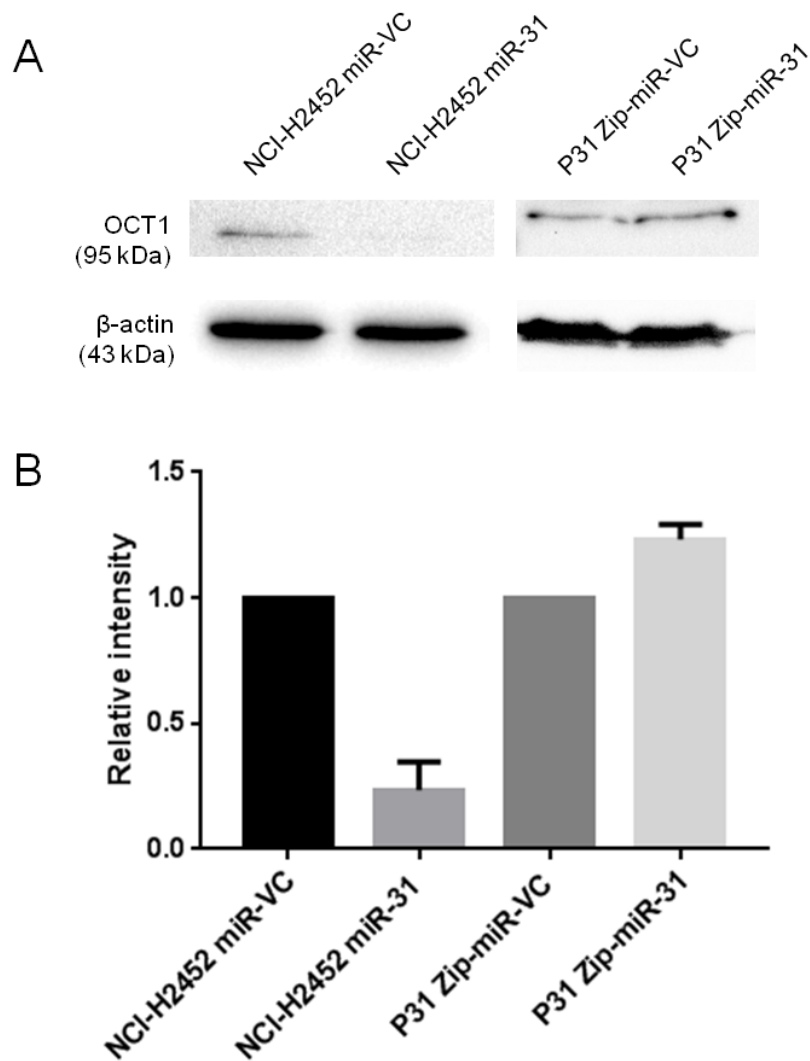
Figure 4.15 The bipotential transcriptional regulator, OCT1, can be associated with miR-31 expression. (A) Representative Western blot illustrating the downregulation of potential negative regulator of both CTR1 and ABCB9 expression, OCT1, with miR-31 reintroduction. Suppression of miR-31 does not affect expression of OCT1. (B) Densitometry analysis of OCT1 expression with miR-31 reintroduction (NCI-H2452) or miR-31 suppression (P31) ($n=2$). Data demonstrates a large decrease in OCT1 with miR-31 re-expression, potentiating miR-31-mediated downregulation of OCT1 leading to upregulation of CTR1 and ABCB9 expression. Data presented as the mean ± SEM. NCI-H2452 miR-VC and P31 Zip-miR-VC utilised as relative control and are set to 1, as such no error is associated.

4.5 Discussion

Cisplatin contributes to the mainstay of treatment in MPM patients. Unfortunately, however, patients often develop or are inherently resistant to this therapeutic strategy [245]. In the previous chapter, it was observed that the re-introduction of a particular miRNA, miR-31, increased resistance to platinum-based chemotherapeutics. This chapter aimed to explore as to how miR-31 potentially modulated therapy resistance, and explored differences in the trafficking of cisplatin through the intracellular environment. Overall, it has been established that miR-31 appears to indirectly affect the cellular machinery involved in the sequestration and transfer of cisplatin from the cytoplasm to the nucleus, which may involve increased drug trafficking into lysosomal regions via ABCB9.

Membrane-bound transporters of cisplatin are well characterised, and are known to function in cellular uptake and efflux of platinum agents throughout cells [297]. Here, there was no observed change in efflux transporters ATP7A and ATP7B, or influx transporter CTR1. An increase in CTR1 expression would denote an influx of platinum into the intracellular environment. As in this chapter, Fang *et al.* [316] described the upregulation of CTR1 in highly cisplatin-resistant cell lines of cervical adenocarcinoma and hepatoma origin. The relationship was forecasted to be a result of mis-localisation or a defect in post-translational modification of the protein. The upregulation of CTR1 and corresponding increase in platinum accumulation was also noted in NSCLC cell lines [317].

In contrast with the results established here, Ishida *et al.* [318] reported high expression of CTR1 being correlated with an increase in disease free survival, however, this study was limited to mRNA levels, rather than the more functional protein level. Although not explored within the context of this chapter, CTR2 has

also been correlated with therapeutic resistance; however, its cellular location is ambiguous. It has been proposed that CTR1 and CTR2 work on opposing mechanisms, with knockdown of CTR2 increasing sensitivity to cisplatin [70, 286]. Increased expression of CTR2 has been demonstrated to promote a greater level of cleaved CTR1, which has a lower affinity for platinum and, thus leads to a reduction in platinum influx [70]. CTR2 was not investigated here as its role is immaterial to resistance persisting despite an increased platinum burden in the intracellular environment.

Glutathione is a three-amino-acid peptide and an abundant antioxidant found in all human cells [289]. Most cellular glutathione exists in a reduced form (GSH) however, some oxidised GSH forms exist, termed GSSG. The phrase "redox state" describes the ratio of GSH/GSSG. Chemotherapies can react with GSH to form adducts or to increase the GSSG levels, decreasing the redox state. Alterations in redox state can be correlated with sensitivity to drugs as well as mechanisms associated with cancer [241, 319]. Post influx, cisplatin can be chelated with GSH throughout the cellular environment, which also has a role as a redox regulating protector in response to cisplatin treatment [289]. No significant differences were observed in the levels of GSH or GSH/GSSG in MPM miR-31 positive cells treated with cisplatin. This result is in contrast with previous reports where a more resistant phenotype correlated with increased GSH [320, 321]; this may suggest miR-31 functioning to modulate other molecules which may affect GSH levels. An additional chaperone of cisplatin has been identified in Atox1, which binds with cisplatin via its conserved metal-binding motif, and reportedly convoys the molecule through the cytoplasmic compartment [71, 290]. The relationship between Atox1 expression and resistance has not been documented, but has been highlighted as an area of potential

future investigation, due the protein potentially contributing to the regulation of cisplatin accumulation [61, 291].

Export of cisplatin is facilitated by the ATPases ATP7A and ATP7B. ATP7A and ATP7B are located in the trans-golgi network and are actively trafficked to the plasma membrane to efflux cisplatin from the cell [322]. Increased ATP7A and ATP7B expression has been associated with poorer response in clinical studies [275, 286, 323, 324], however no alteration in ATP7A or ATP7B transcript or protein expression was determined here; this suggests that miR-31 affects the influx of cisplatin into the cell but does not affect efflux, potentially supporting cisplatin accumulation over time. Although no gross change in efflux was observed, the translocation of these proteins has been shown to be of importance in resistance [325], and an immunoflourescent study could be undertaken to facilitate this. With an increased influx, yet a persisting resistant phenotype determined, investigations focussed upon the intracellular sequestration of cisplatin.

Here, the focus is upon a 2-dimensional *in vitro*-based assays to characterise the alterations in chemosensitivity seen with miR-31 modulation in MPM cell lines, however there is potential to also analyse the flux of chemotherapy within a 3-dimensional system, which may be more closely allied to *in vivo*. 3-dimensional systems such as spheroids are widely adopted in MPM research [326]. Within Curran *et al.* [327], the investigation of drug flux in cells within a spheroid based system is particularly interesting, where high expressors of the multi-drug resistant-associated pump ABCG2 can arrange on the outer edges of spheroids, ensuring less chemotherapy enters the inner more sensitive cells, this is particularly interesting in the context of this research and may be a potential route for future investigation.

Modified *in vitro* systems with mixed MPM cells may better model the tumour environment and potentially add strength to the 2-dimensional model studied here.

Importantly, miR-31 was found to modulate the amount of platinum in the nuclear compartment of MPM cells; this was supported by changes observed in the induction of DNA damage, as measured by phospho-histone H2A.X. Cho *et al.* [328] measured phospho-histone H2A.X levels as a marker of DNA damage in breast cancer, and found that upon miR-31 overexpression there was an increase in foci formation, suggesting that the cells would be more sensitive, rather than the resistance observed here. Similarly, Tseng *et al.* [329], established that in human oral squamous tumours phospho-histone H2A.X was induced at a greater level in miR-31 transgenic mice. Lynam-Lennon *et al.* [256] concluded from their analysis of miR-31 in a radioresistant oesophageal cell line that miR-31 did not play a functional role in the context of DNA DSB repair kinetics. With the results here, it may be that miR-31 is functioning to modulate DNA damage using a mechanism that is specific for MPM.

With the decrease in DNA damage induction upon miR-31 re-introduction, it was important to analyse whether this was a platinum-based therapy-specific response. In clinical practice cisplatin is used in combination with pemetrexed, a potent anti-folate. Unfortunately, due to toxicity issues *in vitro*, the study here could not assess response to pemetrexed (appendix 3), however, a related drug, 5-FU, which is also a thymidylate synthase inhibitor, was utilised as a replacement. DNA damage induction was decreased in miR-31 re-expressing cells in response not only to 5-FU, but also, unexpectedly, to its vehicle control DMSO. This suggests a possible modulation of the overall permeability of the cell membrane [330, 331], as both DMSO and 5-FU can passively diffuse into the cellular environment [330], or possibly a more generalised change to the response to DNA damage or repair. As the

modulation of DNA damage initiation was seen broadly across different chemotherapy treatments, to ensure this was not a generalised response to DNA-damaging agents, radiation treatment was used in miR-31 modified MPM cells. There was no change to DNA damage between radiation treated samples, suggesting the accumulation of cisplatin within the intracellular environment was a paramount contributing factor in the noted resistant phenotype. Accumulation defects were noted in Lanzi *et al.* [332], where increased tolerance to induced damage was observed as one of a range of changes to contribute to resistance.

Astoundingly, research focussing upon nuclear trafficking and transport of chemotherapy is extremely limited. Notably, the multi-drug resistance protein 2 (MRP2) or ABCC2, which normally functions to transport metabolites across the plasma membrane, was found to be frequently located on the nuclear membrane of poorly differentiated or stem-like ovarian cancer cells [333]. Here, however, with pre-existing literature lacking, we focussed upon potential proteins that may be affected by miR-31, leading to the sequestration of platinum in the cytosolic compartment.

Interestingly, the top candidate involving cisplatin sequestration and miR-31 was a lysosomal bound drug transporter known as ABCB9 [312, 313]. Following analysis, ABCB9 was found to be upregulated with miR-31 reintroduction, suggesting more active transport of drugs across the lysosomal membrane into the lysosomal lumen. Theoretically, the greater level of ABCB9 could signify that MPM cells with miR-31 may have greater levels of chemotherapy within them overall, but these cells are better able to sequester cisplatin into lysosomes, away from the nucleus. ABCB9 expression has been associated with resistance to therapy in yeast [334], and in NSCLC [313]. Whilst the increase in ABCB9 could explain, at least in part, the

observed sequestering of platinum in miR-31 positive MPM cells, owing to the traditional mechanisms of miRNA, it would suggest that miR-31 does not directly target the ABCB9 transcript. Therefore, the examination of potential negative regulators of ABCB9 transcription, which also can be repressed by miR-31, uncovered the modulation of bipotential transcription factor OCT1. The transcription factor is widely expressed in tissues, and can be associated with a stress response [335]. Genes associated with oxidative and metabolic stresses are dysregulated in OCT1 deficient conditions [336]. Fundamentally for this research, Shakya *et al.* [315] investigated OCT1 and found that the protein is a transcription factor which can switch between repressive and antirepressive modes, meaning this complex transcription factor can upregulate or downregulate its targets. Here, the proposition is that miR-31 downregulates OCT1 by translational repression, which therefore leads to an increase in CTR1 and ABCB9 expression, which may contribute to the modulation of chemoresistance observed within MPM cell lines.

This chapter has uncovered a potentially novel mechanism behind miR-31 mediated chemoresistance in MPM, potentially mediated via the modulation of the lysosomal drug transporter ABCB9, as summarised in Fig. 5.16. Therefore, to further investigate the significance of the contribution of ABCB9 to MPM resistance, in the next chapter ABCB9 was independently expressed to evaluate its contribution to the miR-31-mediated chemoresistant phenotype.
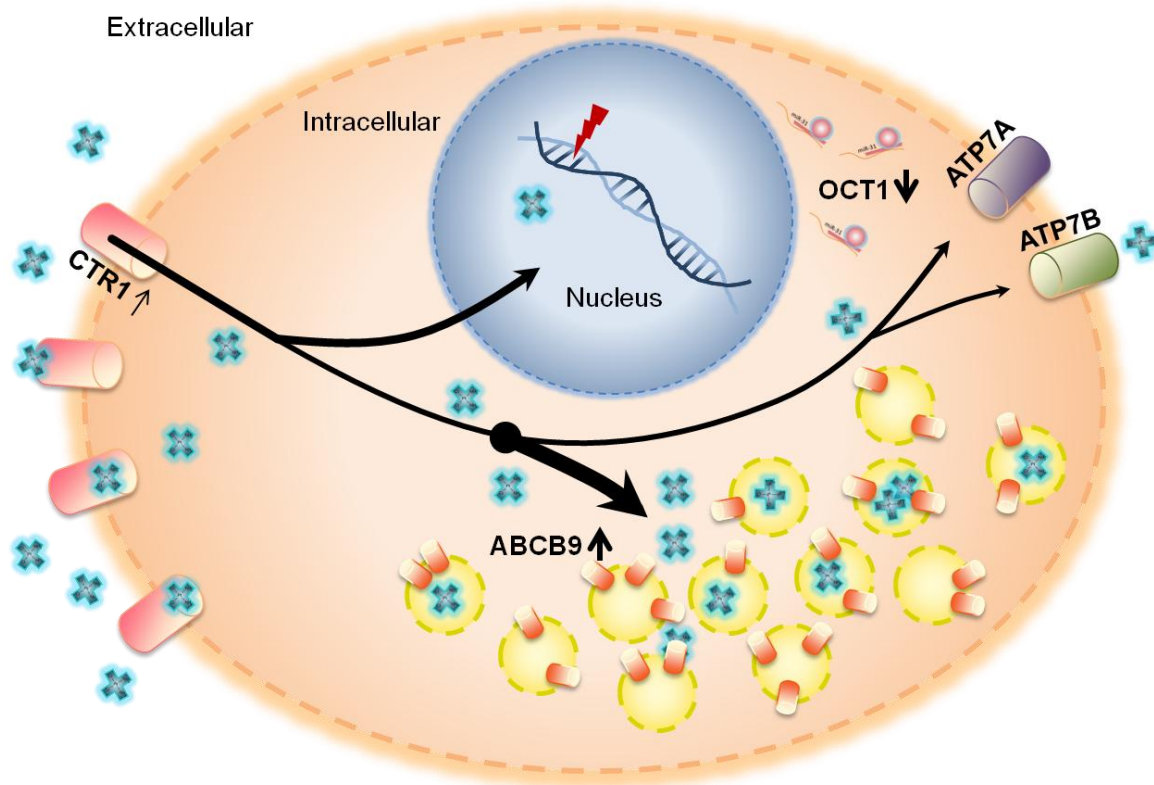
Figure 4.16 Summary of the effect of miR-31-mediated transport on MPM cell. The MPM cell (orange) has notable increased resistance to chemotherapy (blue cross structures) with miR-31 reintroduction. Resulting from the data obtained in chapter 4, the addiation of the increased lysosomally (yellow) bound drug transporter ABCB9 (orange cylinder), as well as the downregulation of bipotential transcription factor OCT-1, may contribute to the sequestration of cisplatin away from the nuclear region, resulting in less DNA damage and increased chemoresistance.

Chapter 5:

The role of ABCB9 in

miR-31-modulated intracellular

drug accumulation

5.1 Introduction

The possible mechanisms by which miRNAs may modulate intracellular accumulation are vast. Due to the pleotropic nature of miRNAs, and the prospect of a single miRNA targeting hundreds of different mRNA, the probability of modulating to targets that affect cellular transport systems is great. In the previous chapter, a potential route by which miR-31 may modulate the intracellular accumulation of cisplatin, whilst selectively depleting the nuclear region of platinum adducts, was identified.

Lysosomes, which range from 50 nm to 500 nm in diameter, are membrane bound organelles that account for the breakdown and recycling of cellular components. Generally, lysosomes have a low pH, ~5.5, and serve as a 'sink' for toxins, drugs and heavy metals [312, 337], and have previously been identified to regulate drug sequestration [314]. The ability of lysosomes to sequester various drugs within their environments has been documented in renal, colorectal and angiosarcoma cell lines [311, 314]. Of particular interest to this study, a known lysosomally-bound drug transporter, ABCB9, has been linked with resistance and is proposed to be regulated by miR-31. Here, however, an upregulation in ABCB9 with miR-31 re-expression has been observed, pertaining ABCB9 being an indirect target of miR-31 in our MPM cell based model.

The family of ATP binding cassette (ABC) transporters represents one of the largest gene families known in eukaryotic cells. ABC transporters function to facilitate the movements of various molecules across membranes, including lipids, nutrients, metabolic products and drugs [312, 338, 339]. Members of this super family include antigen processing (TAP) and multidrug resistance (MDR) transporters [334]. Highly conserved, ABC transporters across the gene family share a general architecture of

two cytosolic nucleotide-binding domains (NBDs) and two transmembrane domains (TMDs) [340], although some have half of this and are found in the endoplasmic reticulum [312]. Zhang *et al.* [312] first identified an ABC transporter localised to the lysosomal membrane, namely ABCB9. ABCB9 is also known as TAPL (transporter associated with antigen processing-like), and is broadly expressed across human tissue, with highest expression noted in the testis, heart and spinal chord [312]. The expression of ABCB9 is upregulated during maturation of immune cells, particularly the maturation of monocytes to dendritic cells and macrophages [341]; however it is not considered to be involved in the MHC class I pathway unlike TAP. Predominantly, ABCB9 operates to translocate peptides into the lumen of lysosomes [338], these can vary in size from 6 to 59 residues [342]. The confidence that ABCB9 is located in the lysosomal membrane is reported in several publications, due to its co-localisation with the lysosome-associated membrane proteins LAMP-1 and LAMP-2 [312, 343]. Recently, Dong *et al.* [313] found that inhibition of ABCB9 enhanced cisplatin resistance, with a reduced uptake of cisplatin and suppression of cisplatin-mediated apoptosis in a NSCLC cell line. Thus far, a conflicting relationship has been observed, suggesting that results presented here may oppose that of Dong *et al.* [313], in that miR-31 re-expression in MPM cell lines increases overall resistance in cells, and also increases ABCB9 expression. This chapter therefore aims to clarify the relationship between ABCB9 and resistance to cisplatin with the landscape of MPM; this is to be done independently of miR-31, and with miR-31 re-expression to explore the contribution of ABCB9 to the resistant phenotype that has been observed.

5.2 Rationale, Aims and Objectives

The lysosomal drug transporter ABCB9 is upregulated upon miR-31 re-expression in MPM cells. The upregulation of ABCB9 in association with increased expression of miR-31 suggests that MPM cells expressing ABCB9 at greater levels than baseline may be better able to sequester chemotherapeutics into lysosomal regions, away from the nucleus and cytosolic compartment. With previous research indicating miR-31 associated regulation of ABCB9 having a role in cisplatin resistance [313], it is hypothesized that ABCB9, as a target of miR-31 is the functional facilitator of the chemoresistant phenotype.

The objectives of this chapter were to 1) determine whether ABCB9, independent of miR-31, contributes to MPM chemoresistance, 2) explore the effect of ABCB9 modulation on platinum transport into lysosomes, in order to identify whether ABCB9 plays a functional role in intracellular platinum sequestration.

5.3 Experimental design

5.3.1 *ABCB9 overexpression*

ABCB9 was overexpressed in the parent NCI-H2452 cell line via stable plasmid transfection, in order to isolate whether the protein affected sensitivity to chemotherapy treatment, in line with observations noted in miR-31 stably transfected cells. The approach to independently express ABCB9 was adopted in order to view whether ABCB9 contributed to the resistant phenotype identified in previous chapters. Importantly, the analysis of stable miR-31 expression with the addition of stable ABCB9 overexpression was also determined to functionally observe whether cells had enhanced chemoresistance compared to that of miR-31 expression alone, this would denote whether ABCB9 contributed to the pathway observed and uncovered in chapter 4.

5.3.2 *The effect of ABCB9 on chemoresistance*

To determine the overall effect of chemoresistance with ABCB9 overexpression, the clonogenic assay was utilised, with support from analysis of γH2A.X using Western blot. Similarly to chapter 4, ICP-MS analysed the content of intracellular platinum within the whole cell and individual organelles. Wholly these approaches would facilitate the investigation as to whether ABCB9, as a lysosomal drug transporter, increased sequestration into the lysosomes, and therefore determine if ABCB9 was the functional facilitator of the miR-31-mediated increase in chemoresistance observed within the *in vitro* MPM systems studied here.

5.4 Results

5.4.1 *Establishing a stable model of ABCB9 expression*

The cell line NCI-H2452 was utilised to stably transfect ABCB9 overexpression (ABCB9+) or vector control plasmids (EX-NEG). Additionally, the already stably transfected NCI-H2452 miR-31 cell line was also transfected with either ABCB9 overexpression, or vector control plasmids. With the absence of a reporter sequence on the ABCB9 plasmids, reliance upon puromycin selection was paramount, as presented in Fig. 5.1 and Fig. 5.2. A puromycin kill curve, as in appendix 4, was analysed via light microscopy to determine optimal dosing of the antibiotic for selection. Cells that had incorporated the plasmid stably were able to survive selection, whilst untransfected and Lipofectamine only controls died in the selection process (far right panel in Fig. 5.1 and Fig. 5.2). Post selection, cells were maintained in 0.5 µg/ml puromycin with medium to ensure escapee populations were minimised.

ABCB9 expression post selection was assessed after clonal populations had been selected and expanded. The expression of ABCB9 was assessed via Western blot (Fig. 5.3), and a selection of high and low clones were chosen for further analysis. Clones B3 (vector control, EX-NEG) and C3 ('high'ABCB9 overexpressor, ABCB9+) were carried forward for immunofluorescence microscopy, clonogenic and ICP-MS analysis. Stable transfection of the NCI-H2452 miR-31 cell line with ABCB9 plasmids appeared to not overexpress ABCB9, relative to the vector control; this may be due to the upregulation of ABCB9 with miR-31 reintroduction meaning ABCB9 expression has already reached threshold levels that cannot be exceeded with the current system.

Immunofluorescence microscopy studies of ABCB9 in the ABCB9+ population, as in Fig. 5.4, reported successful overexpression of ABCB9 within the NCI-H2452
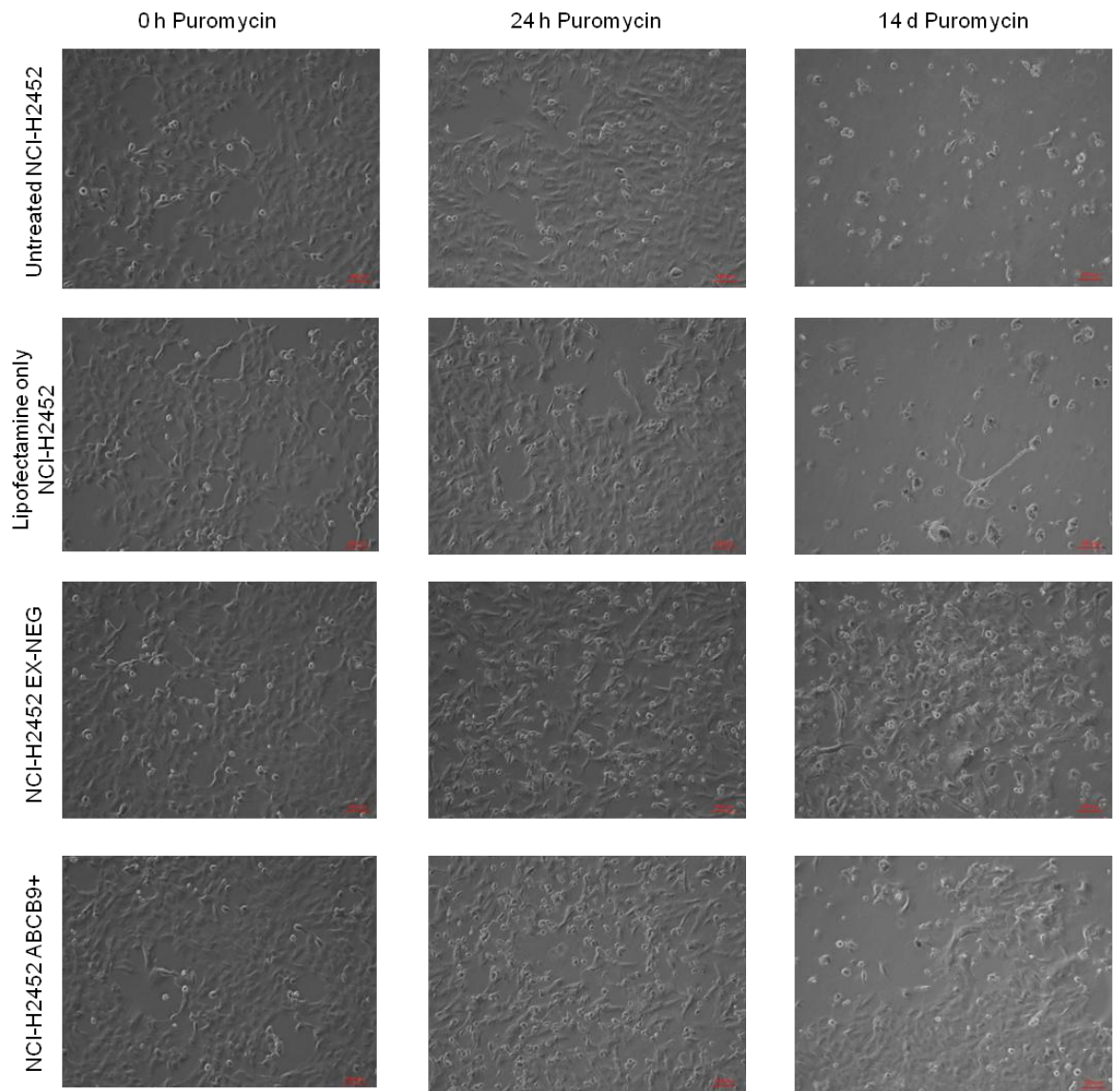
Figure 5.1 Stable expression of ABCB9 in the NCI-H2452 cell line. Time course of microscopy images collected at 0 h, 24 h and 14 days post transfection with 2 µg/ml puromycin. After 14 days under selection, it is apparent that the untreated and Lipofectamine only controls are largely dead, with substantial growth evident in the EX-NEG and ABCB9+ populations. Representative brightfield images captured on Zeiss Axio Vert.A1 with LD A-Plan 10x/0.25 Ph1 objective. Red line at bottom right of images equal to 100 µm.
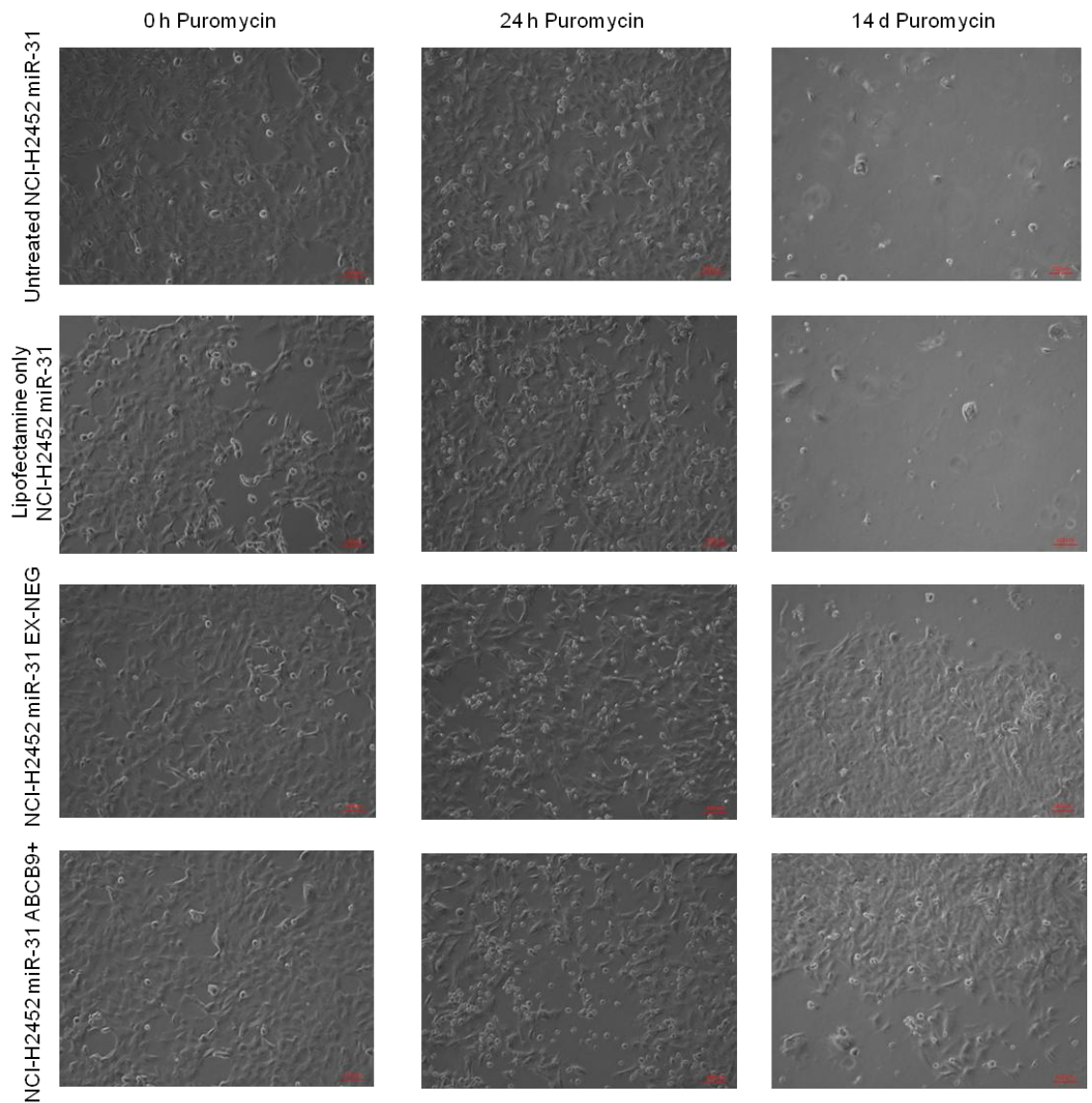
Figure 5.2 Stable expression of ABCB9 in the NCI-H2452 miR-31-expressing cell line. Time course of microscopy images collected at 0 h, 24 h and 14 days post transfection with 2 µg/ml puromycin. After 14 days under selection, it is apparent that the untreated and Lipofectamine only controls are largely dead, with substantial growth evident in the EX-NEG and ABCB9+ populations. Representative brightfield images captured on Zeiss Axio Vert.A1 with LD A-Plan 40x or 10x objectives. Red line at bottom right of images equal to 10 µm at 0 h puromycin, on other images the line represents 100 µm.
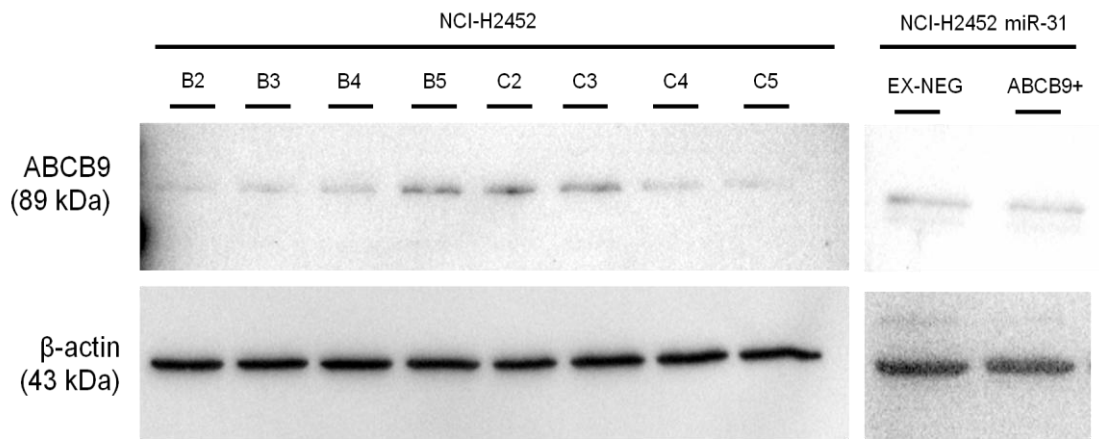
Figure 5.3 ABCB9 overexpression in stable selected clonal populations. The NCI-H2452 miR-31-null cell line was transfected with EX-NEG vector control plasmid (termed EX-NEG) and an ABCB9 overexpression plasmid (termed ABCB9+). Clonal populations were selected and grown under puromycin selection. Clones B2, B3, B4 and B5 correspond to EX-NEG vector control populations. Clones C2, C3, C4, C5 correspond to ABCB9 overexpressing clones. Clones C2 and C3 were selected as high expressing clones, C4 and C5 classified as low ABCB9 expressing clones. EX-NEG vector control clone B5 was seen as an anomalous clonal variant and not carried forward, this may have resulted from multimers. The expression of ABCB9 in NCI-H2452 miR-31 double-transfected with the ABCB9 overexpression plasmid did not highly express ABCB9. β-actin was employed as the endogenous control for data normalisation.
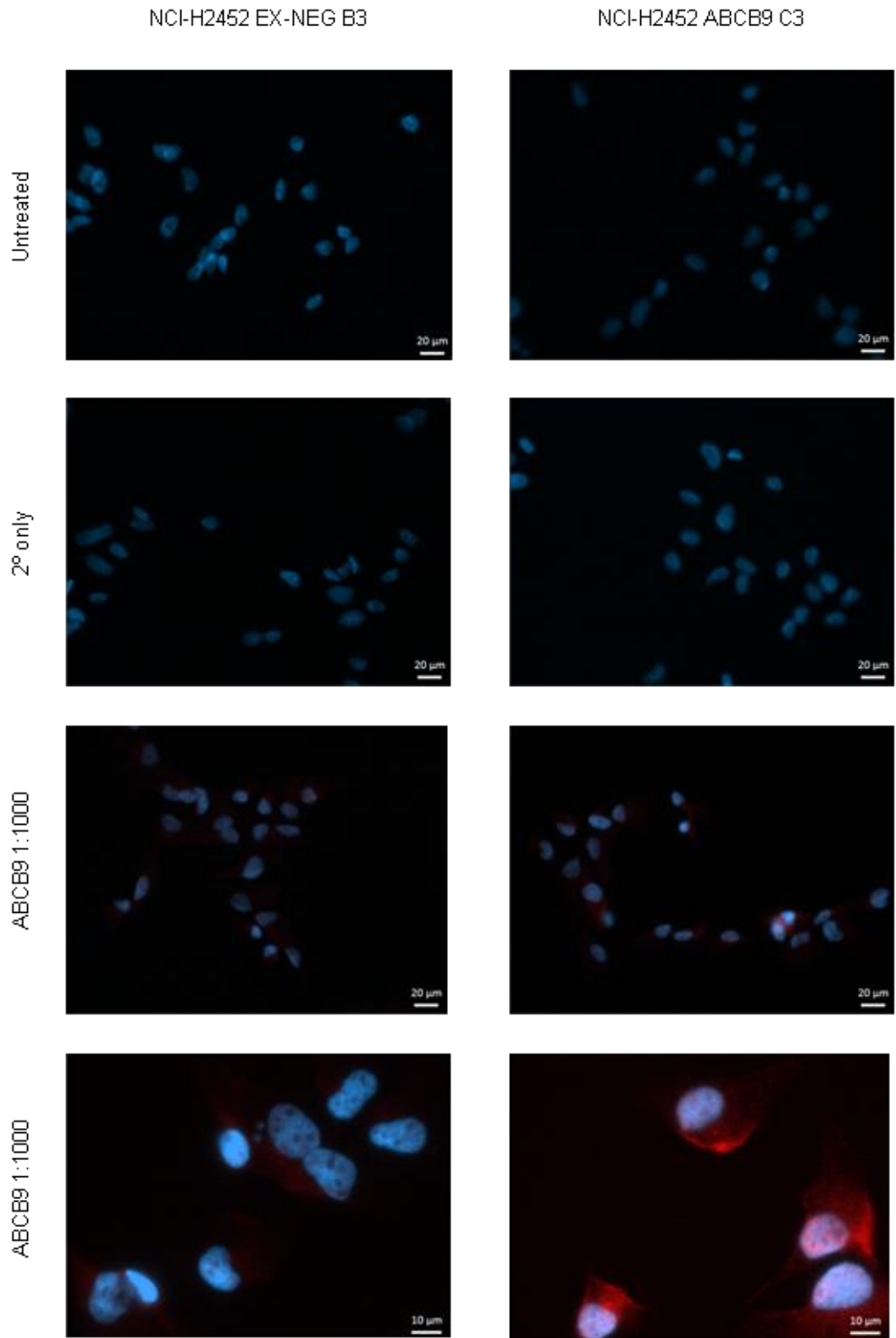
Figure 5.4 ABCB9 overexpression in NCI-H2452 clonal variants.
Immunoflourescent images showing overexpression of ABCB9 in transfected cells.
ABCB9 staining (red), nuclei stained with DAPI (blue). Images captured on Zeiss Axio
Vert.A1 with N-Achroplan 100x objective for bottom ABCB9 images, and EC Plan-
Neofluar 40x objective for top images. Images for both EX-NEG and ABCB9
overexpressing populations are set at the same exposure in the same channels.

population. It is apparent that the ABCB9 overexpression transfection group has increased ABCB9 expression, consistent with lysosomal expression. Small red foci represent the ABCB9 stained lysosomal regions, although there is evidence of a greater concentration of foci toward the cellular membrane, also noted in Dong *et al.*[279]. No change in ABCB9 expression is apparent between the NCI-H2452 miR-31 EX-NEG and NCI-H2452 miR-31 ABCB9+ (Fig. 5.5), with the expression of ABCB9 appearing diffuse. Mean signal intensities of the images captured at 100X magnification (bottom images in panels of Fig .5.4 and Fig. 5.5) show an increase in signal intensity in the ABCB9+ C3 clone compared to the EX-NEG B3 clone (Fig. 5.6).

5.4.2 *Direct ABCB9 overexpression promotes chemosensitivity, not chemoresistance, of MPM cells, independent of miR-31 expression*

With a correlation between miR-31 reintroduction and ABCB9 overexpression possibly modulating the intracellular accumulation of platinum-based therapeutics established in chapter 4, independent overexpression of ABCB9 was performed in the miR-31-null NCI-H2452 cell line, as described in section 5.4.1. Surprisingly, when the clonogenic capacity of the ABCB9 overexpressing NCI-H2452 cells were assessed with a clinically-relevant dose of cisplatin, a more chemosensitive phenotype was displayed, rather than the expected chemoresistant phenotype observed described in Fig. 3.5 with miR-31 mediated ABCB9 overexpression. The NCI-H2452 ABCB9 population had a surviving fraction of 64% ± 19% compared to 93% ± 9% in the vector control (termed EX-NEG) population, meaning ABCB9 overexpressing cells were on average 29% more sensitive to chemotherapy compared with the vector control equivalent (Fig. 5.7). This suggests the enhancement of the lysosomal drug transporter ABCB9 promoting chemosensitivity.
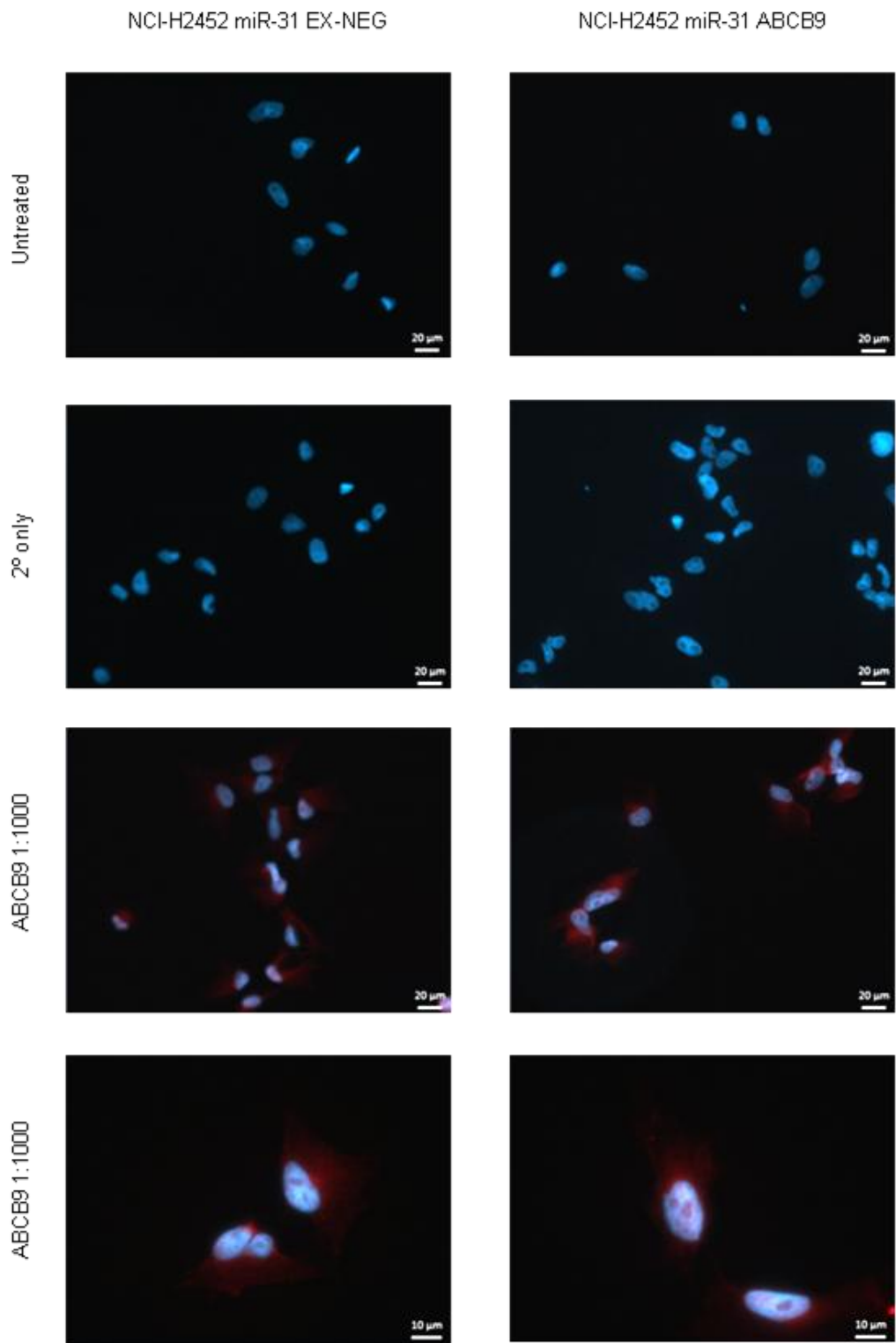
Figure 5.5 ABCB9 overexpression in NCI-H2452 miR-31 appears diffuse throughout the cytoplasmic compartment. Immunoflourescent images showing overexpression of ABCB9 in NCI-H2452 cells transfected with both miR-31 and ABCB9 overexpression plasmids. ABCB9 stained red, nuclei are stained with DAPI (blue). Images were captured on Zeiss Axio Vert.A1 with N-Achroplan 100x objective for the bottom ABCB9 images, and EC Plan-Neofluar 40x objective for the top images. Images for both EX-NEG and ABCB9 overexpressing populations are set at the same exposure in the same channels.
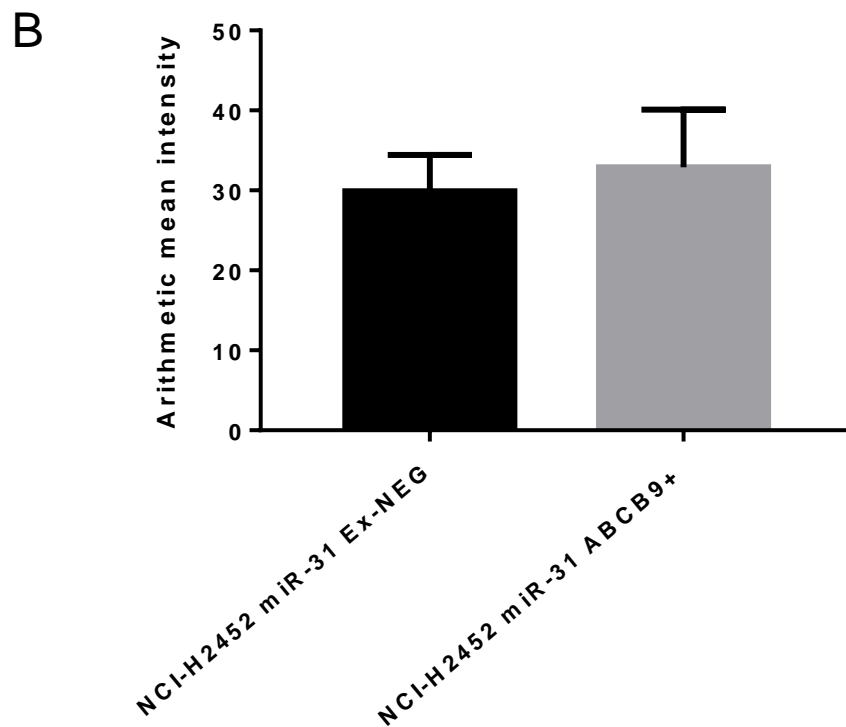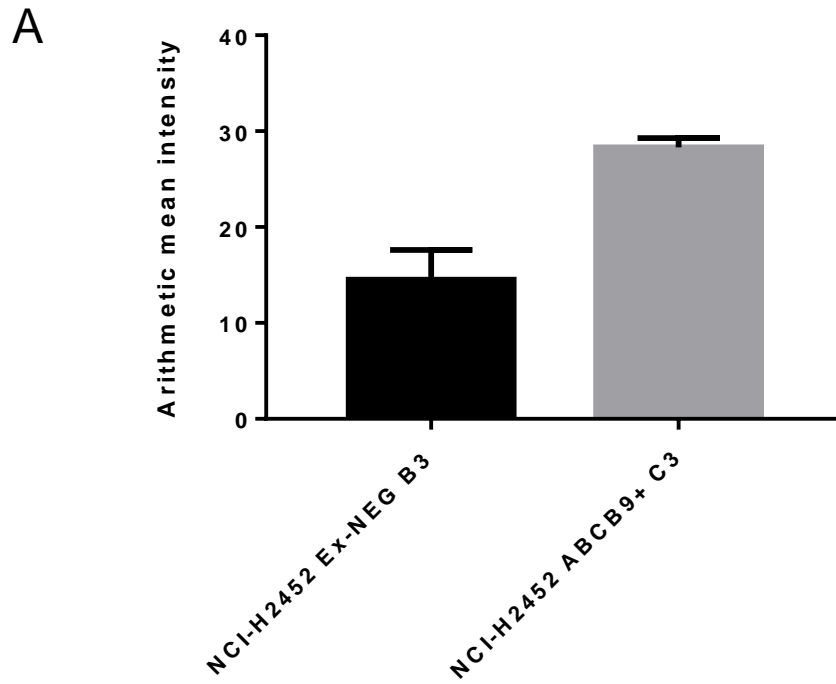
Figure 5.6 ABCB9 overexpression is greater in the NCI-H2452 ABCB9-transfected clonal population. Mean signal intensities of NCI-H2452 transfected cells immunofluorescently stained with ABCB9 represented by Fig. 5.3 and Fig. 5.4. Intensities captured in the Texas Red Channel for the images acquired on Zeiss Axio Vert.A1 with N-Achroplan 100x objective (represented in Fig. 5.3 and Fig. 5.4). Error bars are utilised as mean intensity per field (*n=2*).
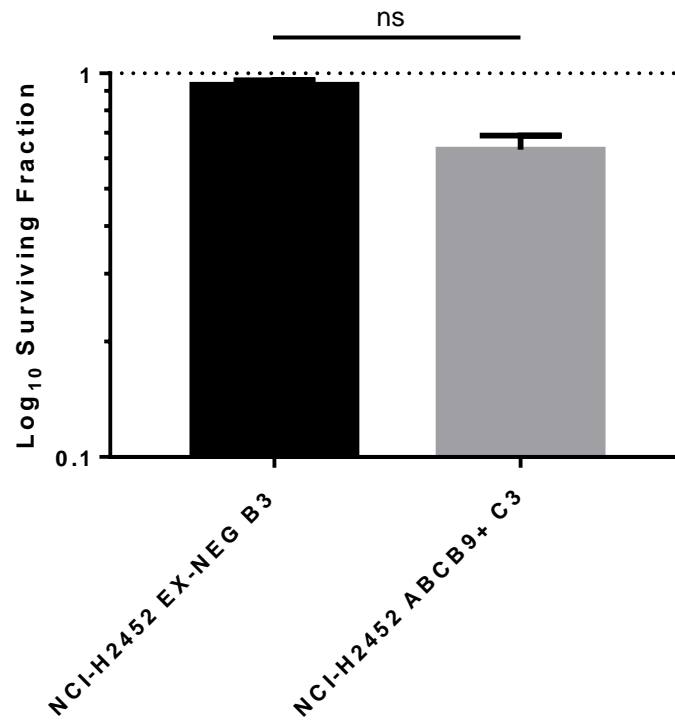
Figure 5.7 Overexpression of the lysosomal drug transporter ABCB9 increases cisplatin sensitivity in NCI-H2452 cells. Clonogenic assay revealed ABCB9 overexpression sensitises miR-31-null NCI-H2452 cells to cisplatin after treatment with 1 μM cisplatin for 24 h, with near significance reached ($p=0.0516$) ($n=3$). The dotted line represents vehicle control treatment, to which data was normalised to and accounted for in calculating the surviving fraction. Data demonstrates that the overexpression of ABCB9 independent of miR-31 expression increases sensitivity to cisplatin treatment. Data are presented as the mean ± SEM. Statistical analysis performed using Student's *t*-test.

5.4.3 *ABCB9 overexpression affects cisplatin-induced DNA damage initiation, but does not significantly affect intranuclear platinum accumulation*

To determine if the increase in chemosensitivity to cisplatin observed with miR-31 independent ABCB9 overexpression was associated with altered DNA damage, we assessed levels of γH2A.X. Supporting the increase in sensitivity with ABCB9 overexpression observed in section 5.4.2, overexpression of ABCB9 lead to greater levels of γH2A.X induction, suggesting that the high ABCB9 expressing clone C3 may be more chemosensitive (Fig. 5.8 and Fig. 5.9).

Additionally, as a measure of cisplatin-induced DNA damage, γH2A.X phosphorylation was reduced in NCI-H2452 cells with co-overexpression of ABCB9 and miR-31 (Fig. 5.8). This supports that the ABCB9 overexpression in the presence of miR-31 is not sufficient to promote a chemosensitive phenotype, thereby inferring that while miR-31 expression promotes ABCB9 expression, the miR-31-mediated chemoresistant phenotype is independent of ABCB9, and is likely driven by additional, as yet unidentified, miR-31-mediated gene or protein changes that influence MPM biology.

Whilst miR-31 mediated alterations to the intracellular accumulation of platinum are observed with the passive increase in ABCB9 expression (Fig. 4.1), the independent ABCB9 overexpression model suggests that ABCB9 does not function to enhance platinum accumulation. On a whole cell level, the high ABCB9+ clone C3 had a decrease in the amount of platinum within the intracellular environment (Fig 5.10), which is in contrast to the increase seen in chapter 4 (Fig. 4.1). Similarly, in the intranuclear region (Fig. 5.11), and in the lysosomal region of high expressing ABCB9+ C3 clone (Fig. 5.12), compared to that of EX-NEG vector control, there was a reduction in platinum content, this may relate to the apparent decrease in the
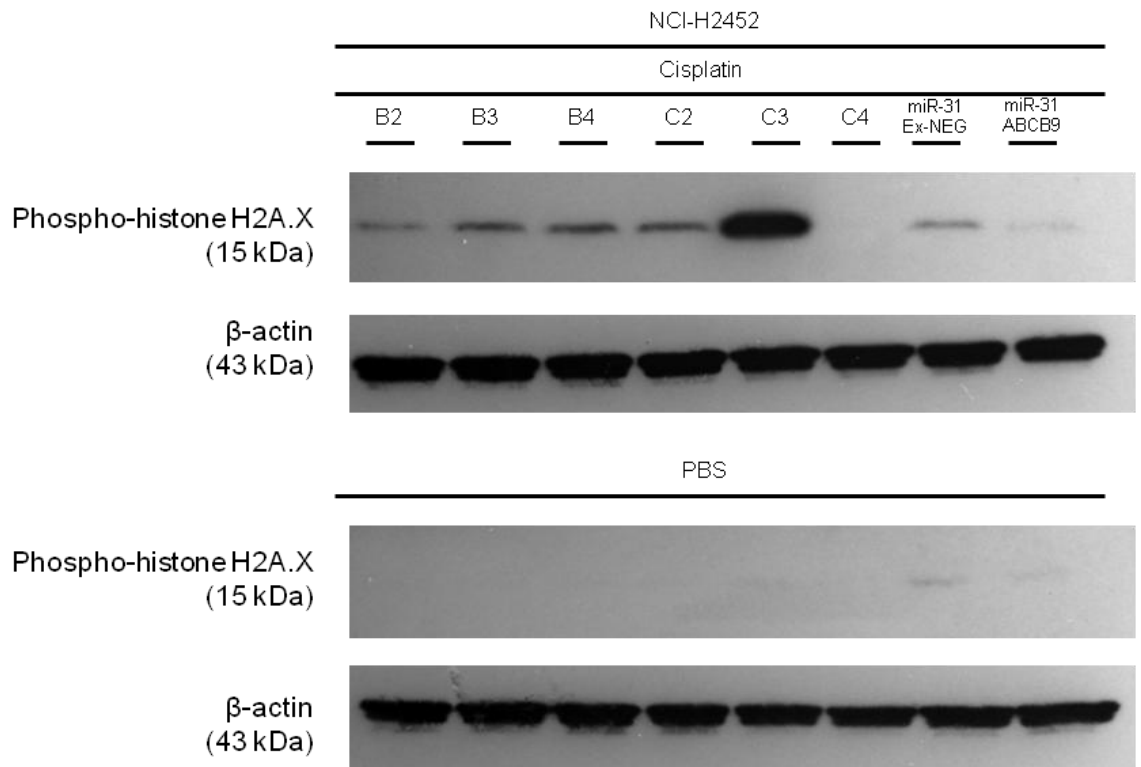
Figure 5.8 Overexpression of lysosomal drug transporter ABCB9 affects DNA damage induction. Representative Western blot demonstrating the increased levels of phospho-histone H2A.X (γH2A.X) with high expression of ABCB9. Clones B2, B3, B4 correlate to EX-NEG vector control clones. Clones C2 and C3 correlate to high expressors of ABCB9, and C4 is a low expressor of ABCB9. Clone C4 appears to demonstrate a lack of DDR, this may be due to this clone having differential expression of additional proteins involved in chemotherapy flux. All clones were treated for 24 h with 50 µM cisplatin. Data demonstrates that greater DNA damage initiation is induced when ABCB9 is highly expressed and perceptibly lower when ABCB9 has low expression.
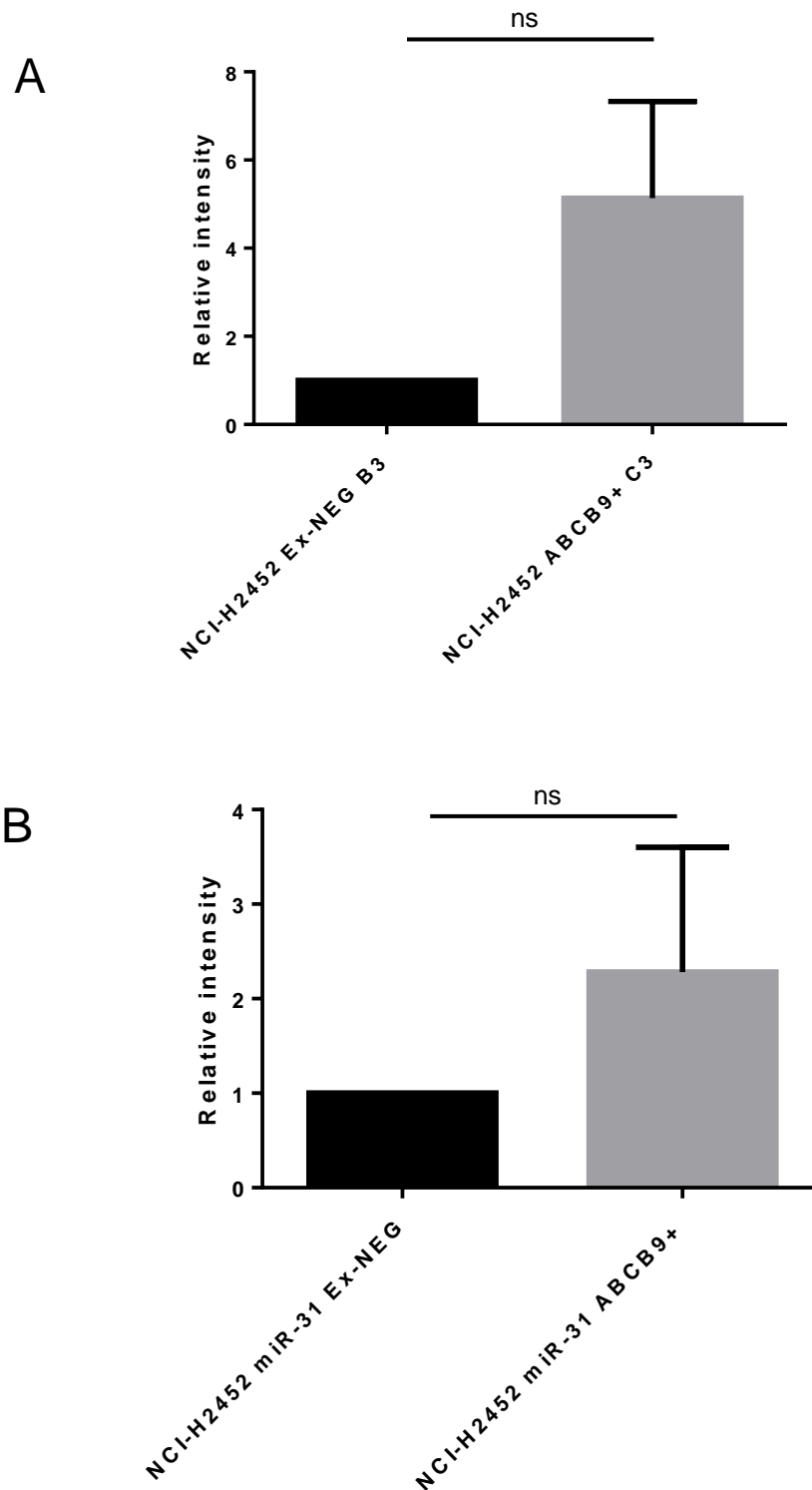
Figure 5.9 Overexpression of lysosomal drug transporter ABCB9 affects DNA damage induction. Densitometry analysis of Western blot demonstrating the increased levels of phospho-histone H2A.X with high expression of ABCB9 in the NCI-H2452 population (A) (n=3), and the NCI-H2452 miR-31 population (B) (n=3). Data demonstrates that although not significant, high ABCB9 expression connotes greater DNA damage. Data presented as the mean ± SEM. Statistical method of Student's t-test adopted for analysis. NCI-H2452 Ex-NEG B3 and miR-31 Ex-NEG utilised as relative control and are set to 1; as such no error is associated.
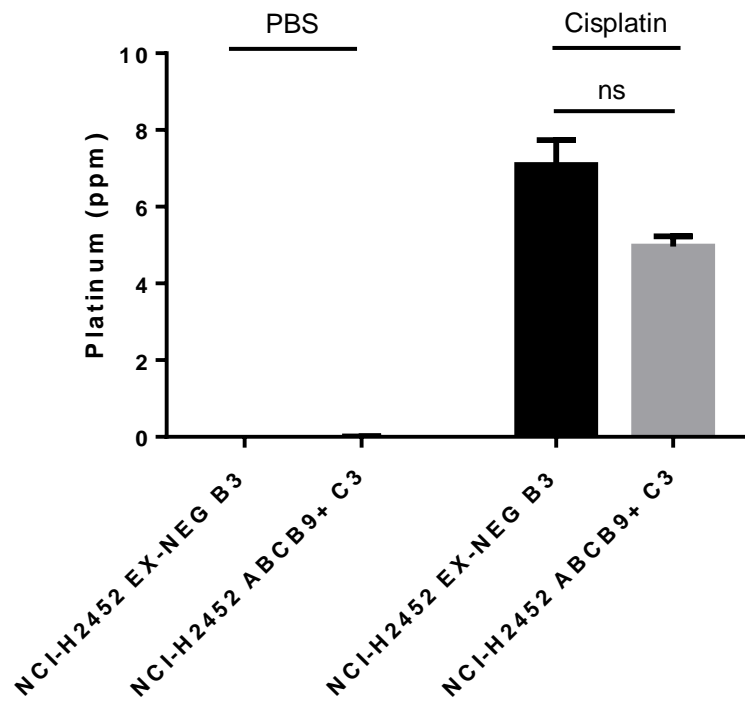
Figure 5.10 Intracellular platinum content may be altered by ABCB9 manipulation. ICP-MS analysis of whole ABCB9 manipulated cells treated with 50 µM cisplatin for 24 h. There is a decrease in levels of platinum in NCI-H2452 ABCB9+ high expressing cells (*n*=3). Data demonstrates that although not significant, high ABCB9 expression may negatively influence the amount of platinum accumulating in MPM cells. Data presented as the mean ± SEM. Statistical method of Student's *t*-test adopted for analysis.
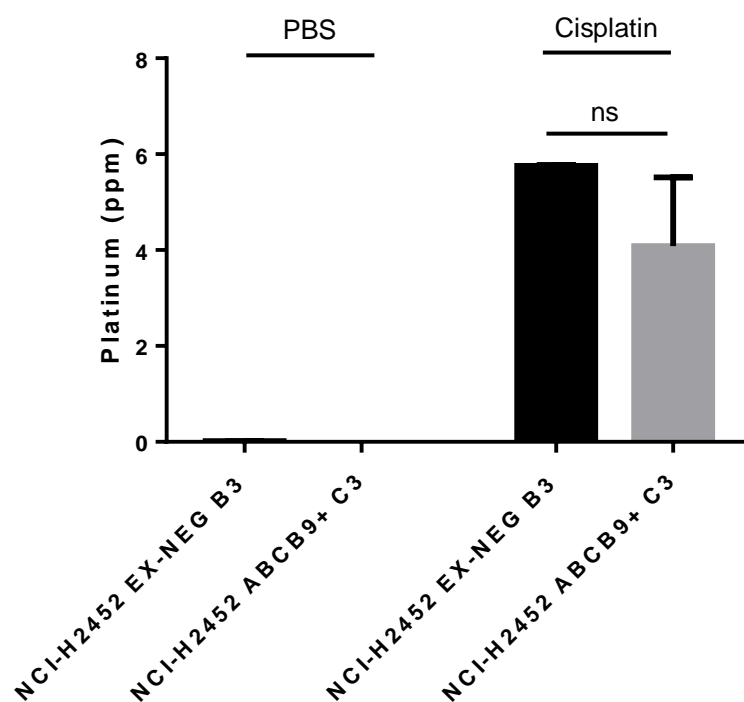
Figure 5.11 Intranuclear platinum content may be altered by ABCB9 manipulation. ICP-MS analysis of nuclear fraction collected from ABCB9 manipulated cells treated with 50 µM cisplatin for 24 h. There is a decrease in levels of platinum in NCI-H2452 ABCB9+ high expressing cells (*n*=3). Data demonstrates that high ABCB9 expression does not affect nuclear accumulation of platinum in MPM cells. Data presented as the mean ± SEM. Statistical method of Student's *t*-test adopted for analysis.
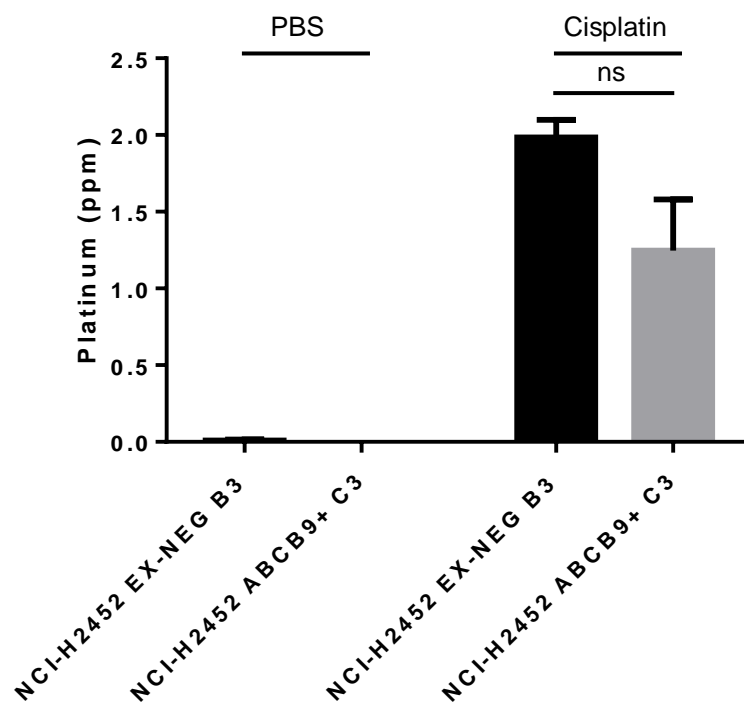
Figure 5.12 Lysosomal platinum content may be altered by ABCB9 manipulation.
ICP-MS analysis of the lysosomal fraction collected from ABCB9 manipulated cells
treated with 50 μM cisplatin for 24 h. There is a decrease in levels of platinum in NCI-
H2452 ABCB9+ high expressing cells (*n*=3). Data demonstrates that although not
significant, high ABCB9 expression may decrease the amount of platinum within the
lysosomal fraction. Data presented as the mean ± SEM. Statistical method of Student's
t-test adopted for analysis.

overall amount of platinum within the ABCB9 high expressing cells as a whole. Overall, this is in contrast to the observations made with the miR-31-mediated sequestration noted in chapter 4, suggesting that ABCB9 overexpression, independent of miR-31, may not functionally modulate this route of chemoresistance. The lysosomal drug transporter ABCB9 does appear to contribute to the modulation of the cellular response to chemotherapeutics, whereby MPM cells with high expression of ABCB9 increases sensitivity to cisplatin, however the model utilised may limit the scope of the results obtained. Further investigation with the use of confocal microscopy to co-localise LAMP-1 and ABCB9 expression may benefit the understanding of how the plasmid based model of ABCB9 overexpression differs between miR-31 driven and independently driven systems.

5.5 Discussion

The lysosomal transporter ABCB9 [342] has widely been established as a modulator of chemoresistance [313, 334, 339]. Here, surprisingly, whilst miR-31 overexpressing, more resistant MPM cells demonstrate an upregulation of ABCB9, upon direct manipulation of ABCB9 in parent NCI-H2452 cells, there is a sensitising affect to cisplatin treatment.

Intrinsic or acquired resistance is attributed to several major mechanisms [284], including the involvement of the ABC super-family, which broadly includes breast cancer resistance protein ABCG2 (BCRP), P-glycoprotein ABCB1 (P-gp) and multidrug-resistance protein 2 ABCC2 (MRP2) [344, 345]. Generally, enhanced expression of these protein leads to ATP-driven efflux of drugs and a reduction in the intracellular concentration of many toxins, ultimately contributing to MDR [344]. ABC transporters are ubiquitously expressed in normal tissue, and many drugs targeting these transporters have been adopted as chemosensitisers in clinical trials. Unfortunately, due to the ubiquitous nature of these proteins, many first generation targeted therapies have proven toxic to patients, with unacceptable pharmacokinetic interactions [344]. Here, the hypothesis was that ABCB9, as a drug transporter, aided the sequestration of cisplatin into lysosomal regions. However, the independent overexpression of ABCB9, as discussed in this chapter, supported the widely accepted consensus that as an ABC transporter, ABCB9 is involved in efflux, as the concentration of intracellular platinum decreased upon ABCB9 overexpression. Whilst the data demonstrated a reduced amount of platinum in ABCB9+ cells, according to general ABC transporter mechanisms, the increase in efflux should imply increased resistance to therapy [345], whereas here, we observed an increase

in sensitivity, which is supported by the notable affects on cisplatin induced DNA damage with multiple clones, as observed in Fig. 5.8.

The roles of ABC transporters have recently been reviewed, with newly discovered roles in the modification of distribution of ABC transporters to intra- and extra-cellular compartments to increase sequestration efficacy [345]. In yeast it has been reported that ectopic expression of ABCB9 promoted an enhancement in drug sensitivity, and its accumulation into lysosomes may contribute to the increase in sensitivity observed. Here, the observation of ABCB9 overexpression connoting increased drug sensitivity would be in agreement with the reported results in Ohashi-Kobayashi *et al.* [334], yet the replication of increased lysosomal drug sequestration was not apparent.

The relationship between ABC transporters and miRNA has been well discussed and is an area of particular interest within the field [344]. Primarily, research has focussed upon miRNA as novel therapies to overcome MDR via the exploration of miRNA-mediated ABC transporter regulation [346, 347]. Ma *et al.* [347] isolated the miRNA miR-487a as a resensitiser to mitoxantrone resistant breast cancer cells; its functionality was shown to target and suppress breast cancer resistance protein, BCRP, whereas Pan *et al.* [346] reported that miR-328 negatively regulated BCRP. The literature exploring the relationship between miRNA and ABCB9 is extremely limited, with only one particular publication relating to miR-31. Dong *et al.* [313] explored the interaction between ABCB9 and the miRNA miR-31 in NSCLC. Their research correlated cisplatin resistant cell lines expressing greater levels of miR-31, which our MPM data is synonymous with. However, the Dong *et al.* [313] group went on to correlate the higher expression of miR-31 with a downregulation in ABCB9, the suggestion being that miR-31 directly targets ABCB9, thus repressing

the translation of the transporter. Here, within this MPM study, there is an observed increase in ABCB9 associated with the miR-31-mediated chemoresistant phenotype; it is possible that miRNA can positively regulate expression [348, 349], whereby miR-31 could be positively regulating ABCB9 directly. Prospectively, the difference in response may be attributed to the pleiotropic function of miR-31 targeting a transcriptional regulator (OCT-1) that modulates ABCB9 expression in MPM. Furthermore, Dong *et al.* [313] focussed upon ABCB9 downregulation increasing resistance to cisplatin in non small cell lung cancer, our ABCB9 overexpression model essentially supports the findings reported, however the research describes ABCB9 as being plasma membrane located, which is not observed here until ABCB9 is directly overexpressed, and is in conflict with other reports of ABCB9 location [312, 343].

Whilst the manipulation of ABCB9 expression was of logical and interesting investigation in terms of the intracellular platinum sequestration observed in chapter 4, there remains potential to modulate OCT-1 expression to observe its effect upon MPM chemoresistance. Potentially, manipulating OCT-1 expression may recapitulate the increase in ABCB9 observed through miR-31-mediation, which may increase the chemoresistant phenotype in a similar manner to that of chapter 3. There is however, a limitation to the manipulation or overexpression of OCT-1 as it functions bipotentially [315]. OCT-1 is known to be dynamically phosphorylated following oxidative or genotoxic cell stress, and its functionality is complex [335, 336, 350]. OCT-1 maintains many gene expression levels including Polr2a, which encodes a subunit of RNA polymerase II, where in an OCT-1 deficient environment Polr2a mRNA is inappropriately repressed. OCT-1 plays an unusual functional role as a Polr2a anti-repressor only in stress response conditions, relaying the intricacy of this homologous transcription factor [350].

In addition to lysosomal transport, miR-31 can potentially regulate other sequestration pathways which may potentially support our findings. As previously discussed, there is potential for alterations in nuclear envelope structure; the packaging of cisplatin into exosomes; and rearrangements of the cytoskeleton to modulate resistance to platinum based therapeutics [308-310]. Alterations in proteins involved in the morphology of the nuclear envelope may directly contribute to tumourigenesis [351, 352]. Particularly interestingly, although the nuclear envelope protein lamin B1 is not directly targeted by miR-31, there is a relationship between lamin B1 expression, OCT-1 and miR-31 [353]. Malhas *et al.* [353] described mutated lamin B1 resulting in the loss of OCT-1 sequestration in the nuclear periphery, which led to dysregulation of OCT-1 targets. Nuclear lamins were demonstrated to regulate miR-31 levels, adding further intricacy to how the mechanisms of the nuclear envelope can contribute to gene expression and potentially cellular resistance [353]. Briefly, miR-31 may regulate OCT-1, and therefore its targets, however OCT-1 may also influenced by lamin B1, and lamin B1 may be influenced by a indirect effect of miR-31 overexpression, which consequently may affect nuclear transport and potentially sequestration of chemotherapeutics.

Although, here, the focus has been to analyse the affect of ABCB9 has on the chemosensitive phenotype of MPM cells by artificially driving increased expression, there are a number of ways in which this may not fully recapitulate the response of ABCB9 if it were indirectly under the control of miR-31. The plasmid overexpression system may, for example, encode the ABCB9 protein which could then be subjected to post-translational modification, affecting the activity of the protein, which may not occur within the miRNA controlled pathway. In order to assess whether additional modifications have occurred, a number of techniques could

be utiliused including Western blot to analyse glycosylation and phosphorylation, as in Li *et al.* [354].

Ultimately, we have shown miR-31 mediation of a chemoresistant phenotype within *in vitro* studies of MPM, with an observed increase in ABCB9 expression. However, when ABCB9 is overexpressed independently of miR-31, an increase in sensitivity is observed, opposing the initial hypothesis, and perhaps indicating that the increase in ABCB9 is in fact passive, as miR-31 is mediating other molecules that potentially contribute more to the regulation of cisplatin intracellular accumulation, as summarised in Fig. 5.13. Altogether, this insinuates that ABCB9 expression is important within the context of MPM; however ABCB9 upregulation, in this case, may not contribute to the specific pathway mediated by miR-31 to enhance MPM chemoresistance, however further investigation of the model used may be needed.
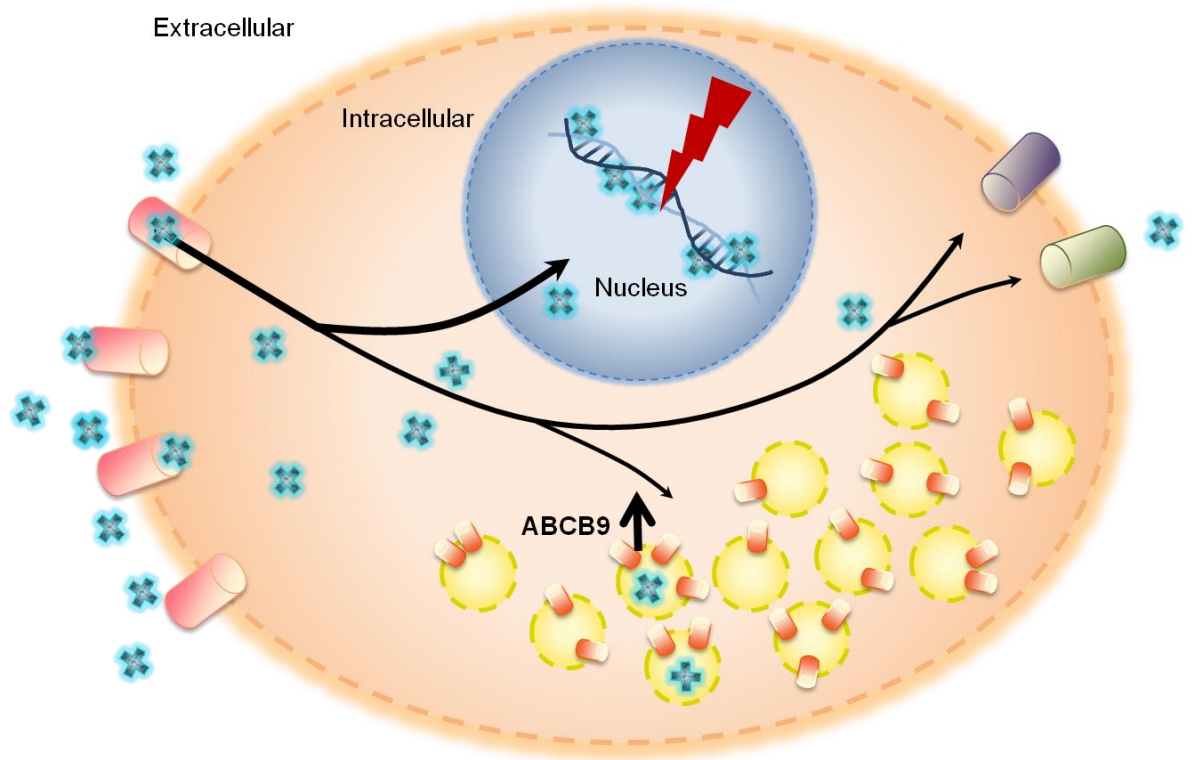
Figure 5.13 Summary of the effect of ABCB9 overexpression on MPM cell. The MPM cell (orange) has notable increased sensitivity to chemotherapy (blue cross structures) with ABCB9 overexpression, independent of miR-31 modulation. Overall, it can be noted that the increase in ABCB9 expression is important within the context of MPM chemosensivity; however ABCB9 upregulation may not contribute to the specific pathway mediated by miR-31 to enhance MPM chemoresistance.

Chapter 6:

Concluding discussion

6.1 Concluding discussion

MPM is an aggressive and debilitating asbestos related disease which is associated with an extremely poor prognosis, mainly owing to inherent or developed chemoresistance [74, 82, 355]. The investigation here aimed to develop an understanding of why MPM cells are resistant to chemotherapy, and to expand a clinically viable route by which sensitivity could be enhanced. A group of non coding molecules named microRNAs are established regulators of many cancer pathways [356]. A particular miRNA, miR-31, is encoded on a fragile site often deleted in MPM patients [188], which led to the potential for miR-31 to be functionally explored in the context of chemoresistance.

It is evident that the role of miR-31 within differing tumour types is multi-faceted and its exact functions remain unclear, with context dependent evidence supporting both oncogenic and tumour suppressive functions [195, 254, 256, 357]. Within MPM, deletion of the fragile site at which miR-31 is encoded has been correlated with poor prognosis [188], however, it has also been reported that miR-31 expression is allied with aggressive tumour subtypes in patient cohorts [189]. Surprisingly, the present study has determined that miR-31 expression in MPM promotes resistance to platinum-based therapy *in vitro*.

Data from this study indicates the loss of miR-31 in MPM tumours may actually confer a chemosensitive phenotype. Although the data represented here is generated in *in vitro* based 2D models, there may be allied results *in vivo* which could confirm and validate miR-31 suppression having sensitising affects to chemotherapeutic treatment. Contrasting with the initial hypothesis, the data support the alternative hypothesis that miR-31 loss in MPM confers a positive prognostic influence. The potential mechanism by which miR-31 mediates resistance appears to be reliant upon

regulation of intracellular transport. Dependence upon nuclear transport has previously been noted in breast cancer [358], with associations between altered transport of platinum containing agents within the cellular environment and resistance to therapy being comprehensively reviewed [275]. Laurila *et al.* [359] detailed the involvement of a nuclear transport protein, KPNA7, with promotion of malignancy in pancreatic cancer. The silencing of KPNA7 lead to the inhibition of malignancy in pancreatic cell lines, which highlights the importance of transportation from the cytoplasmic to nuclear compartment, and its involvement with resistance to therapy.

Cellular accumulation of chemotherapeutics has been comprehensively reviewed [360]. With a higher overall amount of platinum in miR-31 expressing cells (Fig. 4.1), and a reduction in the concentration of platinum in the nuclear fraction (Fig. 4.5), the question remained as to how cells were able to survive an increased intracellular concentration of cisplatin. There is evidence supporting that miRNAs can mediate cellular sequestration, through the alteration of calcium signalling, or the mediation of multi-drug resistant proteins [361-363]. Here, following further fractionation of cellular components, a change in lysosomal accumulation was observed; this promoted the investigation of possible drug transporters that were bound to lysosomes, and indeed promoted the investigation as to whether miR-31 expressing cells had a higher aggregate burden of lysosomes. Notably, Pennati *et al.* [362] showed that miR-205 replacement in prostate cancer cells down-regulated lysosome function and protein trafficking, leading to alterations in the autophagic flux of cells, which changed the detoxifying capabilities by which cells become cisplatin resistant. Drayton *et al.* [364] correlated a reduced miR-27a expression with the cysteine and glutamate exchanger SLC7A11. Cisplatin resistant bladder cancer cell lines were resensitized by initiating miR-27a expression, or reducing the activity

of SLC7A11 via siRNA, which supports the findings that miRNA can regulate cellular transporters, thus connoting regulation of cellular chemoresistance.

The lysosomally bound drug transporter ABCB9 [312] has been identified as a modulator of resistance, with up- or down- regulation of the protein enhancing or reducing response to therapeutics [334]. Surprisingly, whilst ABCB9 appears to be increased with the miR-31 overexpressing more resistant phenotype, upon manipulation of ABCB9 in miR-31-null NCI-H2452 cells, there is a sensitising affect to cisplatin treatment (Fig. 5.7). Recently, Dong *et al.* [313] examined the relationship between miR-31 and ABCB9. The investigation established a link in NSCLC cisplatin resistant cell lines having higher expression of miR-31, and the downregulation drug transporter ABCB9, potentiating that miR-31 directly targeted ABCB9 and so repressed its translation. Whilst the results here suggested ABCB9 may not be directly associated with the overriding mechanism behind cellular accumulation and chemoresistance, there are many other routes by which sequestration of chemotherapeutics can be modulated. There is emerging evidence that extracellular vesicles, including exosomes [308], which are known to package cisplatin, can be modulated by multidrug resistance proteins and can themselves control the uptake of drugs into vesicles, limiting the bioavailability of chemotherapeutics [365]. Federici *et al.* [366] portrayed cisplatin accumulation in extracellular vesicles to be enhanced in acidic pH levels, with a reduction in cellular resistance resulting from the use of proton pump inhibitors.

The movement of platinum based chemotherapeutics within the intracellular environment is widely characterised, with CTR1, ATP7A and ATP7B known to play significant trafficking roles [70, 75]. Here, although no significant changes are apparent for the influx and efflux transporters CTR1 (Fig. 4.2), ATP7A and ATP7B

(Fig. 4.3 and Fig. 4.4), there may still be contributions to the overall phenotypic resistance observed with miR-31 reintroduction. Stordal *et al.* [367] and Kalayda *et al.* [293] illustrated the importance of localisation of these key proteins, which can modulate accumulation and orchestrate the sequestration of cisplatin within resistant cells although there is typically no change in overall expression. ATP7A and ATP7B have been established as golgi network transporters, however within resistant models, a translocation to outer vesicular structures has been noted [293], signifying that whilst the present results show no gross difference, these molecules may be modulating sensitivity through alterations in their localisation.

The effect of miR-31 reintroduction on increasing chemoresistance was contrary to our initial hypothesis, as previously the group had associated miR-31 overexpression with increased sensitivity to therapy in oesophageal adenocarcinoma (OAC) [256]. A downregulation of miR-31 in radioresistant OAC cells was identified, and upon subsequent re-expression of miR-31, a radiosensitising effect was observed [256]. Although unanticipated, a potentially novel mechanism behind enhanced resistance, which may potentiate a modified strategy of treatment in the future, has been uncovered. Many MPM patients are inherently resistant to chemotherapy, and most have extremely poor prognosis [368]; this has driven the field to find an alternative therapeutic, or indeed enhance the ability of the readily available therapeutics to combat this disease [245], as observed in the effective co-treatment of cisplatin and pineapple extract bromelain in malignant peritoneal mesothelioma [369]. Prospectively, the consequence of further investigating this mechanism within an *in vivo* system may lead to the ability to screen patients for miR-31 status. Patients who express high levels of miR-31 could potentially be stratified to have an antagomir administered to suppress miR-31 expression, which could mean the efficiency of platinum based chemotherapy cytotoxicity would be enhanced. Zhang *et al.* [370]

recently co-treated with both paclitaxal and antagomir miR-10b in breast cancer cell lines, using the chemotherapeutic to treat the primary tumor and suppressing miR-10b to decrease metastasis, the results were promising and concluded successful administration of both the antagomir and the paclitaxal via a liposomal based system.

Interestingly, miRNA treatment in the form of nucleic acid-modified DNA phosphorothioate antisense oligonucleotides has already entered human clinical trials in treatment of disease [219]. Although not in cancer, miR-122, the abundant liver expressed miR, is sequestered by the oligonucleotide and bound in a duplex, which inhibits endogenous function within hepatitis C virus infection. Results thus far have shown promise, with long-standing dose-dependent decreases in infection levels without evidence of acquired resistance [219]. In relation to mesothelioma, there has been recent progress in clinical trials using miR to modulate the disease, Kao *et al.* [371] reported both a metabolic and radiological response with miR-16 based mimics. Interestingly, the development of TargomiRs, miRNA delivered via bacterial minicells, to treat thoracic cancers has also shown promise [235].

Within the context of this study, miR-31 expression in MPM facilitates resistance to platinum-based chemotherapy. MiR-31-mediated changes in ABCB9 expression and lysosomal uptake of cisplatin are not sufficient to promote chemoresistance, indicating that miR-31 mediates chemoresistance in MPM through a yet unidentified molecular mechanism involving reduced nuclear trafficking of chemotherapeutic agents. Overall, the data suggests that while deletions in chromosome 9p21.3 may be associated with an overall poor prognosis, the specific loss of miR-31 from this region may not contribute to the chemoresistance observed in MPM patients. Screening patients for miR-31 expression status and corresponding suppression of

the miRNA may promote enhanced sensitivity to platinum based chemotherapeutics, improving patient outcomes.

6.2 Future work

Prospectively, with the observed increase in chemoresistance with miR-31 reintroduction in MPM *in vitro*, it would be advantageous to firstly develop a 3-dimensional based system to mimic that of the 2-dimensional model utilised within this study, with potential to move forward to an *in vivo* model that could explicate cisplatin sensitivity at a more clinically relevant level. With an *in vivo* model of MPM, not only would this add to our understanding of miR-31 increasing resistance in MPM, it would be interesting to develop the potential delivery of a miR-31 suppressing construct, and assess response to chemotherapy post administration.

Additionally, analysis of patient derived samples stratified into pre- and post-treatment, with response data would add greatly to the impact of this study. The patient derived samples stratified by response could be utilised to analyse predictive biomarkers, including potentially miR-31. Unfortunately, patient samples that have response data completed are currently limited; however, the expansion of local tumour banks and the development of the nationwide Mesobank are addressing this issue.

Furthermore, a screen for miR-31-regulated genes and proteins by transcriptome and proteome analysis, respectively, may be completed. The undertaking of this investigation would comprehensively identify miR-31 targets, which could be further analysed by pathway analysis to identify potential new avenues to chemoresistance.

The pathways modulated by miR-31 in intracellular accumulation are still unknown. There is potential to investigate chaperones of cisplatin, including Atox1; this is currently being considered for investigation. Furthermore, with the unexpected relationship between ABCB9 overexpression and increased sensitivity, the focus should be as to how miR-31 modulates the intranuclear drug accumulation. Potentially, the accumulation question could be answered by the investigation of nuclear transport proteins, an area which is currently under researched.

References

1.   van Meerbeeck JP, Scherpereel A, Surmont VF, Baas P: **Malignant pleural mesothelioma: The standard of care and challenges for future management**. *Critical Reviews in Oncology/Hematology* 2011, **78**(2):92-111.

2.   Markaki S, Protopapas A, Milingos S, Lazaris D, Antsaklis A, Michalas S: **Primary malignant mesothelioma of the peritoneum: a clinical and immunohistochemical study**. *Gynecologic Oncology* 2005, **96**(3):860-864.

3.   Mensi C, Giacomini S, Sieno C, Consonni D, Riboldi L: **Pericardial mesothelioma and asbestos exposure**. *International Journal of Hygiene and Environmental Health* 2011, **214**(3):276-279.

4.   Weng C-H, Ho P-Y, Chen C-K, Tsai W-K: **Incidentally discovered malignant mesothelioma of the tunica vaginalis**. *Journal of the Formosan Medical Association* 2013, **112**(1):57-58.

5.   Haberkorn U: **Positron emission tomography in the diagnosis of mesothelioma**. *Lung Cancer* 2004, **45, Supplement**(0):S73-S76.

6.   MacLeod N, Price A, O'Rourke N, Fallon M, Laird B: **Radiotherapy for the treatment of pain in malignant pleural mesothelioma: A systematic review**. *Lung Cancer* 2014, **83**(2):133-138.

7.   Muers MF, Stephens RJ, Fisher P, Darlison L, Higgs CMB, Lowry E, Nicholson AG, O'Brien M, Peake M, Rudd R *et al*: **Active symptom control with or without chemotherapy in the treatment of patients with malignant pleural mesothelioma (MS01): a multicentre randomised trial**. *The Lancet* 2008, **371**(9625):1685-1694.

8.   Thompson SK, Mason E: **Asbestos related malignancy: Mesothelioma**. *Chemical Health and Safety* 2003, **10**(1):4-6.

9.   Bonomo L, Feragalli B, Sacco R, Merlino B, Storto ML: **Malignant pleural disease**. *European Journal of Radiology* 2000, **34**(2):98-118.

10.   Linton A, Vardy J, Clarke S, van Zandwijk N: **The ticking time-bomb of asbestos: Its insidious role in the development of malignant mesothelioma**. *Critical Reviews in Oncology/Hematology* 2012, **84**(2):200-212.

11. Flores RM, Rusch VW: **Staging of Mesothelioma**. In: *Malignant Mesothelioma: Advances in Pathogenesis, Diagnosis, and Translational Therapies.* edn. Edited by Pass HI, Vogelzang NJ, Carbone M. New York, NY: Springer New York; 2005: 402-415.

12. Herth F: **Diagnosis and staging of mesothelioma transthoracic ultrasound**. *Lung Cancer* 2004, **45, Supplement**:S63-S67.

13. Inai K: **Pathology of mesothelioma**. *Environmental Health and Preventive Medicine* 2008, **13**(2):60-64.

14. Meyerhoff RR, Yang C-FJ, Speicher PJ, Gulack BC, Hartwig MG, D'Amico TA, Harpole DH, Berry MF: **Impact of mesothelioma histologic subtype on outcomes in the Surveillance, Epidemiology, and End Results database**. *Journal of Surgical Research* 2015, **196**(1):23-32.

15. Mansfield AS, Symanowski JT, Peikert T: **Systematic review of response rates of sarcomatoid malignant pleural mesotheliomas in clinical trials**. *Lung Cancer* 2014, **86**(2):133-136.

16. O'Kane SL, Pound RJ, Campbell A, Chaudhuri N, Lind MJ, Cawkwell L: **Expression of bcl-2 family members in malignant pleural mesothelioma**. *Acta oncologica (Stockholm, Sweden)* 2006, **45**(4):449-453.

17. Bianchi C, Bianchi T: **Malignant mesothelioma: global incidence and relationship with asbestos**. *Industrial health* 2007, **45**(3):379-387.

18. Pinto C, Novello S, Torri V, Ardizzoni A, Betta PG, Bertazzi PA, Casalini GA, Fava C, Fubini B, Magnani C *et al*: **Second Italian Consensus Conference on Malignant Pleural Mesothelioma: State of the art and recommendations**. *Cancer Treatment Reviews* 2013, **39**(4):328-339.

19. Executive HaS: **Mesothelioma Mortality in Great Britain: Analyses by Geographical Area and Occupation 2005**. 2005.

20. Chapman A, Mulrennan S, Ladd B, Muers MF: **Population based epidemiology and prognosis of mesothelioma in Leeds, UK**. *Thorax* 2008, **63**(5):435-439.

21.   McElvenny DM, Darnton AJ, Price MJ, Hodgson JT: **Mesothelioma mortality in Great Britain from 1968 to 2001**. *Occupational medicine (Oxford, England)* 2005, **55**(2):79-87.

22.   Executive HaS: **Mesothelioma in Great Britain**. 2014, **Mesothelioma mortality in Great Britain 1968-2014**.

23.   Hilliard AK, Lovett JK, McGavin CR: **The rise and fall in incidence of malignant mesothelioma from a British Naval Dockyard, 1979-1999**. *Occupational medicine (Oxford, England)* 2003, **53**(3):209-212.

24.   Nymark P, Wikman H, Hienonen-Kempas T, Anttila S: **Molecular and genetic changes in asbestos-related lung cancer**. *Cancer Letters* 2008, **265**(1):1-15.

25.   Ross M, Langer AM, Nord GL, Nolan RP, Lee RJ, Van Orden D, Addison J: **The mineral nature of asbestos**. *Regulatory Toxicology and Pharmacology* 2008, **52**(1, Supplement):S26-S30.

26.   Thompson SK, Mason E: **Asbestos: Mineral and fibers**. *Chemical Health and Safety* 2002, **9**(4):21-23.

27.   Magnani C, Dalmasso P, Biggeri A, Ivaldi C, Mirabelli D, Terracini B: **Increased risk of malignant mesothelioma of the pleura after residential or domestic exposure to asbestos: a case-control study in Casale Monferrato, Italy**. *Environmental health perspectives* 2001, **109**(9):915-919.

28.   Huang SXL, Jaurand M-C, Kamp DW, Whysner J, Hei TK: **Role of Mutagenicity in Asbestos Fiber-Induced Carcinogenicity and Other Diseases**. *Journal of Toxicology and Environmental Health Part B, Critical Reviews* 2011, **14**(1-4):179-245.

29.   Emri S, Demir AU: **Malignant pleural mesothelioma in Turkey, 2000–2002**. *Lung Cancer* 2004, **45, Supplement**(0):S17-S20.

30.   Kokturk N, Firat P, Akay H, Kadilar C, Ozturk C, Zorlu F, Gungen Y, Emri S: **Prognostic significance of Bax and Fas Ligand in erionite and asbestos induced Turkish malignant pleural mesothelioma**. *Lung Cancer* 2005, **50**(2):189-198.

31.   Bertino P, Marconi A, Palumbo L, Bruni BM, Barbone D, Germano S, Dogan AU, Tassi GF, Porta C, Mutti L *et al*: **Erionite and asbestos differently cause transformation of human mesothelial cells**. *International journal of cancer Journal international du cancer* 2007, **121**(1):12-20.

32.   Carbone M, Rdzanek MA: **Pathogenesis of Malignant Mesothelioma**. *Clinical Lung Cancer* 2004, **5, Supplement 2**(0):S46-S50.

33.   Roushdy-Hammady I, Siegel J, Emri S, Testa JR, Carbone M: **Genetic-susceptibility factor and malignant mesothelioma in the Cappadocian region of Turkey**. *The Lancet* 2001, **357**(9254):444-445.

34.   Gazdar AF, Carbone M: **Molecular Pathogenesis of Malignant Mesothelioma and its Relationship to Simian Virus 40**. *Clinical Lung Cancer* 2003, **5**(3):177-181.

35.   Rizzo P, Bocchetta M, Powers A, Foddis R, Stekala E, Pass HI, Carbone M: **SV40 and the pathogenesis of mesothelioma**. *Seminars in Cancer Biology* 2001, **11**(1):63-71.

36.   Barbanti-Brodano G, Sabbioni S, Martini F, Negrini M, Corallini A, Tognon M: **Simian virus 40 infection in humans and association with human diseases: results and hypotheses**. *Virology* 2004, **318**(1):1-9.

37.   Batra H, Antony VB: **Pleural mesothelial cells in pleural and lung diseases**. *Journal of thoracic disease* 2015, **7**(6):964-980.

38.   Testa JR, Giordano A: **SV40 and cell cycle perturbations in malignant mesothelioma**. *Seminars in Cancer Biology* 2001, **11**(1):31-38.

39.   Testa JR, Cheung M, Pei J, Below JE, Tan Y, Sementino E, Cox NJ, Dogan AU, Pass HI, Trusa S *et al*: **Germline BAP1 mutations predispose to malignant mesothelioma**. *Nat Genet* 2011, **43**(10):1022-1025.

40.   Cigognetti M, Lonardi S, Fisogni S, Balzarini P, Pellegrini V, Tironi A, Bercich L, Bugatti M, Rossi G, Murer B *et al*: **BAP1 (BRCA1-associated protein 1) is a highly specific marker for differentiating mesothelioma from reactive mesothelial proliferations**. *Modern pathology : an official journal of the United States and Canadian Academy of Pathology, Inc* 2015, **28**(8):1043-1057.

41.   Wolf AS, Flores RM: **Current Treatment of Mesothelioma: Extrapleural Pneumonectomy Versus Pleurectomy/Decortication**. *Thorac Surg Clin* 2016, **26**(3):359-375.

42.   Sugarbaker DJ, Wolf AS: **Surgery for malignant pleural mesothelioma**. *Expert review of respiratory medicine* 2010, **4**(3):363-372.

43.   van Zandwijk N, Clarke C, Henderson D, Musk AW, Fong K, Nowak A, Loneragan R, McCaughan B, Boyer M, Feigen M *et al*: **Guidelines for the diagnosis and treatment of malignant pleural mesothelioma**. *Journal of thoracic disease* 2013, **5**(6):E254-E307.

44.   Treasure T, Lang-Lazdunski L, Waller D, Bliss JM, Tan C, Entwisle J, Snee M, O'Brien M, Thomas G, Senan S *et al*: **Extra-pleural pneumonectomy versus no extra-pleural pneumonectomy for patients with malignant pleural mesothelioma: clinical outcomes of the Mesothelioma and Radical Surgery (MARS) randomised feasibility study**. *The Lancet Oncology* 2011, **12**(8):763-772.

45.   Trust RBHNF: **MARS 2: A Feasibility Study Comparing (Extended) Pleurectomy Decortication Versus no Pleurectomy Decortication in Patients With Malignant Pleural Mesothelioma (MARS2)**. *Royal Brompton & Harefield NHS Foundation Trust [web]* 2013.

46.   Opitz I: **Management of malignant pleural mesothelioma—The European experience**. *Journal of thoracic disease* 2014, **6**(Suppl 2):S238-S252.

47.   Parker C, Neville E: **Lung cancer • 8: Management of malignant mesothelioma**. *Thorax* 2003, **58**(9):809-813.

48.   Haas AR, Sterman DH: **Malignant Pleural Mesothelioma: Update on Treatment Options with a Focus on Novel Therapies**. *Clinics in Chest Medicine* 2013, **34**(1):99-111.

49.   Flores RM: **Surgical Options in Malignant Pleural Mesothelioma: Extrapleural Pneumonectomy or Pleurectomy/Decortication**. *Seminars in Thoracic and Cardiovascular Surgery* 2009, **21**(2):149-153.

50. van Sandick JW, Kappers I, Baas P, Haas RL, Klomp HM: **Surgical Treatment in the Management of Malignant Pleural Mesothelioma: A Single Institution's Experience**. *Annals of Surgical Oncology* 2008, **15**(6):1757-1764.

51. Waite K, Gilligan D: **The Role of Radiotherapy in the Treatment of Malignant Pleural Mesothelioma**. *Clinical Oncology* 2007, **19**(3):182-187.

52. van Zandwijk N: **Clinical practice guidelines for malignant pleural mesothelioma**. *Journal of thoracic disease* 2013, **5**(6):724-725.

53. MacLeod N, Chalmers A, O'Rourke N, Moore K, Sheridan J, McMahon L, Bray C, Stobo J, Price A, Fallon M *et al*: **Is Radiotherapy Useful for Treating Pain in Mesothelioma?: A Phase II Trial**. *Journal of thoracic oncology : official publication of the International Association for the Study of Lung Cancer* 2015, **10**(6):944-950.

54. Bissett D, Macbeth FR, Cram I: **The role of palliative radiotherapy in malignant mesothelioma**. *Clinical oncology (Royal College of Radiologists (Great Britain))* 1991, **3**(6):315-317.

55. Ceresoli GL, Vavassori V: **Radiotherapy to intervention sites in mesothelioma: no more?** *The Lancet Oncology* 2016, **17**(8):1025-1027.

56. UK CR: **A trial of higher dose radiotherapy to treat pain caused by mesothelioma (SYSTEMS-2)**. *Cancer Research UK [web]* 2016, **2017**(04/01/2017):Phase 2 trial.

57. Rimner A, Zauderer MG, Gomez DR, Adusumilli PS, Parhar PK, Wu AJ, Woo KM, Shen R, Ginsberg MS, Yorke ED *et al*: **Phase II Study of Hemithoracic Intensity-Modulated Pleural Radiation Therapy (IMPRINT) As Part of Lung-Sparing Multimodality Therapy in Patients With Malignant Pleural Mesothelioma**. *Journal of clinical oncology : official journal of the American Society of Clinical Oncology* 2016, **34**(23):2761-2768.

58. Alam MS, Hossain MA, Algoul S, Majumader MAA, Al-Mamun MA, Sexton G, Phillips R: **Multi-objective multi-drug scheduling schemes for cell cycle specific cancer treatment**. *Computers & Chemical Engineering* 2013, **58**(0):14-32.

59.   Fulda S, Debatin K-M: **Sensitization for Anticancer Drug-Induced Apoptosis by Betulinic Acid**. *Neoplasia* 2005, **7**(2):162-170.

60.   Melnikov SV, Söll D, Steitz TA, Polikanov YS: **Insights into RNA binding by the anticancer drug cisplatin from the crystal structure of cisplatin-modified ribosome**. *Nucleic Acids Research* 2016.

61.   Messori L, Merlino A: **Cisplatin binding to proteins: A structural perspective**. *Coordination Chemistry Reviews* 2016, **315**:67-89.

62.   Fulda S, Debatin KM: **Extrinsic versus intrinsic apoptosis pathways in anticancer chemotherapy**. *Oncogene* 2006, **25**(34):4798-4811.

63.   Astanehe A, Arenillas D, Wasserman WW, Leung PC, Dunn SE, Davies BR, Mills GB, Auersperg N: **Mechanisms underlying p53 regulation of PIK3CA transcription in ovarian surface epithelium and in ovarian cancer**. *Journal of cell science* 2008, **121**(Pt 5):664-674.

64.   Day TW, Najafi F, Wu C-H, Safa AR: **Cellular FLICE-like inhibitory protein (c-FLIP): A novel target for Taxol-induced apoptosis**. *Biochemical pharmacology* 2006, **71**(11):1551-1561.

65.   Kitagawa M, Shiozaki A, Ichikawa D, Nakashima S, Kosuga T, Konishi H, Komatsu S, Fujiwara H, Okamoto K, Otsuji E: **Tumor necrosis factor-α-induced apoptosis of gastric cancer MKN28 cells: Accelerated degradation of the inhibitor of apoptosis family members**. *Archives of Biochemistry and Biophysics* 2015, **566**(0):43-48.

66.   Vaillant F, Merino D, Lee L, Breslin K, Pal B, Ritchie ME, Smyth GK, Christie M, Phillipson LJ, Burns CJ *et al*: **Targeting BCL-2 with the BH3 mimetic ABT-199 in estrogen receptor-positive breast cancer**. *Cancer cell* 2013, **24**(1):120-129.

67.   Ricci MS, Zong W-X: **Chemotherapeutic Approaches for Targeting Cell Death Pathways**. *The oncologist* 2006, **11**(4):342-357.

68.   Elmore S: **Apoptosis: A Review of Programmed Cell Death**. *Toxicologic pathology* 2007, **35**(4):495-516.

69. Crowe DL, Yoon E: **A common pathway for chemotherapy-induced apoptosis in human squamous cell carcinoma lines distinct from that of receptor-mediated cell death**. *Anticancer research* 2003, **23**(3B):2321-2328.

70. Ohrvik H, Thiele DJ: **The role of Ctr1 and Ctr2 in mammalian copper homeostasis and platinum-based chemotherapy**. *Journal of trace elements in medicine and biology : organ of the Society for Minerals and Trace Elements (GMS)* 2014.

71. Dolgova NV, Nokhrin S, Yu CH, George GN, Dmitriev OY: **Copper chaperone Atox1 interacts with the metal-binding domain of Wilson's disease protein in cisplatin detoxification**. *The Biochemical journal* 2013, **454**(1):147-156.

72. Dasari S, Bernard Tchounwou P: **Cisplatin in cancer therapy: Molecular mechanisms of action**. *European Journal of Pharmacology* 2014, **740**(0):364-378.

73. Leonhardt K, Gebhardt R, Mossner J, Lutsenko S, Huster D: **Functional interactions of Cu-ATPase ATP7B with cisplatin and the role of ATP7B in the resistance of cells to the drug**. *The Journal of biological chemistry* 2009, **284**(12):7793-7802.

74. Kitazono-Saitoh M, Takiguchi Y, Kitazono S, Ashinuma H, Kitamura A, Tada Y, Kurosu K, Sakaida E, Sekine I, Tanabe N *et al*: **Interaction and cross-resistance of cisplatin and pemetrexed in malignant pleural mesothelioma cell lines**. *Oncology reports* 2012, **28**(1):33-40.

75. Zisowsky J, Koegel S, Leyers S, Devarakonda K, Kassack MU, Osmak M, Jaehde U: **Relevance of drug uptake and efflux for cisplatin sensitivity of tumor cells**. *Biochemical pharmacology* 2007, **73**(2):298-307.

76. Di Pasqua AJ, Goodisman J, Dabrowiak JC: **Understanding how the platinum anticancer drug carboplatin works: From the bottle to the cell**. *Inorganica Chimica Acta* 2012, **389**:29-35.

77.   Becker JP, Weiss J, Theile D: **Cisplatin, oxaliplatin, and carboplatin unequally inhibit in vitro mRNA translation**. *Toxicology Letters* 2014, **225**(1):43-47.

78.   Kelland L: **The resurgence of platinum-based cancer chemotherapy**. *Nat Rev Cancer* 2007, **7**(8):573-584.

79.   Chattopadhyay S, Moran RG, Goldman ID: **Pemetrexed: biochemical and cellular pharmacology, mechanisms, and clinical applications**. *Molecular cancer therapeutics* 2007, **6**(2):404-417.

80.   Curtin NJ, Hughes AN: **Pemetrexed disodium, a novel antifolate with multiple targets**. *The Lancet Oncology* 2001, **2**(5):298-306.

81.   Green MR: **Alimta (pemetrexed disodium): a multitargeted antifolate for the treatment of mesothelioma**. *Lung Cancer* 2002, **38, Supplement 2**(0):55-57.

82.   Vogelzang NJ, Rusthoven JJ, Symanowski J, Denham C, Kaukel E, Ruffie P, Gatzemeier U, Boyer M, Emri S, Manegold C *et al*: **Phase III study of pemetrexed in combination with cisplatin versus cisplatin alone in patients with malignant pleural mesothelioma**. *Journal of clinical oncology : official journal of the American Society of Clinical Oncology* 2003, **21**(14):2636-2644.

83.   Ivanova AV, Ivanov SV, Cruz C, Beck A, Pass HI: **C5-07: Mechanisms of innate drug sensitivity in malignant pleural mesotheliomas**. *Journal of Thoracic Oncology*, **2**(8):S374-S375.

84.   Mossman BT, Shukla A, Heintz NH, Verschraegen CF, Thomas A, Hassan R: **New Insights into Understanding the Mechanisms, Pathogenesis, and Management of Malignant Mesotheliomas**. *The American Journal of Pathology* 2013, **182**(4):1065-1077.

85.   Hudson AL, Weir C, Moon E, Harvie R, Klebe S, Clarke SJ, Pavlakis N, Howell VM: **Establishing a panel of chemo-resistant mesothelioma models for investigating chemo-resistance and identifying new treatments for mesothelioma**. *Scientific Reports* 2014, **4**:6152.

86.   Remon J, Lianes P, Martínez S, Velasco M, Querol R, Zanui M: **Malignant mesothelioma: New insights into a rare disease**. *Cancer Treatment Reviews* 2013, **39**(6):584-591.

87.   Shi WJ, Gao JB: **Molecular mechanisms of chemoresistance in gastric cancer**. *World journal of gastrointestinal oncology* 2016, **8**(9):673-681.

88.   O'Reilly EA, Gubbins L, Sharma S, Tully R, Guang MHZ, Weiner-Gorzel K, McCaffrey J, Harrison M, Furlong F, Kell M *et al*: **The fate of chemoresistance in triple negative breast cancer (TNBC)**. *BBA Clinical* 2015, **3**:257-275.

89.   Singh S, Chitkara D, Mehrazin R, Behrman SW, Wake RW, Mahato RI: **Chemoresistance in Prostate Cancer Cells Is Regulated by miRNAs and Hedgehog Pathway**. *PloS one* 2012, **7**(6):e40021.

90.   Peng X-X, Shi Z, Damaraju VL, Huang X-C, Kruh GD, Wu H-C, Zhou Y, Tiwari A, Fu L, Cass CE *et al*: **Up-regulation of MRP4 and down-regulation of influx transporters in human leukemic cells with acquired resistance to 6-mercaptopurine**. *Leukemia Research* 2008, **32**(5):799-809.

91.   NCBI: **Compound Summary**. *PubChem* 2016, **2016**(12/9/16).

92.   Drozd E, Krzysztoń-Russjan J, Marczewska J, Drozd J, Bubko I, Bielak M, Lubelska K, Wiktorska K, Chilmonczyk Z, Anuszewska E *et al*: **Up-regulation of glutathione-related genes, enzyme activities and transport proteins in human cervical cancer cells treated with doxorubicin**. *Biomedicine & Pharmacotherapy* 2016, **83**:397-406.

93.   Tsurutani J, Nitta T, Hirashima T, Komiya T, Uejima H, Tada H, Syunichi N, Tohda A, Fukuoka M, Nakagawa K: **Point mutations in the topoisomerase I gene in patients with non-small cell lung cancer treated with irinotecan**. *Lung Cancer* 2002, **35**(3):299-304.

94.   Rocha JC, Busatto FF, de Souza LK, Saffi J: **Influence of nucleotide excision repair on mitoxantrone cytotoxicity**. *DNA Repair* 2016, **42**:33-43.

95.   Ling K-S, Chen G-D, Tsai H-J, Lee M-S, Wang P-H, Liu F-S: **Mechanisms Involved in Chemoresistance in Ovarian Cancer**. *Taiwanese Journal of Obstetrics and Gynecology* 2005, **44**(3):209-217.

96. O'Grady S, Finn SP, Cuffe S, Richard DJ, O'Byrne KJ, Barr MP: **The role of DNA repair pathways in cisplatin resistant lung cancer**. *Cancer Treatment Reviews* 2014, **40**(10):1161-1170.

97. Røe OD, Anderssen E, Sandeck H, Christensen T, Larsson E, Lundgren S: **Malignant pleural mesothelioma: Genome-wide expression patterns reflecting general resistance mechanisms and a proposal of novel targets**. *Lung Cancer* 2010, **67**(1):57-68.

98. Rosell R, Lord RVN, Taron M, Reguart N: **DNA repair and cisplatin resistance in non-small-cell lung cancer**. *Lung Cancer* 2002, **38**(3):217-227.

99. Vogelzang NJ: **Standard therapy for the treatment of malignant pleural mesothelioma**. *Lung Cancer* 2005, **50, Supplement 1**(0):S23-S24.

100. Hiddinga BI, Rolfo C, van Meerbeeck JP: **Mesothelioma treatment: Are we on target? A review**. *Journal of Advanced Research* 2015, **6**(3):319-330.

101. Federico R, Adolfo F, Giuseppe M, Lorenzo S, Martino DT, Anna C, Adriano P, Gino C, Francesca R, Matteo C *et al*: **Phase II trial of neoadjuvant pemetrexed plus cisplatin followed by surgery and radiation in the treatment of pleural mesothelioma**. *BMC Cancer* 2013, **13**:22.

102. Govindan R, Kratzke RA, Herndon JE, 2nd, Niehans GA, Vollmer R, Watson D, Green MR, Kindler HL: **Gefitinib in patients with malignant mesothelioma: a phase II study by the Cancer and Leukemia Group B**. *Clinical cancer research : an official journal of the American Association for Cancer Research* 2005, **11**(6):2300-2304.

103. Garland LL, Rankin C, Gandara DR, Rivkin SE, Scott KM, Nagle RB, Klein-Szanto AJP, Testa JR, Altomare DA, Borden EC: **Phase II Study of Erlotinib in Patients With Malignant Pleural Mesothelioma: A Southwest Oncology Group Study**. *Journal of Clinical Oncology* 2007, **25**(17):2406-2413.

104. Couzin-Frankel J: **Cancer Immunotherapy**. *Science* 2013, **342**(6165):1432-1433.

105. Alley EW, Molife LR, Santoro A, Beckey K, Yuan S, Cheng JD, Piperdi B, Schellens JHM: **Abstract CT103: Clinical safety and efficacy of**

pembrolizumab (MK-3475) in patients with malignant pleural mesothelioma: Preliminary results from KEYNOTE-028. *Cancer research* 2015, **75**(15 Supplement):CT103-CT103.

106. Hanahan D, Weinberg RA: **The hallmarks of cancer**. *Cell* 2000, **100**(1):57-70.

107. Hanahan D, Weinberg RA: **Hallmarks of cancer: the next generation**. *Cell* 2011, **144**(5):646-674.

108. DeBerardinis RJ, Lum JJ, Hatzivassiliou G, Thompson CB: **The Biology of Cancer: Metabolic Reprogramming Fuels Cell Growth and Proliferation**. *Cell Metabolism* 2008, **7**(1):11-20.

109. Ou S-HI, Moon J, Garland LL, Mack PC, Testa JR, Tsao AS, Wozniak AJ, Gandara DR: **SWOG S0722: Phase II Study of mTOR Inhibitor Everolimus (RAD001) in Advanced Malignant Pleural Mesothelioma (MPM)**. *Journal of Thoracic Oncology* 2015, **10**(2):387-391.

110. Bograd AJ, Suzuki K, Vertes E, Colovos C, Morales EA, Sadelain M, Adusumilli PS: **Immune responses and immunotherapeutic interventions in malignant pleural mesothelioma**. *Cancer Immunology, Immunotherapy* 2011, **60**(11):1509-1527.

111. Landskron G, De la Fuente M, Thuwajit P, Thuwajit C, Hermoso MA: **Chronic Inflammation and Cytokines in the Tumor Microenvironment**. *Journal of Immunology Research* 2014, **2014**:19.

112. Izzi V, Masuelli L, Tresoldi I, Foti C, Modesti A, Bei R: **Immunity and malignant mesothelioma: From mesothelial cell damage to tumor development and immune response-based therapies**. *Cancer Letters* 2012, **322**(1):18-34.

113. Vinay DS, Ryan EP, Pawelec G, Talib WH, Stagg J, Elkord E, Lichtor T, Decker WK, Whelan RL, Kumara HMCS *et al*: **Immune evasion in cancer: Mechanistic basis and therapeutic strategies**. *Seminars in Cancer Biology* 2015, **35, Supplement**:S185-S198.

114. Pass HI, Vogelzang N, Hahn S, Carbone M: **Malignant pleural mesothelioma**. *Current Problems in Cancer* 2004, **28**(3):93-174.

115.	Gonzalez MJ, Miranda Massari JR, Duconge J, Riordan NH, Ichim T, Quintero-Del-Rio AI, Ortiz N: **The bio-energetic theory of carcinogenesis**. *Med Hypotheses* 2012, **79**(4):433-439.

116.	Vander Heiden MG, Cantley LC, Thompson CB: **Understanding the Warburg effect: the metabolic requirements of cell proliferation**. *Science* 2009, **324**(5930):1029-1033.

117.	Zhang X, Varin E, Briand M, Allouche S, Heutte N, Schwartz L, Poulain L, Icard P: **Novel therapy for malignant pleural mesothelioma based on anti-energetic effect: an experimental study using 3-Bromopyruvate on nude mice**. *Anticancer research* 2009, **29**(4):1443-1448.

118.	Yaswen P, MacKenzie KL, Keith WN, Hentosh P, Rodier F, Zhu J, Firestone GL, Matheu A, Carnero A, Bilsland A *et al*: **Therapeutic targeting of replicative immortality**. *Semin Cancer Biol* 2015, **35 Suppl**:S104-128.

119.	Chiappori AA, Kolevska T, Spigel DR, Hager S, Rarick M, Gadgeel S, Blais N, Von Pawel J, Hart L, Reck M *et al*: **A randomized phase II study of the telomerase inhibitor imetelstat as maintenance therapy for advanced non-small-cell lung cancer**. *Ann Oncol* 2015, **26**(2):354-362.

120.	Au AYM, Hackl T, Yeager TR, Cohen SB, Pass HI, Harris CC, Reddel RR: **Telomerase activity in pleural malignant mesotheliomas**. *Lung Cancer* 2011, **73**(3):283-288.

121.	Petrovic N: **Targeting Angiogenesis in Cancer Treatments: Where do we Stand?** *Journal of pharmacy & pharmaceutical sciences : a publication of the Canadian Society for Pharmaceutical Sciences, Societe canadienne des sciences pharmaceutiques* 2016, **19**(2):226-238.

122.	Su MT, Tsai PY, Tsai HL, Chen YC, Kuo PL: **miR-346 and miR-582-3p-regulated EG-VEGF expression and trophoblast invasion via matrix metalloproteinases 2 and 9**. *BioFactors (Oxford, England)* 2016.

123.	Kron P, Linecker M, Limani P, Schlegel A, Kambakamba P, Lehn JM, Nicolau C, Graf R, Humar B, Clavien PA: **Hypoxia-driven Hif2a coordinates mouse**

liver regeneration by coupling parenchymal growth to vascular expansion. *Hepatology (Baltimore, Md)* 2016.

124. Zhang Y, Liu J, Wang S, Luo X, Li Y, Lv Z, Zhu J, Lin J, Ding L, Ye Q: **The DEK oncogene activates VEGF expression and promotes tumor angiogenesis and growth in HIF-1alpha-dependent and -independent manners**. *Oncotarget* 2016, **7**(17):23740-23756.

125. Chen J, Lai L, Liu S, Zhou C, Wu C, Huang M, Lin Q: **Targeting HIF-1alpha and VEGF by lentivirus-mediated RNA interference reduces liver tumor cells migration and invasion under hypoxic conditions**. *Neoplasma* 2016(6).

126. Wheatley-Price P, Chu Q, Bonomi M, Seely J, Gupta A, Goss G, Hilton J, Feld R, Lee CW, Goffin JR *et al*: **A Phase II Study of PF-03446962 in Patients with Advanced Malignant Pleural Mesothelioma. CCTG Trial IND.207**. *Journal of Thoracic Oncology*.

127. Yoshida GJ: **Emerging role of epithelial-mesenchymal transition in hepatic cancer**. *Journal of experimental & clinical cancer research : CR* 2016, **35**(1):141.

128. Yang X, Jing D, Liu L, Shen Z, Ju J, Ma C, Sun M: **Downregulation of p53 promotes in vitro perineural invasive activity of human salivary adenoid cystic carcinoma cells through epithelial-mesenchymal transition-like changes**. *Oncology reports* 2015, **33**(4):1650-1656.

129. Casarsa C, Bassani N, Ambrogi F, Zabucchi G, Boracchi P, Biganzoli E, Coradini D: **Epithelial-to-mesenchymal transition, cell polarity and stemness-associated features in malignant pleural mesothelioma**. *Cancer Letters* 2011, **302**(2):136-143.

130. Hugo H, Ackland ML, Blick T, Lawrence MG, Clements JA, Williams ED, Thompson EW: **Epithelial--mesenchymal and mesenchymal--epithelial transitions in carcinoma progression**. *Journal of cellular physiology* 2007, **213**(2):374-383.

131. Ivanova AV, Ivanov SV, Prudkin L, Nonaka D, Liu Z, Tsao A, Wistuba I, Roth J, Pass HI: **Mechanisms of FUS1/TUSC2 deficiency in mesothelioma and its tumorigenic transcriptional effects**. *Molecular Cancer* 2009, **8**:91-91.

132. Wheler JJ, Janku F, Naing A, Li Y, Stephen B, Zinner R, Subbiah V, Fu S, Karp D, Falchook GS *et al*: **TP53 Alterations Correlate with Response to VEGF/VEGFR Inhibitors:Implications for Targeted Therapeutics**. *Molecular cancer therapeutics* 2016.

133. Hylebos M, Van Camp G, van Meerbeeck JP, Op de Beeck K: **The Genetic Landscape of Malignant Pleural Mesothelioma: Results from Massively Parallel Sequencing**. *Journal of Thoracic Oncology* 2016, **11**(10):1615-1626.

134. Fradet-Turcotte A, Sitz J, Grapton D, Orthwein A: **BRCA2 functions: from DNA repair to replication fork stabilization**. *Endocrine-related cancer* 2016.

135. Sottoriva A, Kang H, Ma Z, Graham TA, Salomon MP, Zhao J, Marjoram P, Siegmund K, Press MF, Shibata D *et al*: **A Big Bang model of human colorectal tumor growth**. *Nature genetics* 2015, **47**(3):209-216.

136. Siddik ZH: **Chapter 12 - Apoptosis in Cancer: Mechanisms, Deregulation, and Therapeutic Targeting**. In: *Cancer Drug Design and Discovery (Second Edition).* edn. Edited by Neidle S. San Diego: Academic Press; 2014: 357-390.

137. de Assis LVM, Locatelli J, Isoldi MC: **The role of key genes and pathways involved in the tumorigenesis of Malignant Mesothelioma**. *Biochimica et Biophysica Acta (BBA) - Reviews on Cancer* 2014, **1845**(2):232-247.

138. Hao W, Luo W, Bai M, Li J, Bai X, Guo J, Wu J, Wang M: **MicroRNA-206 Inhibited the Progression of Glioblastoma Through BCL-2**. *Journal of molecular neuroscience : MN* 2016.

139. Arora H, Qureshi R, Rizvi MA, Shrivastava S, Parihar MS: **Study of apoptosis-related interactions in colorectal cancer**. *Tumour biology : the journal of the International Society for Oncodevelopmental Biology and Medicine* 2016.

140. Bartel DP: **MicroRNAs: genomics, biogenesis, mechanism, and function**. *Cell* 2004, **116**(2):281-297.

141. He L, Hannon GJ: **MicroRNAs: small RNAs with a big role in gene regulation**. *Nature reviews Genetics* 2004, **5**(7):522-531.

142. Malumbres M: **miRNAs and cancer: an epigenetics view**. *Mol Aspects Med* 2013, **34**(4):863-874.

143. Lee RC, Feinbaum RL, Ambros V: **The C. elegans heterochronic gene lin-4 encodes small RNAs with antisense complementarity to lin-14**. *Cell* 1993, **75**(5):843-854.

144. Wightman B, Burglin TR, Gatto J, Arasu P, Ruvkun G: **Negative regulatory sequences in the lin-14 3'-untranslated region are necessary to generate a temporal switch during Caenorhabditis elegans development**. *Genes Dev* 1991, **5**(10):1813-1824.

145. Wightman B, Ha I, Ruvkun G: **Posttranscriptional regulation of the heterochronic gene lin-14 by lin-4 mediates temporal pattern formation in C. elegans**. *Cell* 1993, **75**(5):855-862.

146. Slack FJ, Basson M, Liu Z, Ambros V, Horvitz HR, Ruvkun G: **The lin-41 RBCC gene acts in the C. elegans heterochronic pathway between the let-7 regulatory RNA and the LIN-29 transcription factor**. *Mol Cell* 2000, **5**(4):659-669.

147. Lagos-Quintana M, Rauhut R, Lendeckel W, Tuschl T: **Identification of novel genes coding for small expressed RNAs**. *Science* 2001, **294**(5543):853-858.

148. Lee RC, Ambros V: **An extensive class of small RNAs in Caenorhabditis elegans**. *Science* 2001, **294**(5543):862-864.

149. Borchert GM, Lanier W, Davidson BL: **RNA polymerase III transcribes human microRNAs**. *Nature structural & molecular biology* 2006, **13**(12):1097-1101.

150. Lee Y, Kim M, Han J, Yeom KH, Lee S, Baek SH, Kim VN: **MicroRNA genes are transcribed by RNA polymerase II**. *EMBO J* 2004, **23**(20):4051-4060.

151. Han J, Lee Y, Yeom KH, Kim YK, Jin H, Kim VN: **The Drosha-DGCR8 complex in primary microRNA processing**. *Genes Dev* 2004, **18**(24):3016-3027.

152. Lee Y, Jeon K, Lee JT, Kim S, Kim VN: **MicroRNA maturation: stepwise processing and subcellular localization**. *EMBO J* 2002, **21**(17):4663-4670.

153. Bohnsack MT, Czaplinski K, Gorlich D: **Exportin 5 is a RanGTP-dependent dsRNA-binding protein that mediates nuclear export of pre-miRNAs**. *RNA (New York, NY)* 2004, **10**(2):185-191.

154. Schwarz DS, Hutvagner G, Du T, Xu Z, Aronin N, Zamore PD: **Asymmetry in the assembly of the RNAi enzyme complex**. *Cell* 2003, **115**(2):199-208.

155. Ketting RF, Fischer SE, Bernstein E, Sijen T, Hannon GJ, Plasterk RH: **Dicer functions in RNA interference and in synthesis of small RNA involved in developmental timing in C. elegans**. *Genes Dev* 2001, **15**(20):2654-2659.

156. Maher SG, Bibby BAS, Moody HL, Reid G: **Chapter 4 - MicroRNAs and Cancer**. In: *Epigenetic Cancer Therapy*. edn. Edited by Gray SG. Boston: Academic Press; 2015: 67-90.

157. Peters L, Meister G: **Argonaute proteins: mediators of RNA silencing**. *Mol Cell* 2007, **26**(5):611-623.

158. Meister G, Landthaler M, Patkaniowska A, Dorsett Y, Teng G, Tuschl T: **Human Argonaute2 mediates RNA cleavage targeted by miRNAs and siRNAs**. *Mol Cell* 2004, **15**(2):185-197.

159. Lewis BP, Shih IH, Jones-Rhoades MW, Bartel DP, Burge CB: **Prediction of mammalian microRNA targets**. *Cell* 2003, **115**(7):787-798.

160. Pasquinelli AE, Reinhart BJ, Slack F, Martindale MQ, Kuroda MI, Maller B, Hayward DC, Ball EE, Degnan B, Muller P *et al*: **Conservation of the sequence and temporal expression of let-7 heterochronic regulatory RNA**. *Nature* 2000, **408**(6808):86-89.

161. Friedman RC, Farh KK, Burge CB, Bartel DP: **Most mammalian mRNAs are conserved targets of microRNAs**. *Genome Res* 2009, **19**(1):92-105.

162. Saito T, Saetrom P: **MicroRNAs--targeting and target prediction**. *N Biotechnol* 2010, **27**(3):243-249.

163. Lytle JR, Yario TA, Steitz JA: **Target mRNAs are repressed as efficiently by microRNA-binding sites in the 5' UTR as in the 3' UTR**. *Proceedings of the National Academy of Sciences of the United States of America* 2007, **104**(23):9667-9672.

164. Saito T, Sætrom P: **MicroRNAs – targeting and target prediction**. *New Biotechnology* 2010, **27**(3):243-249.

165. Grimson A, Farh KK, Johnston WK, Garrett-Engele P, Lim LP, Bartel DP: **MicroRNA targeting specificity in mammals: determinants beyond seed pairing**. *Mol Cell* 2007, **27**(1):91-105.

166. Stark A, Brennecke J, Bushati N, Russell RB, Cohen SM: **Animal MicroRNAs confer robustness to gene expression and have a significant impact on 3'UTR evolution**. *Cell* 2005, **123**(6):1133-1146.

167. Lim LP, Lau NC, Garrett-Engele P, Grimson A, Schelter JM, Castle J, Bartel DP, Linsley PS, Johnson JM: **Microarray analysis shows that some microRNAs downregulate large numbers of target mRNAs**. *Nature* 2005, **433**(7027):769-773.

168. Filipowicz W, Bhattacharyya SN, Sonenberg N: **Mechanisms of post-transcriptional regulation by microRNAs: are the answers in sight?** *Nature reviews Genetics* 2008, **9**(2):102-114.

169. Bhattacharyya SN, Habermacher R, Martine U, Closs EI, Filipowicz W: **Relief of microRNA-mediated translational repression in human cells subjected to stress**. *Cell* 2006, **125**(6):1111-1124.

170. Brengues M, Teixeira D, Parker R: **Movement of eukaryotic mRNAs between polysomes and cytoplasmic processing bodies**. *Science* 2005, **310**(5747):486-489.

171. Parker R, Song H: **The enzymes and control of eukaryotic mRNA turnover**. *Nature structural & molecular biology* 2004, **11**(2):121-127.

172.   Younger ST, Pertsemlidis A, Corey DR: **Predicting potential miRNA target sites within gene promoters**. *Bioorganic & medicinal chemistry letters* 2009, **19**(14):3791-3794.

173.   Huang V, Li LC: **miRNA goes nuclear**. *RNA biology* 2012, **9**(3):269-273.

174.   Lu J, Getz G, Miska EA, Alvarez-Saavedra E, Lamb J, Peck D, Sweet-Cordero A, Ebert BL, Mak RH, Ferrando AA *et al*: **MicroRNA expression profiles classify human cancers**. *Nature* 2005, **435**(7043):834-838.

175.   Li M, Li J, Ding X, He M, Cheng SY: **microRNA and cancer**. *The AAPS journal* 2010, **12**(3):309-317.

176.   Bourassa MW, Ratan RR: **The interplay between microRNAs and histone deacetylases in neurological diseases**. *Neurochemistry International* 2014, **77**:33-39.

177.   Hébert SS, De Strooper B: **Alterations of the microRNA network cause neurodegenerative disease**. *Trends in Neurosciences* 2009, **32**(4):199-206.

178.   Farazi TA, Hoell JI, Morozov P, Tuschl T: **MicroRNAs in human cancer**. *Advances in experimental medicine and biology* 2013, **774**:1-20.

179.   Jansson MD, Lund AH: **MicroRNA and cancer**. *Molecular Oncology* 2012, **6**(6):590-610.

180.   Vandenboom Ii TG, Li Y, Philip PA, Sarkar FH: **MicroRNA and Cancer: Tiny Molecules with Major Implications**. *Current genomics* 2008, **9**(2):97-109.

181.   Calin GA, Dumitru CD, Shimizu M, Bichi R, Zupo S, Noch E, Aldler H, Rattan S, Keating M, Rai K *et al*: **Frequent deletions and down-regulation of micro-RNA genes miR15 and miR16 at 13q14 in chronic lymphocytic leukemia**. *Proceedings of the National Academy of Sciences of the United States of America* 2002, **99**(24):15524-15529.

182.   Calin GA, Croce CM: **MicroRNA-cancer connection: the beginning of a new tale**. *Cancer research* 2006, **66**(15):7390-7394.

183. Reid G: **MicroRNAs in mesothelioma: from tumour suppressors and biomarkers to therapeutic targets**. *Journal of thoracic disease* 2015, **7**(6):1031-1040.

184. Khodayari N, Mohammed KA, Goldberg EP, Nasreen N: **EphrinA1 inhibits malignant mesothelioma tumor growth via let-7 microRNA-mediated repression of the RAS oncogene**. *Cancer gene therapy* 2011, **18**(11):806-816.

185. Xu Y, Zheng M, Merritt RE, Shrager JB, Wakelee H, Kratzke RA, Hoang CD: **miR-1 induces growth arrest and apoptosis in malignant mesothelioma**. *Chest* 2013, **144**(5):1632-1643.

186. Reid G, Pel ME, Kirschner MB, Cheng YY, Mugridge N, Weiss J, Williams M, Wright C, Edelman JJ, Vallely MP *et al*: **Restoring expression of miR-16: a novel approach to therapy for malignant pleural mesothelioma**. *Ann Oncol* 2013, **24**(12):3128-3135.

187. Pass HI, Goparaju C, Ivanov S, Donington J, Carbone M, Hoshen M, Cohen D, Chajut A, Rosenwald S, Dan H *et al*: **hsa-miR-29c* is linked to the prognosis of malignant pleural mesothelioma**. *Cancer research* 2010, **70**(5):1916-1924.

188. Ivanov SV, Goparaju CM, Lopez P, Zavadil J, Toren-Haritan G, Rosenwald S, Hoshen M, Chajut A, Cohen D, Pass HI: **Pro-tumorigenic effects of miR-31 loss in mesothelioma**. *The Journal of biological chemistry* 2010, **285**(30):22809-22817.

189. Matsumoto S, Nabeshima K, Hamasaki M, Shibuta T, Umemura T: **Upregulation of microRNA-31 associates with a poor prognosis of malignant pleural mesothelioma with sarcomatoid component**. *Medical oncology (Northwood, London, England)* 2014, **31**(12):303.

190. Maki Y, Asano H, Toyooka S, Soh J, Kubo T, Katsui K, Ueno T, Shien K, Muraoka T, Tanaka N *et al*: **MicroRNA miR-34b/c enhances cellular radiosensitivity of malignant pleural mesothelioma cells**. *Anticancer research* 2012, **32**(11):4871-4875.

191. Tomasetti M, Monaco F, Manzella N, Rohlena J, Rohlenova K, Staffolani S, Gaetani S, Ciarapica V, Amati M, Bracci M *et al*: **MicroRNA-126 induces**

autophagy by altering cell metabolism in malignant mesothelioma. *Oncotarget* 2016.

192. Cioce M, Ganci F, Canu V, Sacconi A, Mori F, Canino C, Korita E, Casini B, Alessandrini G, Cambria A *et al*: **Protumorigenic effects of mir-145 loss in malignant pleural mesothelioma**. *Oncogene* 2014, **33**(46):5319-5331.

193. Fassina A, Cappellesso R, Guzzardo V, Dalla Via L, Piccolo S, Ventura L, Fassan M: **Epithelial-mesenchymal transition in malignant mesothelioma**. *Modern pathology : an official journal of the United States and Canadian Academy of Pathology, Inc* 2012, **25**(1):86-99.

194. Laurila EM, Kallioniemi A: **The diverse role of miR-31 in regulating cancer associated phenotypes**. *Genes, chromosomes & cancer* 2013. 2013 **52**(12):1103-13.

195. Cekaite L, Rantala JK, Bruun J, Guriby M, Ågesen TH, Danielsen SA, Lind GE, Nesbakken A, Kallioniemi O, Lothe RA *et al*: **MiR-9, -31, and -182 Deregulation Promote Proliferation and Tumor Cell Survival in Colon Cancer**. *Neoplasia* 2012, **14**(9):868-IN821.

196. He L, Thomson JM, Hemann MT, Hernando-Monge E, Mu D, Goodson S, Powers S, Cordon-Cardo C, Lowe SW, Hannon GJ *et al*: **A microRNA polycistron as a potential human oncogene**. *Nature* 2005, **435**(7043):828-833.

197. Suarez Y, Fernandez-Hernando C, Yu J, Gerber SA, Harrison KD, Pober JS, Iruela-Arispe ML, Merkenschlager M, Sessa WC: **Dicer-dependent endothelial microRNAs are necessary for postnatal angiogenesis**. *Proceedings of the National Academy of Sciences of the United States of America* 2008, **105**(37):14082-14087.

198. Sylvestre Y, De Guire V, Querido E, Mukhopadhyay UK, Bourdeau V, Major F, Ferbeyre G, Chartrand P: **An E2F/miR-20a autoregulatory feedback loop**. *The Journal of biological chemistry* 2007, **282**(4):2135-2143.

199. Gao B, Gao K, Li L, Huang Z, Lin L: **miR-184 functions as an oncogenic regulator in hepatocellular carcinoma (HCC)**. *Biomedicine & Pharmacotherapy* 2014, **68**(2):143-148.

200. Tsai WC, Hsu PW, Lai TC, Chau GY, Lin CW, Chen CM, Lin CD, Liao YL, Wang JL, Chau YP *et al*: **MicroRNA-122, a tumor suppressor microRNA that regulates intrahepatic metastasis of hepatocellular carcinoma**. *Hepatology (Baltimore, Md)* 2009, **49**(5):1571-1582.

201. Li P, Xu Q, Zhang D, Li X, Han L, Lei J, Duan W, Ma Q, Wu Z, Wang Z: **Upregulated miR-106a plays an oncogenic role in pancreatic cancer**. *FEBS Letters* 2014, **588**(5):705-712.

202. Mace TA, Collins AL, Wojcik SE, Croce CM, Lesinski GB, Bloomston M: **Hypoxia induces the overexpression of microRNA-21 in pancreatic cancer cells**. *Journal of Surgical Research* 2013, **184**(2):855-860.

203. Muller DW, Bosserhoff AK: **Integrin [beta]3 expression is regulated by let-7a miRNA in malignant melanoma**. *Oncogene* 2008, **27**(52):6698-6706.

204. Dang D, Bamburg JR, Ramos DM: **αvβ3 integrin and cofilin modulate K1735 melanoma cell invasion**. *Experimental Cell Research* 2006, **312**(4):468-477.

205. Koturbash I, Zemp FJ, Pogribny I, Kovalchuk O: **Small molecules with big effects: The role of the microRNAome in cancer and carcinogenesis**. *Mutation Research/Genetic Toxicology and Environmental Mutagenesis* 2011, **722**(2):94-105.

206. Zhang X, Dong Y, Ti H, Zhao J, Wang Y, Li T, Zhang B: **Down-regulation of miR-145 and miR-143 might be associated with DNA methyltransferase 3B overexpression and worse prognosis in endometrioid carcinomas**. *Human pathology* 2013, **44**(11):2571-2580.

207. Robertson KD, Uzvolgyi E, Liang G, Talmadge C, Sumegi J, Gonzales FA, Jones PA: **The human DNA methyltransferases (DNMTs) 1, 3a and 3b: coordinate mRNA expression in normal tissues and overexpression in tumors**. *Nucleic Acids Research* 1999, **27**(11):2291-2298.

208. Fabbri M, Garzon R, Cimmino A, Liu Z, Zanesi N, Callegari E, Liu S, Alder H, Costinean S, Fernandez-Cymering C *et al*: **MicroRNA-29 family reverts aberrant methylation in lung cancer by targeting DNA methyltransferases**

3A and 3B. *Proceedings of the National Academy of Sciences of the United States of America* 2007, **104**(40):15805-15810.

209. Martinez I, Cazalla D, Almstead LL, Steitz JA, DiMaio D: **miR-29 and miR-30 regulate B-Myb expression during cellular senescence**. *Proceedings of the National Academy of Sciences of the United States of America* 2011, **108**(2):522-527.

210. Wang Y, Zhang X, Li H, Yu J, Ren X: **The role of miRNA-29 family in cancer**. *European Journal of Cell Biology* 2013, **92**(3):123-128.

211. Abdelmohsen K, Srikantan S, Kuwano Y, Gorospe M: **miR-519 reduces cell proliferation by lowering RNA-binding protein HuR levels**. *Proceedings of the National Academy of Sciences of the United States of America* 2008, **105**(51):20297-20302.

212. Zhou X, Wei M, Wang W: **MicroRNA-340 suppresses osteosarcoma tumor growth and metastasis by directly targeting ROCK1**. *Biochemical and Biophysical Research Communications* 2013, **437**(4):653-658.

213. Chen X, Zhang Y, Yan J, Sadiq R, Chen T: **miR-34a suppresses mutagenesis by inducing apoptosis in human lymphoblastoid TK6 cells**. *Mutation Research/Genetic Toxicology and Environmental Mutagenesis* 2013, **758**(1–2):35-40.

214. Benetti R, Gonzalo S, Jaco I, Munoz P, Gonzalez S, Schoeftner S, Murchison E, Andl T, Chen T, Klatt P *et al*: **A mammalian microRNA cluster controls DNA methylation and telomere recombination via Rbl2-dependent regulation of DNA methyltransferases**. *Nature structural & molecular biology* 2008, **15**(3):268-279.

215. Hua Z, Lv Q, Ye W, Wong C-KA, Cai G, Gu D, Ji Y, Zhao C, Wang J, Yang BB *et al*: **MiRNA-Directed Regulation of VEGF and Other Angiogenic Factors under Hypoxia**. *PloS one* 2006, **1**(1):e116.

216. Ruan K, Fang X, Ouyang G: **MicroRNAs: Novel regulators in the hallmarks of human cancer**. *Cancer Letters* 2009, **285**(2):116-126.

217. Shaw A, Bradley MD, Elyan S, Kurian KM: **Tumour biomarkers: diagnostic, prognostic, and predictive**. *BMJ : British Medical Journal* 2015, **351**.

218. Schwarzenbach H, Nishida N, Calin GA, Pantel K: **Clinical relevance of circulating cell-free microRNAs in cancer**. *Nat Rev Clin Oncol* 2014, **11**(3):145-156.

219. Janssen HL, Reesink HW, Lawitz EJ, Zeuzem S, Rodriguez-Torres M, Patel K, van der Meer AJ, Patick AK, Chen A, Zhou Y *et al*: **Treatment of HCV infection by targeting microRNA**. *The New England journal of medicine* 2013, **368**(18):1685-1694.

220. Croce CM: **Causes and consequences of microRNA dysregulation in cancer**. *Nature reviews Genetics* 2009, **10**(10):704-714.

221. Kelly WS, Mir AH, Balazs D, Balazs H, Walter K, Glen JW: **The Role of microRNAs in the Diagnosis and Treatment of Malignant Pleural Mesothelioma - A Short Review**. *MicroRNA* 2012, **1**(1):40-48.

222. Cheng CJ, Slack FJ: **The Duality of OncomiR Addiction in the Maintenance and Treatment of Cancer**. *Cancer Journal (Sudbury, Mass)* 2012, **18**(3):232-237.

223. Li C, Feng Y, Coukos G, Zhang L: **Therapeutic MicroRNA Strategies in Human Cancer**. *The AAPS journal* 2009, **11**(4):747.

224. Stenvang J, Petri A, Lindow M, Obad S, Kauppinen S: **Inhibition of microRNA function by antimiR oligonucleotides**. *Silence* 2012, **3**(1):1.

225. Pan X, Wang ZX, Wang R: **MicroRNA-21: a novel therapeutic target in human cancer**. *Cancer biology & therapy* 2010, **10**(12):1224-1232.

226. Hong L, Han Y, Zhang Y, Zhang H, Zhao Q, Wu K, Fan D: **MicroRNA-21: a therapeutic target for reversing drug resistance in cancer**. *Expert opinion on therapeutic targets* 2013, **17**(9):1073-1080.

227. Zhou X, Ren Y, Moore L, Mei M, You Y, Xu P, Wang B, Wang G, Jia Z, Pu P *et al*: **Downregulation of miR-21 inhibits EGFR pathway and suppresses the**

growth of human glioblastoma cells independent of PTEN status. *Lab Invest* 2010, **90**(2):144-155.

228. Leone E, Morelli E, Di Martino MT, Amodio N, Foresta U, Gulla A, Rossi M, Neri A, Giordano A, Munshi NC *et al*: **Targeting miR-21 inhibits in vitro and in vivo multiple myeloma cell growth**. *Clinical cancer research : an official journal of the American Association for Cancer Research* 2013, **19**(8):2096-2106.

229. Li J, Huang H, Sun L, Yang M, Pan C, Chen W, Wu D, Lin Z, Zeng C, Yao Y *et al*: **MiR-21 indicates poor prognosis in tongue squamous cell carcinomas as an apoptosis inhibitor**. *Clinical cancer research : an official journal of the American Association for Cancer Research* 2009, **15**(12):3998-4008.

230. Iliopoulos D, Jaeger SA, Hirsch HA, Bulyk ML, Struhl K: **STAT3 activation of miR-21 and miR-181b-1 via PTEN and CYLD are part of the epigenetic switch linking inflammation to cancer**. *Molecular cell* 2010, **39**(4):493-506.

231. Haussecker D, Kay MA: **miR-122 Continues to Blaze the Trail for MicroRNA Therapeutics**. *Mol Ther* 2010, **18**(2):240-242.

232. Davis S, Propp S, Freier SM, Jones LE, Serra MJ, Kinberger G, Bhat B, Swayze EE, Bennett CF, Esau C: **Potent inhibition of microRNA in vivo without degradation**. *Nucleic Acids Research* 2009, **37**(1):70-77.

233. Misso G, Di Martino MT, De Rosa G, Farooqi AA, Lombardi A, Campani V, Zarone MR, Gulla A, Tagliaferri P, Tassone P *et al*: **Mir-34: A New Weapon Against Cancer?** *Mol Ther Nucleic Acids* 2014, **3**:e194.

234. Reid G, Pel ME, Kirschner MB, Cheng YY, Mugridge N, Weiss J, Williams M, Wright C, Edelman JJB, Vallely MP *et al*: **Restoring expression of miR-16: a novel approach to therapy for malignant pleural mesothelioma**. *Annals of Oncology* 2013.

235. Reid G, Kao SC, Pavlakis N, Brahmbhatt H, MacDiarmid J, Clarke S, Boyer M, van Zandwijk N: **Clinical development of TargomiRs, a miRNA mimic-based treatment for patients with recurrent thoracic cancer**. *Epigenomics* 2016.

236. Balatti V, Maniero S, Ferracin M, Veronese A, Negrini M, Ferrocci G, Martini F, Tognon MG: **MicroRNAs dysregulation in human malignant pleural mesothelioma**. *Journal of thoracic oncology : official publication of the International Association for the Study of Lung Cancer* 2011, **6**(5):844-851.

237. Williams M, Kirschner MB, Cheng YY, Hanh J, Weiss J, Mugridge N, Wright CM, Linton A, Kao SC, Edelman JJ *et al*: **miR-193a-3p is a potential tumor suppressor in malignant pleural mesothelioma**. *Oncotarget* 2015, **6**(27):23480-23495.

238. Quinn L, Finn SP, Cuffe S, Gray SG: **Non-coding RNA repertoires in malignant pleural mesothelioma**. *Lung Cancer* 2015, **90**(3):417-426.

239. Dalby B, Cates S, Harris A, Ohki EC, Tilkins ML, Price PJ, Ciccarone VC: **Advanced transfection with Lipofectamine 2000 reagent: primary neurons, siRNA, and high-throughput applications**. *Methods* 2004, **33**(2):95-103.

240. Livak KJ, Schmittgen TD: **Analysis of relative gene expression data using real-time quantitative PCR and the 2(-Delta Delta C(T)) Method**. *Methods* 2001, **25**(4):402-408.

241. Owen JB, Butterfield DA: **Measurement of oxidized/reduced glutathione ratio**. *Methods in molecular biology (Clifton, NJ)* 2010, **648**:269-277.

242. Eskelinen EL: **Roles of LAMP-1 and LAMP-2 in lysosome biogenesis and autophagy**. *Mol Aspects Med* 2006, **27**(5-6):495-502.

243. Morrison JG, White P, McDougall S, Firth JW, Woolfrey SG, Graham MA, Greenslade D: **Validation of a highly sensitive ICP-MS method for the determination of platinum in biofluids: application to clinical pharmacokinetic studies with oxaliplatin**. *Journal of pharmaceutical and biomedical analysis* 2000, **24**(1):1-10.

244. Van Schil PE, Baas P, Gaafar R, Maat AP, Van de Pol M, Hasan B, Klomp HM, Abdelrahman AM, Welch J, van Meerbeeck JP: **Trimodality therapy for malignant pleural mesothelioma: results from an EORTC phase II multicentre trial**. *European Respiratory Journal* 2010, **36**(6):1362-1369.

245. Bonelli MA, Fumarola C, La Monica S, Alfieri R: **New therapeutic strategies for malignant pleural mesothelioma**. *Biochemical pharmacology*.

246. ClinicalTrial.gov: **Clinical and Histopathologic Characteristics of BAP1 Mutations**. *ClinicalTrialgov* 2016, **2016** (June 2016).

247. Raffit Hassan AT, Manish R. Patel, John J. Nemunaitis, Jaafar Bennouna, John D. Powderly, Matthew H. Taylor, Afshin Dowlati, Franklin Chen, Joseph Leach, Ulka N. Vaishampayan, Claire F. Verschraegen, Jean-Pierre Delord, Hans Juergen Grote, Anja von Heydebreck, Jean-Marie Cuillerot, James L. Gulley: **Avelumab (MSB0010718C; anti-PD-L1) in patients with advanced unresectable mesothelioma from the JAVELIN solid tumor phase Ib trial: Safety, clinical activity, and PD-L1 expression**. *2016 ASCO Annual Meeting* 2016:J Clin Oncol 34, 2016 (suppl; abstr 8503).

248. Baas P, Fennell D, Kerr KM, Van Schil PE, Haas RL, Peters S: **Malignant pleural mesothelioma: ESMO Clinical Practice Guidelines for diagnosis, treatment and follow-up**. *Annals of Oncology* 2015, **26**(suppl 5):v31-v39.

249. Lin RCY, Kirschner MB, Cheng YY, van Zandwijk N, Reid G: **MicroRNA gene expression signatures in long-surviving malignant pleural mesothelioma patients**. *Genomics Data* 2016, **9**:44-49.

250. Xuan Y, Yang H, Zhao L, Lau WB, Lau B, Ren N, Hu Y, Yi T, Zhao X, Zhou S *et al*: **MicroRNAs in colorectal cancer: Small molecules with big functions**. *Cancer Letters* 2015, **360**(2):89-105.

251. Yu Z, Baserga R, Chen L, Wang C, Lisanti MP, Pestell RG: **microRNA, Cell Cycle, and Human Breast Cancer**. *The American Journal of Pathology* 2010, **176**(3):1058-1064.

252. Kirschner MB, Cheng YY, Armstrong NJ, Lin RCY, Kao SC, Linton A, Klebe S, McCaughan BC, van Zandwijk N, Reid G: **MiR-Score: A novel 6-microRNA signature that predicts survival outcomes in patients with malignant pleural mesothelioma**. *Molecular Oncology* 2015, **9**(3):715-726.

253.   Yang MH, Yu J, Chen N, Wang XY, Liu XY, Wang S, Ding YQ: **Elevated MicroRNA-31 Expression Regulates Colorectal Cancer Progression by Repressing Its Target Gene SATB2**. *PloS one* 2013, **8**(12):e85353.

254.   Hua D, Ding D, Han X, Zhang W, Zhao N, Foltz G, Lan Q, Huang Q, Lin B: **Human miR-31 targets radixin and inhibits migration and invasion of glioma cells**. *Oncology reports* 2012, **27**(3):700-706.

255.   Kim SB, Zhang L, Barron S, Shay JW: **Inhibition of microRNA-31-5p protects human colonic epithelial cells against ionizing radiation**. *Life Sciences in Space Research* 2014, **1**:67-73.

256.   Lynam-Lennon N, Reynolds JV, Marignol L, Sheils OM, Pidgeon GP, Maher SG: **MicroRNA-31 modulates tumour sensitivity to radiation in oesophageal adenocarcinoma**. *Journal of molecular medicine (Berlin, Germany)* 2012, **90**(12):1449-1458.

257.   Buikhuisen WA, Hiddinga BI, Baas P, van Meerbeeck JP: **Second line therapy in malignant pleural mesothelioma: A systematic review**. *Lung Cancer* 2015, **89**(3):223-231.

258.   Bibby BAS, Reynolds JV, Maher SG: **MicroRNA-330-5p as a Putative Modulator of Neoadjuvant Chemoradiotherapy Sensitivity in Oesophageal Adenocarcinoma**. *PloS one* 2015, **10**(7):e0134180.

259.   Mirzayans R, Andrais B, Scott A, Tessier A, Murray D: **A sensitive assay for the evaluation of cytotoxicity and its pharmacologic modulation in human solid tumor-derived cell lines exposed to cancer-therapeutic agents**. *Journal of pharmacy & pharmaceutical sciences : a publication of the Canadian Society for Pharmaceutical Sciences, Societe canadienne des sciences pharmaceutiques* 2007, **10**(2):298s-311s.

260.   Stewart DJ: **Mechanisms of resistance to cisplatin and carboplatin**. *Critical Reviews in Oncology/Hematology* 2007, **63**(1):12-31.

261.   Nutt JE, Razak ARA, O'Toole K, Black F, Quinn AE, Calvert AH, Plummer ER, Lunec J: **The role of folate receptor alpha (FRα) in the response of**

malignant pleural mesothelioma to pemetrexed-containing chemotherapy. *British journal of cancer* 2010, **102**(3):553-560.

262. Kim HS, Lee KS, Bae HJ, Eun JW, Shen Q, Park SJ, Shin WC, Yang HD, Park M, Park WS *et al*: **MicroRNA-31 functions as a tumor suppressor by regulating cell cycle and epithelial-mesenchymal transition regulatory proteins in liver cancer**. *Oncotarget* 2015, **6**(10):8089-8102.

263. Liu X, Sempere LF, Ouyang H, Memoli VA, Andrew AS, Luo Y, Demidenko E, Korc M, Shi W, Preis M *et al*: **MicroRNA-31 functions as an oncogenic microRNA in mouse and human lung cancer cells by repressing specific tumor suppressors**. *The Journal of Clinical Investigation*, **120**(4):1298-1309.

264. Wang N, Zhou Y, Zheng L, Li H: **MiR-31 is an independent prognostic factor and functions as an oncomir in cervical cancer via targeting ARID1A**. *Gynecol Oncol* 2014, **134**(1):129-137.

265. Gu F, Pfeiffer RM, Bhattacharjee S, Han SS, Taylor PR, Berndt S, Yang H, Sigurdson AJ, Toro J, Mirabello L *et al*: **Common genetic variants in the 9p21 region and their associations with multiple tumours**. *British journal of cancer* 2013, **108**(6):1378-1386.

266. Sasaki S, Kitagawa Y, Sekido Y, Minna JD, Kuwano H, Yokota J, Kohno T: **Molecular processes of chromosome 9p21 deletions in human cancers**. *Oncogene* 0000, **22**(24):3792-3798.

267. Bertino JR, Waud WR, Parker WB, Lubin M: **Targeting tumors that lack methylthioadenosine phosphorylase (MTAP) activity: Current strategies**. *Cancer biology & therapy* 2011, **11**(7):627-632.

268. Kanehisa M, Goto S: **KEGG: kyoto encyclopedia of genes and genomes**. *Nucleic Acids Res* 2000, **28**(1):27-30.

269. Kuhn DE, Martin MM, Feldman DS, Terry AV, Nuovo GJ, Elton TS: **Experimental Validation of miRNA Targets**. *Methods (San Diego, Calif)* 2008, **44**(1):47-54.

270. Ogoh H, Tanuma N, Matsui Y, Hayakawa N, Inagaki A, Sumiyoshi M, Momoi Y, Kishimoto A, Suzuki M, Sasaki N *et al*: **The protein phosphatase 6**

catalytic subunit (Ppp6c) is indispensable for proper post-implantation embryogenesis. *Mechanisms of Development* 2016, **139**:1-9.

271.   Hayashi K, Momoi Y, Tanuma N, Kishimoto A, Ogoh H, Kato H, Suzuki M, Sakamoto Y, Inoue Y, Nomura M *et al*: **Abrogation of protein phosphatase 6 promotes skin carcinogenesis induced by DMBA**. *Oncogene* 2015, **34**(35):4647-4655.

272.   Wouters MD, van Gent DC, Hoeijmakers JHJ, Pothof J: **MicroRNAs, the DNA damage response and cancer**. *Mutation Research/Fundamental and Molecular Mechanisms of Mutagenesis* 2011, **717**(1–2):54-66.

273.   Takano M, Otani Y, Tanda M, Kawami M, Nagai J, Yumoto R: **Paclitaxel-resistance Conferred by Altered Expression of Efflux and Influx Transporters for Paclitaxel in the Human Hepatoma Cell Line, HepG2**. *Drug Metabolism and Pharmacokinetics* 2009, **24**(5):418-427.

274.   Liu FS: **Mechanisms of chemotherapeutic drug resistance in cancer therapy--a quick review**. *Taiwanese journal of obstetrics & gynecology* 2009, **48**(3):239-244.

275.   Burger H, Loos WJ, Eechoute K, Verweij J, Mathijssen RHJ, Wiemer EAC: **Drug transporters of platinum-based anticancer agents and their clinical significance**. *Drug Resistance Updates* 2011, **14**(1):22-34.

276.   Ho GY, Woodward N, Coward JIG: **Cisplatin versus carboplatin: comparative review of therapeutic management in solid malignancies**. *Critical Reviews in Oncology/Hematology* 2016, **102**:37-46.

277.   Lladó V, López DJ, Ibarguren M, Alonso M, Soriano JB, Escribá PV, Busquets X: **Regulation of the cancer cell membrane lipid composition by NaCHOleate: Effects on cell signaling and therapeutical relevance in glioma**. *Biochimica et Biophysica Acta (BBA) - Biomembranes* 2014, **1838**(6):1619-1627.

278.   MacDonagh L, Gray SG, Finn SP, Cuffe S, O'Byrne KJ, Barr MP: **The emerging role of microRNAs in resistance to lung cancer treatments**. *Cancer Treatment Reviews* 2015, **41**(2):160-169.

279. Dong Z, Zhong Z, Yang L, Wang S, Gong Z: **MicroRNA-31 inhibits cisplatin-induced apoptosis in non-small cell lung cancer cells by regulating the drug transporter ABCB9**. *Cancer Lett* 2014, **343**(2):249-257.

280. Kanakkanthara A, Miller JH: **MicroRNAs: Novel mediators of resistance to microtubule-targeting agents**. *Cancer Treatment Reviews* 2013, **39**(2):161-170.

281. Tong JL, Zhang CP, Nie F, Xu XT, Zhu MM, Xiao SD, Ran ZH: **MicroRNA 506 regulates expression of PPAR alpha in hydroxycamptothecin-resistant human colon cancer cells**. *FEBS Letters* 2011, **585**(22):3560-3568.

282. Samuel P, Pink RC, Caley DP, Currie JM, Brooks SA, Carter DR: **Over-expression of miR-31 or loss of KCNMA1 leads to increased cisplatin resistance in ovarian cancer cells**. *Tumour biology : the journal of the International Society for Oncodevelopmental Biology and Medicine* 2016, **37**(2):2565-2573.

283. Liu H, Qi B, Guo X, Tang L-Q, Chen Q-Y, Zhang L, Guo L, Luo D-H, Huang P-Y, Mo H-Y *et al*: **Genetic Variations in Radiation and Chemotherapy Drug Action Pathways and Survival in locoregionally Advanced Nasopharyngeal Carcinoma Treated with Chemoradiotherapy**. *PloS one* 2013, **8**(12):e82750.

284. De Mattia E, Cecchin E, Toffoli G: **Pharmacogenomics of intrinsic and acquired pharmacoresistance in colorectal cancer: Toward targeted personalized therapy**. *Drug Resistance Updates* 2015, **20**:39-70.

285. Wee NK, Weinstein DC, Fraser ST, Assinder SJ: **The mammalian copper transporters CTR1 and CTR2 and their roles in development and disease**. *Int J Biochem Cell Biol* 2013, **45**(5):960-963.

286. Amable L: **Cisplatin resistance and opportunities for precision medicine**. *Pharmacological Research* 2016, **106**:27-36.

287. Lin X, Okuda T, Holzer A, Howell SB: **The copper transporter CTR1 regulates cisplatin uptake in Saccharomyces cerevisiae**. *Molecular pharmacology* 2002, **62**(5):1154-1159.

288. Kalayda GV, Wagner CH, Jaehde U: **Relevance of copper transporter 1 for cisplatin resistance in human ovarian carcinoma cells**. *Journal of inorganic biochemistry* 2012, **116**:1-10.

289. Chen HHW, Kuo MT: **Role of Glutathione in the Regulation of Cisplatin Resistance in Cancer Chemotherapy**. *Metal-Based Drugs* 2010, **2010**.

290. Palm ME, Weise CF, Lundin C, Wingsle G, Nygren Y, Bjorn E, Naredi P, Wolf-Watz M, Wittung-Stafshede P: **Cisplatin binds human copper chaperone Atox1 and promotes unfolding in vitro**. *Proceedings of the National Academy of Sciences of the United States of America* 2011, **108**(17):6951-6956.

291. Palm-Espling ME, Lundin C, Bjorn E, Naredi P, Wittung-Stafshede P: **Interaction between the anticancer drug Cisplatin and the copper chaperone Atox1 in human melanoma cells**. *Protein and peptide letters* 2014, **21**(1):63-68.

292. Samimi G, Katano K, Holzer AK, Safaei R, Howell SB: **Modulation of the cellular pharmacology of cisplatin and its analogs by the copper exporters ATP7A and ATP7B**. *Molecular pharmacology* 2004, **66**(1):25-32.

293. Kalayda GV, Wagner CH, Buß I, Reedijk J, Jaehde U: **Altered localisation of the copper efflux transporters ATP7A and ATP7B associated with cisplatin resistance in human ovarian carcinoma cells**. *BMC Cancer* 2008, **8**:175-175.

294. Liu Y, Pilankatta R, Hatori Y, Lewis D, Inesi G: **Comparative features of copper ATPases ATP7A and ATP7B heterologously expressed in COS-1 cells**. *Biochemistry* 2010, **49**(46):10006-10012.

295. Ip V, Liu JJ, Mercer JF, McKeage MJ: **Differential expression of ATP7A, ATP7B and CTR1 in adult rat dorsal root ganglion tissue**. *Molecular Pain* 2010, **6**(1):1-10.

296. Mangala LS, Zuzel V, Schmandt R, Leshane ES, Halder JB, Armaiz-Pena GN, Spannuth WA, Tanaka T, Shahzad MM, Lin YG *et al*: **Therapeutic Targeting of ATP7B in Ovarian Carcinoma**. *Clinical cancer research : an official journal of the American Association for Cancer Research* 2009, **15**(11):3770-3780.

297. Ciarimboli G: **Membrane Transporters as Mediators of Cisplatin Effects and Side Effects**. *Scientifica* 2012, **2012**:18.

298. Raymond E, Faivre S, Chaney S, Woynarowski J, Cvitkovic E: **Cellular and Molecular Pharmacology of Oxaliplatin¹**. *Molecular cancer therapeutics* 2002, **1**(3):227-235.

299. Barr MP, Gray SG, Hoffmann AC, Hilger RA, Thomale J, O'Flaherty JD, Fennell DA, Richard D, O'Leary JJ, O'Byrne KJ: **Generation and characterisation of cisplatin-resistant non-small cell lung cancer cell lines displaying a stem-like signature**. *PloS one* 2013, **8**(1):e54193.

300. Xia G, Kumar SR, Masood R, Koss M, Templeman C, Quinn D, Zhu S, Reddy R, Krasnoperov V, Gill PS: **Up-Regulation of EphB4 in Mesothelioma and Its Biological Significance**. *Clinical Cancer Research* 2005, **11**(12):4305-4315.

301. Schröter CJ, Braun M, Englert J, Beck H, Schmid H, Kalbacher H: **A rapid method to separate endosomes from lysosomal contents using differential centrifugation and hypotonic lysis of lysosomes**. *Journal of Immunological Methods* 1999, **227**(1–2):161-168.

302. Baghirova S, Hughes BG, Hendzel MJ, Schulz R: **Sequential fractionation and isolation of subcellular proteins from tissue or cultured cells**. *MethodsX* 2015, **2**:440-445.

303. Ishida S, Lee J, Thiele DJ, Herskowitz I: **Uptake of the anticancer drug cisplatin mediated by the copper transporter Ctr1 in yeast and mammals**. *Proceedings of the National Academy of Sciences of the United States of America* 2002, **99**(22):14298-14302.

304. Ishida S, Lee J, Thiele DJ, Herskowitz I: **Uptake of the anticancer drug cisplatin mediated by the copper transporter Ctr1 in yeast and mammals**. *Proceedings of the National Academy of Sciences of the United States of America* 2002, **99**.

305. Kuo LJ, Yang LX: **Gamma-H2AX - a novel biomarker for DNA double-strand breaks**. *In vivo (Athens, Greece)* 2008, **22**(3):305-309.

306. Wilson PM, Danenberg PV, Johnston PG, Lenz H-J, Ladner RD: **Standing the test of time: targeting thymidylate biosynthesis in cancer therapy**. *Nat Rev Clin Oncol* 2014, **11**(5):282-298.

307. Danson S, Ranson M, Denneny O, Cummings J, Ward TH: **Validation of the comet-X assay as a pharmacodynamic assay for measuring DNA cross-linking produced by the novel anticancer agent RH1 during a phase I clinical trial**. *Cancer Chemother Pharmacol* 2007, **60**(6):851-861.

308. Xiao X, Yu S, Li S, Wu J, Ma R, Cao H, Zhu Y, Feng J: **Exosomes: Decreased Sensitivity of Lung Cancer A549 Cells to Cisplatin**. *PloS one* 2014, **9**(2):e89534.

309. Krajci D, Mares V, Lisa V, Spanova A, Vorlicek J: **Ultrastructure of nuclei of cisplatin-treated C6 glioma cells undergoing apoptosis**. *Eur J Cell Biol* 2000, **79**(5):365-376.

310. Kopf-Maier P, Muhlhausen SK: **Changes in the cytoskeleton pattern of tumor cells by cisplatin in vitro**. *Chemico-biological interactions* 1992, **82**(3):295-316.

311. Gotink KJ, Broxterman HJ, Labots M, de Haas RR, Dekker H, Honeywell RJ, Rudek MA, Beerepoot LV, Musters RJ, Jansen G *et al*: **Lysosomal sequestration of sunitinib: a novel mechanism of drug resistance**. *Clinical cancer research : an official journal of the American Association for Cancer Research* 2011, **17**(23):7337-7346.

312. Zhang F, Zhang W, Liu L, Fisher CL, Hui D, Childs S, Dorovini-Zis K, Ling V: **Characterization of ABCB9, an ATP binding cassette protein associated with lysosomes**. *The Journal of biological chemistry* 2000, **275**(30):23287-23294.

313. Dong Z, Zhong Z, Yang L, Wang S, Gong Z: **MicroRNA-31 inhibits cisplatin-induced apoptosis in non-small cell lung cancer cells by regulating the drug transporter ABCB9**. *Cancer Letters* 2014, **343**(2):249-257.

314. Gorden BH, Saha J, Khammanivong A, Schwartz GK, Dickerson EB: **Lysosomal drug sequestration as a mechanism of drug resistance in**

vascular sarcoma cells marked by high CSF-1R expression. *Vascular cell* 2014, **6**:20.

315. Shakya A, Kang J, Chumley J, Williams MA, Tantin D: **Oct1 is a switchable, bipotential stabilizer of repressed and inducible transcriptional states**. *The Journal of biological chemistry* 2011, **286**(1):450-459.

316. Fung KL, Tepede AK, Pluchino KM, Pouliot LM, Pixley JN, Hall MD, Gottesman MM: **Uptake of Compounds That Selectively Kill Multidrug-Resistant Cells: The Copper Transporter SLC31A1 (CTR1) Increases Cellular Accumulation of the Thiosemicarbazone NSC73306**. *Molecular Pharmaceutics* 2014, **11**(8):2692-2702.

317. Jiang P, Wu X, Wang X, Huang W, Feng Q: **NEAT1 upregulates EGCG-induced CTR1 to enhance cisplatin sensitivity in lung cancer cells**. *Oncotarget* 2016.

318. Ishida S, McCormick F, Smith-McCune K, Hanahan D: **Enhancing tumor-specific uptake of the anticancer drug cisplatin with a copper chelator**. *Cancer cell* 2010, **17**(6):574-583.

319. Balendiran GK, Dabur R, Fraser D: **The role of glutathione in cancer**. *Cell biochemistry and function* 2004, **22**(6):343-352.

320. Meijer C, Mulder NH, Hospers GA, Uges DR, de Vries EG: **The role of glutathione in resistance to cisplatin in a human small cell lung cancer cell line**. *British journal of cancer* 1990, **62**(1):72-77.

321. Zheng Z-G, Xu H, Suo S-S, Xu X-L, Ni M-W, Gu L-H, Chen W, Wang L-Y, Zhao Y, Tian B *et al*: **The Essential Role of H19 Contributing to Cisplatin Resistance by Regulating Glutathione Metabolism in High-Grade Serous Ovarian Cancer**. *Scientific Reports* 2016, **6**:26093.

322. Samimi G, Katano K, Holzer AK, Safaei R, Howell SB: **Modulation of the cellular pharmacology of cisplatin and its analogs by the copper exporters ATP7A and ATP7B**. *Molecular pharmacology* 2004, **66**.

323. Li Z-h, Qiu M-z, Zeng Z-l, Luo H-y, Wu W-j, Wang F, Wang Z-q, Zhang D-s, Li Y-h, Xu R-h: **Copper-transporting P-type adenosine triphosphatase**

(ATP7A) is associated with platinum-resistance in non-small cell lung cancer (NSCLC). *Journal of Translational Medicine* 2012, **10**(1):1-9.

324. Rose MC, Kostyanovskaya E, Huang RS: **Pharmacogenomics of Cisplatin Sensitivity in Non-small Cell Lung Cancer**. *Genomics, Proteomics & Bioinformatics* 2014, **12**(5):198-209.

325. Kalayda GV, Wagner CH, Buss I, Reedijk J, Jaehde U: **Altered localisation of the copper efflux transporters ATP7A and ATP7B associated with cisplatin resistance in human ovarian carcinoma cells**. *BMC Cancer* 2008, **8**.

326. Ruppen J, Cortes-Dericks L, Marconi E, Karoubi G, Schmid RA, Peng R, Marti TM, Guenat OT: **A microfluidic platform for chemoresistive testing of multicellular pleural cancer spheroids**. *Lab on a chip* 2014, **14**(6):1198-1205.

327. Curran S, Vantangoli MM, Boekelheide K, Morgan JR: **Architecture of Chimeric Spheroids Controls Drug Transport**. *Cancer Microenvironment* 2015, **8**(2):101-109.

328. Cho J-H, Dimri M, Dimri GP: **MicroRNA-31 Is a Transcriptional Target of Histone Deacetylase Inhibitors and a Regulator of Cellular Senescence**. *The Journal of biological chemistry* 2015, **290**(16):10555-10567.

329. Tseng SH, Yang CC, Yu EH, Chang C, Lee YS, Liu CJ, Chang KW, Lin SC: **K14-EGFP-miR-31 transgenic mice have high susceptibility to chemical-induced squamous cell tumorigenesis that is associating with Ku80 repression**. *International journal of cancer Journal international du cancer* 2015, **136**(6):1263-1275.

330. He F, Liu W, Zheng S, Zhou L, Ye B, Qi Z: **Ion transport through dimethyl sulfoxide (DMSO) induced transient water pores in cell membranes**. *Molecular membrane biology* 2012, **29**(3-4):107-113.

331. Imoto M, Azuma H, Yamamoto I, Otagiri M, Imai T: **Permeability of 5-fluorouracil and its prodrugs in Caco-2 cell monolayers: evidence for shift from paracellular to transcellular transport by prodrug formation**. *Journal of Drug Delivery Science and Technology* 2009, **19**(1):37-41.

332. Lanzi C, Perego P, Supino R, Romanelli S, Pensa T, Carenini N, Viano I, Colangelo D, Leone R, Apostoli P *et al*: **Decreased drug accumulation and increased tolerance to DNA damage in tumor cells with a low level of cisplatin resistance**. *Biochemical pharmacology* 1998, **55**(8):1247-1254.

333. Surowiak P, Materna V, Kaplenko I, Spaczynski M, Dolinska-Krajewska B, Gebarowska E, Dietel M, Zabel M, Lage H: **ABCC2 (MRP2, cMOAT) can be localized in the nuclear membrane of ovarian carcinomas and correlates with resistance to cisplatin and clinical outcome**. *Clinical cancer research : an official journal of the American Association for Cancer Research* 2006, **12**(23):7149-7158.

334. Ohashi-Kobayashi A, Ohashi K, Du W-b, Omote H, Nakamoto R, Al-shawi M, Maeda M: **Examination of drug resistance activity of human TAP-like (ABCB9) expressed in yeast**. *Biochemical and Biophysical Research Communications* 2006, **343**(2):597-601.

335. Kang J, Shakya A, Tantin D: **Stem cells, stress, metabolism and cancer: a drama in two Octs**. *Trends in Biochemical Sciences* 2009, **34**(10):491-499.

336. Tantin D, Schild-Poulter C, Wang V, Hache RJ, Sharp PA: **The octamer binding transcription factor Oct-1 is a stress sensor**. *Cancer research* 2005, **65**(23):10750-10758.

337. Bandyopadhyay D, Cyphersmith A, Zapata JA, Kim YJ, Payne CK: **Lysosome Transport as a Function of Lysosome Diameter**. *PloS one* 2014, **9**(1):e86847.

338. Ween MP, Armstrong MA, Oehler MK, Ricciardelli C: **The role of ABC transporters in ovarian cancer progression and chemoresistance**. *Critical Reviews in Oncology/Hematology* 2015, **96**(2):220-256.

339. Hlavata I, Mohelnikova-Duchonova B, Vaclavikova R, Liska V, Pitule P, Novak P, Bruha J, Vycital O, Holubec L, Treska V *et al*: **The role of ABC transporters in progression and clinical outcome of colorectal cancer**. *Mutagenesis* 2012, **27**(2):187-196.

340. Demirel Ö, Bangert I, Tampé R, Abele R: **Tuning the Cellular Trafficking of the Lysosomal Peptide Transporter TAPL by its N-terminal Domain**. *Traffic* 2010, **11**(3):383-393.

341. Demirel Ö, Waibler Z, Kalinke U, Grünebach F, Appel S, Brossart P, Hasilik A, Tampé R, Abele R: **Identification of a Lysosomal Peptide Transport System Induced during Dendritic Cell Development**. *Journal of Biological Chemistry* 2007, **282**(52):37836-37843.

342. Fujimoto Y, Kamakura A, Motohashi Y, Ohashi-Kobayashi A, Maeda M: **Transporter associated with antigen processing-like (ABCB9) stably expressed in Chinese hamster ovary-K1 cells is sorted to the microdomains of lysosomal membranes**. *Biological & pharmaceutical bulletin* 2011, **34**(1):36-40.

343. Demirel O, Jan I, Wolters D, Blanz J, Saftig P, Tampe R, Abele R: **The lysosomal polypeptide transporter TAPL is stabilized by interaction with LAMP-1 and LAMP-2**. *Journal of cell science* 2012, **125**(Pt 18):4230-4240.

344. Chen Z, Shi T, Zhang L, Zhu P, Deng M, Huang C, Hu T, Jiang L, Li J: **Mammalian drug efflux transporters of the ATP binding cassette (ABC) family in multidrug resistance: A review of the past decade**. *Cancer Letters* 2016, **370**(1):153-164.

345. Li W, Zhang H, Assaraf YG, Zhao K, Xu X, Xie J, Yang D-H, Chen Z-S: **Overcoming ABC transporter-mediated multidrug resistance: Molecular mechanisms and novel therapeutic drug strategies**. *Drug Resistance Updates* 2016, **27**:14-29.

346. Pan YZ, Morris ME, Yu AM: **MicroRNA-328 negatively regulates the expression of breast cancer resistance protein (BCRP/ABCG2) in human cancer cells**. *Molecular pharmacology* 2009, **75**(6):1374-1379.

347. Ma MT, He M, Wang Y, Jiao XY, Zhao L, Bai XF, Yu ZJ, Wu HZ, Sun ML, Song ZG *et al*: **MiR-487a resensitizes mitoxantrone (MX)-resistant breast cancer cells (MCF-7/MX) to MX by targeting breast cancer resistance protein (BCRP/ABCG2)**. *Cancer Lett* 2013, **339**(1):107-115.

348.   Place RF, Li L-C, Pookot D, Noonan EJ, Dahiya R: **MicroRNA-373 induces expression of genes with complementary promoter sequences**. *Proceedings of the National Academy of Sciences* 2008, **105**(5):1608-1613.

349.   Pasquinelli AE: **MicroRNAs and their targets: recognition, regulation and an emerging reciprocal relationship**. *Nature reviews Genetics* 2012, **13**(4):271-282.

350.   Kang J, Gemberling M, Nakamura M, Whitby FG, Handa H, Fairbrother WG, Tantin D: **A general mechanism for transcription regulation by Oct1 and Oct4 in response to genotoxic and oxidative stress**. *Genes & Development* 2009, **23**(2):208-222.

351.   Chow K-H, Factor RE, Ullman KS: **The nuclear envelope environment and its cancer connections**. *Nat Rev Cancer* 2012, **12**(3):196-209.

352.   Strambio-De-Castillia C, Niepel M, Rout MP: **The nuclear pore complex: bridging nuclear transport and gene regulation**. *Nat Rev Mol Cell Biol* 2010, **11**(7):490-501.

353.   Malhas A, Saunders NJ, Vaux DJ: **The nuclear envelope can control gene expression and cell cycle progression via miRNA regulation**. *Cell cycle (Georgetown, Tex)* 2010, **9**(3):531-539.

354.   Li C-W, Lim S-O, Xia W, Lee H-H, Chan L-C, Kuo C-W, Khoo K-H, Chang S-S, Cha J-H, Kim T *et al*: **Glycosylation and stabilization of programmed death ligand-1 suppresses T-cell activity**. *Nature Communications* 2016, **7**:12632.

355.   Favoni RE, Florio T: **Combined chemotherapy with cytotoxic and targeted compounds for the management of human malignant pleural mesothelioma**. *Trends in pharmacological sciences* 2011, **32**(8):463-479.

356.   Lynam-Lennon N, Maher SG, Reynolds JV: **The roles of microRNA in cancer and apoptosis**. *Biological reviews of the Cambridge Philosophical Society* 2009, **84**(1):55-71.

357. Valastyan S, Reinhardt F, Benaich N, Calogrias D, Szasz A, Wang Z, Brock J, Richardson A, Weinberg R: **A pleiotropically acting microRNA, miR-31, inhibits breast cancer metastasis**. *Cell* 2009, **137**:1032 - 1046.

358. Kuusisto HV, Jans DA: **Hyper-dependence of breast cancer cell types on the nuclear transporter Importin β1**. *Biochimica et Biophysica Acta (BBA) - Molecular Cell Research* 2015, **1853**(8):1870-1878.

359. Laurila E, Vuorinen E, Savinainen K, Rauhala H, Kallioniemi A: **KPNA7, a nuclear transport receptor, promotes malignant properties of pancreatic cancer cells in vitro**. *Experimental Cell Research* 2014, **322**(1):159-167.

360. Ouar Z, Lacave R, Bens M, Vandewalle A: **Mechanisms of altered sequestration and efflux of chemotherapeutic drugs by multidrug-resistant cells**. *Cell Biology and Toxicology* 1999, **15**(2):91-100.

361. Boac BM, Xiong Y, Marchion DC, Abbasi F, Bush SH, Ramirez IJ, Khulpateea BR, Clair McClung E, Berry AL, Zgheib NB *et al*: **Micro-RNAs associated with the evolution of ovarian cancer cisplatin resistance**. *Gynecologic Oncology* 2016, **140**(2):259-263.

362. Pennati M, Lopergolo A, Profumo V, De Cesare M, Sbarra S, Valdagni R, Zaffaroni N, Gandellini P, Folini M: **miR-205 impairs the autophagic flux and enhances cisplatin cytotoxicity in castration-resistant prostate cancer cells**. *Biochemical pharmacology* 2014, **87**(4):579-597.

363. Dehghanzadeh R, Jadidi-Niaragh F, Gharibi T, Yousefi M: **MicroRNA-induced drug resistance in gastric cancer**. *Biomedicine & Pharmacotherapy* 2015, **74**:191-199.

364. Drayton RM, Dudziec E, Peter S, Bertz S, Hartmann A, Bryant HE, Catto JWF: **Reduced expression of microRNA-27a modulates cisplatin resistance in bladder cancer by targeting the cystine/glutamate exchanger SLC7A11**. *Clinical cancer research : an official journal of the American Association for Cancer Research* 2014, **20**(7):1990-2000.

365. Soekmadji C, Nelson CC: **The Emerging Role of Extracellular Vesicle-Mediated Drug Resistance in Cancers: Implications in Advanced Prostate Cancer**. *BioMed research international* 2015, **2015**:13.

366. Federici C, Petrucci F, Caimi S, Cesolini A, Logozzi M, Borghi M, D'Ilio S, Lugini L, Violante N, Azzarito T *et al*: **Exosome release and low pH belong to a framework of resistance of human melanoma cells to cisplatin**. *PloS one* 2014, **9**(2):e88193.

367. Stordal B, Hamon M, McEneaney V, Roche S, Gillet J-P, O'Leary JJ, Gottesman M, Clynes M: **Resistance to Paclitaxel in a Cisplatin-Resistant Ovarian Cancer Cell Line Is Mediated by P-Glycoprotein**. *PloS one* 2012, **7**(7):e40717.

368. Quinn L, Finn SP, Cuffe S, Gray SG: **Non-coding RNA repertoires in malignant pleural mesothelioma**. *Lung Cancer* 2015, **90**(3):417-426.

369. Pillai K, Ehteda A, Akhter J, Chua TC, Morris DL: **Anticancer effect of bromelain with and without cisplatin or 5-FU on malignant peritoneal mesothelioma cells**. *Anticancer Drugs* 2014, **25**(2):150-160.

370. Zhang Q, Ran R, Zhang L, Liu Y, Mei L, Zhang Z, Gao H, He Q: **Simultaneous delivery of therapeutic antagomirs with paclitaxel for the management of metastatic tumors by a pH-responsive anti-microbial peptide-mediated liposomal delivery system**. *Journal of Controlled Release* 2015, **197**:208-218.

371. Kao SC, Fulham M, Wong K, Cooper W, Brahmbhatt H, MacDiarmid J, Pattison S, Sagong JO, Huynh Y, Leslie F *et al*: **A Significant Metabolic and Radiological Response after a Novel Targeted MicroRNA-based Treatment Approach in Malignant Pleural Mesothelioma**. *American journal of respiratory and critical care medicine* 2015, **191**(12):1467-1469.

372. Yoshida D, Ebara T, Sato Y, Kaminuma T, Takahashi T, Asao T, Nakano T: **Interaction of radiation and pemetrexed on a human malignant mesothelioma cell line in vitro**. *Anticancer research* 2011, **31**(9):2847-2851.
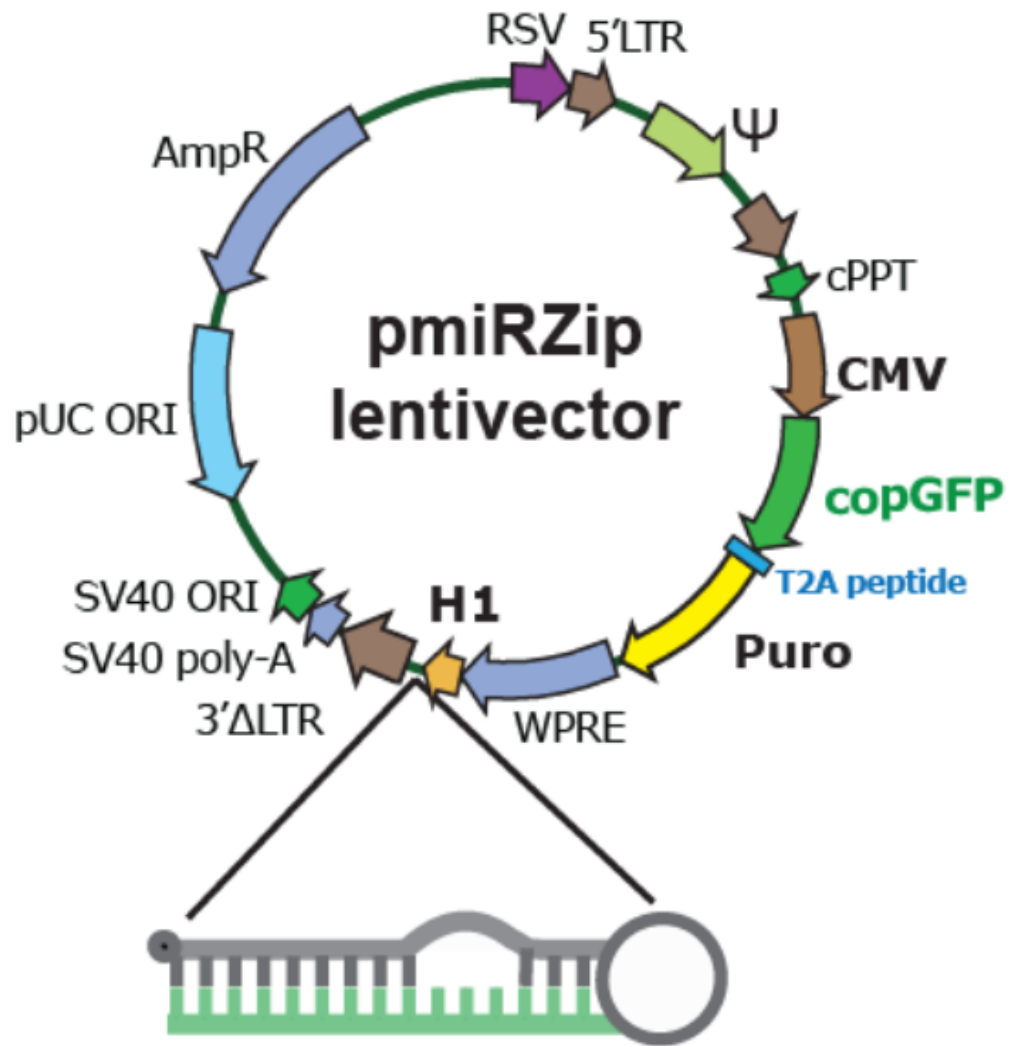
Appendices

Appendix 1
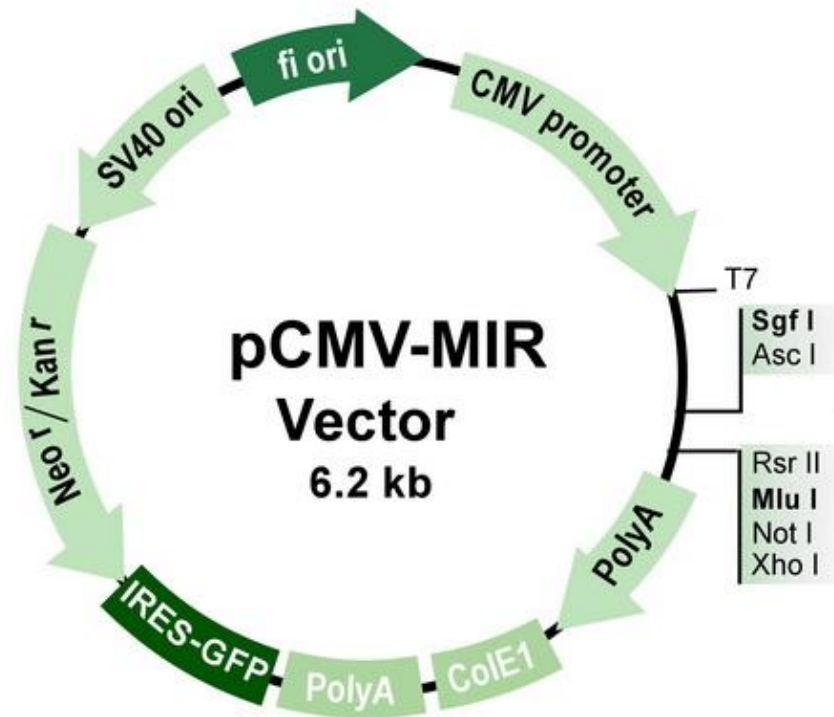
Figure A1.1 Plasmid map for miR-31 overexpression/reintroduction. Under the control of a CMV promoter, miR-31 was produced from the plasmid. A GFP reporter was encoded on the plasmid. A kanamycin resistance gene was encoded for bacterial selection; a neomycin (also known as G418 or geneticin) resistance gene was encoded for mammalian selection. The plasmid was purchased from Origene.

Image sourced at: http://www.origene.com/MicroRNA/pCMV-MIR-Vector.aspx

Figure A1.2 Plasmid map for Zip-miR-31 suppression. Under the control of a CMV promoter, an antisense-miR-31 (termed anti-miRNA) was produced from the plasmid, which bound to endogenous miR-31, effectively inhibiting its functionality. A GFP reporter was encoded on the plasmid. An ampicillin resistance gene was encoded for bacterial selection; a puromycin resistance gene was encoded for mammalian selection. The plasmid was purchased from SBI.

Image sourced at:

https://www.systembio.com/microrna-research/microRNA-knockdown/mirzip/technical-details
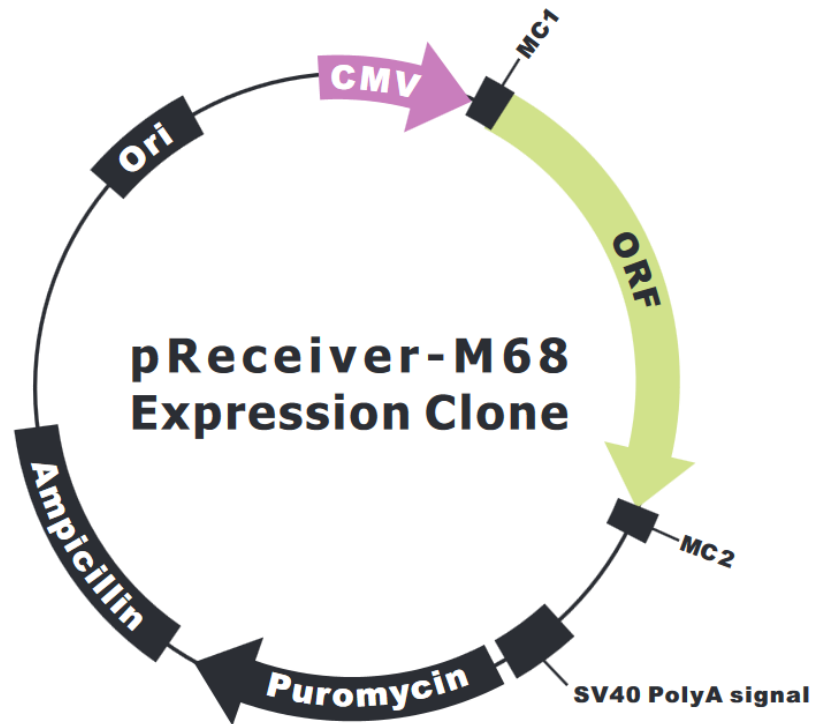
Figure A1.3 Plasmid map for ABCB9 overexpression. Under the control of a CMV promoter, ABCB9 was produced from the plasmid. An ampicillin resistance gene was encoded for bacterial selection; a puromycin resistance gene was encoded for mammalian selection. The plasmid was purchased from Genecopoeia.

Image sourced at:

http://www.genecopoeia.com/product/search/detail.php?prt=1&cid=&key=T8156

Appendix 2

Table A2. Gel Casting Recipes

Stacking Gel:

Component	
H_2O	6.1 mL
0.5 M Tris pH 6.8	2.5 mL
Acrylamide	1.3 mL
10% SDS	100 μL
10% APS	100 μL
TEMED	20 μL

Resolving gel:

| Component	6 %	7.5%	10%	12%	15%	20%
H_2O	8.13 mL	7.4 mL	6.07 mL	5.2 mL	3.75 mL	1.1 mL
1.5 M Tris pH 8.8	3.75 mL	3.75 mL	3.75 mL	3.75 mL	3.75 mL	3.75 mL
Acrylamide	2.92 mL	3.65 mL	4.95 mL	5.8 mL	7.25 mL	10 mL
10% SDS	150 μL	150 μL	150 μL	150 μL	150 μL	150 μL
10% APS	75 μL	75 μL	75 μL	75 μL	75 μL	75 μL
TEMED	18 μL	18 μL	18 μL	18 μL	18 μL	18 μL

Appendix 3

Table A3.1 Optimising cell seeding densities for the clonogenic assay. The number of cells seeded per well of a six welled plate was optimised to ensure a minimum of ~200 colonies after fixing and staining. Mean colony number taken from all wells for all experiments.

Cell line	Treatment	Cell seeding density	Mean colony number ±SEM
NCI-H2452 miR-VC	PBS	5×10^2	265 ± 56
	1 µM cisplatin	1.5×10^3	203 ± 76
	10 µM carboplatin	$7.5 \times 10^2 - 1.5 \times 10^3$	211 ± 54
NCI-H2452 miR-31	PBS	5×10^2	321 ± 39
	1 µM cisplatin	1.5×10^3	283 ± 79
	10 µM carboplatin	$7.5 \times 10^2 - 1.5 \times 10^3$	359 ± 37
P31 Zip-miR-VC	PBS	5×10^2	311 ± 59
	2 µM cisplatin	$5 \times 10^2 - 7.5 \times 10^2$	145 ± 84
	40 µM carboplatin	1.0×10^3	499 ± 45
P31 Zip-miR-31	PBS	5×10^2	268 ± 59
	2 µM cisplatin	$5 \times 10^2 - 7.5 \times 10^2$	141 ± 82
	40 µM carboplatin	1.0×10^3	450 ± 27

Table A3.2 Optimised Compact Hough and Radial Map (CHARM) settings for NCI-H2452. The algorithm was optimised to ensure that sufficient colonies were analysed, without taking anomalies into account.

| Panel	Function	Setting
F1 Pre-processed	Smoothing	0
F2 Edge detection	Edge detection sensitivity	72/100
F3 Centre detection	Detection mode	Dark on light
	Centre detection sensitivity	65.3/100
	Soft colony diameter range	Lower 40 μm, Upper 1500 μm
	Min centre to centre separation	40 μm
	Auto-select	Yes
	Smoothing	3
F4 Shape controls	Circularity factor	50/100
	Edge distance threshold	0.89
	No. Spokes	32
	Shape filtering	Fast Gaussian, Filter size 3
	Shape processing	Best fit circle
F5 Filtering controls	Colony diameter filter	Min 66 μm, Max 1500 μm
	Colony intensity	Min 0.1, Max 2.0
	Good edge factor	0.5/1
	Borders from centroids	Yes
F6 Overlap controls	Merge overlapping objects	Yes
	Overlap threshold	1.00
	Overlap calculation	Area
	Retain the	Most intense
	Calculate new cluster boundaries	Yes
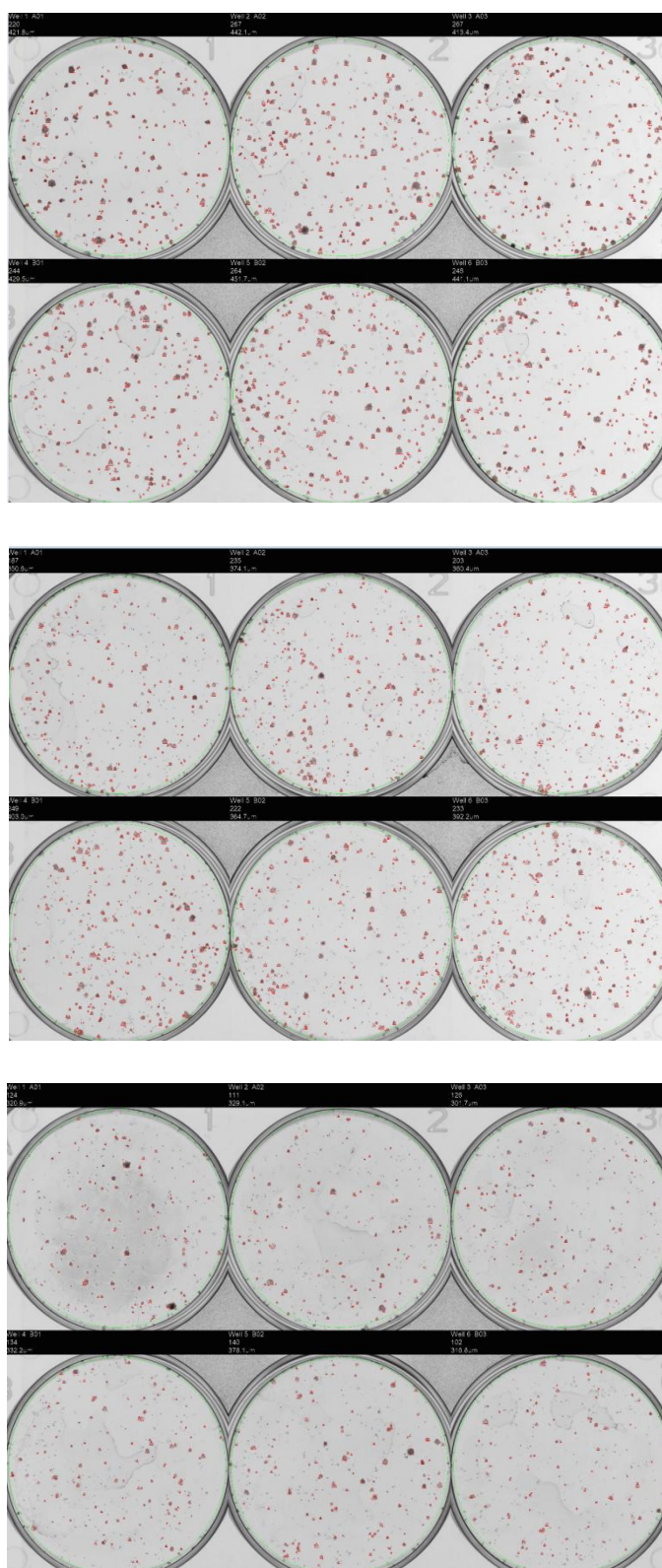
Figure A3.1 Example of typical clonogenic assay plates. Top, PBS treated NCI-H2452 miR-VC with an average colony count of 251 (500 cells per well seeded), middle, carboplatin treated NCI-H2452 miR-VC with an average colony count of 221 (1000 cells per well seeded), bottom, carboplatin treated NCI-H2452 miR-VC with an average colony count of 122 (1500 cells per well seeded).
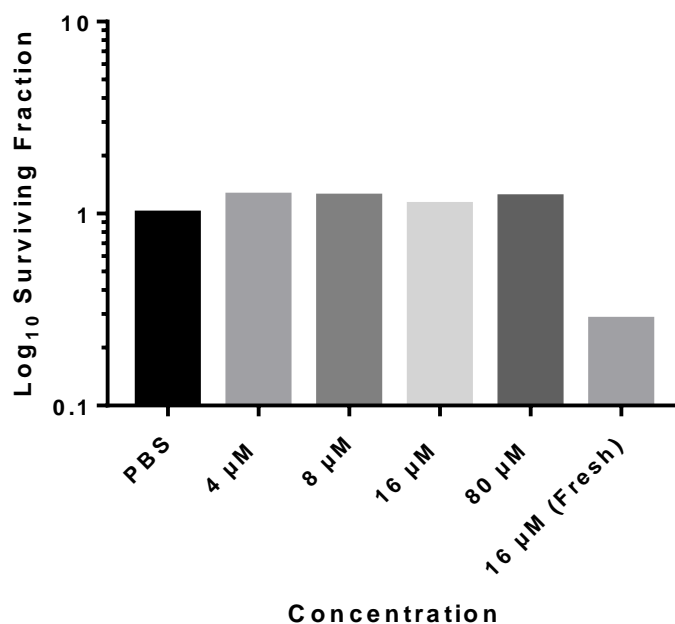
Figure A3.2 Pemetrexed treated clonogenic of NCI-H2452. NCI-H2452 cell line response to pemetrexed disodium. It was concluded that pemetrexed toxicity was affected by storage at -20ºC. While multiple solubilising agents were tried, the toxicity of pemetrexed in storage remained poor. As apparent in the last bar, with the use of 16 μM (fresh) pemetrexed, which was solubilised in PBS and used immediately for treatment, pemetrexed was only effective when prepared directly prior to use, this was impracticable for the dose range required for clonogenic assay.

Pemetrexed has been successfully utilised in other publications, such as Yoshida *et al.* [372], where pemetrexed was purchased as a liquid stock solution, and then frozen at -80°C, this may potentially be a route by which pemetrexed toxicity could be restored.

Appendix 4
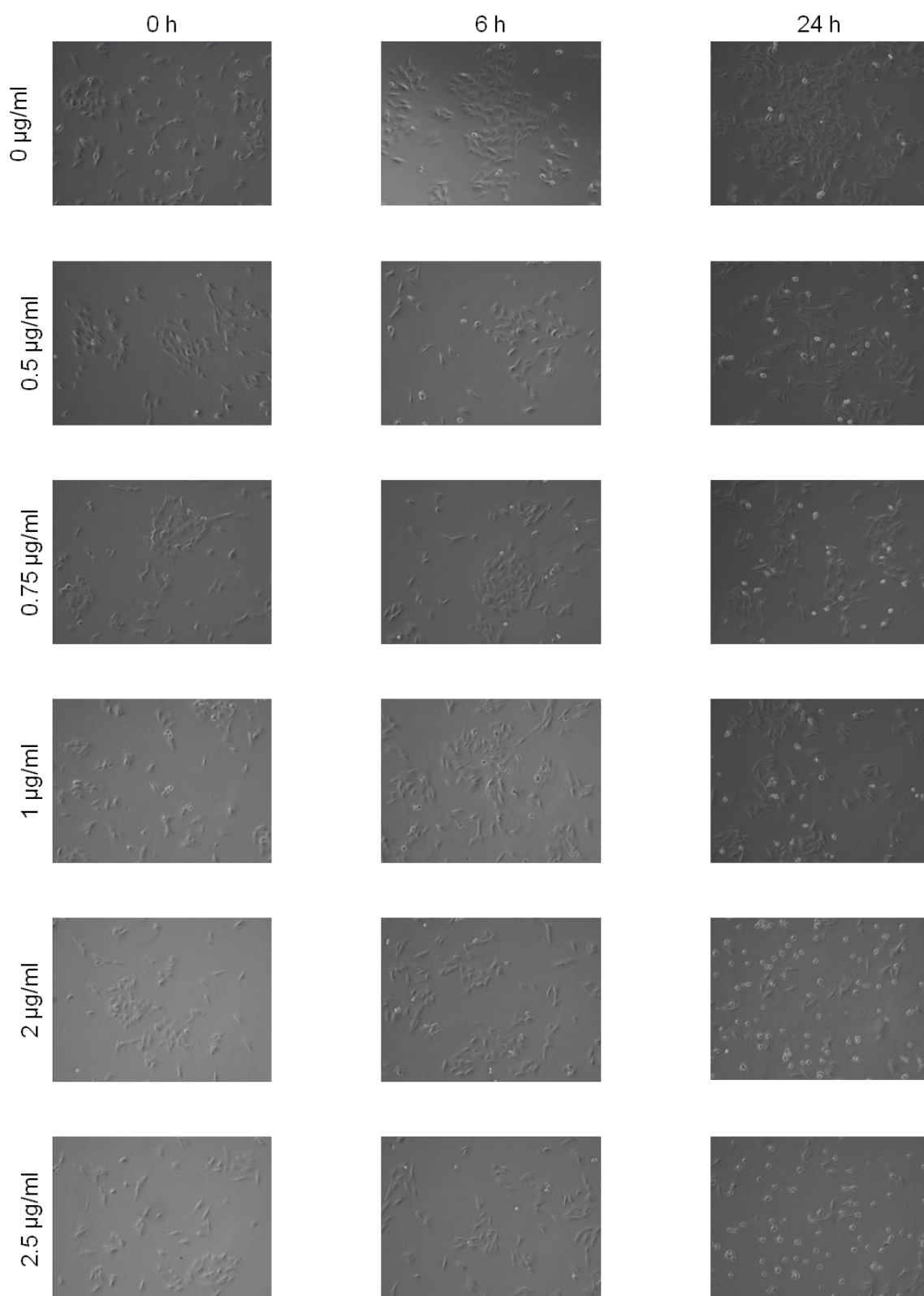
Figure A4. Puromycin kill response in NCI-H2452. The response of NCI-H2452 cell line treated with varying concentrations of puromycin. The dose of 2 µg/ml was utilised as the optimal killing dose without overwhelming the cell line.
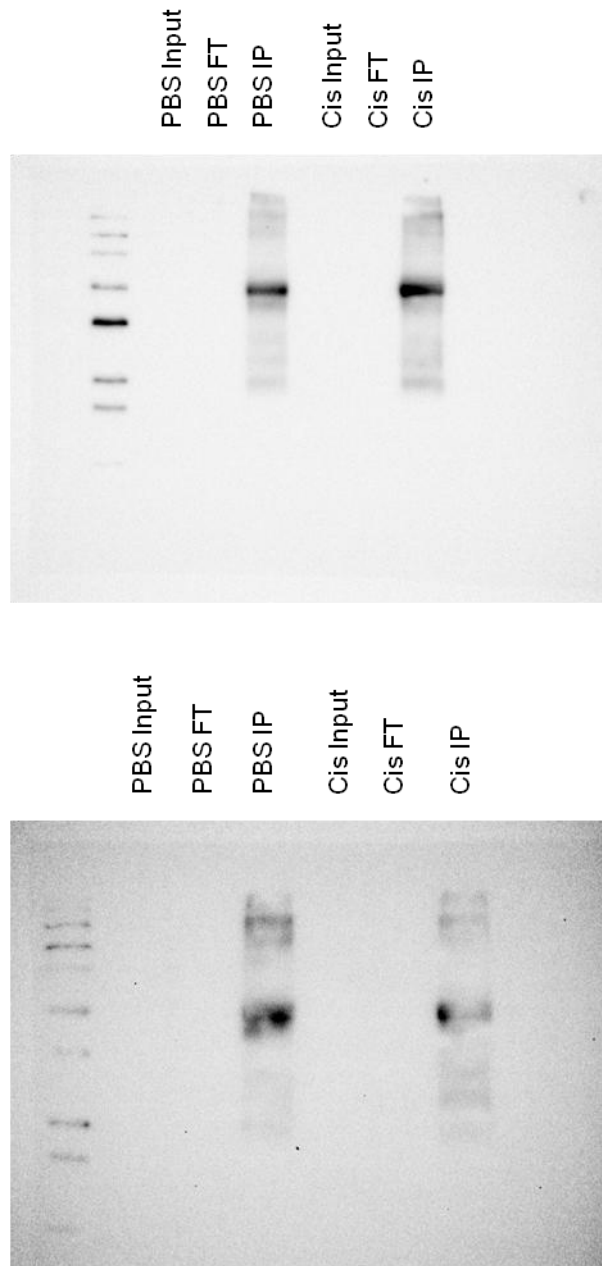
Figure A5. LAMP-1 immuno-pull down. Representative Western blots illustrating pull down of LAMP-1 post novel lysosomal isolation method. The NCI-H2452 miR-VC cell line (top) demonstrated successful pull down of LAMP-1 protein in PBS and cisplatin treated samples. The NCI-H2452 miR-31 cell line (bottom) demonstrated successful pull down of LAMP-1 protein in both PBS and cisplatin treated cell samples.
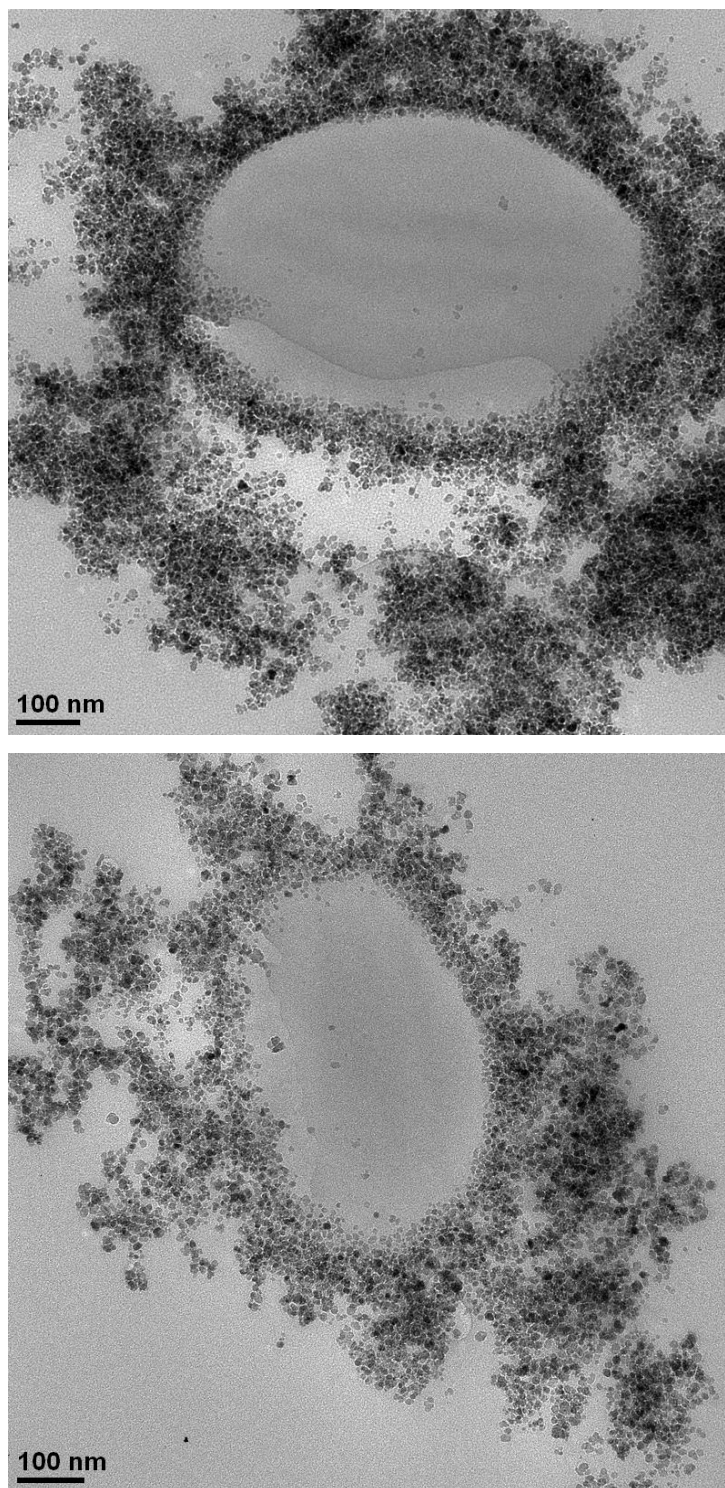
Figure A6. Transmission electron microscopy (TEM) of lysosomal pull down. TEM images using osmium contrast, captured after novel immuno-pull down method to isolate lysosomes. The method to obtain confirmation of successful isolation of lysosomes was deemed insufficient, as the beads only control (top) appeared structurally the same as the lysosome isolated samples (bottom).

Definitions	
3'	3 prime
5'	5 prime
5-FU	5-Fluorouracil
ABCB9	ATP binding cassette subfamily B member 9
Ago	argonaut protein
Amp	ampicillin
ANOVA	analysis of variance
APS	ammonium persulphate
ATP	adenosine triphosphate
ATP7A	ATPase copper transporting alpha
ATP7B	ATPase copper transporting beta
BCA	bicinchoninic acid
BER	base excision repair
BSA	bovine serum albumin
cDNA	complimentary DNA
CHARM	compact Hough and radial map
cis	cisplatin
CTLA-4	cytotoxic T-lymphocyte-associated protein 4
CTR1	copper transporter 1
DACH	diaminocyclohexane
DAPI	4', 6-diamidino-2-phenylindole
DDR	DNA damage response
DGCR	DiGeorge syndrome chromosomal region
DMSO	dimethyl sulphoxide

DNA	deoxyribosenucleic acid
dNTPs	deoxyribose nucelotide triphosphates
dsDNA	double strand DNA
dTTP	deoxythymidine triphosphate
E.coli	*Escherichia coli*
EDTA	ethylenediaminetetraacetic Acid
EGFR	epithelial growth factor receptor
EMT	epithelial-mesenchymal transition
EtOH	ethanol
FBS	foetal bovine serum
FITC	fluorescin isothiocynate
G418	geneticin antibiotic
gDNA	genomic DNA
GFP	green fluorescent protein
GSH	glutathione
GSSG	glutathione disulfide
HRP	horseradish peroxidise
IC$_{50}$	concentration of a drug where the response is reduced by half
IgG	immunoglobulin
IHC	immunohistochemistry
Kan	kanamycin
KEGG	Kyoto Encyclopedia of Genes and Genomes
LAMP-1	Lysosomal-associated membrane protein 1
LB	Lysogeny broth
MDR	multi-drug resistance

MeOH	methanol
MHC	major histocompatibility complex
miR-	microRNA-
miRNA	microRNA
miR-Zip	microRNA suppression plasmid
MM	malignant mesothelioma
MMR	mismatch repair
MPM	malignant pleural mesothelioma
mRNA	messenger RNA
n	number of replicates
NCI-H2452	National Cancer Institute H2452 epithelioid MPM cell line
NER	nucleotide excision repair
ns	non significant
NSCLC	non small cell lung cancer
OCT1	Organic Cation Transporter 1
p	probability
P31	P31 MPM epithelioid cell line
PBS	phosphate buffered saline
PCR	polymerase chain reaction
PD-1	programmed cell death protein 1
Pre-miRNA	pre-microRNA
Pri-miRNA	primary-microRNA
Puro	puromycin
PVDF	polyvinylidene fluoride
qPCR	quantitative PCR

RB	retinoblastoma
RIPA	radioimmunoprecipitation assay buffer
RISC	RNA-induced silencing complex
RNA	ribose nucleic acid
RNase	ribonuclease
ROS	reactive oxygen species
RPMI-1640	Roswell Park Memorial Institute cell culture medium
RT	reverse transcription
SEM	standard error of mean
SD	standard deviation
SDS	sodium dodecyl sulfate
SDS-PAGE	sodium dodecyl sulphate-polyacrylamide gel electrophoresis
TBS	tris buffered saline
TBST	tris buffered saline with tween 20
TEM	Transmission electron microscopy
TEMED	tetramethylethylenediamine
TSP-1	Thrombospondin type-1
UK	United Kingdom
USA	United States of America
VEGF	vascular endothelial growth factor

Units	
β	beta
ɣ	gamma
bp	base pairs
ºC	degrees Celsius
g	grams
×*g*	acceleration (gravity)
Gy	Gray (radiation)
h	hours
kb	kilobase
kDa	kiloDalton
L	litres
M	molar
mg	milligram
min	minute
mL	millilitre
mM	millimolar
ms	milliseconds
µg	micrograms
µL	microlitres
µM	micromolar
µm	micrometer
ng	nanogram
nm	nanometer
s	seconds

V	Volts
v/v	volume per volume
w/v	weight per volume